Functional and genetic approaches to decipher novel roles of Src homology region 2 domain-containing phosphatase-1 (SHP1) in physiology and metabolism Thèse

Amit Kumar

Functional and genetic approaches to decipher novel roles of Src homology region 2 domain-containing phosphatase-1 (SHP1) in physiology and metabolism

Thesis · July 2024

DOI: 10.13140/RG.2.2.12113.13923

1 author:

Amit Kumar
University Health Network
63 PUBLICATIONS **1,413** CITATIONS

SEE PROFILE

Functional and genetic approaches to decipher novel roles of Src homology region 2 domain-containing phosphatase-1 (SHP1) in physiology and metabolism

Thèse

Amit Kumar

Doctorat en médecine moléculaire
Philosophiæ doctor (Ph. D.)

Québec, Canada

Functional and genetic approaches to decipher novel roles of Src homology region 2 domain-containing phosphatase-1 (SHP-1) in physiology and metabolism

Thèse

Amit KUMAR

Sous la direction de :

André Marette, directeur de recherche

Résumé

La résistance à l'insuline associée à l'obésité est une condition qui favorise les troubles métaboliques tels que le diabète de type 2 (T2D) et la stéatose hépatique non alcoolique (NAFLD). Des altérations de l'homéostasie des lipides et du glucose, ainsi qu'une inflammation chronique de bas grade sont les caractéristiques du T2D et de la NAFLD. SHP-1 (codé par le gène *PTPN6*) est une tyrosine phosphatase avec deux domaines SH2 et est connu pour agir comme modulateur du métabolisme du glucose et des lipides. SHP-1 régule également la signalisation des cytokines et l'expression des gènes inflammatoires. En plus d'être localisé dans le cytoplasme, SHP-1 se trouve également dans le noyau des cellules épithéliales. La fonction de ce SHP-1 nucléaire reste inconnue. Ici, nous avons étudié les fonctions dépendantes et indépendantes de la tyrosine phosphatase de SHP-1 dans le contrôle des voies métaboliques.

Des découvertes antérieures de notre laboratoire ont établi un lien entre SHP-1 et l'activité du récepteur activé par les proliférateurs de peroxysomes γ2 (PPARγ2). PPARγ2 est un facteur de transcription activé par des ligands et contrôle le métabolisme des lipides. Dans le chapitre II, nous avons constaté que SHP-1 interagit avec PPARγ2 principalement via son domaine SH2 en N-terminal et peut déphosphoryler PPARγ2 *in vitro*. Nos données suggèrent que PPARγ2 est phosphorylé sur le résidu tyrosine 78 (Y78) et que la déphosphorylation catalysée par SHP-1 est associée à la stabilité de PPARγ2. L'invalidation génétique de SHP-1 dans des cellules exprimant PPARγ2 augmente l'expression des cibles transcriptionnelles de PPARγ2 telles que *FABP4* et *CD36* en plus d'augmenter l'adipogenèse. Ces effets étaient atténués dans des cellules exprimant une forme mutée de PPARγ2 où la tyrosine 78 avait été remplacée par une phénylalanine ne pouvant être phosphorylée (Y78F). Collectivement, ces résultats indiquent que l'activité phosphatase de SHP-1 contrôle la stabilité de PPARγ2 et donc affecte l'adipogenèse.

SHP-1 est un modulateur de la signalisation de l'insuline. L'invalidation génétique de SHP-1 spécifiquement dans les hépatocytes chez la souris (SHP-1 KO) est associée à une glycémie à jeun plus basse que celle de leurs congénères non transgéniques. Les souris SHP-1 KO présentaient également une diminution importante de la production hépatique de glucose, suggérant donc l'existence d'une autre fonction de SHP-1 sur l'homéostasie du glucose, possiblement indépendante de l'insuline.

Dans le chapitre III, nous avons découvert que SHP-1 agit comme coactivateur pour contrôler la transcription du gène phosphoénolpyruvate carboxykinase 1 (PCK1) et donc régule la gluconéogenèse. SHP-1 est recruté à la région régulatrice du gène *PCK1*, le cite potentiel où il interagit avec l'ARN polymérase II (RNAPII). Le recrutement de SHP-1 à la chromatine est dépendant du facteur de transcription transducteur de signal et activateur de transcription 5 (STAT5). L'épuisement de STAT5 ainsi que SHP-1 résulte en une diminution du niveau de transcrit de *PCK1* et une réduction de la gluconéogenèse. Ensemble, ces résultats indiquent que nous avons découvert une nouvelle fonction de SHP-1 où la phosphatase agit comme un co-régulateur transcriptionnel clef du gène *PCK1* et exerce un contrôle sur la gluconéogenèse.

Abstract

Insulin resistance coupled with obesity is a condition that promotes metabolic disorders such as type 2 diabetes (T2D) and non-alcoholic fatty liver disease (NAFLD). Alterations in lipid and glucose homeostasis, as well as low-grade chronic inflammation are the hallmarks of T2D and NAFLD. SHP-1 (encoded by the gene Protein Tyrosine Phosphatase Non-Receptor Type 6, *PTPN6*) is a tyrosine phosphatase with two SH2 domains and is known to act as a modulator of glucose and lipid metabolism. In addition, SHP-1 also regulates cytokine signaling and inflammatory gene expression. Besides being localized in the cytoplasm, SHP-1 is also found in the nucleus of epithelial cells. The function of this nuclear SHP-1 remains elusive. Here, we investigated tyrosine phosphatase dependent and independent functions of SHP-1 in controlling metabolic pathways.

Previous findings from our laboratory established a link between SHP-1 and peroxisome proliferator-activated receptor γ2 (PPARγ2) activity. PPARγ2 is a ligand-activated transcription factor that controls lipid metabolism. In chapter II, we found that SHP-1 interacts with PPARγ2 mainly via its N-terminal SH2 domain and can dephosphorylate PPARγ2 *in vitro*. Our data suggest that PPARγ2 is tyrosine phosphorylated mainly on tyrosine residue 78 (Y78) and SHP-1-mediated dephosphorylation of PPARγ2 is associated with its stability. The knockdown of SHP-1 in PPARγ2 expressing cells resulted in enhanced expression of the classical PPARγ2 targets *FABP4* and *CD36* coupled with increased adipogenesis. These effects were blunted in cells expressing mutant PPARγ2 where tyrosine 78 has been replaced with the non-phosphorylatable phenylalanine (Y78F). Collectively, phosphatase activity of SHP-1 controls the stability of PPARγ2 thereby affecting lipid metabolism.

SHP-1 is a modulator of insulin signaling. Hepatocyte-specific SHP-1 KO mice compared to their wild type control littermates exhibited lower fasting glucose and

markedly decreased hepatic glucose production suggesting the existence of an additional insulin-independent effect of SHP-1 on glucose homeostasis. In Chapter III, we found that SHP-1 acts as a co-activator for controlling the transcription of the phosphoenolpyruvate carboxykinase 1 (*PCK1*) gene thereby regulating gluconeogenesis. SHP-1 is recruited to the regulatory region of the *PCK1* gene, the potential site where it interacts with RNA polymerase II (RNAPII). The recruitment of SHP-1 to the chromatin was mediated by the transcription factor signal transducer and activator of transcription 5 (STAT5). Depletion of STAT5 as well as SHP-1 resulted in a decrease in *PCK1* transcript levels and blunted gluconeogenesis. Taken together, we discovered a novel function of SHP-1 whereby it acts as a key transcriptional co-regulator of the *PCK1* gene and exerts control over gluconeogenesis.

Collectively, findings from these studies provide novel functions of SHP-1 in controlling lipid and glucose metabolism.

Contents

List of figures

INTRODUCTION

CHAPTER II

CHAPTER III

CONCLUSION

List of tables

CHAPTER II

CHAPTER III

CONCLUSION

List of abbreviations

(Cbl)-b	Casitas-B-lineage lymphoma
ACACA	Acetyl-CoA carboxylase
ALT	Alanine aminotransferase
AP-MS	Affinity-purification mass spectrometry
AST	Aspartate aminotransferase
BAT	Brown adipose tissue
BAT	Brown adipose tissue
BMI	Basal mass index
CBP	CREB binding protein
CC	Coiled-coil
CEACAM1	Carcinoembryonic antigen-related cell adhesion molecule 1
c-JNK	c-Jun amino-terminal kinase
CREB	CREB1 Gene - CAMP Responsive Element Binding Protein
CRTC2	CREB Regulated Transcription Coactivator 2
CTD	C terminal domain
CVD	Cardiovascular diseases
DBD	DNA binding domain
DN	Dominant negative
DNL	de novo lipogenesis
DSIF	DRB sensitivity inducing factor
ECM	Extracellular matrix
EGF	Epidermal growth factor
eWAT	Epididymal white adipose tissue
FA	Fatty acid
FAS	Fatty acid synthase
FOXO1	Forkhead Box Protein O1
G6P	Glucose-6-phosphate

GCGR	Glucagon receptor
GDM	Gestational diabetes mellitus
GLUT4	Glucose transporter 4
GTFs	General transcription factors
HbA1C	Hemoglobin A1c
HS	Hepatic steatosis
IL-1β	Interleukin 1 beta
IL-6	Interleukin-6
INSIGs	Insulin-induced genes
ipITT	Intraperitoneal insulin tolerance test
IR	Insulin receptor
IRS	Insulin receptor substrates
iWAT	Inguinal white adipose tissue
JAK	Janus Kinase
KD	Knockdown
KO	Knockout
MAPK	Mitogen-activated protein kinase kinase
MODY	Maturity-onset diabetes of the young
mTOR	Mammalian target of rapamycin
mWAT	Mesenteric white adipose tissue
NAFLD	Non-alcoholic fatty liver disease
NASH	Non-alcoholic steatotic hepatitis
NCoR	Nuclear receptor corepressor
NDM	Neonatal diabetes mellitus
NELF	Negative elongation factor
NF-κB	Nuclear factor kappa-light-chain-enhancer of activated B cells
NR	Nuclear Receptor
NTD	N terminal domain
NTTPs	Non-transmembrane tyrosine phosphatases

OAA	oxaloacetate
ob/ob	Obese/obese
oGTT	Glucose tolerance test
oGTT	Oral glucose tolerance tests
PAX8	Paired box 8
PDK-1	3-phosphoinositide-dependent protein kinase 1
PEP	phosphoenolpyruvic acid
PI3K	Phophoinositide3-kinase
PIC	Pre-initiation complex
PKA	Protein kinase A
PPARγ2	Peroxisome proliferator-activated receptor-γ
PPARs	Peroxisome proliferator-activated receptors
PPRE	PPAR response elements
PTMs	Post-translational modifications
PTP	Proteintyrosine phosphatase
PTP1B	Protein tyrosine phosphatase
RNAP	DNA-directed RNA polymerase
RPTPs	Receptor-like protein- tyrosine phosphatases
rpWAT	Retroperitoneal white adipose tissue
RXR	Retinoic acid receptor
SCD1	Stearoyl-CoA Desaturase 1
SH2	Src-homology 2 containing domain
SHP-1	Src homology 2 domain-containing protein tyrosine phosphatase 1
SHP-2	SH2 domain containing non protein tyrosine phosphatase 2
SNP	Single nucleotide polymorphism
SOCS	Suppressor of cytokine signaling
SREBP-1	Sterol regulatory element-binding protein-1
STAT	Signal Transducer and Activator of Transcription Protein
T1D	Type 1 diabetes

T2DM	Type 2 diabetes mellitus
TAD	Transactivation domain
TFs	Transcription factors
TG	Triglycerides
TG	Triglyceride
TNFα	TNA alpha
TPO	Thrombopoietin
TSS	Transcription start site
UC	Ulcerative colitis
uSTAT5	Unphosphorylated STAT5
WAT	White adipose tissue
WAT	White adipose tissue
WHO	World Health Organization
WT	Wild type

Acknowledgments

First, I thank my supervisor, Dr. André Marette for giving me an opportunity to pursue a Ph.D. in his esteemed laboratory. I thank him for his continuous encouragement, support, and mentorship throughout my Ph.D. studies. You provided me with several opportunities to present our research in several avenues around the world and this has significantly contributed to my scientific development.

I would like to sincerely thank my advisory committee, Dr. Mathieu Laplante, Dr. Steve Bilodeau for their guidance and constructive criticism throughout my Ph.D. I am very fortunate to have had a committee full of marvelous scientists.

I would like to thank direct supervisors Dr. Michael Schwab and Dr. Kerstin Bellmann. I have learned a lot from you. I thank you for always being approachable. I appreciate your thorough feedbacks that always pushed me to do better. Your vigorous training, suggestions, critical comments, writing inputs and endless help, helped me throughout my wet lab and the writing of my thesis. Because of you I am finally able to submit my thesis. I will be always grateful to you.

I thank our cell culture expert: Bruno Marcotte and animal lab technicians: Christine Dallaire, Joanie Dupont-Morissette, Jacinthe Julien, and Geneviève Guèvremont for their time that they invested in me in training, and experimental troubleshooting whenever required.

A special thanks to my lab colleague Dr. Marie Julie Dubois for ordering reagents in a very efficient way that was crucial for the successful completing of my doctoral work.

A special thanks to Trish (Dr. Patricia Mitchell) for providing her expertise in real time PCR and lipid biology whenever required.

I would like to also thank my colleagues: Dr. Cristina Bosoi, Lais, Arianne, Beatrice, Jean-Philippe, Amélie, and Adia for helping me during the animal protocol and on the bench whenever required.

I would also like to acknowledge all of the help and support from our collaborators: Dr. Mathieu Morissette, Dr. François Maltais and his student Marie Pineault at the IUCPQ for their support and for providing Ala457Thr mice for the experiments.

Special thanks to Dr. Mathieu Laplante and members of his team: Romain, Mathilde, Audrey Manal, and Yves for providing plasmids, reagents, and scientific inputs.

Special thanks to Dr. Vanessa Houde for her in vitro training and help in animal protocol. I thank Besma for her help whenever required.

Special thanks to Dr. Frédérik Desmarais for translating all abstracts to French. I also thank him for his help in wet lab experiments whenever required.

Further, I am especially grateful for Beisy Laborit Labrada. Thank you for being always by my side. You are a great teammate and a friend forever.

I want to acknowledge IUCPQ for awarding me IUCPQ Ph.D. fellowship. Their financial support further helped me to carry out my research and improve my future prospects.

A special thanks to Rashmi Shah and Dr. Girish Shah and members of the Indian gang in Quebec City (Anjana, Angana, Prashad, Naidu and Nisar) for helping me when I needed a family member in Québec city.

Finally, I would like to thank my adorable wife Dr. Charu Kothari, whose constant encouragement, limitless giving, and great understanding and sacrifice, helped me accomplish my graduate studies.

Last but not the least, I would like to thank my daughter Iwa Kothari for her unconditional love. You make Quebec snowy winter a real fun time for me.

Foreword

The Chapter II of the thesis comprises the manuscript under preparation for submission to Molecular Metabolism. I participated in planning the study, have performed all the experiments, analyzed the data, and wrote the draft of the manuscript. The manuscript has been thoroughly reviewed and corrected by Dr. Michael Schwab and Dr. Kerstin Bellmann.

Chapter III of the thesis is under review in the Journal of Biological Chemistry. I am the first of the two co-authors with Dr. Michael Schwab. As a first co-author, I am responsible for planning the study, performing experiments, analyzing data, and writing the manuscript. Dr. Michael Schwab has generated Figure 1 & 3 and has generated the CHIP-Seq data. Beisy Laborit Labrada has isolated primary mouse hepatocytes and performed some of the experiments. Dr. Eric Fournier and Dr. Steve Bilodeau have helped in the analysis CHIP-Seq data. I have written the draft of the manuscript and that have been reviewed and corrected by Dr. Michael Schwab and Dr. Kerstin Bellmann.

For Iwa Kothari, Charu Kothari, Digambari Devi and Udali Devi

Introduction

1. Global obesity pandemic

Obesity is defined as condition of excessive fat accumulation in the body that may impair health (Hruby & Hu, 2015; Panuganti *et al*, 2021). Body mass index (BMI) of 30.0 or higher falls within the obesity range. Although obesity is considered as a predisposing factor for several comorbidities there is a disagreement whether obesity is itself recognized as a chronic disease or a behavioral risk factor, similar to alcohol, smoking and drug abuse that eventually lead to diseases (Hruby & Hu, 2015). Data by the World Health Organization (WHO) showed that the prevalence of obesity has increased approximately threefold worldwide from 1975 to 2016. The global burden of obesity has taken pandemic shape and more than 4 million people die each year due to comorbidities directly or indirectly related to obesity. According to an estimate by WHO, in 2016, more than 1.9 billion adults (aged 18 years and older) were overweight out of which 650 million were obese (Figure 1). According to Canadian Community Health Survey in 2018, 26.8% of Canadians (18 years or old) were classified as obese according to their BMI measurements. Another 36.8% of adults were classified as overweight suggesting that 63.6% of the adult Canadian population are at health risk due to excess weight.

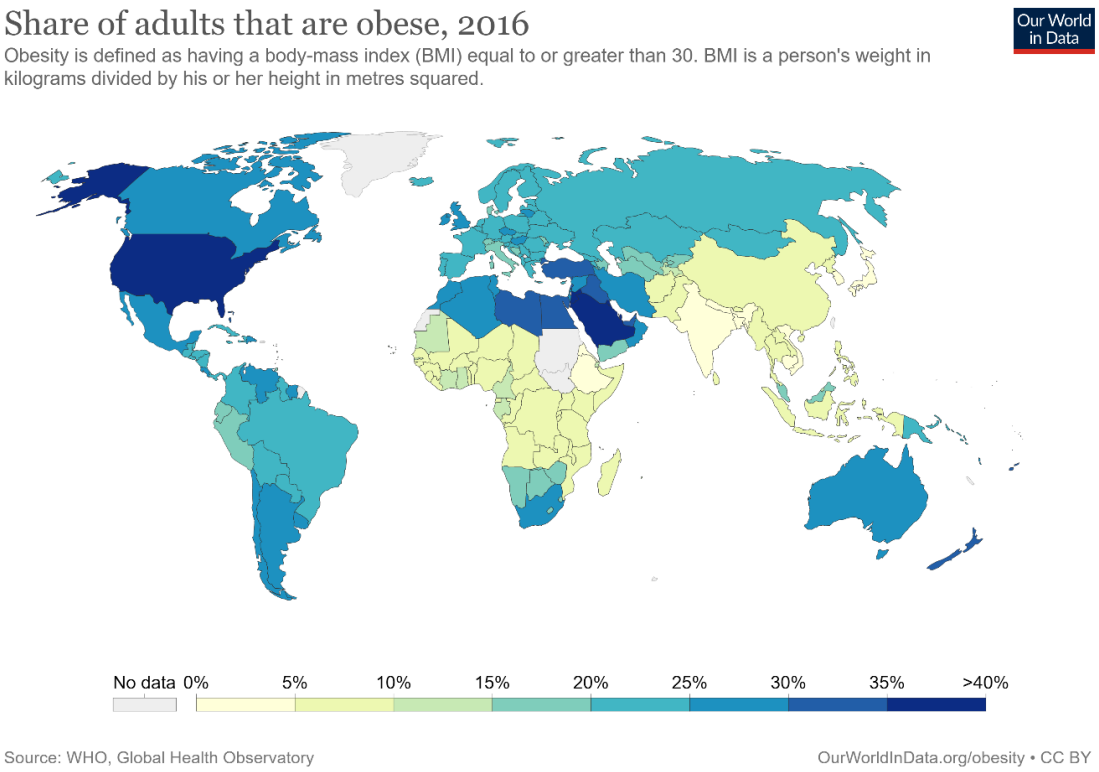

Figure 1. Word obesity map showing the percentage of adult obese individuals across the globe. Source: https://ourworldindata.org/obesity. The license of the figure: CCBY: "CC BY: This license allows reusers to distribute, remix, adapt, and build upon the material in any medium or format, so long as attribution is given to the creator. The license allows for commercial use.

2. Obesity and associated comorbidities

Obesity is one of the predisposing factors for several pathologies including, non-alcoholic fatty liver disease (NAFLD), type 2 diabetes mellitus (T2DM), hypertension, cardiovascular diseases (CVD), kidney disease, dyslipidemia, and even cancer (Han & Lean, 2016; Leitner *et al*, 2017; Engin, 2017; GBD 2015 Obesity Collaborators *et al*, 2017).

According to a WHO report between 2006 and 2016, there was a 5% increase in the premature mortality associated with T2DM. In high-income groups, the premature mortality due to diabetes decreased from the period of 2000 to 2010 then

increased from 2010 to 2016. However, in low-income groups, there was an increase in premature deaths due to diabetes from 2000 to 2016 (WHO, 2016).

Nearly 29% of Canadians live with either diabetes or are pre-diabetic. According to the Public Health Agency of Canada (2011), diabetes can reduce a person's lifespan by 5 to 15 years. People with diabetes are three times more susceptible to be hospitalized due to CVD and 12 times more likely to be hospitalized due to kidney disease (Leon & Maddox, 2015; Anja & Laura, 2017). Other diabetes-associated complications involve lower limb amputation and blindness.

In addition to the non-infectious comorbidities mentioned above, obesity has been linked to higher susceptibility to infectious diseases (Casqueiro *et al*, 2012). Obesity can weaken the immune system by several mechanisms (Andersen *et al*, 2016). For instance, obesity has emerged as one of the important risk factors that determines the severity of coronavirus disease of 2019 (COVID-19) infection. Studies suggest that individuals with a BMI greater than 23 kg/m^2 are associated with an adverse outcome of COVID-19 infection (Gao *et al*, 2021). Association of obesity with the severity of COVID-19 infection, subsequent hospitalization, and even death has been reported (Hamer *et al*, 2020).

2.1 Non-alcoholic fatty liver disease (NAFLD)

Non-alcoholic fatty liver disease (NAFLD) refers to a range of liver diseases affecting people that drink little or no alcohol at all (Pouwels *et al*, 2022). NAFLD is the most common liver disease affecting people worldwide and is the leading cause of liver disease related mortality (Riazi *et al*, 2022). The prerequisite for NAFLD is the accumulation of an abnormal amount of fat in the liver (Abd El-Kader & El-Den Ashmawy, 2015). Hepatic steatosis (HS), non-alcoholic steatohepatitis (NASH), hepatic fibrosis and cirrhosis are different forms of NAFLD that differ in severity and reversibility (Vuppalanchi & Chalasani, 2009). Poor diet choice, increased calorie intake and less physical activity are some of the important factors that can lead to

NAFLD (Salehi-sahlabadi *et al*, 2021). There is a growing trend of NAFLD worldwide, especially in Western countries (Mitra *et al*, 2020). For instance, NAFLD is the most common liver condition affecting nearly 20% of Canadians (Swain *et al*, 2020). Overweight and obese people are more prone to develop NAFLD. Hepatic steatosis, the mildest form of NALFD, is characterized by intrahepatic fat of at least 5% of the liver weight in the absence of liver injury (McCullough, 2006; Serfaty & Lemoine, 2008). Clinically, HS is classified into three grades depending on the percentage of fat within the liver. Grade 0: liver fat less than five percent of liver weight; grade 1: mild (liver fat between 5 and 33%), grade 2: (moderate, liver fat between 34 and 66%) and grade 3: severe (liver fat more than 66% of liver weight) (Qayyum *et al*, 2012; Nassir *et al*, 2015). Although a small accumulation of fat in the liver can even have beneficial effects , a chronic increase and large amounts of fat in the liver have been associated with inflammation, liver metabolic dysfunction, advanced forms of NAFLD and type 2 diabetes (Al Rifai *et al*, 2015; Godoy-Matos *et al*, 2020). HS is often reversible but may progress to NASH. NASH is characterized by hepatocyte injury with ballooning, inflammation, presence of Mallory-Denk bodies and signs of fibrosis (Takahashi & Fukusato, 2014). Liver fibrosis is characterized by excessive accumulation of extracellular matrix (ECM) proteins in the liver such as collagen (Takahashi & Fukusato, 2014). Liver fibrosis may progress to cirrhosis and liver failure that often requires liver transplantation (Bataller & Brenner, 2005). The accumulation of ECM proteins in the liver results in changes of hepatic architecture by forming a fibrous scar followed by the development of nodules for regenerating hepatocytes, a feature of cirrhosis (Bataller & Brenner, 2005; Smith *et al*, 2019).

2.2 Diabetes

Diabetes is a chronic disease that occurs when either pancreas fails to produce the glucose-lowering hormone insulin or when insulin fails to exert its biological effect called insulin resistance (Cantley & Ashcroft, 2015). The pancreas is the key organ involved in regulating glucose homeostasis (Figure 2). Islets of Langerhans cells

make only 1-2% of the pancreas (Da Silva Xavier, 2018). These islets contain alpha and beta cells that secrete glucagon and insulin, respectively (Da Silva Xavier, 2018; Honzawa & Fujimoto, 2021). The beta cells secrete insulin in response to higher glucose levels following food intake (Cerf, 2013; Wilcox, 2005). The insulin action results in the uptake of glucose by metabolically active organs such as skeletal muscle and adipose tissue (Chadt & Al-Hasani, 2020). In skeletal muscle, insulin promotes glucose transport to the cells and supports glycogen synthesis (Samuel & Shulman, 2012). In adipose tissue, insulin promotes triglyceride synthesis and inhibits lipolysis. In liver, insulin inhibits endogenous glucose production called gluconeogenesis, promotes glycogenesis and *de novo* lipid synthesis (Samuel & Shulman, 2012). In patients with diabetes, glycemic control is lost due to absence or inactivity, or both, of insulin (Cantley & Ashcroft, 2015).

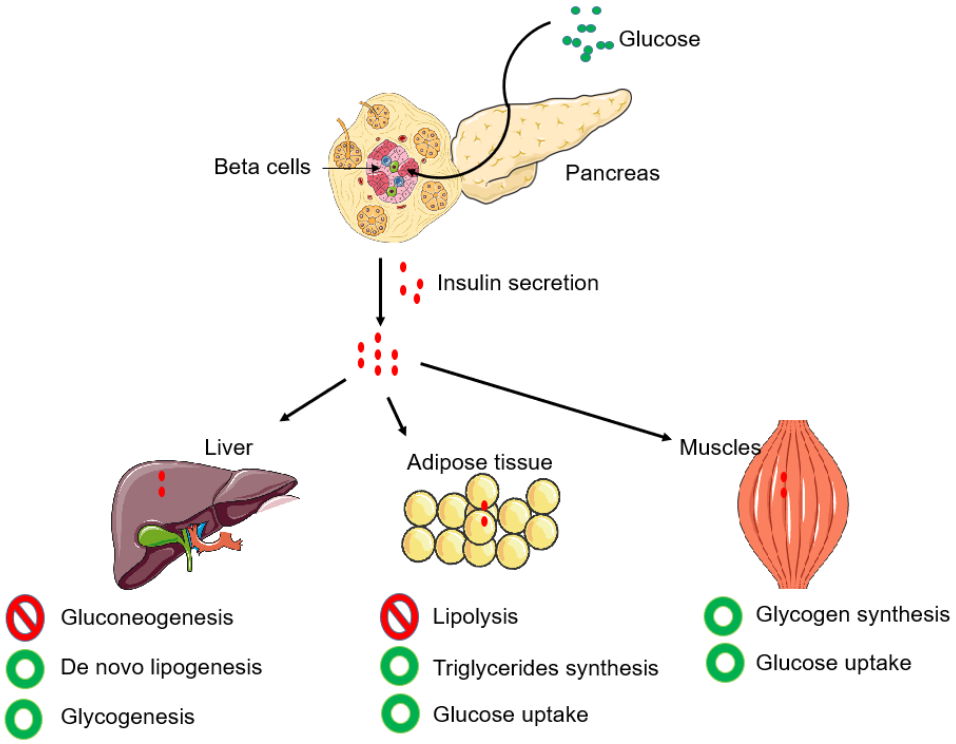

Figure 2. Physiologic insulin action in insulin responsive, metabolically active organs. Figure is generated with the help of graphics from Servier Medical Art (https://smart.servier.com/). License type: CC BY 3.0 (free to use, no permission required).

2.2.1 Type 2 Diabetes (T2D): Diabetes mellitus

Obesity (Hamman *et al*, 2006), low levels of physical activity (Jarvie *et al*, 2019), family history of diabetes (Amador *et al*, 2020), the occurrence of gestational diabetes mellitus (GDM) (Bian *et al*, 2000; Moosazadeh *et al*, 2017), and age are important risk factors for T2D (Wu *et al*, 2014). Individuals above the age of 45 are two to four times more at risk for the development of T2D. Both genetic and environmental factors affect the pathogenesis of T2D (Kirkman *et al*, 2012). Several studies suggest that T2D has a strong genetic disposition. In addition, the prevalence of diabetes varies in different ethnicities sharing the same environmental conditions (Spanakis & Golden, 2013). Furthermore, GDM has been associated with the increased risk of developing T2D for both offspring (Bianco & Josefson, 2019) and mother (Sacks *et al*, 2012) later in life.

T2D is due to the development of insulin resistance in target tissues such as muscle, liver and adipose tissue (Wilcox, 2005). Insulin resistance, in clinical terms, refers to a metabolic condition wherein cells exhibit reduced responsiveness to the effects of insulin, leading to impaired glucose uptake and utilization. To compensate for insulin resistance, beta cells of the pancreas secrete higher amounts of insulin, resulting in their exhaustion and eventually loss (Cerf, 2013). In T2D more than 60% decrease in beta-cell mass has been reported (Butler *et al*, 2003). Insulin resistance is often the earliest sign of the development of T2D. However, T2D is not detected until beta cells cannot secrete sufficient insulin to compensate for insulin resistance (Chen *et al*, 2017a; Mezza *et al*, 2019).

T2D is diagnosed by measuring the fasting blood glucose level and long-term levels of hemoglobin A1c (HbA1C) (ADA, 2009; Weykamp, 2013). HbA1C refers to the glycosylated hemoglobin A1C. Glucose interacts with hemoglobin in red blood cells and glycosylates a fraction of it called HbA1c. HbA1C can be detected in blood for 120 days (Sherwani *et al*, 2016). Therefore, HbA1C levels represent the long-term glucose levels of individuals. In addition, a two-hour oral glucose tolerance test

(oGTT) is the gold standard used in the clinic to detect impaired fasting hyperglycemia and impaired glucose tolerance (Woerle *et al*, 2004).

2.2.2. Other forms of diabetes

Type 1 diabetes (T1D) results from immune-mediated destruction of beta-cells leading to insulin deficiency. T1D can be distinguished from T2D by the presence of lower levels of C-peptides and the presence of autoimmune antibodies (Atkinson *et al*, 2014).

GDM refers to the elevated levels of blood glucose during pregnancy (McIntyre *et al*, 2019). Studies suggest that during pregnancy placenta secretes a variety of hormones necessary for the development of the fetus. Some of these hormones such as cortisol and estrogen may hamper the function of insulin (Ahmed & Shalayel, 1999; Root-Bernstein *et al*, 2014; Feng *et al*, 2020).

Monogenic diabetes is a rare form of diabetes caused by mutations in a single gene. It represents a non-autoimmune mediated form of diabetes. There are more than 20 genes so far associated with monogenic diabetes (Greeley *et al*, 2011; Urakami, 2019). Maturity-onset diabetes of the young (MODY) and neonatal diabetes mellitus (NDM) are two monogenic diabetes.

MODY is a rare, genetically inherited young-onset form of diabetes. So far, 14 genes have been characterized in MODY (Urakami, 2019). These genes include *HNF4α*, *HNF1α*, *HNF-1β*, *GCK*, *PDX/IPF1*, *NEUROD1*, *KLF11*, *BLK*, *INSABCC8*, *PAX4*, and *KCNJ11* (Ellard *et al*, 2008; Greeley *et al*, 2011). Unlike T2D, individuals with MODY exhibit no obesity, partly conserved insulin secretion, no sign of insulin resistance, and no immune-mediated beta cell loss (Firdous *et al*, 2018).

NDM is rarer than MODY. NDM occurs in one out of 100,000 to 500,000 neonates (Hattersley *et al*, 2018). It is diagnosed before the age of 12 months as compared to MODY that is usually diagnosed before adolescence or before age of 25 years (Gaál

& Balogh, 2019). NDM diagnosed before the age of 6 months has been associated with genetic causes (Gaál & Balogh, 2019).

3. Insulin signaling

The year 2021 marks the 100th year of the discovery of the fascinating hormone insulin (Banting *et al*, 1922a, 1922b; Marette, 2021). The insulin receptor (IR) is the key receptor that recognizes insulin and executes its physiological functions. Although ubiquitously expressed, IR is more relevant in the metabolically active tissues. IR is a member of the receptor tyrosine kinase superfamily comprised of two extracellular alpha and two transmembrane beta subunits. Insulin binds to the alpha subunit of IR causing a trans-auto-phosphorylation of the beta subunits. IR subsequently phosphorylates a variety of intracellular substrates/adapter proteins that interact with the cytoplasmic domain of IR (Figure 3). These intracellular substrates include insulin receptor substrates (IRS1-4), IRS/DOK5, IRS5/DOK, Shc, Gab-1, Grb2, Cbl, and APS (Kido *et al*, 2001).

Insulin Receptor Substrate (IRS) proteins are examples of adaptor proteins that bind to the activated IR and serve as docking sites for several other downstream effectors. Insulin signaling broadly affects two pathways: Ras/Raf/MAPK signaling pathway and phophoinositide3-kinase (PI3K)/Protein kinase B (Akt) Pathway (Figure 3).

PI3K-AKT Pathway : Activated IRS binds to the regulatory subunit of PI3K (p85), which activates the catalytic subunit of PI3K (p110) (Luo *et al*, 2005). Activated PI3K promotes the synthesis of secondary messenger molecules, such as phosphatidylinositol (4,5)-bisphosphate (PIP2) and phosphatidylinositol (3,4,5)-trisphosphate (PIP3), which ultimately activates AKT via 3-phosphoinositide-dependent protein kinase 1 (PDK1) (Toker & Cantley, 1997). Activated AKT signaling promotes several changes in the cell (Figure 3).

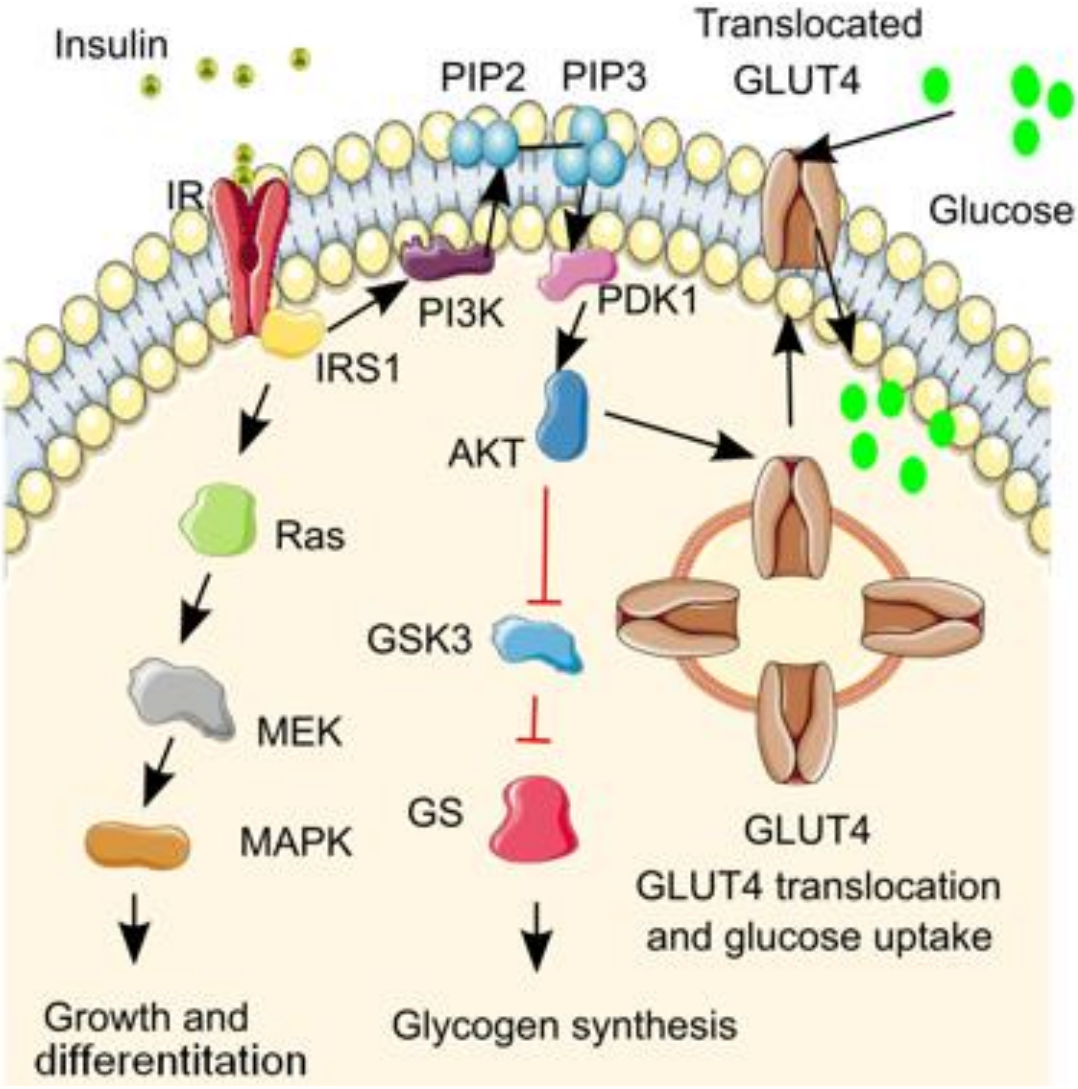

Figure 3. Simplified insulin signaling pathway. This figure is generated with the help of graphics from Servier Medical Art (https://smart.servier.com/) and Inkspace software Inkspace Project. (2020).

In adipose tissue and muscle, insulin facilitates the recruitment of glucose transporter 4 (GLUT4) to the plasma membrane (Martin *et al*, 2000; Saltiel & Kahn, 2001; Slot *et al*, 1991). GLUT4 is the glucose transporter that permits the uptake of extracellular glucose into the cell (Bogan & Kandror, 2010). In the absence of insulin, GLUT4 resides in the vesicular bodies within the cell and is slowly recycled (Figure 3). Mice with muscle- or adipose-specific knockout (KO) of GLUT4 show glucose intolerance and insulin resistance phenotypes (Abel *et al*, 2001; Zisman *et al*, 2000). One of the substrates of activated AKT in muscle and adipose tissue is TBC1

Domain Family Member 4 (TBC1D4) (Cartee, 2015). TBC1D4 is a Rab-GTPase-activating protein that helps in the intracellular retention of GLUT4 within the intracellular vesicular membrane. TBC1D4 has several AKT phosphorylation-motifs (Stöckli *et al*, 2008; Tan *et al*, 2012). AKT-mediated phosphorylation of TBC1D4 promotes its dissociation from GLUT4 (Stöckli *et al*, 2008) resulting in the localization of GLUT4 to the plasma membrane (Stöckli *et al*, 2008; Klip *et al*, 2019). Katome and coworkers demonstrated using AKT isoform-specific siRNA that insulin-mediated GLUT4 translocation is largely regulated by AKT2 and to a lesser extent by AKT1 (Katome *et al*, 2003). A recent study shows that AKT can negatively regulate insulin signaling by phosphorylating IRS2 at S306 and S577 in humans. As a result of this inhibitory phosphorylation, AKT controls the PIP3 abundance (Kearney *et al*, 2021). The activated AKT also promotes glycogen synthesis by inhibiting glycogen synthase kinase 3 (GSK3) via phosphorylation (Beurel *et al*, 2015).

Ras/Raf/MAPK pathway: Insulin is a pleiotropic hormone. In addition to its clear effect on glucose and lipid metabolism, insulin also exerts proliferative effects mediated by IRS-1 (Araki *et al*, 1994; Tamemoto *et al*, 1994; Miele *et al*, 1999). IRS-1 deficient mice show a reduction in intrauterine growth in addition to impaired glucose tolerance and reduced glucose uptake (Tamemoto *et al*, 1994, 1994). IRS-1 possesses multiple tyrosine residues that can be phosphorylated (Mothe & Van Obberghen, 1996). As a result, IRS-1 attracts several substrates that have SH2 domains. For instance, IRS-1 phosphorylates growth factor receptor-bound protein 2 (GRB2) (Skolnik *et al*, 1993a), which interacts with guanine nucleotide exchange factor SOS (son of Sevenless) further activating Ras (Skolnik *et al*, 1993b). Ras through Raf triggers MAPK/ERK kinase (MEK)1/2 dual-specificity kinases into functional state (Garrington & Johnson, 1999) which then further phosphorylates MAPK (ERK1 and ERK2) (Lenormand *et al*, 1993) resulting in nuclear translocation of ERK where it phosphorylates multiple transcription factors (TFs) that regulate several genes involved in cell growth, differentiation, and cell survival (Lenormand *et al*, 1993; Buscà *et al*, 2016, 1).

3.1 Insulin action in liver: insight into glucose metabolism

In addition to muscle and adipose tissue, insulin regulates glucose and lipid metabolism in the liver (Nakae *et al*, 1999; Kido *et al*, 2001). In hepatocytes, insulin activates AKT that in turn phosphorylates Forkhead Box Protein O1 (FOXO1) (Nakae *et al*, 1999). FOXO1 is a transcription factor that regulates several genes involved in gluconeogenic and glycolytic pathways and lipogenesis (Zhang *et al*, 2006, 2018). In the liver, FOXO1 interacts with Peroxisome Proliferator-Activated Receptor Gamma Coactivator 1 to activate the expression of its target genes (Puigserver *et al*, 2003).

AKT controls hepatic glucose production via phosphorylation of FOXO1 at serine 256 in humans that results in the nuclear exclusion of this protein (Figure 4) and thereby in the suppression of its target genes including rate-limiting enzymes such as Phosphoenolpyruvate Carboxykinase 1 (PCK1) and Glucose-6-Phosphatase (G6PC) (Guo *et al*, 1999; O'Brien *et al*, 1990). FOXO1 has been shown to regulate glucose production in isolated hepatocytes and (Figure 4) ablation of FOXO1 improves glucose tolerance in mice. Interestingly, in the absence of both FOXO1 and AKT, mice are still able to suppress hepatic glucose production in response to insulin suggesting the presence of other insulin-independent pathways (Lu *et al*, 2012). Titchenell and colleagues (2015) further dissected this observation and demonstrated that mice with liver-specific ablation of insulin receptor and *Foxo1* gene were still able to control hepatic glucose production and genes involved in gluconeogenesis suggesting the presence of extrahepatic tissues where insulin may act to produce secondary signals that are eventually recognized by the liver (Titchenell *et al*, 2015). These studies suggest the presence of some other cell-non-autonomous regulation of gluconeogenesis (Matsumoto *et al*, 2007; O-Sullivan *et al*, 2015; Titchenell *et al*, 2015).

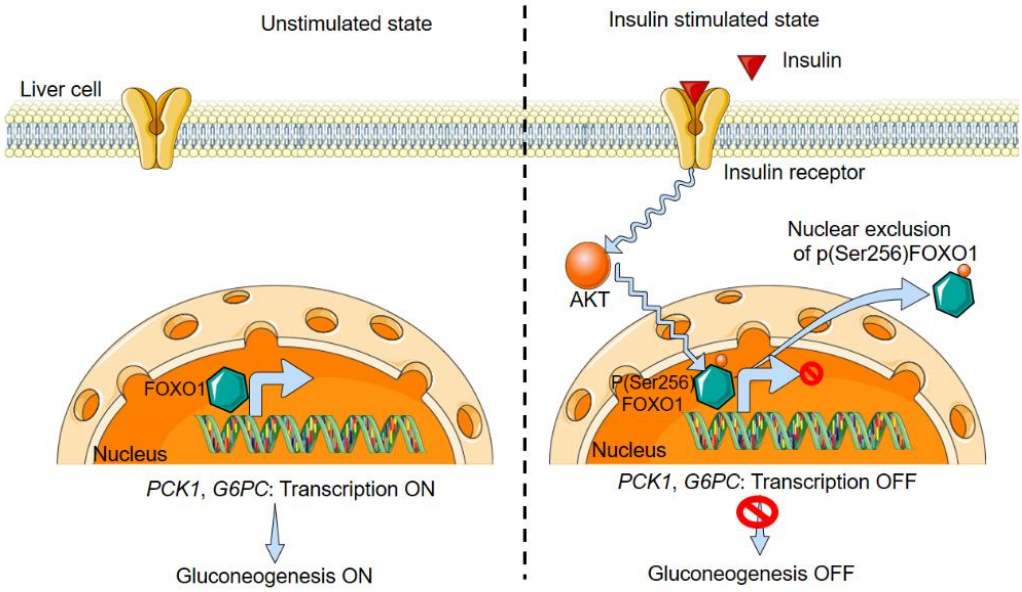

Figure 4. Insulin mediated control of FOXO1 to control gluconeogenesis in liver cells. This figure is generated with the help of graphics from Servier Medical Art (https://smart.servier.com/).

3.2 Insulin action in liver: insight into Lipid metabolism

When energy intake exceeds the energy demand of the body, the body converts the excess glucose generated from food into fatty acid (FA) molecules. This process is called de novo lipogenesis (DNL) (Kersten, 2001). FA are further stored in the form of triglycerides (TG) in the liver and adipose tissue that may act as a source of energy when needed (Song *et al*, 2018). Insulin plays an important role in the activation of DNL. Insulin-mediated activation of PI3K-AKT axis activates sterol regulatory element-binding protein-1 (SREBP-1) (Figure 5). SREBP-1 is a transcription factor that regulates the expression of key genes involved in fatty acid, TG and cholesterol biosynthesis in the liver and adipose tissue (Horton *et al*, 2002). SREBP-1 gene codes for two different forms, SREBP-1a and SREPB-1c. SREBP1a participates in cholesterol homeostasis and FA synthesis whereas SREBP-1c activates genes involved in FA synthesis only (Amemiya-Kudo *et al*, 2002). The activated insulin-PI3K-AKT-mTOR axis is important for the nuclear localization of SREBP-1 where it regulates the transcription of genes involved in lipid metabolism (Porstmann *et al*,

2008; Sanders & Griffin, 2016) (Figure 5). Some of the key SREBP-1 regulated genes that are involved in lipid metabolism include ATP citrate-lyase (ACLY) (Sato *et al*, 2000), acetyl-CoA carboxylase (ACACA) (Horton *et al*, 2002), fatty acid synthase (FASN), and stearoyl-CoA Desaturase 1 (SCD1) (Horton *et al*, 2002). ACLY is the first enzyme that starts the DNL process. ACLY converts citrate into acetyl CoA. Further acetyl CoA is converted into fatty acid by the sequential activity of ACACA, FASN and SCD1 (Horton *et al*, 2002). Mammalian target of rapamycin (mTOR) is a multimeric serine-threonine kinase complex that can sense several biological signals and regulates processes involved in growth and development (Bakan & Laplante, 2012; Laplante & Sabatini, 2009). mTOR forms two kinds of distinct complexes mTORC1 and mTORC2. AKT activates mTORC1 by inhibiting PRAS40 and TSC1/2, the inhibitors of mTORC1 (Bakan & Laplante, 2012). Inhibition of mTOR by rapamycin blocks the AKT mediated nuclear accumulation of SREBP-1 suggesting that mTOR could be a connecting link between AKT and SREBP-1 (Porstmann *et al*, 2008). Several studies show that mTORC1 plays an important role in the induction of the lipogenic program in liver, but mTORC1 alone is not sufficient to induce DNL (Li *et al*, 2010; Porstmann *et al*, 2008; Yecies *et al*, 2011).

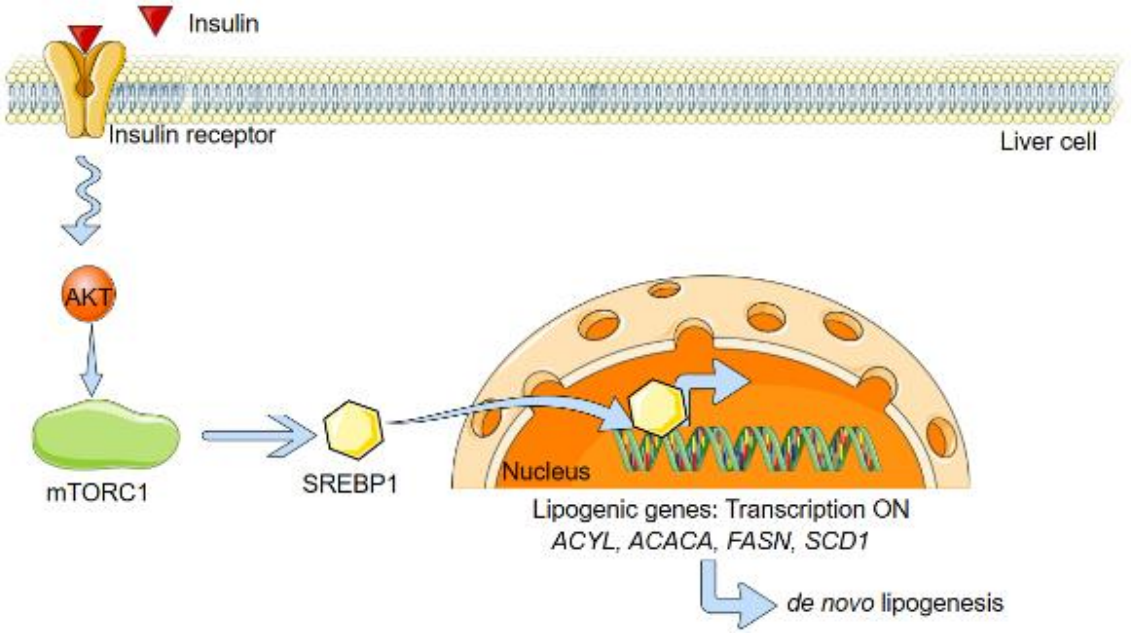

Figure 5. Insulin mediated control of de novo lipogenesis in liver cells.

The role of FOXO1 in regulating DNL is debatable as different studies yield different outcomes. Wan et al., 2011 discovered that insulin signaling through Akt2 can drive lipogenesis independently of FOXO1 or FOXO2 (Wan *et al*, 2011). On the other hand, Titchenell et al., 2016 demonstrated that insulin-dependent AKT-mediated FOXO1 inhibition and mTORC1 activation are sufficient to induce DNL in the liver (Titchenell *et al*, 2016). Alternatively, liver specific deletion of FOXOs (L-Fox1,3,4) has been shown to result in inhibition of glucose-6-phosphatase and repression of glucokinase during fasting. This results in an increase in lipogenesis at the expense of glucose production (Haeusler *et al*, 2014). The debate is still open and more studies are required to elaborate the role of FOXO1 in regulating lipogenesis.

3.3 Insulin Resistance

In addition to its role in fat storage, white adipose tissue (WAT) acts as an endocrine organ (Coelho *et al*, 2013). WAT secretes adipokines and free fatty acids that target distant tissues and affect insulin sensitivity (Zhang and Zhang, 2010). In obesity and metabolic disease, with adipose tissue expansion, there is also immune cell infiltration and secretion of inflammatory cytokines by the infiltrating immune cells and adipocytes (Nteeba *et al*, 2013; Lu *et al*, 2019) (Figure 6). Interleukin-6 (IL-6), interleukin-1 beta (IL-1β), and TNF-alpha (TNF-α) are well-known examples of pro-inflammatory cytokines released by adipocytes and immune cells in response to obesity resulting in low-grade chronic inflammation (Stenlöf *et al*, 2003; Stępień *et al*, 2014; Ellulu *et al*, 2017) (Figure 6). In addition, these pro-inflammatory cytokines activate nuclear factor kappa-light-chain-enhancer of activated B cells (NF-κB) and c-Jun terminal kinase pathways that ultimately result in insulin resistance (Yung & Giacca, 2020; Choubey *et al*, 2020; Daniel *et al*, 2021). Briefly, under basal conditions, NF-κB is sequestered in the cytoplasm by a family of inhibitory proteins such as IκBα (Baeuerle & Baltimore, 1988). In response to stimuli that includes growth factors, cytokines, mitogens, microbial components and stress inducing agents, IκBα is degraded after site-specific phosphorylation through the IκB kinase (IKK) complex that results in rapid nuclear translocation of NF-κB members and associated gene expression.

Activated IKK also phosphorylates IRS-1 at ser 312 in humans and serine 307 in mice (Gao *et al*, 2002). Similar to IKK, c-Jun amino-terminal kinase (JNK) a member of the MAPK family can also phosphorylate IRS at serine residues (Aguirre *et al*, 2000). In addition to Serine 307, serine 302 can be phosphorylated by JNK in vitro and in vivo (Werner *et al*, 2004). Levels of pSer302 and pSer307 are increased in diet induced obesity and insulin resistance animal models (Werner *et al*, 2004). These phosphorylations abrogate IR-IRS1 binding and thus hamper insulin signaling (Werner *et al*, 2004; Boucher *et al*, 2014). Like NF-κB, JNK also promotes the

expression of pro-inflammatory cytokines by the activation of activator protein-1 (AP-1) (Boucher *et al*, 2014).

The cytokines induced by NF-κB and JNK create a loop, in which NF-κB and JNK induced cytokines that again activate NF-κB and JNK themselves that ultimately results in insulin resistance (Cargnello & Roux, 2011) (Figure 6). NF-κB and AP-1 dependent pro-inflammatory pathways can also be activated by IL1-β (Cargnello & Roux, 2011). Several studies reported elevated levels of TNF-α , IL-6 and IL-1β in obese and diabetic individuals further linking the inflammatory state to the insulin resistant state (Mirza *et al*, 2012; Sindhu *et al*, 2015; Caër *et al*, 2017). Obese mice with a targeted disruption of the *TNFa* gene exhibit improved insulin sensitivity compared to control mice (Ventre *et al*, 1997).

IL-6 promotes the nuclear localization of Signal Transducer and Activator of Transcription Proteins (STATs) mediated by activation of Janus Kinase (JAK) (Li, 2008) (Figure 6). JAK/STAT pathways induce the suppressor of cytokine signaling (SOCS) proteins. SOCS have been shown to promote insulin resistance by preventing the action of IRS protein through inhibition of IRS-1 tyrosine phosphorylation (Ueki *et al*, 2004). Furthermore, mice injected with IL-6 display signs of hepatic insulin resistance revealed by elevated levels of insulin and glucose levels (Klover *et al*, 2003). Taken together the crosstalk between pro-inflammatory cytokines and insulin signaling players contributes to obesity-induced insulin resistance state.

4. Physiological processes in Liver

The liver is a heterogeneous organ composed of several cell types including hepatocytes, cholangiocytes, kupffer cells, stellate cells, and liver sinusoidal

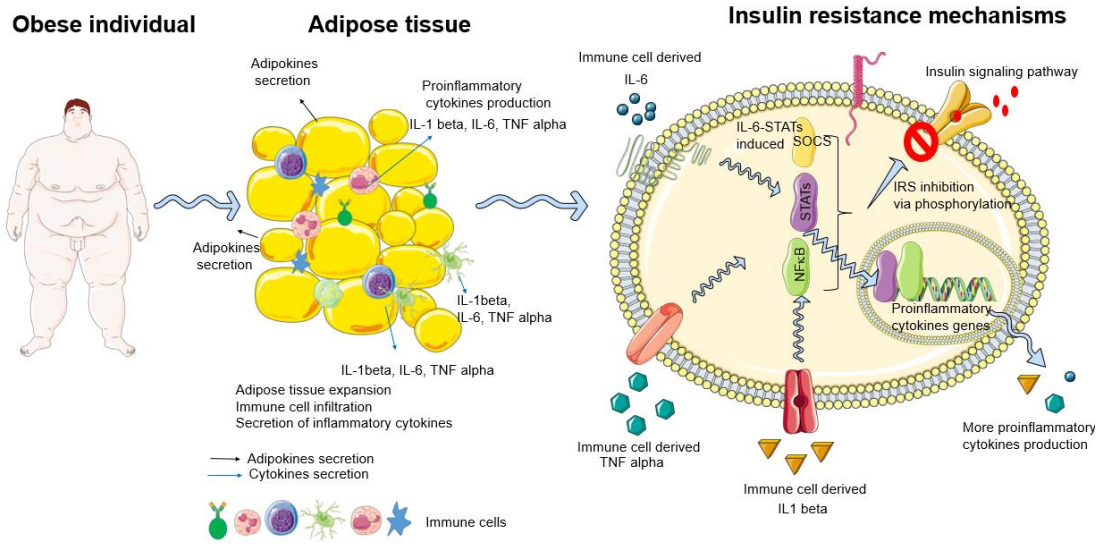

Figure 6. Schematic diagram depicting the relationship between obesity, inflammation and development of insulin resistance. This figure is generated with the help of graphics from Servier Medical Art (https://smart.servier.com/).

endothelial cells (Trefts *et al*, 2017). Hepatocytes, the major cell type in the liver, perform several metabolic functions described below. The liver is a hub of several important physiological processes including glucose and lipid metabolism. The liver plays an important role in energy homeostasis by participating in the metabolism of macronutrients (van den Berghe, 1991). Depending upon the nutritional status of the body, liver can provide glucose or convert it into complex molecules that play an important role in keeping blood glucose in the physiological range. During the physiological fasting stage, also called short term fasting, the liver provides glucose to the systemic circulation by a biochemical pathway called glycogenolysis in which glycogen is catabolized into glucose-1-phosphate and glycogen (n-1) (Paredes-Flores & Mohiuddin, 2021). During prolonged fasting (refers to starvation) liver synthesizes glucose using non-carbohydrate sources such as pyruvate, lactate, amino acids, and glycerol (Owen *et al*, 1969). This process is known as gluconeogenesis (Owen et al, 1969; Chung et al, 2015; Zhang et al, 2018; Melkonian

et al, 2021). Muscle, adipose tissue and the gut act as important sources for providing these non-carbohydrate precursors for glucose synthesis (Rui, 2014). During the feeding stage, the liver stores excess glucose in the form of glycogen and lipid which are produced by glycogenesis and lipogenesis, respectively (Adeva-Andany et al, 2016). The glucose-maintaining processes in the liver are tightly regulated by the endocrine system and are regulated by the ratio of insulin and glucagon hormone (Muller et al, 1971; Edgerton et al, 2009; Perry et al, 2020).

4.1 Regulation of Hepatic Glucose production–Gluconeogenesis

The gluconeogenesis pathway is activated by glucagon upon severe dietary restriction (Jiang & Zhang, 2003). Glucagon was discovered in 1922 by Kimball and Murlin by injecting a pancreatic fraction in dogs and rabbits that resulted in increased blood glucose. With this observation, they concluded that the pancreas produces a factor that has the potential to neutralize the effect of insulin and named the substance “glucose agonist” or glucagon (Kimball and Murlin, 1923). Glucagon secreated by the alpha cells of pancreas exerts its effect on several tissues as its receptor called glucagon receptor (GCGR) is found in several tissue types including cells of Langerhans, liver, heart, and muscle (Hansen *et al*, 1995). Binding of glucagon to its receptor followed by glucagon receptor conformational changes activates G protein. There are several types of G proteins. G protein subunit alpha Q (Gαq) and stimulatory G-protein (Gαs) proteins are the key players that participate in glucagon signaling. Activated Gαq protein triggers phospholipase C-inositol triphosphate channel that results in the release of calcium from the endoplasmic reticulum. On the other hand, activated Gαs activates adenylate cyclase that results in an increase in intracellular cAMP levels that consequently activates protein kinase A (PKA). PKA in turn results in phosphorylation of several transcription factors involved in glucose homeostasis. This pathway is known as the PKA pathway. GCGR is abundantly expressed in the liver. During hypoglycemia, the action of glucagon in the liver enhances gluconeogenesis and glycogenolysis. The PKA pathway in the liver activates CREB1, CAMP Responsive Element Binding Protein

(CREB) that transactivates genes involved in gluconeogenesis and glycogenolysis. The activation of CREB is influenced by co-activator CREB Regulated Transcription Coactivator 2 (CRTC2). During high energy state, high levels of ATP trigger phosphorylation of CRTC2 at several sites by AMP-activated protein kinase (AMPK) or salt-inducible kinase that results in the sequestration of CRTC2 in the cytoplasm. During low energy state, CRTC2 undergoes dephosphorylation resulting in its nuclear translocation and activation of CREB to its full potential that ultimately leading to the activation of genes involved in gluconeogenesis and glycogenolysis (Wang *et al*, 2009). For instance, PKA-CREB-CRCT2 pathway activated by glucagon increases the expression of one of the key enzymes involved in gluconeogenesis called phosphoenolpyruvate carboxykinase (PEPCK or PCK1) described later in the thesis. Glucagon boosts hepatic gluconeogenesis through diverse mechanisms, including the augmentation of hepatic adipose triglyceride lipase activity, intrahepatic lipolysis, hepatic acetyl-CoA levels, and pyruvate carboxylase flux. Moreover, glucagon stimulates mitochondrial fat oxidation by activating the inositol triphosphate receptor-1 (InsP3R-I) (Perry *et al*, 2020). Further, studies show that this pathway can be activated during exercise and cellular stress conditions (Emhoff *et al*, 2013; Nirupama *et al*, 2012).

In addition, glucagon activates the PKA pathway and exerts an impact on glucose homeostasis by targeting liver glycogen. Activated PKA can phosphorylate glycogen phosphorylase kinase, which further activates glycogen phosphorylase. The latter enzyme triggers the breakdown of glycogen into glucose-6-phosphate (G6P). G6P can further act as a substrate for glucose-6-phosphatase to produce glucose. This process is called glycogenolysis (Jiang & Zhang, 2003). This process occurs mainly in the liver and muscle tissue with the primary purpose of rapidly releasing glucose, formed by the catalysis of glycogen, when energy demands increase, such as during exercise or in response to low blood glucose levels (hypoglycemia).

Liver and to a lesser extent the kidney and intestine are the sites where gluconeogenesis occurs in humans (Melkonian *et al*, 2021). This pathway involves

at least 11 enzymes, out of which eight enzymes catalyze bidirectional reactions (Adeva-Andany *et al*, 2016) (Figure 7). The three enzymes phosphoenolpyruvate carboxykinase (PEPCK or PCK1), fructose-1-6-bisphosphatase (FBPase), and glucose-6-phosphatase (G6Pase) catalyze the reaction in a unidirectional manner and are specific to gluconeogenesis (Figure 7) (Burchell & Hume, 1995; Hanson & Reshef, 1997; Zhang *et al*, 2018; Timson, 2019).

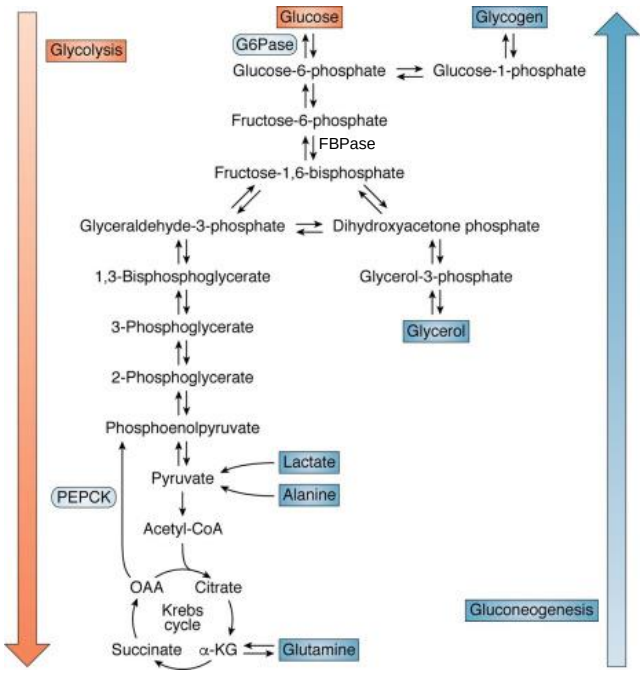

Figure 7. Schematic diagram showing steps involved in gluconeogenesis and glycolysis. The figure is reproduced from Shah et al., 2020 with minor modification. The positon of FBPase is added in the figure. User license: Creative Commons Attribution (CC BY 4.0).

4.1.1 Phosphoenolpyruvate carboxykinase 1 (PCK1/PEPCK)

Phosphoenolpyruvate carboxykinase 1 (PCK1) is recognized as one of the key enzymes that regulates the rate-limiting step of gluconeogenesis. PCK is highly conserved among species. PCK has two isoforms; PCK1 and PCK2. PCK1 is also known as PEPCK1 or PEPCK-C whereas PCK2 is also called PEPCK2 or PEPCK-M. Although *PCK1* and *PCK2* have quite similar gene structures as both contain 10 exons/9 introns in mice, rats, and humans, they exhibit differential activity among different species (Yu et al., 2021). PCK1 is the cytoplasmic isoform whereas PCK2 is restricted to mitochondria. PCK1 is the major isoform in the murine liver whereas PCK2 is the main isoform in birds. In humans, PCK1 and PCK2 are present in equal amounts in the liver (Yang et al., 2009). PCK catalyzes the key step of hepatic gluconeogenesis i.e. oxaloacetate (OAA) to phosphoenolpyruvic acid (PEP) (Yoon et al, 2001; Yu et al, 2021) (Figure 7). PCK1 and PCK2 convert OAA into PEP in cytosol and mitochondria, respectively. In Chapter III of the thesis, our investigation revealed that PCK1 is a pivotal gene subjected to modulation by SHP-1., therefore we will focus on PCK1 afterwards.

Liver specific knock down of PCK1 results in improved glycemic control and insulin sensitivity (Gómez-Valadés *et al*, 2008). Higher levels of *PCK1* transcripts have been reported in patients with diabetes (Giralt *et al*, 2018). Expression of PCK1 is controlled by hormones (glucagon, glucocorticoids, insulin) and by diet (Yoon *et al*, 2001; Puigserver *et al*, 2003; Koo *et al*, 2005). The transcriptional regulation of *PCK1* is controlled by several transcription factors and cofactors (coactivators and corepressors) (Figure 8).

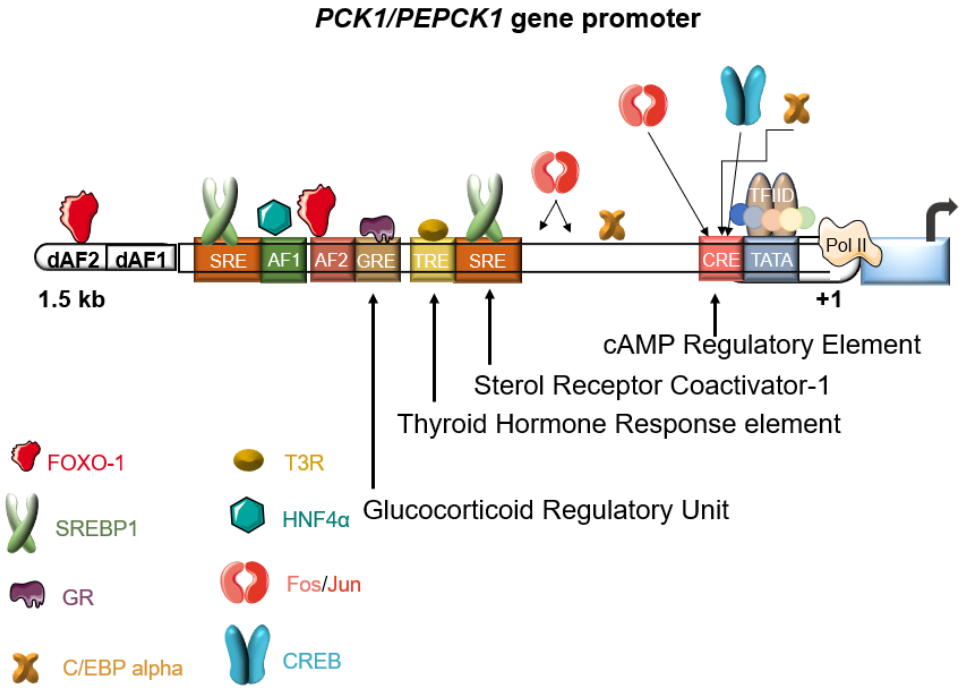

Figure 8. Schematic of PCK1/PEPCK1 gene promoter showing several genetic elements and binding sites for transcription factors and cofactors.

The abbreviations for the elements are: dAF2 - distal Accessory Factor 2, dAF1 - distal Accessory Factor 1, AF1 - Accessory Factor 1; AF2 - Accessory Factor 2, TRE - thyroid hormone response element, GRU - glucocorticoid regulatory unit, SRE - Sterol receptor response element, CRE - cAMP regulatory element.
The transacting factors are FOXO-1 - Forkhead Box O1, SREBP1 - Sterol regulatory element-binding protein 1, GR - Glucocorticoid receptor, C/EBP alpha - CCAAT enhancer binding protein alpha, T3R - thyroid hormone receptor, HNF4α - HNF4A hepatocyte nuclear factor 4 alpha, CREB - CAMP Responsive Element Binding Protein 1.
This figure is generated with the help of graphics from Servier Medical Art (https://smart.servier.com/).

Chromatin immunoprecipitation experiments revealed the presence of several transcription factor binding sites on the *PCK1* promoter including FOXO1 binding site, HFN4 alpha binding site, c-Jun/c-Fos-binding element, CREB, thyroid hormone response element, SREBP-1/Insulin responsive element, glucocorticoid response region and retinoic acid-responsive element (Chakravarty *et al*, 2005; Koo *et al*, 2005; O-Sullivan *et al*, 2015) (Figure 8). The binding of these transcription factors to the *PCK1* promoter has been shown to be influenced by endocrine hormones such as glucocorticoids, insulin, and glucagon (Yoon *et al*, 2001; Puigserver *et al*, 2003; Perry *et al*, 2020). Insulin inhibits FOXO1 and PGC-1 alpha mediated control of *PCK1* transcription as described in previous sections. Glucagon promotes *PCK1* transcription by activating a cAMP/protein kinase A pathway (Herzig *et al*, 2001). Glucocorticoids similar to glucagon exert a positive effect on *PCK1* transcription (Imai *et al*, 1993). Glucocorticoid-activated receptor dimer bind to the GR responsive element on the *PCK1* promoter (Cassuto et al., 2005). Accessory factors (AF1 and AF2) and COUP-TF and HNF-4 are required for the full activation of *PCK1* transcription mediated via glucocorticoids (Hall *et al*, 1995) (Figure 8).

4.1.2 The non-metabolic function of PCK1

The role of PCK1 in mice is more than just controlling gluconeogenesis. For instance, mice that lack PCK1 exhibit severe hypoglycemia right after birth and die. Importantly, glucose supplementation although increasing the systemic blood glucose however does not improve the survival chances indicating another important role of PCK1 in development (Hakimi *et al*, 2005).

In the last few years, upregulation or increased phosphorylation of PCK (PCK1/PCK2) has been reported in several kinds of malignancies including breast cancer, liver cancer, lung cancer and colon cancer (Chen *et al*, 2007; Leithner *et al*, 2015; Li *et al*, 2015; Grasmann *et al*, 2019). A recent research suggests that PCK1 can act as a novel regulator of certain types of cancer. Based on the type of cancer, PCK1 can act as a positive or negative regulator of cancer. For instance, Xu et al.,

2020 showed that PCK1 can promote hepatocellular carcinoma (HCC) growth by activating lipogenesis (Xu *et al*, 2020). In HCC, activated AKT phosphorylates PCK1 at ser90 resulting in the nuclear translocation of this cytosolic form of PCK1. In the nucleus, PCK1 uses GTP as a phosphate donor to phosphorylate insulin-induced genes (INSIGs), INSIG1 and INSIG2, at ser207 and ser151, respectively. These phosphorylation events trigger a cascade that ultimately results in the transcription of downstream genes involved in lipogenesis (Xu *et al*, 2020). However, there are contrasting findings that suggest PCK1 can also act as a negative regulator of HCC (Tuo *et al*, 2019).

5. Transcriptional regulation

Altered gene expression can result in a range of human pathologies. Several different kinds of pathologies and syndromes such as CVD, cancer, autoimmune disorders, obesity and diabetes can result from mutations in regulatory elements, cofactors, transcription factors and non-coding RNAs. (Lee & Young, 2013). Each cell of the human and mouse genome has approximately 20000 and 22000 genes (Bult *et al*, 2016; Salzberg, 2018). However, different cell types express different sets of genes called differential gene expression. Gene expression refers to the process in which DNA is transcribed into mRNA, which is ultimately translated into protein. This definition is applicable to protein coding genes. In addition, cells express a range of non-coding RNAs that directly exert their function upon transcription and as their name suggests do not translate into protein. Gene transcription is often regulated by exogenous and endogenous signals that trigger signaling pathways ultimately resulting in stimulus-specific gene expression (Gibcus & Dekker, 2012). To understand how different cell types acquire different functions it is important to understand the transcriptional process and the factors that make it specific in a particular cellular context. Transcription is a highly complex process that involves coordinated recruitment of co-activators and RNA polymerase to the specific DNA elements that include enhancers and promoters (Figure 9).

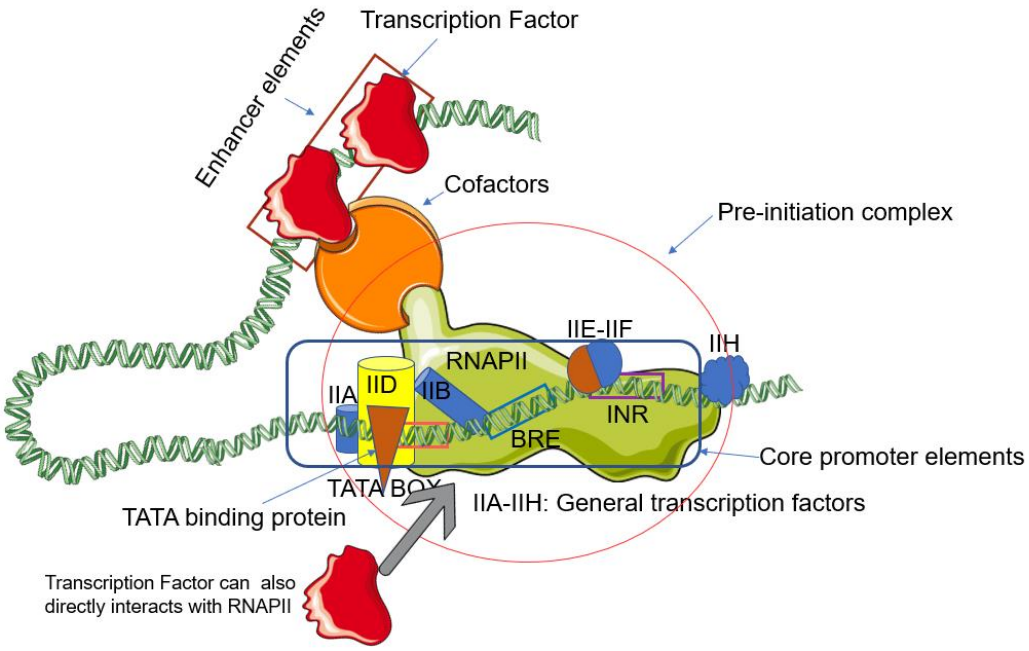

Figure 9. Schematic diagram depicting various genetic elements, proteins (RNAPII, GTFs, TFs and cofactors) involved in the transcription of a hypothetical eukaryotic gene by RNAPII. The abbreviations are RNAPII-RNA polymerase II, GTFs-general transcription factors (IIA,IIB, IID, IIE, IIF,IIH), TFs- transcription factors, INR-Initiator; BRE-B recognition element.

This figure is generated with the help of graphics from Servier Medical Art (https://smart.servier.com/).

5.1 Structure of eukaryotic promoter

The definition of the core prompter sequence is not very precise. Earlier, 50-100bp of DNA elements where RNA polymerase and associated factors assemble resulting in the initiation of transcription was referred to as core promoter. In depth analysis of core promoters suggests that core promoters have a series of conserved DNA elements in various combinations. It is not necessary for core promoters of all genes to have all these conserved elements.

These sequence elements include TATA box, TFIIB-recognition element, Initiator element (Inr), and downstream promoter element (Smale & Kadonaga, 2003; Haberle & Stark, 2018) (Figure 9). The rate-limiting step in transcription is the recruitment of RNA polymerase, also called DNA-directed RNA polymerase (RNAP), to the core promoter. In eukaryotes, there are three types of RNAPs namely RNAPI, RNAPII and RNAPIII (Roeder & Rutter, 1969). RNAPII transcribes mainly protein-coding genes and several non-coding RNAs such as microRNAs whereas RNAPI and RNAPIII transcribe genes coding for ribosomal RNA and transfer RNA, respectively (Roeder & Rutter, 1969).

5.2. Structure of RNA polymerase II

RNAPII is an evolutionarily conserved protein complex that shows a high level of similarity across species. Humans and Yeast RNAPII have 80% similarity at the protein level (Cramer, 2001; Wild & Cramer, 2012; Osman & Cramer, 2020). RNA polymerase II is a large 500kDa heterocomplex comprising 12 polypeptides (Rpb1-12) (Cramer, 2001; Osman & Cramer, 2020) (Figure 10), out of which Rpb1 is the largest subunit (Cramer, 2001; Hsin & Manley, 2012) (Figure 10). Rpb1, also called POLR2A, possesses the enzymatic activity and a regulatory C-terminal domain (CTD). CTD contains several tandem heptad repeats (“consensus Tyr1–Ser2–Pro3–Thr4–Ser5–Pro6–Ser7”) that vary from 26 to 56 in number depending on the species (Hsin & Manley, 2012; Eick & Geyer, 2013). For instance, budding yeast has 26

repeats whereas vertebrates have 52 repeats (Corden, 1990). The CTD plays an important role in all stages of transcription (initiation, elongation, and termination) (Eick & Geyer, 2013; Haberle & Stark, 2018). CTD has several regulatory sites that undergo post-translational modifications (PTMs) (Hsin & Manley, 2012). The most widely studied PTMs in CTD include phosphorylation, methylation, glycosylation and ubiquitination (Li *et al*, 2007; Sims *et al*, 2011; Hsin & Manley, 2012).

In addition to RPB1, RNAPII subunits RPB3 (POLR2C) and RPB11 (POLR2J) need a mention here as we discovered these subunits as the interacting partners of SHP-1 which will be described in detail in later parts of the thesis. RPB3, the third largest subunit of RNAPII is an essential component for the mRNA transcription complex in eukaryotes (Kolodziej & Young, 1989). RBP3 exists as a heterodimer with RPB11. RPB2-RPB3-RPB11 complex has been proposed to represent a core subassembly of RNAPII. Both free RPB1 as well as RPB2-RPB3-RPB11 complex exhibit DNA binding affinity, but far less compared to intact RNAPII suggesting that coordinated assembly of all peptides of RNAPII is essential for the full potential of this enzyme.

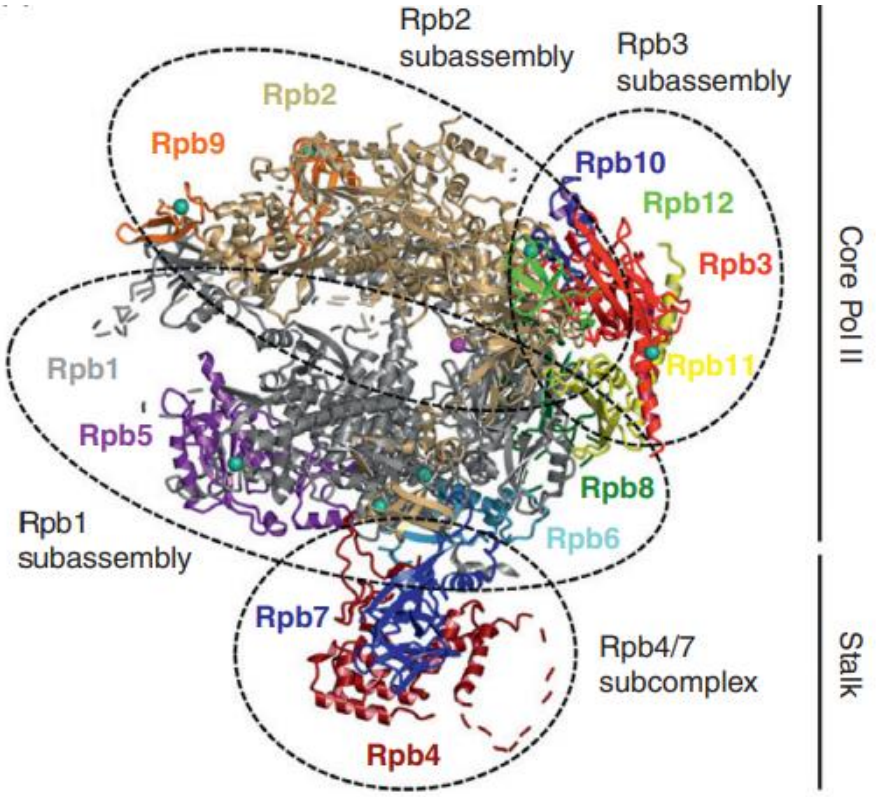

Figure 10. Crystal structure of RNAPII. This figure is reproduced from Wild and Cramer, 2012 with permission.

5.3. Steps involved in general transcription

RNAPII is not able to initiate the transcription and transcribe along DNA consistently. RNAPII needs so-called general transcription factors (GTFs) to successfully execute the transcription process (Haberle & Stark, 2018). In vitro transcription experiments revealed that RNAPII can recognize DNA at non-specific positions in the absence of GTFs (Matsui *et al*, 1980; Samuels & Sharp, 1986; Conaway *et al*, 1987; Sayre *et al*, 1992). GTFs (TFIID, TFIIA, TFIIB, TFIIF, TFIIE, TFIIH) are sequentially assembled at the core promoter which eventually results in the recruitment of RNAPII to the core promoter (Figure 9). The assembly of GTFs, RNAPII and mediator at core promoters is called pre-initiation complex (PIC) (Haberle & Stark, 2018; Rengachari *et al*, 2021) (Figure 9). The mediator complex consist of 30 subunits in human and is 1.4MDa in size (Plaschka *et al*, 2015). This complex controls transcription initiation and elongation by helping in the recruitment of general

or specific transcription factors to the gene promoter and by interacting with RNAPII (Allen & Taatjes, 2015). However, the precise mechanisms by which mediator influences transcription is poorly understood.

Biochemical and structural experiments revealed that TFIID is the first factor that recognizes and binds to the core promoter followed by TFIIA and TFIIB (Figure 9). The binding of TFIIA and TFIIB is followed by the recruitment of RNAPII-TFIIF complex. Finally, TFIIE and TFIIH join the complex (Nikolov & Burley, 1997; Haberle & Stark, 2018) (Figure 9). PIC assembly at the promoter results in melting of the DNA that allows RNAPII to start transcription at the transcription start site (TSS). The carboxy-terminal domain (CTD) of RNAPII likely helps to recruit Mediator to the promoter (Kim *et al*, 1994; Robinson *et al*, 2016) (Figure 9). To continue the transcription, RNAPII needs to dissociate from the PIC (termed as promoter escape). After escape, RNAPII synthesizes a 20-60 nucleotide long nascent RNA and then pauses downstream of TSS (Rougvie & Lis, 1988; Rasmussen & Lis, 1993). RNAPII pausing seems to give time for the proper 5'-capping of the nascent RNA (Rasmussen & Lis, 1993; Tome *et al*, 2018). At this stage, DRB sensitivity inducing factor (DSIF) and negative elongation factor (NELF) bind to RNAPII and help to maintain RNA pausing. The productive elongation phase is regulated by cyclin-dependent kinase 9 (CDK9) which phosphorylates DSIF, NELF, and RNAPII CTD at ser2. CTD phosphorylation at ser2 is considered one of the hallmarks of transcription elongation (Haberle & Stark, 2018).

5.4. Transcription factors (TFs)

In addition to the players mentioned before, transcription factors play an important role in ensuring tissue-specific transcription. TFs refer to proteins that are capable of binding DNA in a sequence-specific manner thereby regulating transcription (Fulton *et al*, 2009; Vaquerizas *et al*, 2009; Lambert *et al*, 2018). There are approximately 1600 transcription factors in the human proteome. Aberrant

expression of TFs is frequently associated with several kinds of cancer, developmental disorders, and other human pathologies. The affinity of TFs towards their specific DNA sequence is 1000 fold higher than to non-specific sequences (Lambert *et al*, 2018). Based on the structure of their DNA binding domains, TFs have been classified into several families that include nuclear hormone receptors, STATs, basic helix loop helix, homeodomain, C2H2-zinc finger and basic leucine zipper proteins (Struhl, 1989; de Souza *et al*, 2018; Lambert *et al*, 2018).

The differential presence and activity of transcription factors results in transcription of specific sets of genes in different cell types. TFs can bind to either the proximal promoter or enhancers in a combinatorial manner with the help of several other factors in addition to TFs. Enhancers are non-coding regulatory DNA sequences present in the genome that enhance the transcription of genes transcribed by RNAPII (Banerji *et al*, 1981; Bulger & Groudine, 2011; Kim & Shiekhattar, 2015; Oh *et al*, 2021). The key feature that distinguishes enhancers from promoters is that enhancers can activate transcription being located in either direction and irrespective of the distance and location to the target gene. Depending on the cell type and condition, promoters or enhancers are bound by several different kinds of proteins. These proteins include RNAPII, coactivators, TFs, architectural proteins such as histones and reader proteins that modify histones (Bulger & Groudine, 2011; Lambert *et al*, 2018). Different combinations of these proteins result in the transcription of a specific subset of genes at a specific time and location (Panigrahi & O'Malley, 2021).

There are several mechanisms, by which TFs can control gene expression. TFs can regulate gene expression either by direct recruitment of the RNAPII or by the recruitment of coactivators and corepressors (Bulger & Groudine, 2011) (Figure 9). TFs can also regulate transcription simply by steric mechanisms or by blocking the binding to other proteins on the same sequence. Coactivators are regulatory proteins that increase the transcription of the gene without binding to the DNA. Coactivators exert their function by binding to the TFs and modifying the chromatin. CBP, p300,

BRG1 and BRM (mammalian orthologue of SWI/SNF family) are few examples of coactivators (Kim *et al*, 1994; Zaret & Carroll, 2011; Allen & Taatjes, 2015). In the next chapters, the STAT- and nuclear receptor-family will be described in more detail as examples of TFs with the focus on PPARγ and STAT5, respectively.

6. Signal Transducer and Activator of Transcription-Family

The members of the STAT-family were discovered as key DNA binding proteins involved in cytokine signaling. In response to IFNα/β, STAT1/STAT2 rapidly binds to an IFN responsive element (Schindler *et al*, 1992; Ihle, 1996; Meraz *et al*, 1996; Levy & Darnell, 2002; Au-Yeung *et al*, 2013; Verhoeven *et al*, 2020). Following the cloning of STAT1 and STAT2, other members of the STAT-family were discovered (Liu *et al*, 1995; Au-Yeung *et al*, 2013). The STAT-family is comprised of seven family members (STAT1, 2, 3, 4, 5A, 5B and 6) (Verhoeven *et al*, 2020). Each family member has six domains namely the N-terminal domain (NTD), followed by the coiled-coil domain (CC). The CC domain is followed by a DNA binding domain (DBD). A helical linker connects the DBD to the SH2 domain. The SH2 domain is followed by C-terminal transactivation domain (TAD). TAD is the most divergent part among all domains (Ihle, 1996; Verhoeven *et al*, 2020) (Figure 11). During activation, SH2 domain along with the N-terminal domain mediates homo- and heterodimerization of STAT molecules. Coiled-coil domain helps in the nuclear localization of STATs mediated by protein-protein interaction. DNA binding domain is responsible for the binding of STATs to the DNA consequences sequence. The TAD domain has regulatory phosphorylation sites that upon phosphorylation help in the recruitment of additional factors resulting in enhanced STAT activity.

STAT	Consensus binding site
STAT1	TTCC(G>C)GGAA
STAT2	None Definable
STAT3	TTCC(G=C)GGAA
STAT4	TTCC(G>C)GGAA
STAT5	TTCC(A>T)GGAA
STAT6	TTCC(A>T,N)GGAA

Figure 11. Structure and consensus binding sites of STATs.

STAT proteins regulate a variety of fundamental cellular processes that induce growth and differentiation, immune response, inflammation and development. STAT1 and STAT2 mediated signaling is implicated in the growth and apoptosis of immune cells (Adámková *et al*, 2007, 1) and exerting antiviral effects (Gamero *et al*, 2010). STAT3 is important for embryonic development as STAT3-deficient mouse embryos die within a few days of birth (Akira, 1999) . IL-12-STAT4 activated signaling plays an important role in the differentiation of TH1 cells (Szabo *et al*, 2003). Classical STAT5 signaling is important for mammary gland development, milk production and haematopoiesis (Buitenhuis *et al*, 2003). The last member, STAT6, is activated by IL-4 and IL-13 and is important for immune functions (Hou *et al*, 1994; Chiba *et al*, 2009).

6.1. Signal Transducer and Activator of Transcription 5 (STAT5)

STAT5 was discovered from sheep as prolactin regulated transcription factor (Wakao *et al*, 1994). Subsequently, it was found that two isoforms of STAT5 exist in mice. STAT5A and STAT5B share 94-96% sequence similarity at the amino acid level with the highest degree of dissimilarity at TAD (Liu *et al*, 1995). STAT5A and STATB genes are located on chromosome 17 and chromosome 11 of the human and mouse genome, respectively. The promoters of STAT5A and STAT5B are separated by 10kb. These proteins show a differential expression pattern. For instance, STAT5A (Liu *et al*, 1995; Barash, 2006) is predominantly expressed in the mammary gland, whereas STAT5B is highly expressed in natural killer cells (Gotthardt *et al*, 2016), liver (Udy *et al*, 1997) and muscle (Paul *et al*, 2019).

STAT5 undergoes several post-translational modifications that regulate its activity and stability. STAT5 is activated and mediates cell signaling in response to several

kinds of ligands including different growth hormones, different kinds of cytokines such as IL-2, IL-3, IL-4, and IL-7, GM-CSF, CSF1, thrombopoietin and erythropoietin. The canonical activation of these latent cytoplasmic transcription factors depends on tyrosine phosphorylation within the SH2 domain. STAT5A is tyrosine phosphorylated at Tyr694 and STAT5B is phosphorylated at Tyr699 by Janus kinase (JAK) in response to several cytokine and growth factors as mentioned above (Gouilleux *et al*, 1994). The tyrosine phosphorylation results in homo/heterodimer formation (STAT5A-5A, STAT5B-5B, STAT5A-5B) followed by their nuclear translocation and subsequent activation of target genes. Ser725 of Stat5A and Ser730 of Stat5B are phosphorylated in response to IL-2 and prolactin stimulation (Kirken *et al*, 1997b, 1997a; Decker & Kovarik, 2000). Point mutation studies showed that these serine residues are not important for the transcriptional regulation and transactivation potential of STAT5 (Yamashita *et al*, 2001). Other kinds of modification such as lysine acetylation (Ma *et al*, 2010; Kosan *et al*, 2013), lysine SUMOylation (Geiss-Friedlander & Melchior, 2007; Van Nguyen *et al*, 2012) and O-GlcNAcylation (Freund *et al*, 2017) have been shown to affect STAT5 transactivation capabilities.

STAT5 plays an important role in growth and differentiation. Double knockout mice (Stat5a-/Stat5b-) exhibit perinatal lethality 92-96% (Kerenyi *et al*, 2008; Socolovsky *et al*, 1999) due to severe anemia and severe combined immunodeficiency (Yao *et al*, 2006). Furthermore, surviving Stat5a-/Stat5b-mice fail to develop CD8+T lymphocytes and B cell maturation suggesting an important role of STAT5 in immune cell development (Hoelbl *et al*, 2010). Liver-specific invalidation of Stat5a-/Stat5b in mice leads to signs of severe hepatic steatosis, and the mice develop liver cancer at the age of 17 months without any chemical treatment (Yu *et al*, 2012). Collectively these finds suggest that STAT5A and 5B are important for growth and development.

The precise role of STAT5A and STAT5B was investigated using single mutants. Deletion of *Sta5A* but not *Stat5B* gene results in developmental issues in the mammary gland and decrease in milk secretion in mice (Liu *et al*, 1997) suggesting an important role of STAT5A in the development and function of the mammary gland.

Stat5B specific deletion in mice results in loss of sexual dimorphism in mice. Male mice with *Stat5B* deletion show growth rate and liver-specific gene expression similar to wild-type female mice (Udy *et al*, 1997). Collectively these studies show that STAT5A and STAT5B have redundant and non-redundant functions. These non-redundant functions may be attributed to their differential gene expression and different protein interaction patterns.

6.2. Unphosphorylated STAT5 (uSTAT5)

Most of the studies showed that growth hormone and cytokine mediated activation of STAT5 resulted in its phosphorylation. Phosphorylated STAT5 is the active molecule that is translocated into the nucleus and binds to the target sequence in the DNA thereby regulating gene expression. However, several studies suggest that unphosphorylated STAT5 (uSTAT5) can enter the nucleus and regulate gene expression. Shin and Reich, 2013 demonstrated that STAT5 nuclear import can be mediated by an unconventional nuclear localization signal (NLS) that resides within the CC domain (Shin & Reich, 2013). Interestingly, they demonstrated that STAT5 nuclear import is mediated by importin-alpha3/β1 and was independent of STAT5 activation by tyrosine phosphorylation. Functional assays demonstrated that the CC domain is important for the STAT5 mediated activation of the β-casein gene in response to prolactin treatment (Shin & Reich, 2013). Structural analysis of the unphosphorylated STAT5A homodimer lacking the N-terminal and C-terminal domains showed a high degree of resemblance with phosphorylated STAT5 (Neculai *et al*, 2005). The structural key difference between uSTAT5 and pSTAT5 was the mode of dimerization. uSTAT5 dimerizes in a completely different manner mediated via interaction between their "β-barrel and four-helix bundle domain" (Neculai *et al*, 2005).

Park et al.,2016 demonstrated that in the absence of signal, uSTAT5 can still bind to the DNA and may act as a repressor. In the absence of thrombopoietin (TPO), uSTAT5 co-localizes with CCAAT box-binding transcription factor and subsequently

represses the megakaryocytic transcriptional program. In the presence of TPO, uSTAT5 is phosphorylated and the canonical STAT5 pathway is activated (Park *et al*, 2016). These findings suggest that uSTAT5 is not an inert player, but its precise function needs to be further elucidated.

7. The Nuclear Receptor (NR) Superfamily

The nuclear receptor superfamily comprises ligand-activated transcription factors that play important roles in growth, development, inflammation, immunity, and metabolism (Mazaira *et al*, 2018; Dias *et al*, 2020; Christofides *et al*, 2021). Since the discovery of the first member of the NR family in 1985 until now 48 members have been added to this family (Hollenberg *et al*, 1985; Mazaira *et al*, 2018). NRs are divided into three classes. Class I consists of ligand-activated transcription factors. Glucocorticoid receptors and estrogen receptors (Novac & Heinzel, 2004) are examples of this class. In the absence of ligand, these TFs reside in the cytoplasm. Upon ligand activation, these TFs translocate to the nucleus where they initiate the transcription of several target genes (Nagy & Schwabe, 2004). The second class comprises orphan receptors since their endogenous ligand has not been identified (Giguère, 1999). Class III comprises ligand-activated TFs that require retinoic X receptors for their activity. Members of this class form complexes with RXR to bind to the promoter of their target genes. Peroxisome proliferator-activated receptors (PPARs) and retinoic acid receptors are members of this class (Tyagi *et al*, 2011).

PPARs are ligand-activated transcription factors that regulate a variety of genes involved in metabolic homeostasis, development, and immunity (Tyagi *et al*, 2011). PPARs were originally identified by their ability to induce proliferation of peroxisome (Lazarow & De Duve, 1976), but this function of PPARs is not found in humans. PPARs comprise three closely related members namely PPARα (NR1C1), PPAR ß/δ (NR1C2), and PPARγ (NR1C3) (Tyagi *et al*, 2011). These members are encoded

by three independent genes in rodents and humans (Zoete *et al*, 2007). Although co-expressed in several cell types, the different PPARs exhibit ligand specificity and specific functional characteristics (Braissant *et al*, 1996). PPARs are recognized as nuclear lipid sensing receptors, whose natural ligands include various kinds of endogenous lipids such as omega 3 fatty acids, eicosanoids and Vitamin B3 (Tyagi *et al*, 2011). PPARα is abundant in the liver, brown adipose tissue, skeletal muscle, endocrine tissue, and to a lesser extent in kidney and immune cells (Varga *et al*, 2011). PPARα has been detected in a specific area of the brain, where it exerts an anti-inflammatory effect (Esmaeili et al., 2016; Warden et al., 2016). In addition, PPARα regulates liver specific genes involved in fatty acid catabolism which provides energy to peripheral organs (Varga *et al*, 2011). PPAR ß/δ is ubiquitously expressed and plays an important role in the modulation of inflammatory responses (Liu *et al*, 2018). Studies suggest that PPAR ß/δ imparts protective function in the brain by exerting anti-inflammatory and anti-oxidant properties (Iwashita *et al*, 2007; Warden *et al*, 2016; Gamdzyk *et al*, 2018). However, there are contrasting studies that suggest a role for PPAR ß/δ in promoting inflammation (Liu *et al*, 2018). In addition, PPAR ß/δ plays important roles in controlling cell proliferation and cell cycle (Lim *et al*, 2009) and helps in inhibiting cell death by promoting the expression of proteins like PDK1 in several cell types (Pedchenko *et al*, 2008). The third member of PPAR family, PPARγ significantly contributes to the regulation of adipogenesis, lipid metabolism, energy balance and inflammation. PPARγ will be mentioned in more detail in following section.

The structure of nuclear receptors is highly conserved (Chandra *et al*, 2008). The PPARs are composed of five domains (designated as AF1, DBD, domain D, LBD, and AF2). The N-terminal AF-1 domain also called ligand-independent activation domain precedes the DNA-binding domain (DBD, domain C). The DBD contains two zinc-finger motifs that are responsible for the recognition of the consensus sequence on DNA. DBD is followed by the hinge domain D, which provides structural flexibility between DBD and ligand-binding domain (LBD) domain. The hinge domain is followed by the C-terminal LBD. As the name suggests LBD has a site for the

activation by ligand, sites for dimerization, and bears the AF-2 domain (Tyagi *et al*, 2011) (Figure 12). The LBD domain is large enough to accommodate a variety of endogenous lipid molecules such as eicosanoids and fatty acids. In the presence of an agonist, the AF2 domain plays a crucial role in mediating the recruitment of coactivators leading to enhanced expression of target genes. This recruitment occurs by displacing corepressors. Conversely, in the absence of an agonist, the AF2 domain exhibits a stronger association with corepressors. Additionally, the AF2 domain is responsible for both agonist binding and heterodimerization with RXR. Ligand binding to LBD domain is thought to induce conformational changes in the AF-2 domain resulting in the recruitment of co-activator proteins that further assist in regulation of gene expression (Tyagi *et al*, 2011).

PPARs bind to DNA on a region known as PPAR response elements (PPRE) containing two hexameric direct repeats (AGGTCA) with a single nucleotide space called DR1 or dinucleotide spacer called DR2 (Heinäniemi *et al*, 2007). PPRE is present in the promoter and enhancer region of PPAR target genes (Heinäniemi *et al*, 2007). PPARs interact with retinoic acid receptor (RXR) α and bind to PPRE to regulate target gene transcription (Chandra *et al*, 2008). In the absence of ligand,
Upon ligand binding, the PPARG2-RXRα heterodimer undergoes a conformational change, leading to the recruitment of co-activators essential for transcriptional activation. These co-activators include members of the p160 protein family, CREB-binding protein/p300. The cooperative interaction between the ligand-bound heterodimer and these co-activators facilitates the activation of target genes, resulting in transactivation. Conversely, in the absence of their cognate ligands, RXRα exhibit a different transcriptional response. Under such conditions, RXRα interact with co-repressors such as nuclear receptor corepressor (NCoR) and silencing mediator of retinoic acid (SMRT). This interaction plays a crucial role in transcriptional silencing, thereby regulating the expression of target genes (Powell *et al*, 2007). The binding of hydrophobic ligand to LBD results in conformational changes promoting the recruitment of co-activator complexes containing CREB binding protein (CBP), steroid receptor coactivator 1 and p300 to the PPAR:RXR

heterodimer, which subsequently results in transcription of the target genes (Zoete *et al*, 2007; Chandra *et al*, 2008; Chan & Wells, 2009; Tyagi *et al*, 2011; Ahmadian *et al*, 2013).

7.1. PPAR gamma

PPAR gamma was discovered by Tontonoz et al., 1994 while characterizing the adipocyte *P2* gene (Tontonoz et al., 1994). In humans, four splice variants of *PPARG* transcripts exist, of which *PPARG1*, *PPARG3* and *PPARG4* translate into PPARγ1 protein (Meirhaeghe & Amouyel, 2004). In addition to white adipose tissue, PPARγ is also expressed in liver, skeletal muscle, heart, colon, immune cells such as monocytes/macrophages, dendritic cells, and T cells, and various cells of epithelial origin (Figure 12) (Arck et al., 2010).

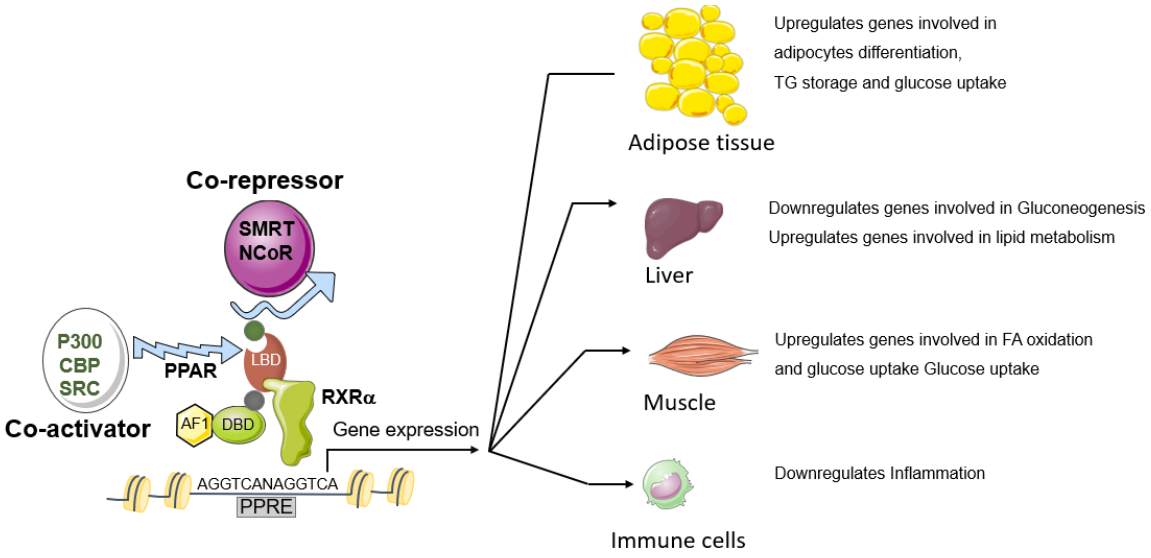

Figure 12. Mechanism of PPAR gamma activation and its impact on various organs.

AF1-Activation function 1, DBD-DNA-binding domain, LBD-ligand-binding domain, AF2- Activation function 2, RXR a-Retinoic acid receptor alpha, SMRT- Silencing mediator of retinoic acid, NCoR- Nuclear receptor corepressor, SRC- Steroid receptor coactivator, CBP-CREB-binding protein, PPRE- Peroxisome proliferator-activated receptor-gamma response element.
This figure is generated with the help of graphics from Servier Medical Art (https://smart.servier.com/)

PPARγ is regulated at transcriptional and post-translational levels (Zhu *et al*, 1995; van Beekum *et al*, 2009; Wadosky & Willis, 2012; Brunmeir & Xu, 2018; Hajri *et al*, 2021). PPARγ has two isoforms PPARγ1 and PPARγ2 resulting from different promoter usage and alternative splicing (Zhu *et al*, 1995). PPARγ2 is the longer form with an additional 30 amino acids (aa) at its N-terminus. PPARγ1 is expressed in several tissue types including liver, macrophages, small intestine, and WAT. On the other hand, PPARγ2 is mainly expressed in WAT, but also to a low extent in the liver (Zhu *et al*, 1995). In addition to PPARγ1 and PPARγ2, recently two other forms of PPARγ have been discovered, designated as PPARγ1Δ5, and PPARγ2Δ5 (Aprile *et al*, 2018). PPARγ1Δ5 and PPARγ2Δ5 are produced by skipping of exon 5 resulting in the deletion of the entire LBD (Aprile *et al*, 2018). These protein variants are

expressed in human adipose tissue where they exert a dominant-negative effect that may result in adipocyte dysfunction (Aprile *et al*, 2018).

7.1.1 Post-translational regulation of PPARγ

The activity of PPARγ is also governed by various post-translational modifications that include phosphorylation (Camp et al., 1999; Keshet et al., 2014; Hall et al., 2020), acetylation (Jiang *et al*, 2014), O-GlcNAcylation (Ji et al., 2012), ubiquitination (Keshet *et al*, 2014), and SUMOylation (Diezko & Suske, 2013; Katafuchi *et al*, 2018; Hall *et al*, 2020) (Figure 13). These PTMs affect protein stability, PPARγ transactivation potential and its interaction with coactivators and suppressors (Burns & Vanden Heuvel, 2007) (Figure 13). The position of the key amino acid residues that undergo PTMs and associated enzymes is shown in Figure 13. Indeed, some of the PTMs have been associated with metabolic syndrome (Burns & Vanden Heuvel, 2007; Brunmeir & Xu, 2018).

Phosphorylation is the most studied PTM in PPARγ biology. Several studies reported a variety of signals that could trigger PPARγ phosphorylation including epidermal growth factor, transforming growth factor β and prostaglandin F2α through the activation of ERK1/2 or JNK (Hu *et al*, 1996; Reginato *et al*, 1998; Brunmeir & Xu, 2018). One of the well-studied PPARγ phosphorylations is the one of ser112 that is located in the AF-1 region within a MAPK consensus sequence site. Phosphorylation of S112 results in decreased transcriptional activity of PPARγ at least in part by enhancing SUMOylation of K107. Mutagenesis experiments revealed that expression of a non-phosphorylatable form (S122A) led to an increase in transcriptional activity and adipogenesis (Camp *et al*, 1999; Ristow *et al*, 1998). Ser273 is another residue that undergoes phosphorylation in PPARγ by cyclin dependent kinase 5 and shares some similarity with S112. The loss of Ser273 phosphorylation increases PPARγ activation, however it does not affect adipogenesis but rather influences insulin sensitivity by affecting a subset of target

genes (Choi *et al*, 2015). In addition, Keshet et al., 2014 discovered that tyrosine residues 78 (Y78) and 112 (Y112) could be phosphorylated in PPARγ by c-Abl and phosphorylation was associated with increased PPARγ stability and promoted adipogenesis (Keshet *et al*, 2014). Interestingly, another group found that Y78 phosphorylation was regulated by SRC kinase and the phospho Y78 was involved in the regulation of a set of cytokine genes (Choi *et al*, 2015).

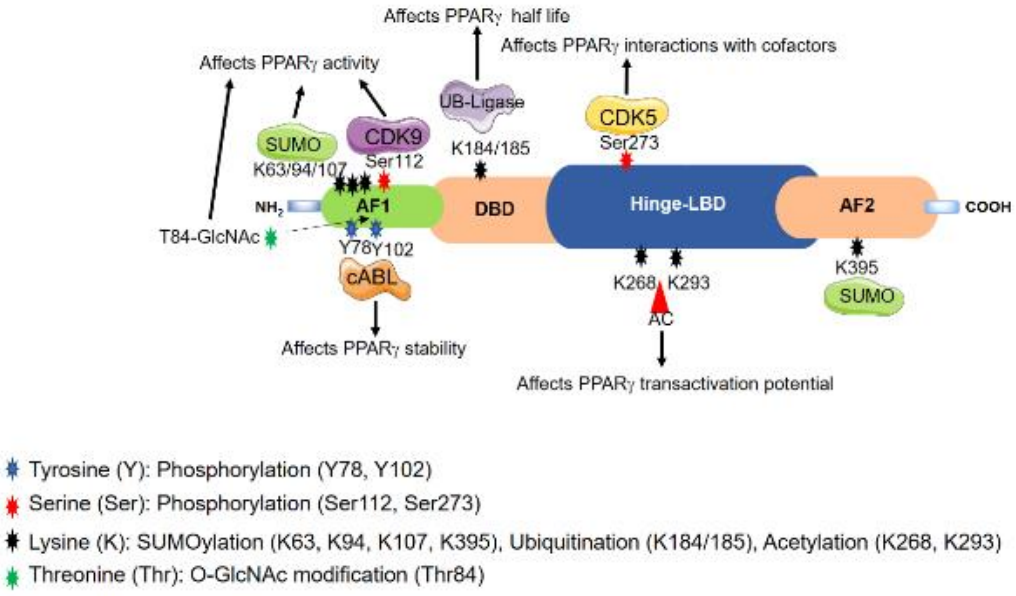

Figure 13. Schematic diagram of PPARγ showing key amino acids can undergo post-translational modifications.

The abbreviations are: CDK9-Cyclin Dependent Kinase 9, UB-Ligase-Ubituitin ligase, CDK5-Cyclin Dependent Kinase 5, cABL-Abelson Tyrosine-Protein ,Kinase 1, AF1-Activation function 1, DBD-DNA-binding domain, LBD-ligand-binding domain, AF2-Activation function 2, SUMO-Small Ubiquitin-related modifier.

This figure is generated with the help of graphics from Servier Medical Art (https://smart.servier.com/).

7.1.2 Biological role of PPARγ

PPARγ plays a special and indispensable role in the development, functionality and differentiation of adipose tissue. PPARγ is the master regulator of lipid storage and adipogenesis (Cataldi *et al*, 2021). The highest level of PPARγ is expressed in adipose tissue. Ectopic expression and activation of PPARγ is sufficient to induce adipogenesis in fibroblasts (Tontonoz *et al*, 1994b). In addition, forced expression of PPARγ in myoblasts causes cells to express adipocyte-specific genes leading to lipid accumulation, a phenomenon known as transdifferentiation (Hu *et al*, 1995). Using chimeric wild-type and *PPARG* null cells, Rosen et al. demonstrated that PPARγ is of utmost importance for the development of adipose tissue (Rosen *et al*, 1999).
Under the action of different ligands, PPARγ forms different transcriptional complexes comprised of different sets of cofactors that regulate different gene sets at various stages of adipocyte lifespan. Mice with an adipose tissue-specific KO of PPARγ exhibit marked abnormalities in the development and function of white as well as brown adipose tissue (BAT) (Jones *et al*, 2005). These mice have low levels of adiponectin and leptin hormones that play important roles in metabolism.

In addition to adipose tissue, PPARγ also plays important roles in several other tissues (Gavrilova et al., 2003). Although liver expresses lower amounts of PPARγ, liver specific deletion of *PPARG* shows the functional relevance of PPARγ in the liver. For instance, Matsusue et al., 2003 observed that PPARγ-deficient liver of obese/obese (ob/ob) mice exhibits lower levels of TG as compared to control littermates. Importantly, liver specific deletion of PPARγ increases the severity of diabetes in ob/ob mice due to decreased insulin sensitivity in adipose tissue and muscle (Matsusue *et al*, 2003). Furthermore, obesity results in the dysfunction of adipose tissue promoting lipolysis and hyperlipidemia. In such a situation, the liver can act as a site of lipid storage (Gavrilova *et al*, 2003). Excess lipid storage can activate the expression of PPARγ in the liver. Activated PPARγ can induce the

expression of genes involved in lipid metabolism such as *FABP4* and *CD36* that help in free fatty acid uptake in the liver and can contribute to steatosis (Ipsen *et al*, 2018). In Kupffer cells, PPARγ promotes the activation of the M2 macrophage phenotype and inhibits the M1 macrophage phenotype (Luo *et al*, 2017). The shift to the more anti-inflammatory M2 phenotype results in reduced inflammation levels. On one hand, PPARγ induces hepatic steatosis, on the other hand, PPARγ reduces inflammation. These observations suggest a dual role of PPARγ in the liver (Liss & Finck, 2017).

Gavrilova et al., 2003 demonstrated that ablation of PPARγ in the liver of lipodystrophic A-ZIP/F-1 (AZIP) mice reduces hepatic steatosis (Gavrilova *et al*, 2003). However, this deletion is accompanied by hyperlipidemia and muscle insulin resistance. Interestingly, rosiglitazone's hypoglycemic and hypolipidemic effects were lost upon the inactivation of PPARγ in AZIP mice, but not in wild-type mice (Gavrilova *et al*, 2003). Rosiglitazone, a member of the thiazolidinediones family, exerts its pharmacological effects by specifically binding to and activating PPARγ). These observations indirectly suggest that in the absence of adipose tissue, the liver may be the main site of rosiglitazone activity. Collectively liver PPARγ may play an important role in triglyceride homeostasis and inflammation under obese conditions.

The role of PPARγ in tumorigenesis is controversial (Mueller *et al*, 1998; Sarraf *et al*, 1998; Hernandez-Quiles *et al*, 2021). In several kinds of cancers, loss of function-, gain of function- and the presence of somatic PPARγ fusion-proteins have been documented (Sarraf *et al*, 1999; Hernandez-Quiles *et al*, 2021). PPARγ is highly expressed in the small intestine. Activation of PPARγ in colon cancer cells resulted in reduction in clonogenic growth (Sarraf *et al*, 1998). Furthermore, transplantation of tumors derived from human colon cancer cells showed a reduction in growth in mice treated with PPARγ agonists. A similar reduction in cancer growth upon PPARγ activation has been reported in prostate (Kubota *et al*, 1998), breast (Bonofiglio *et al*, 2009), and lung cancer (Bren-Mattison *et al*, 2005). The somatic mutation that

results in loss of function of PPARγ has been reported in nearly 8% of sporadic colorectal cancers (Hernandez-Quiles *et al*, 2021). PPARγ focal amplification has been reported for bladder carcinomas. The loss of function of PPARγ expression in bladder cancer cells resulted in reduced cell viability. In the luminal bladder cancer, mutations have been found in PPARγ that activate the PPARγ pathway and confer PPARγ dependency to the cancer cells (Rochel *et al*, 2019).

PPARγ expression in thyroid tissue is extremely low and its physiological relevance is not clear. In 30% of follicular thyroid carcinomas, t(2;3)(q13;p25) chromosomal translocation has been detected that results in plugging of PPARγ gene in frame to the paired box 8 (PAX8) gene (Kroll *et al*, 2000). PAX8 is an important transcription factor involved in the development of the thyroid gland (Kroll *et al*, 2000). In vitro and in vivo studies suggest that PAX8-PPARγ can act as an oncogenic transcription factor as it has DBDs from both proteins. The presence of this novel transformed transcription factor has been detected in poorly differentiated thyroid carcinomas, follicular thyroid adenomas, and follicular tumors. However, the presence of PAX-PPARγ does not correlate with the invasiveness of thyroid carcinomas (Boos *et al*, 2013).

8. Protein tyrosine phosphatases

8. 1. A brief history of Tyrosine (Tyr) phosphorylation

Protein phosphorylation and dephosphorylation indispensably contributes to several biological processes including cell signaling and gene expression. These processes ultimately govern metabolism, immune response and reproduction. The dysregulation of phosphorylation and dephosphorylation is one of the factors that instigate several human pathologies including diabetes, NAFLD, immunological diseases, and even cancer. In the eukaryotic proteome, approximately 30% of all proteins have phosphate groups added to them by kinases (Hunter, 2014). Among

all amino acids, phosphorylation at serine residues makes up 95% of total phosphoproteins (Hunter & Sefton, 1980; Tautz *et al*, 2006), threonine is accountable for 5% of total phosphoproteins. Tyrosine phosphorylation contributes to only 0.01-0.1% of all protein-bound phosphate groups (Hunter & Sefton, 1980; Tautz *et al*, 2006).

From a historical prospective, Ser/Thr kinases were discovered several years before protein tyrosine phosphorylation and tyrosine kinases (Eckhart *et al*, 1979; Hunter & Sefton, 1980). Tyr phosphorylation in general is relatively short-lived as compared to Ser/Thr phosphorylation and therefore often harder to detect. This is due to the presence of extremely active protein tyrosine phosphatases, which dephosphorylate any unprotected phospho-tyrosine residue within a few seconds (Kleiman *et al*, 2011). Another reason for the late discovery of phospho-tyrosine residues was the previous method of identifying phospho-amino acid residues. Electrophoretic migration of partial acid hydrolysates of ^{32}P labeled protein at pH 1.9 was the main method to detect phospho-amino acids (Ushiro & Cohen, 1980). At pH 1.9, phospho-Tyr (pTyr) and phospho-Thr (pThr) migrate together and pThr being abundant and relatively long-lived as compared to pTyr masks the pTyr signal (Hunter, 2014). For instance, EGF receptor kinase was mistakenly discovered as threonine kinase (Carpenter *et al*, 1978). With the discovery of two-dimensional electrophoresis that can distinguish between pTyr and pSer/pThr residues, it was demonstrated that pTyr-proteins exist and the level of their phosphorylation increases when activated Tyr-kinases were expressed in the cells (Hunter & Sefton, 1980). The development of pan-phospho-tyrosine antibodies (Frackelton *et al*, 1983), site-specific pTyr antibodies coupled with immunoblotting and finally affinity-purification mass spectrometry (AP-MS) resulted in the discovery of many phospho-tyrosine sites in a wide range of proteins.

8.2 Discovery of tyrosine phosphatases (PTP) and their classification

Tanks et al., 1988 identified and purified the first protein tyrosine phosphatase (PTP) called PTP1B from the human placenta (Tonks *et al*, 1988). Invention of PCR, low stringency screening, and further whole genome sequencing resulted in the discovery of several diverse members of the PTP family. Upon the completion of the sequencing of the human genome, the PTP family can be categorized into two groups (Tonks, 2006) (Figure 14). Group I comprises classical PTPs and dual-specificity phosphatases (DSPs) (Tonks, 2006). Some members of the PTP family are also classified as pseudo-phosphatase.

8.2.1 Classical phospho-tyrosine specific phosphatases

The classical PTPs can be further divided into transmembrane receptor-like protein-tyrosine phosphatases (RPTPs) and non-transmembrane protein tyrosine phosphatases (NTPTPs) (Alonso *et al*, 2004; Tonks, 2006) (Figure 14). Of note, the use of alternative promoters or alternative splicing can result in the production of receptor and non-receptor tyrosine phosphatases from a single gene suggesting the classification is not definitive. PTPRE and PTPRO genes are examples of such PTP genes (Tonks, 2006). There are at least 37 classical PTP genes in humans, mice, and rats. The catalytic domain of classical PTPs comprises several short sequence motifs especially the phospho-Tyr binding signature motif at the active site called active-site signature motif $C(X)_5R$. The average length of the catalytic domain of classical PTPs is 280 amino acids (Andersen *et al*, 2001).

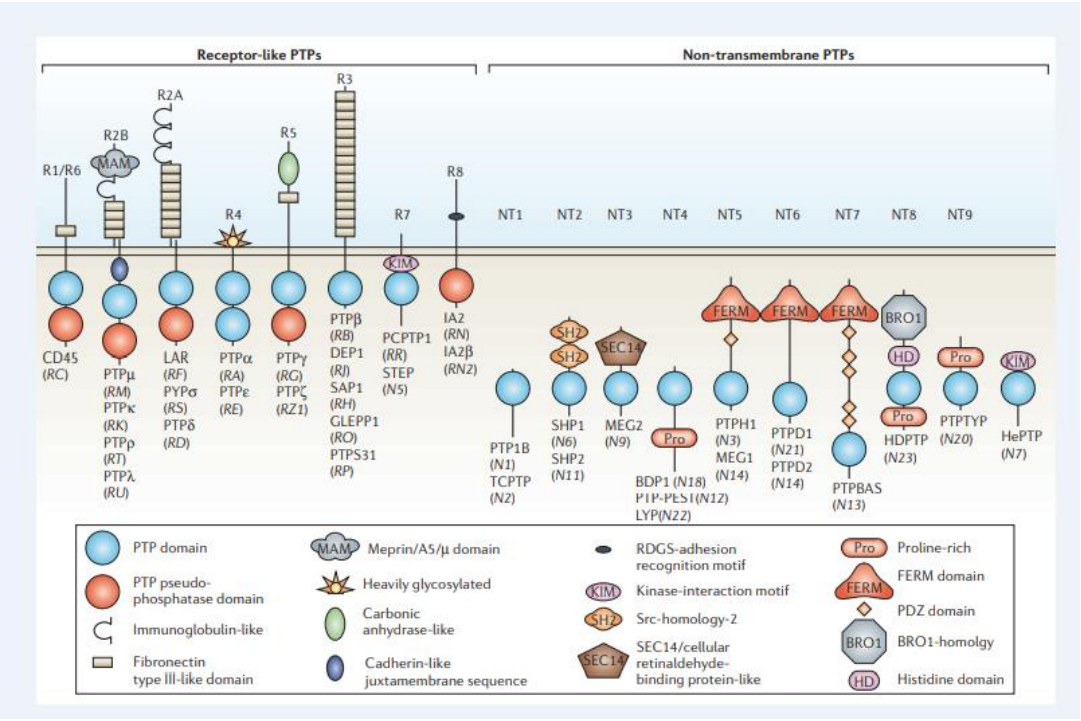

Figure 14. The classical PTPs. The figure is reproduced from Tonks et al., 2006, Springer Nature with permission.

8.2.2 RPTPs

Generally, RPTPs contain two cytoplasmic PTP domains, the membrane-proximal domain (D1) and the membrane distal domain (D2). In addition, RPTPs contain a single transmembrane segment and an extracellular domain (Andersen *et al*, 2001) (Figure 14). Functional studies suggest that most of the activity is attributed to the D1 PTP domain. The D2 domain does not have detectable enzymatic activity except for PTPalpha 11, but structural integrity is important for substrate specificity (Streuli *et al*, 1990).

8.2.3 NTPTPs

Unlike RPTPs that are predominantly found in the plasma membrane, NTPTPs are localized in the cytosol, endoplasmic reticulum and even in the nucleus (Andersen

et al, 2001; Alonso *et al*, 2004; Tonks, 2006). Structurally NTPTPs are comprised of catalytic domains flanked by regulatory sequences. These regulatory sequences play an important role by interacting with the substrate and catalytic domain such as the SH2 domain of SHP-1 and also regulate the subcellular distribution of the protein.

8.2.4 Dual specificity phosphatases (DSPs)

As compared to classical PTPs, DSPs possess a small catalytic domain and exhibit little sequence similarity with classical PTPs. The presence of cysteine-containing signature motifs qualifies them to classify within the PTP family. The mechanism of action of DSPs is similar to classical PTPs. The structural flexibility of the catalytic domain of DSPs allows them to accommodate phospho-serine and phospho-threonine residues in addition to phospho-tyrosine residues. Until now more than 60 genes have been identified that encode diverse members of DSPs (Pulido and Lang, 2019).

8.2.5 Pseudophosphatases

Pseudophosphatases are atypical members of the PTP superfamily that although having a conserved catalytic domain contain a mutation within this domain rendering them inactive. Nevertheless, this inactive catalytic domain, maintains a three-dimensional structure similar to other members of PTPs. For this reason pseudophosphatases were thought of as dead or natural substrate trapping mutants of the PTP family. With the discovery of several other pseudophosphatases (Hinton, 2019) several novel functions of these dead phosphatases have begun to emerge. For example the misregulation of pseudophosphatases has been observed in several kinds of human pathologies such as obesity, breast cancer and Charcot-Marie-Tooth disorder (Bolino *et al*, 2000; Mattei *et al*, 2021).

8.3. Src homology 2 domain-containing protein tyrosine phosphatase 1 (SHP-1)

To decipher the relationship between neoplastic transformation and impact of tyrosine phosphatases, Shen et al., 1991, screened a human breast carcinoma cDNA library with a Leukocyte Antigen-Related Tyrosine Phosphatase probe. Under high stringency conditions, they found two clones with large cDNA inserts (PTP1C4 and PTP1C2) (Shen *et al*, 1991). The sequencing of PTP1C4 indicated the presence of an open reading frame encoding a protein with 609 amino acids. Using PTP1C as a probe on total RNA extracted from ZR-75-1 cells gave a single band of 2.4 kb. The expression of PTP1C resulted in a very high amount of PTPase activity (Shen *et al*, 1991). In 1992, Yi and coworkers discovered the presence of PTP1C in hematopoietic cells and designated the gene that codes for PTP1C as hematopoietic cell phosphatase (HCP). At the same time Plutzky et al.,1992 discovered SH-PTP1 in the libraries of rat megakaryocytes and human erythroleukemia (Plutzky *et al*, 1992). The in vivo significance of SHP-1 (also known as haematopoietic cell phosphatase, HCP) was shown in the study of Tsui et al., 1993 where they found that a spontaneous recessive mutation observed in motheaten mice was due to a defect in the *HCP* gene (Wo Tsui *et al*, 1993).

8.3.1 SHP-1 structure and mechanism of action

SHP-1, also known as PTPN6, PTP-1C, HCP, HCPH, EC3.1.3.48, SH-PTP1 or SHP-1L, is the protein product encoded by the *PTPN6* gene located on chr12:6,946,468-6,961,316(GRCh38/hg38). The size of the *PTPN6* gene is 14,849 bp and the gene is located on the plus strand. Alternative splicing results in two isoforms: 68kDa (called SHP1a in mice and SHP1-1 in humans) and a slightly longer called SHP-1b in mouse and SHP1-2 in human. This second isoform is slightly longer as it carries two extra amino acids at the N-terminus (Banville *et al*, 1995). SHP-1 is predominantly expressed in cells of hematopoietic lineage (astrocytes, macrophages, neuronal cells), but also to a lesser extent in skeletal muscle, adipose

tissue and liver. The shorter isoform of SHP-1 is predominantly expressed in cells of hematopoietic origin whereas the longer isoform is expressed in epithelial cells (Matthews *et al*, 1992; Plutzky *et al*, 1992; Abram & Lowell, 2017). In humans a third C-terminal alternatively spliced form of SHP-1 called SHP-1L exists. SHP-1L, a 70 kDa protein, is 29 aa longer than other forms of SHP-1. SHP-1L is thought to exhibit specificity for specific substrates in certain cell types (Jin *et al*, 1999). The human and mouse SHP-1 shows 94% nucleotide similarity and 95% amino acid similarity.

The two isoforms of SHP-1 a and b are initiated from different initiation codons in exon 1 and exon 2. SHP-1 is expressed in different tissues using tissue-specific promoters. Promoter 1 (called P1) is active in non-hematopoietic cells, whereas Promoter 2 (called P2) is exclusively active in hematopoietic cells. In mice, Promoter 1 is more active in liver, brain, and kidney whereas promoter 2 is nearly 100 fold more active than Promoter 1 in the spinal cord, thymus and spleen (Evren *et al*, 2013). P1 is located 7 kb upstream of promoter 2 (Nakase *et al*, 2009). The P2 promoter, which is studied in more detail, is located within intron 1 (Wlodarski *et al*, 2007). PU.1 transcription factor that plays an important role in the differentiation of myeloid and lymphoid cells, binds to the core P2 promoter. Abolishing PU.1 results in decreased levels of SHP-1 transcripts (Wlodarski *et al*, 2007). In addition, transcription factor binding sites for Oct-1, Sp1, CREB-1 and NF-κB, have been detected in Jurkat and CD4+ T cells. Site-directed mutagenesis experiments revealed that Oct-1 and Sp1 binding is necessary for the basal activity of P2 promoters (Nakase *et al*, 2009). AP-1, AP-2, NF-kB, and RFX-1 binding sites have been identified in the P1 promoter.

Structurally, SHP-1 comprises two N-terminal SH2 domains (designated as N-SH2 & C-SH2 domains), a highly conserved enzymatic phosphatase domain and a flexible C-terminal tail that play a regulatory role (Figure 15-16). The SH2 domain plays important roles in regulating the activity of SHP-1. The crystal structure of SHP-1 revealed that in ligand/substrate-free conditions the N-terminal SH2 domain forms extensive contacts with the PTP domain and keeps the enzyme in an inactive state

(Hof *et al*, 1998; Yang *et al*, 2003; Wang *et al*, 2011) (Figure 15-16) by inserting the NXGDY/F motif into the catalytic cleft of the PTP domain. This inhibition is released by interaction of the N-SH2 domain with appropriate substrates containing phosphotyrosine bearing peptides (Pei *et al*, 1994). Wang et al., 2011 identified interactions between N-SH2 and C-SH2 domain and N-SH2 and catalytic domain. These interactions may be important for the stabilization of SHP-1 in the open confirmation (Wang *et al*, 2011). These structural details prove that SH2 domains are important for substrate recognition and controlling phosphatase activity (Yang *et al*, 2003; Wang *et al*, 2011). Furthermore, the binding of substrates/ phosphopeptides to the N-SH2 domain results in increased phosphatase activity. Wang et al., 2011 identified a sulfate ion, an analogue of phosphate in the binding site of N-SH2 and PTP domain suggesting N-SH2 domain also plays a role in substrate recognition. The binding of phosphopeptides to the N-SH2 domain results in a conformational change in the structure of the SH2 domain (Figure 15-16). This allosteric structural change disturbs the interaction between the N-SH2 domain and phosphatase domain allowing the PTP domain to access its substrate (Wang *et al*, 2011) and subsequently dephosphorylate it (Poole & Jones, 2005).

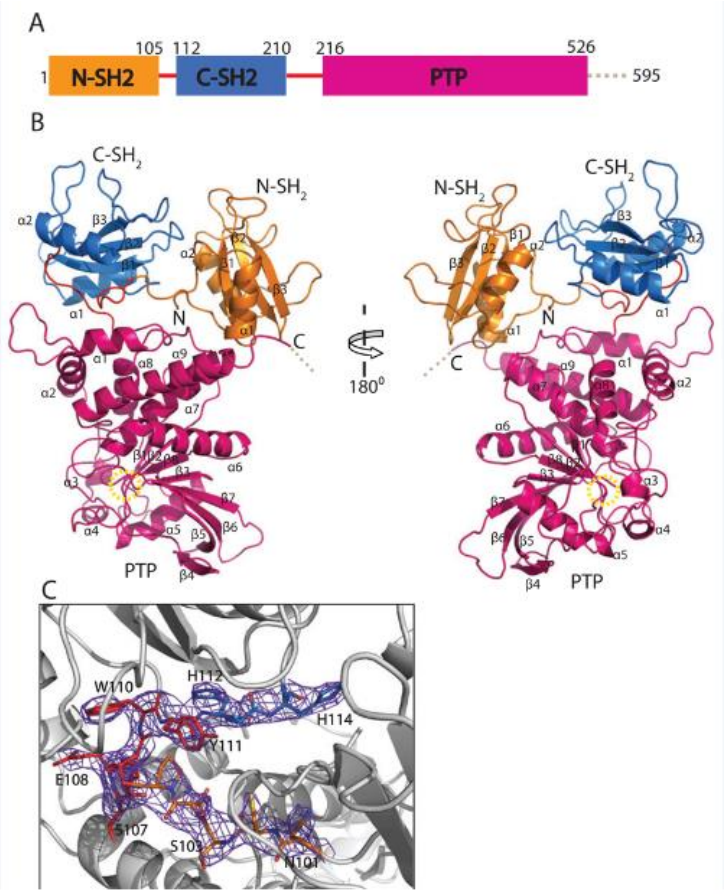

Figure 15. Structure of SHP-1. The figure is reproduced from Wang et al., 2011 with due permission.

A. Schematic representation of the domain organization of SHP-1. The C-terminal tail, shown as a dashed line, is disordered in the structure.

B. Overall structure of SHP-1, highlighting the arrangement of two SH2 domains resembling horns of the PTP domain. The active site is indicated by a yellow dashed circle.

C. Electron density map illustrating the region surrounding the linker connecting the two SH2 domains in SHP-1.

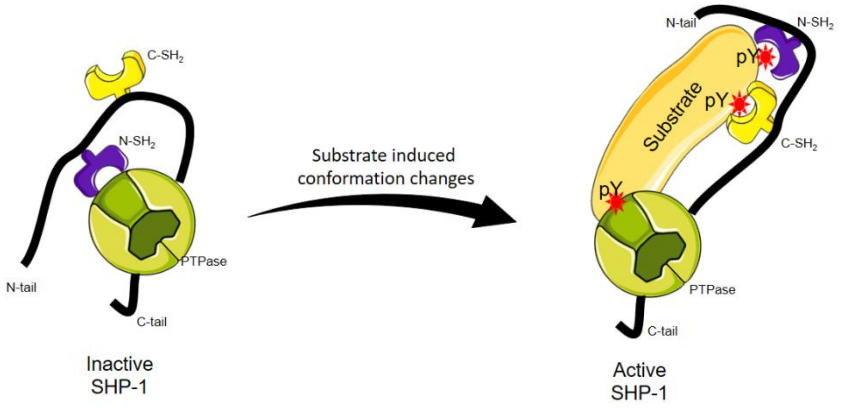

Figure 16. Schematic diagram showing mechanism of action of SHP-1. This figure is generated with the help of graphics from Servier Medical Art (https://smart.servier.com/).

In addition to these domains, the extreme C-terminus of SHP-1, 88 amino acids in length, contains several regulatory sites and signal motifs such as nuclear localization signal (Poole & Jones, 2005; Xu *et al*, 2014b). SHP-1 shows different localization in hematopoietic and epithelial cells. In the latter, SHP-1 is largely localized in the nucleus whereas in hematopoietic cells it exhibits cytoplasmic localization suggesting a differential role of SHP-1 in cells of different origins. This observation could be attributed to upstream signals that may lead to the nuclear localization of SHP-1 in epithelial cells, necessitating additional investigations. Fusion protein and mutagenesis studies revealed the presence of nuclear localization signals (NLS) in the C-terminal domain of SHP-1. This NLS comprises short stretches of basic amino acids (KRK). The SHP-1 C-terminal domain contains three basic regions (designated as BD1, BD2, and BD3) (Craggs & Kellie, 2001) out of which BD3 is responsible for nuclear import. In addition, the C-terminus has two putative tyrosine phosphorylation sites (Y536 and Y564) and several sites that could be phosphorylated by serine/threonine kinases (Zhang *et al*, 2003). These two tyrosine residues become phosphorylated upon various stimuli and are supposed to influence the activity of SHP-1. For instance, Lorenz et al., 1994 found that upon Lck mediated activation SHP-1 is phosphorylated on the Y-564 residue contributing to early T-cell signaling (Lorenz *et al*, 1994).

8.3.2 Biological functions of SHP-1

SHP-1 is present in different cell types performing diverse biological functions. SHP-1 plays important roles in lipid and glucose metabolism and immune cell functions. In addition, SHP-1 is involved in several human pathologies such as hereditary human diseases (Hendriks & Pulido, 2013; Bossé *et al*, 2019), bacterial and viral pathogenesis (Christophi *et al*, 2008; Böhmer *et al*, 2013) and cancer.

8.3.2.1 SHP-1 in metabolism

SHP-1 plays important roles in regulating glucose homeostasis and insulin action (Dubois *et al*, 2006; Bergeron *et al*, 2011; Xu *et al*, 2012; Drapeau *et al*, 2013; Xu *et al*, 2014a; Marín-Juez *et al*, 2014; Lizotte *et al*, 2016; Krüger *et al*, 2016). Dubois et al., 2006 found that viable motheaten mice ($Ptpn6^{(me\text{-}v/me\text{-}v)}$) that express catalytically dead SHP-1 exhibit marked glucose tolerance and insulin sensitivity as compared to their WT control littermates (Dubois *et al*, 2006). These observations were attributed to the enhanced activity of the IRS-PI3K-AKT axis in metabolic active tissues such as liver and muscle. In addition to regulating insulin signaling, SHP-1 also regulates insulin clearance. Tyrosine phosphorylation of carcinoembryonic antigen-related cell adhesion molecule 1 (CEACAM1), a substrate of SHP-1, is a hallmark of insulin clearance. In the absence of functional SHP-1 in viable motheaten mice, enhanced insulin clearance is also observed (Dubois *et al*, 2006). Expression of a dominant-negative mutant of *SHP-1* (C453S) in myocytes resulted in enhanced glucose uptake and glycogen synthesis. At the molecular level, the expression of SHP-1-C453S is accompanied by an increase in insulin-induced AKT phosphorylation (Bergeron *et al*, 2011). In a diet-induced obesity model, liver-specific knockdown of SHP-1 exhibits improved fasting glycaemia and protection from liver insulin resistance (Xu *et al*, 2012, 2014a). Of note, expression of SHP-1 is upregulated in metabolic tissues of high-fat diet-fed mice. In Zebrafish, the expression of SHP-1 is upregulated in

insulin-resistant larvae (Marín-Juez *et al*, 2014). Knockdown of SHP-1 improves insulin sensitivity in zebrafish (Marín-Juez *et al*, 2014). Besides improving insulin sensitivity, SHP-1 also modulates lipid metabolism and obesity linked NAFLD. For instance, Xu et al., 2014 unexpectedly found that hepatocyte specific SHP-1 KO although improving hepatic insulin action, resulted in increased hepatic steatosis in response to HFD (Xu *et al*, 2014a). In another report, hepatocyte specific SHP-1 KO mice showed exacerbated hepatic inflammation, hepatic steatosis and fibrosis in response to a methionine-choline deficient diet. Furthermore adenovirus mediated administration of SHP-1 in SHP-1 KO mice improved hepatic steatosis and inflammatory signs compared to control littermates (Lin *et al*, 2020).

In addition to liver and muscle, SHP-1 plays an important role in podocyte survival (Drapeau *et al*, 2013). Insulin pathways are important for podocyte survival. Elevated expression of SHP-1 is found in type1 diabetic mice. Exposure of podocytes to high glucose results in higher expression of SHP-1, reduced insulin signaling and elevated caspase3/7 activity. The high expression of SHP-1 in glomeruli may cause insulin resistance that can trigger podocyte loss and may contribute to diabetic nephropathy (Drapeau *et al*, 2013).

A high level of glucose induces active histone modifications (H3K4me1 and H3K9/14ac) on the SHP-1 promoter that results in its persistent expression ultimately causing renal insulin resistance and diabetic nephropathy (Lizotte *et al*, 2016).

Collectively these studies showed that SHP-1 acts as a negative regulator of insulin signaling and insulin clearance ultimately influencing glucose homeostasis in several kinds of tissues and organisms. Furthermore, SHP-1 controls lipid metabolism and failure to do so may be one of the factors for the development of NAFLD.

8.3.2.2 SHP-2: a brief introduction

SHP-2 is another SH2 domain containing non protein tyrosine phosphatase encoded by the *PTPN11* gene showing 60% homology on the protein level with

SHP-1 (Lorenz, 2009). Structurally, SHP-2 exhibits similar structural organization compared to SHP-1 and contains two SH2 domains followed by a PTP domain and a C-terminal regulatory tail. Despite of that, SHP-1 and SHP-2 execute opposite biological functions. SHP-2 is ubiquitously present whereas as mentioned earlier SHP-1 is mainly expressed in hematopoietic cells and epithelial cells (Feng *et al*, 1993). SHP-1 is largely considered as a negative regulator of a range of metabolic processes whereas SHP-2 mainly serves as a positive regulator. The role of SHP-2 has been identified in the regulation of several cellular processes like growth, division, differentiation, oncogenesis and metabolism. A study by Zhang et. al., 2004, has shown that mice with postmitotic forebrain neuron deletion of SHP2 showed early-onset of obesity in combination with a high level of leptin, insulin, glucose, and triglycerides in serum (Zhang *et al*, 2004). Furthermore, inhibition of SHP-2 has been shown to reduce both mRNA and protein levels of Acyl-CoA synthetase 4 (ACSL4) which is an important member of the fatty acid metabolism pathway with arachidonic acid thus modulating fatty acid metabolism (Cooke *et al*, 2011). The underlying mechanism behind this observation remains elusive and warrants further in-depth investigation. Another study highlighting the role of SHP-2 in lipid metabolism shows that SHP-2 works as an adaptor for the binding of p38 phosphorylated E3 ligase COP1 to fatty acid synthetase thereby facilitating its degradation by the ubiquitination pathway (Yu *et al*, 2013). The role of SHP-2 has also been established as an enhancer for leptin signaling, which might provide an important therapeutic candidate for obese patients (Feng, 2006). Another aspect of metabolism where the role of SHP-2 has been widely studied is glucose homeostasis and insulin resistance. It has been shown that in diabetic rats SHP-2 knockdown leads to an increase in glucose consumption and improves insulin resistance through phosphorylation of IRS-2 employing AKT and ERK1/2 regulation in the liver (Yue *et al*, 2020). A similar finding suggests that downregulation of SHP-2 in macrophages gives protection to hepatic steatosis and insulin resistance to mice fed a high-fat diet (Liu *et al*, 2020). Furthermore, deletion of SHP-2 in muscle cells has been associated with cardiomyopathy, insulin resistance, and premature death (Princen *et al*, 2009). These findings suggest that SHP-2 like SHP-1 participates in signaling that regulates

lipid biosynthesis and metabolism as well as insulin biosynthesis and glucose homeostasis.

8.3.2.3 SHP-1 and Inflammation

In response to infectious and non-infectious harmful stimuli, several cell types including both immune and non-immune cells activate intracellular signaling pathways resulting in the production of inflammatory mediators. This process is called inflammation and is characterized by redness, swelling, pain, and/or temporary loss of function of the affected area (Chen *et al*, 2017b). The inflammatory response involves several cell types including neutrophils, monocytes/macrophages, natural killer cells, B and T cells. Inflammation is mediated via the binding of cytokines such as IL-1β, IL-6, TNF-alpha to their respective receptors resulting in the activation of intracellular signaling pathways including NFκB, MAPK and JAK/STAT pathway (Germolec *et al*, 2018). SHP-1 is abundantly expressed in myeloid cells (Abram & Lowell, 2017). The role of SHP-1 in inflammation and immunity was evident from the study of motheaten mutants that rapidly develop inflammation and accumulation of immunoglobulins and autoantibodies after birth (Green & Shultz, 1975; Wo Tsui *et al*, 1993).

In 1965, spontaneous recessive mutations occurred in the C57BL/6J strain of the mice in the production colony of Jackson Laboratory. The affected mice have a short life span of 8 weeks and were characterized by the “patchy absence and thinness of hair” that gave the appearance of motheaten (Dickie *et al*, 1969). Genetic analysis revealed that the motheaten phenotype is attributed to the mutation in the *Ptpn6* gene (Green & Shultz, 1975). The systemic inflammation in motheaten mice is attributed to neutrophils and macrophages, not to the adaptive immune response (Yu *et al*, 1996). Double mutant $Ptpn6^{me\text{-}v/me\text{-}v}$ Rag1−/− mice that lack functional B- and T-cells still develop motheaten phenotypes (Yu *et al*, 1996; Croker *et al*, 2008). B cell-specific deletion of SHP-1 results in an increase in B-1a cell population, altered calcium sensing by B-cell antigen receptors, elevated levels of serum immunoglobulins. These mice eventually develop autoimmunity (Pao *et al*, 2007).

Lower levels of SHP-1 have been found in T-cells from psoriatic inflammatory skin disease patients as compared to T-cells derived from non-psoriatic patients (Eriksen *et al*, 2010). Ablation of SHP-1 in the retina enhances LPS-induced retinal dysfunction concomitant with elevated levels of pro-inflammatory cytokines (Zhuang *et al*, 2021). These phenotypes were due to the over-activation of transforming growth factor-β-activated kinase-1 (TAK1)/JNK pathway that otherwise is negatively regulated by SHP-1 (Zhuang *et al*, 2021). In immune cells, several substrates of SHP-1 have been identified including Syk, Slp65, p65Dok, Sirpa, Pirb, Lyn and JAK/STAT (Abram & Lowell, 2017). These proteins play important roles in immune cell survival and function. Taken together, these findings suggest SHP-1 is a critical player in the regulation of inflammation and immune functions.

8.3.2.4 SHP-1 in cancer development

Whether SHP-1 acts as a tumor suppressor or oncogenic promoting agent is still a matter of debate and largely depends on the cellular context. For example, in lymphocytes, SHP-1 terminates activating signals by dephosphorylating substrates such as CD72, FcyRIIB, CD22 and KIR (Unkeless & Jin, 1997; Christensen & Geisler, 2000). Therefore, there is the possibility that dysfunction of SHP-1 in lymphocytes may trigger lymphoma and leukemia formation (Varone *et al*, 2020). There are several studies, in which lower protein and transcript levels of SHP-1 have been documented in different cancer cell lines and cancerous tissues. These findings support the notion that SHP-1 functions as a tumor suppressor, as evidenced by previous studies (Oka *et al*, 2001; Tsui *et al*, 2002; Wu *et al*, 2003; Varone *et al*, 2020). In agreement, overexpression of SHP-1 results in inhibition of particular cancers cell lines (Bruecher-Encke *et al*, 2001; Zapata *et al*, 2002). However, *in vivo* evidence is largely lacking.

Strikingly, several reports suggest that SHP-1 can also exert a positive effect on cell growth (Su *et al*, 1996; You & Zhao, 1997; Rodríguez-Ubreva *et al*, 2010). The overexpression of dominant-negative SHP-1 mutant in HEK293T cells resulted in

suppression of mitogen-activated pathways and reduced cell growth and DNA synthesis (Su *et al*, 1996). In bone marrow mast cells derived from motheaten mice, SHP-1 deficiency results in persistent activation of ERK that results in inhibition of IL3-dependent cell proliferation (Nakata *et al*, 2011). SHP-1 has been shown to interact with proteins responsible for cell cycle regulation such as p27 and CDK2 (López-Ruiz *et al*, 2011). In light of these presumably contradictory reports, it is not clear whether SHP-1 exerts a positive or negative effect on the cell cycle.

8.3 DNA polymorphism in PTPN6 and human pathologies

Single nucleotide polymorphism (SNP) is the most common type of genetic variation in the population that affects only a single building block of the DNA. These minor differences account for approximately 0.1% variation in the DNA sequence between two individuals. Not all of these tiny differences are translated into phenotypes. This tiny difference can be associated with the susceptibility to several human pathologies only if they occur important DNA site that ultimately translate as amino acid in the protein that affects the expression, activity or stability of the protein. According to NCBI, human SNP database, PTPN6 has more than 7000 SNPs documented, out of which only 4 SNPs are classified as pathogenic or likely pathogenic SNPs (NCBI-dsSNP database).

The role of PTPN6 in the development of idiopathic neutrophilic dermatoses has been speculated (Nesterovitch *et al*, 2011; Hendriks & Pulido, 2013). In one patient, sequencing revealed a combined heterozygous mutation (E441G) in the PTP domain of SHP-1 and a heterozygous deletion of 1.7 kb of DNA in the promoter region of the PTPN6 gene. These changes resulted in low levels of SHP-1 that may contribute to pathogenesis in a certain subset of neutrophilic dermatoses (Nesterovitch *et al*, 2011).

Bouzid et al., 2013 investigated the association of a genetic variation of *PTPN6*, *ZAP70*, *BANK1* and *CLEC2D* genes with inflammatory bowel disease in the Tunisian population. Inflammatory bowel disease comprises ulcerative colitis (UC) and

Crohn's disease (Bouzid *et al*, 2013). They found an allelic and genotypic association of SNP-rs7310161 of PTPN6 in a patient with ulcerative colitis. SNP-rs7310161 is located in the 5'-UTR of the PTPN6 gene and results from transversion (A/T) (Bouzid *et al*, 2013). How this SNP affects UC, needs to be further investigated.

Recently Bossé et al., 2019 while investigating the genetic cause of early-onset emphysema in a French Canadian family discovered a rare non-synonymous heterozygous (Ala455Thr) SNP in the PTPN6 gene using whole-genome sequencing (Bossé *et al*, 2019). This mutation was found in 95% (20 out of 21) of the patients in which emphysema was confirmed using computed tomography. The Ala455Thr mutation lies near the catalytic site of the SHP-1 resulting in partial loss of function of the protein (Bossé *et al*, 2019).

All these three reports have two things in common. First, all the pathologies investigated in these different studies are associated with inflammation to some extent and all SNPs are heterozygous in nature. Collectively, these studies show that SHP-1 is an important player in regulating inflammation and any alteration in SHP-1 activity due to pathogenic SNPs can help in understanding the etiology of human pathologies. Currently, there is no documented association between human SHP-1 SNPs/mutations and metabolic effects. However, further investigation is warranted to explore the potential metabolic effects of the aforementioned SHP-1 SNPs.

9. Objectives

The principal aim of this thesis was to discover the new mechanisms by which SHP-1 participates in lipid and glucose metabolism. Previously, we have shown that liver specific deletion of SHP-1 resulted in upregulation of PPAR gamma activity. However, the exact mechanism behind this observation was not elucidated. The objective of Chapter II was to study the mechanisms by which SHP-1 regulates PPARγ activity and further to study the physiological context in the metabolic regulation.

Furthermore, to decipher the novel functions of SHP-1, we decide to discover the novel interacting partners of this protein. Interestingly, our AP-MS experiments revealed that SHP-1 interacts with a component of RNA polymerase machinery called POLR2J. Furthermore, we hypothesize that SHP-1 may play an important role in transcriptional regulation via interacting with RNAP II. In the absence of SHP-1, we found the modulation of several genes involved in metabolism. The transcript levels of PCK1, one of the key genes involved in gluconeogenesis was affected in the absence of SHP-1. Therefore, in chapter III we decide to study the mechanisms by which SHP-1 regulates PCK1 transcription.

Chapter II: Regulation of PPARγ stability and activity by SHP-1

Chapitre II

Régulation de la stabilité et de l'activité de PPARγ par SHP-1

Résumé

La région d'homologie de la protéine tyrosine phosphatase Src 2 contenant le domaine phosphatase-1 (SHP-1) joue un rôle important dans la modulation de l'homéostasie du glucose et des lipides. Précédemment, nous avons établi un lien entre SHP-1 et l'expression et l'activité du récepteur activé par les proliférateurs de peroxysomes -γ (PPARγ). PPARγ est le régulateur principal de l'adipogenèse, mais la façon dont son activité est régulée par la phosphorylation de la tyrosine est largement inconnue.

Ici, nous avons constaté que SHP-1 se lie à PPARγ2 principalement via ses domaines SH2 N-terminaux. Nous avons confirmé la phosphorylation de PPARγ2 sur le résidu tyrosine 78 (Y78), qui a été réduit par SHP-1 in vitro, entrainant donc une diminution de la stabilité de PPARγ2. La perte de SHP-1 entraîne une expression élevée, induite par un agoniste, des cibles PPARγ2 classiques FABP4 et CD36, concomitante à une augmentation de la teneur en lipides dans les cellules exprimant le PPARγ2 de type sauvage. Ces effets ont été atténués dans les cellules exprimant PPARγ2-Y78F, où la tyrosine 78 a été mutée en phénylalanine non phosphorylable. Dans l'ensemble, nous avons découvert que PPARγ2 est substrat de SHP-1 et que SHP-1 influence l'adipogenèse en affectant la stabilité de PPARγ2.

Regulation of PPARγ stability and activity by SHP-1

Amit Kumar[1], Beisy Laborit Labrada[1], Marie-Hélène Lavallée-Bourget[1], Marie-Pier Forest[1], Michael Schwab[1], Kerstin Bellmann[1], Vanessa Houde[1], Nicole Beauchemin[2], Mathieu Laplante[1,3], André Marette [1,4*]

[1]Centre de recherche de l'Institut universitaire de cardiologie et de pneumologie de Québec (CRIUCPQ), Faculté de Médecine, Université Laval, Québec, QC G1V 4G5, Canada.

[2]Rosalind and Morris Goodman Cancer Research Centre, Depts. of Oncology, Medicine and Biochemistry, McGill University, Montreal, QC H3A 1A3, Canada.

[3]Centre de Recherche sur le Cancer de l'Université Laval, Québec, QC G1R 3S3, Canada.

[4]Institute of Nutrition and Functional Foods, Laval University, Québec, QC G1V 0A6, Canada.

Abstract

The protein tyrosine phosphatase Src homology region 2 domain-containing phosphatase-1 (SHP-1) plays an important role in modulating glucose and lipid homeostasis. Previously, we have established a link between SHP-1 and peroxisome proliferator-activated receptor γ (PPARγ) expression and activity. PPARγ is the master regulator of adipogenesis, but how its activity is regulated by tyrosine-phosphorylation is largely unknown. Here, we found that SHP-1 binds to PPARγ2 mainly via its N-terminal SH2-domains. We confirmed the phosphorylation of PPARγ2 on tyrosine-residue 78 (Y78), which was reduced by SHP-1 *in vitro* resulting in decreased PPARγ2 stability. Loss of SHP-1 led to elevated, agonist-induced expression of the classical PPARγ targets *FABP4* and *CD36* concomitant with increased lipid content in cells expressing wild-type PPARγ2. These effects were blunted in cells expressing PPARγ2-Y78F, where tyrosine 78 was mutated to the non-phosphorylatable phenylalanine. Collectively, we discovered that PPARγ2 is a novel substrate of SHP-1 and that SHP-1 influences adipogenesis by affecting the stability of PPARγ2.

Introduction

The Src homology region 2 domain-containing phosphatase-1, (SHP-1) (also known as Protein Tyrosine Phosphatase Non-Receptor Type 6 (PTPN6) regulates signal transduction by dephosphorylating phospho-tyrosine residues on its targets proteins. It is mostly known for its role in hematopoietic cells (Plutzky *et al*, 1992; Mizuno *et al*, 1996; Paling & Welham, 2005) where SHP-1 negatively regulates signaling mediated by cytokine receptors such as interleukin-3 receptor, erythropoietin receptor, colony-stimulating factor 1 receptor, and T cell/B cell antigen receptor (Garg *et al*, 2020). SHP-1 is also expressed to a lesser extent in non-hematopoietic cells such as intestinal epithelial cells (Duchesne *et al*, 2003; Bergeron *et al*, 2011), myocytes (Bergeron *et al*, 2011), adipocytes (Lodeiro *et al*, 2011), and hepatocytes (Xu *et al*, 2012, 2014a).

SHP-1 possesses two N-terminally located SH2 domains, a single phosphatase domain and a C-terminal tail (Wang *et al*, 2011). The C-terminal tail of SHP-1 possesses multiple tyrosine and serine residues harboring regulatory functions (Zhang *et al*, 2003). The structural and molecular analysis of SHP-1 has revealed that its enzymatic function is regulated by structural rearrangement of the SH2 domains, which by binding to the catalytic domain keep the phosphatase inactive (Yang et al., 2003). The catalytic block is lifted when the SH2-domains interact with phospho-tyrosine residues in target proteins, which are then transferred to the C-terminal catalytic domain for dephosphorylation (Wang *et al*, 2011).

Peroxisome proliferator-activated receptor γ (PPARγ), a member of the nuclear hormone receptor superfamily, is a ligand-activated transcription factor that forms a heterodimer with retinoid X receptor α (RXRα) and then binds to its consensus sequence called PPAR responsive element on the DNA to activate transcription (Bardot *et al*, 1993; Schachtrup *et al*, 2004; Nielsen *et al*, 2008). Several natural and synthetic ligands including thiazolidinediones like rosiglitazone (Lehmann et al., 1995) are known to activate PPARγ (Houseknecht *et al*, 2002; Wu *et al*, 2021). Additionally, the activity of PPARγ is modulated by several post-translational

modifications such as phosphorylation (Choi et al., 2010; Hu et al., 1996), SUMOylation (Floyd & Stephens, 2004; Ohshima *et al*, 2004; Pascual *et al*, 2005) and ubiquitination (Hauser *et al*, 2000; Floyd & Stephens, 2002).

PPARγ is expressed predominantly in adipose tissue (Lefterova *et al*, 2014), in immune cells (Toobian *et al*, 2021), and to a lower extent in other metabolic tissues such as the liver (Lehrke & Lazar, 2005). In adipose tissue, PPARγ plays a key role in lipid metabolism and adipocyte differentiation. For instance, fibroblasts that lack PPARγ are not able to mature into mature adipocytes (Farmer, 2006). In addition to lipid metabolism, PPARγ is also known to modulate glucose metabolism, inflammation and cell proliferation, and its functions are organ and context dependent (Lehrke & Lazar, 2005). For instance, adipocyte-specific PPARγ controlled target genes such as *FABP4* and CD36, which are not expressed or at very low levels in the liver, are markedly enhanced in the liver of ob/ob mice upon troglitazone treatment (Memon *et al*, 2000). These findings suggest that an adipocyte-like function of PPARγ in the liver may contribute to NAFLD, and the information derived from one sources of PPARγ can be applied to study its impact on other tissues (He *et al*, 2003).

Previously, we have shown that SHP-1 modulates PPARγ activity, but the underlying molecular mechanisms remain elusive (Xu *et al*, 2014a). Herein, we demonstrate that SHP-1, by directly interacting with PPARγ leads to its dephosphorylation, which results in its degradation and subsequently in altered expression of adipogenic genes. Taken together, our data reveal a new relationship between SHP-1 and PPARγ adding an additional possibility to exploit this novel regulation for new therapeutic opportunities related to obesity and its complications.

Materials and methods

DNA constructs:

SH2-SH2 and *PTPase(-DN)* fragments were PCR-amplified from pcDNA5-FLAG3-SHP-1 constructs and pcDNA5-FLAG3-SHP-1-DN described elsewhere (Xu et al., 2014a) and cloned using *Hind*III and *Eco*RI to generate pcDNA5-FLAG3-SH2-SH2, pcDNA5-PTPase-WT, and pcDNA5-PTPase-DN constructs. pcDNA3.1-Myc3-Pparg2 and pcDNA3-FLAG3-Pparg2 are mammalian expression constructs containing full length mouse *Pparg2* cDNA. WZLneo-PPARγ2 plasmid (#34566) was purchased from Addgene. WZLneo-PPARγ2 plasmid was used as a template to generate WZLneo-PPARγ2-Y78F construct using Q5 Site-directed mutagenesis kit as per manufacturer's instructions (New England Biolabs, cat# E0554S). Lentiviral construct pLKO-shRNA-luciferase (called shControl), pLX304, pLX304-PTPN6-V5, and pLX304-PTP1B-V5 were kind gifts from Mathieu Laplante. shRNA against Shp-1 (*shShp-1*) was purchased from Sigma (shSHP-1.68, TRCN0000028968).

Cell culture, transfection, and treatment

All cell lines were cultured at 37°C in a humidified atmosphere containing 5% CO_2. The cell lines used were human embryonic kidney cells HEK293T, human hepatoma HepG2 cells and NIH3T3 mouse fibroblasts. HEK293T cells and NIH3T3 cells were cultured in DMEM high-glucose (Wisent Bioproducts cat # 319-005-CL) supplemented with 10% fetal bovine serum (FBS). HepG2 cells were cultivated in DMEM low-glucose (Wisent Bioproducts cat # 319-010-CL) supplemented with 10% FBS. All cell lines were transfected using jetPRIME (Polyplus-transfection, New York, USA) transfection reagent according to the manufacturer’s instructions with cell confluence between 60 and 80%. Depending on the experiments, the day after the transfection, some cells were treated with 100 nM of rosiglitazone (SynFine cat# 010301) before further analysis. Cells were treated with 20 µM (HEK293T and HepG2 cells) or 10 µM (HepG2 cells) bpV(HOpic) (Calbiochem, cat# 203701, reconstituted in water) for 30 minutes before harvesting. In the indicated experiments 100µM of cycloheximide (Sigma, cat # 01810-1G) and 20 µM of MG-132 (Calbiochem, cat# 474787-10MG) were added to the cell culture medium.

Virus preparation and generation of stable cell lines

Retro- and Lentiviruses were prepared using HEK293T cells. Retroviruses were prepared by transfecting WZLneo-PPARγ2 or WZLneo-PPARγ2-Y78F plasmid along with Gag-Pol and VSVg constructs. For lentiviral infection, shControl or *shShp-1* constructs were transfected with psPAX2 and pMD2.G plasmids. Transfections were performed using JetPRIME transfection reagent as per the manufacturer's instructions. Virus containing supernatants were collected 48 h after transfection and filtered using a 0.45 µm filter (Cribbs *et al*, 2013).

NIH3T3 cells or HepG2 cells were infected with retroviral supernatants (empty vector or PPARγ2 expressing vector) in the presence of polybrene (8 µg/ml). After 24 h of infection, transduction media was replaced by fresh media. After another 24 h, cells were split and selected using G418 (800 µg/ml). Expression of PPARγ2 protein was determined by western blot using a PPARγ-specific antibody (Cell signaling # 2443S, (81B8), 1:1000 dilution). Similarly, NIH3T3 cells overexpressing mutant PPARγ2-Y78F were generated.

SHP-1 was knocked down in NIH3T3 cells using lentiviral infection. Briefly, NIH3T3 cells were infected with lentiviral supernatant (shControl or *shShp-1*) in the presence of polybrene. Cells were selected using 2 µg/ml of puromycin (Invivogen, Cat# ant-pr-1). The expression level of SHP-1 protein was determined by western blot using a SHP-1-specific antibody (Thermo Fischer Scientific Cat# MA5-11669 (1SH01), 1:500 dilution).

Immunoprecipitation and western blot

Cells were washed with PBS followed by lysis in buffer containing 20 mM Tris-HCl pH 7.5, 140 mM NaCl, 1 mM of $CaCl_2$ and $MgCl_2$, 10 mM NaF, 1% NP-40, 10% glycerol, 2 mM Na-Vanadate, 1 mM PMSF and protease inhibitor cocktail (Roche). For immunoprecipitation, 1000 µg (for phosphoproteins) or 500 µg of total proteins were incubated with either anti-FLAG M2 affinity gel (Sigma) or protein A/G-agarose beads pre-incubated with PPARγ antibody for 2 h followed by five washes with buffer

containing 1X PBS, 1% NP40, 2 mM Na-Vanadate and protease inhibitors. Beads were boiled in 1X Laemmli buffer and western blot was performed as described earlier (Dubois *et al*, 2006; Xu *et al*, 2012, 2014a). The dilutions of the antibodies used in the study were as follows: FLAG antibody (Sigma cat# 088K6018, 1:1000 dilution), Myc antibody (Sigma cat# M4439-100UL, 1:2000 dilution), Actin antibody (Millipore, cat# MAB1501, 1:30000 dilution), SHP-1 antibody (Thermo Fischer Scientific cat# MA5-11669 (1SH01), 1:500 dilution), PPARγ antibody (Cell signaling cat# 2443S, (81B8) 1:1000 dilution), PY20 antibody (Abcam, cat# ab10321, 1:2000) and 4G10 antibody (Millipore, cat # 05-321, 1:2000 dilution).

In vitro dephosphorylation assay

HEK293T cells were transfected individually with either pcDNA3.1-Myc3-Pparg2 , pcDNA5-FLAG3, pcDNA5-FLAG3-SHP-1, or pcDNA5-FLAG3-SHP-1-C453S (dominant-negative) constructs. Cells transfected with Myc3-Pparg2 construct were treated with 20 µM of bpV(HOpic) for 30 minutes. Next, cells were washed three times with PBS containing 1X protease inhibitor cocktail (Sigma)and lysed in NP40 buffer containing 1% NP-40, 150 mM NaCl, 50 mM Tris-HCl, pH 8, and PIs. Phosphorylated Myc3-PPARγ2 was pulled down using anti-Myc agarose beads. Similarly, FLAG3, FLAG3-SHP-1, and FLAG3-SHP-1-DN were prepared by immuno-precipitating using anti-flag-agarose beads. FLAG-precipitated proteins were released from FLAG-agarose beads by incubating with 15 µg of FLAG peptides for 30 min at 4°C with rotation (Sigma, cat# F4799-4MG). Phosphorylated Myc3-PPARγ2 bound to Myc-agarose was incubated with either FLAG3, FLAG3-SHP-1-DN or FLAG3-SHP-1-WT in phosphatase buffer (20 mM HEPES pH7.5, 150 mM of NaCl, 0.5mM DTT, 0.01 β-mercaptoethanol and 1mM PMSF) at 37°C for 30 min (Frank *et al*, 2004). The reaction was stopped by adding Laemmli buffer and levels of phosphorylated Myc3-PPARγ2 were determined by western blotting using phospho-tyrosine specific antibodies (mixture of 4G10 and PY20).

A similar dephosphorylation assay was performed with proteins immunoprecipitated from NIH3T3 cells. Briefly, NIH3T3 cells were transfected individually with either

pcDNA3-FLAG3-Pparg2, pLX304, pLX304-PTPN6-V5 and pLX304-PTP1B-V5 constructs. Cells transfected with FLAG3-Pparg construct were treated with 20 µM of bpV(HOpic) for 30 minutes. Phosphorylated FLAG3-PPARγ2 was pulled down using anti-FLAG agarose beads and eluted using FLAG peptides. Similarly, pLX304, SHP-1-V5 and PTP1B-V5 were prepared by immuno-precipitation using an anti-V5 antibody coupled to agarose beads. Dephosphorylation assay was performed as described above.

In addition, the non-specific phosphatase activity of SHP-1-V5 and PTP1B-V5 were determined using the Molecular Probes™ DiFMUP (6,8-Difluoro-4-Methylumbelliferyl Phosphate) substrate as described previously (Bosse, 2019). Reaction was performed at 37°C for 30 min.

Cycloheximide protein stability experiments

NIH3T3 cells stably expressing PPARγ2 in SHP-1-WT or SHP-1-KD conditions were incubated with 100 µM of cycloheximide (Sigma, cat # 01810-1G, dissolved in DMSO). PPARγ2 protein was measured by western blot at 0, 1, 3, and 6 h of the cycloheximide treatment.

Oil red O staining

To assess the lipid content, NIH3T3 cells stably expressing PPARγ2 or PPARγ2-Y78F in SHP-1-WT or SHP-1-KD cells were cultured to confluence and treated with 100 nM of rosiglitazone for 10 days. On day 10, cells were fixed and stained with oil red O (Sigma O-0625) as described previously (Keshet *et al*, 2014). Oil red O was dissolved in isopropanol and relative intracellular content was measured by measuring OD at 500nm (Keshet *et al*, 2014).

RNA isolation and quantitative PCR

Total RNA was isolated using the Direct-zol™ RNA MiniPrep kit (R2072, Zymoresearch, Irvine, USA) as per the manufacturer's instructions. 2 µg of total RNA was reverse transcribed using high capacity cDNA reverse transcription kit (Thermo Fischer Scientific, cat# 4368813). cDNA was diluted and the expression of

transcripts was determined using Multicell Advanced qPCR master mix (Wisent bioproducts, cat# 800-435-UL). *Hprt1* or *B2M* were included as a reference genes (Supplementary table S1). Relative fold change was calculated using 2^(-delta delta Ct) method (Livak & Schmittgen, 2001).

Statistical Analysis

All values presented in graphs are the average value of at least two independent experiments. The error bar shown in the graph is the standard error of the mean. Student t-test and one-way ANOVA or two-way ANOVA with Tukey's post hoc test were used to determine the statistical significance using GraphPad Prism software version 8. Western blots were quantified using ImageJ software.

Results

SHP-1 interacts with PPARγ2

To elucidate the molecular mechanism of how SHP-1 can regulate PPARγ activity we generated SHP-1 constructs expressing either a FLAG-tagged N-terminal fragment containing only the two SH2-domains (SH2-SH2) or two FLAG-tagged C-terminal fragments without the SH2-domains, but carrying the phosphatase domain in its wild type (WT) or substrate-trapping, dominant negative (DN) form (PTPase WT and PTPase DN) (Figure 1A). Lysates from HepG2 cells co-transfected with these or full length WT or DN SHP-1 and Myc-PPARγ2 were FLAG-immunoprecipitated. As shown in Figure 1B, PPARγ interacted better with full-length DN than WT SHP-1. Deletion of the N-terminus of SHP-1 strongly reduced the association between PPARγ2 and SHP-1, but the DN form of the PTPase domain still bound better to PPARγ2 than the WT version (Figure 1B and 1C). The N-terminal fragments retained the interaction with PPARγ2 at a similar level as full-length SHP-1 (Figure 1B and 1C) indicating that SHP-1 mainly interacts with PPARγ2 via its N-terminal SH2-domains. Thus, recognition of PPARγ2 by the N-terminal SH2 domain

and stronger binding of PPARγ2 to DN SHP-1 imply that PPARγ2 is a direct substrate of SHP-1.

To determine whether the SHP-1-PPARγ2 interaction depends on the activation of PPARγ2, NIH3T3 cells were co-transfected with Myc-PPARγ2 and FLAG-SHP-1 constructs and treated with either DMSO or rosiglitazone for 1 h. No difference in the levels of co-immunoprecipitated PPARγ2 was observed with or without rosiglitazone treatment (Figure 1D and E).

Collectively these findings show that PPARγ2 is a novel binding partner and potential substrate of SHP-1 and that the interaction is independent of exogenous PPARγ2 activation.

SHP-1 dephosphorylates PPARγ2

Next, we investigated whether PPARγ2, which has been shown to be tyrosine-phosphorylated (Keshet et. al, 2014), could be a substrate of SHP-1 *in vitro*. To confirm the tyrosine-phosphorylation of PPARγ2 HEK293T cells were transfected with a FLAG-PPARγ2 construct and were either left untreated or treated with the general tyrosine phosphatase inhibitor bpV(HOpic) for 30 min. Immunoprecipitated PPARγ was strongly tyrosine-phosphorylated as detected with phosphotyrosine-specific antibodies after bpV(HOpic)-treatment (Figure 2A).

To determine whether SHP-1 could directly dephosphorylate PPARγ2 we performed *in vitro* dephosphorylation assays. Phosphorylated Myc-PPARγ2 was immunoprecipitated as substrate from transiently transfected HEK293T cells treated with bpV(HOpic) as before. This substrate was incubated with FLAG-SHP-1-WT or FLAG-SHP-1-DN proteins eluted from FLAG-immunoprecipitates of transfected HEK293T cells. As a negative control, eluates from HEK293T cells transfected with an empty FLAG-vector and as a positive control recombinant lambda-phosphatase were included in the experiment. Similar to lambda phosphatase, SHP-1 WT, but not

SHP-1 DN was able to dephosphorylate PPARγ2 suggesting that PPARγ2 is a substrate of SHP-1 (Figure 2B and C).

Previously, protein tyrosine phosphatase 1B (PTP1B) has been implicated in PPARγ dephosphorylation (Choi *et al*, 2015). Our dephosphorylation assay performed with phosphorylated PPARγ2 as substrate and SHP-1 and PTP1B as enzymes immunoprecipated and purified from transfected NIH3T3 cells revealed that SHP-1, but not PTP1B efficiently dephosphorylated PPARγ2 *in vitro* (Figure 2D and E). However, SHP-1 and PTP1B used in the dephosphorylation assay were equally efficient in dephosphorylating a non-specific tyrosine-phosphatase substrate (DifMUP) ruling out that the difference in the dephosphorylation of PPARγ2 was only due to reduced PTP1B-activity (Figure 2F). Together, these results indicate that tyrosine-phosphorylated PPARγ2 is a specific target of SHP-1.

SHP-1 modulates PPARγ2 stability

Next, we wanted to examine the functional relationship between SHP-1 and PPARγ2 in more detail. We exogenously expressed PPARγ2 in HepG2 and NIH3T3 cells (Figure 3A-B). While HepG2 cells failed to respond to PPARγ overexpression with and without rosiglitazone treatment (Figure 3C), NIH3T3 cells displayed a robust induction of classical PPARγ target genes (*CD36* and *FABP4*) in the presence of PPARγ2, an effect that was further increased after treatment with rosiglitazone (Figure 3D). Therefore, we chose NIH3T3 cells for our future experiments. We generated NIH3T3 cells overexpressing PPARγ2 using retroviral transduction and knocked down (KD) *Shp-1* in these and control cells using lentivirus encoded *Ptpn6* shRNA (Figure 4A). Surprisingly, depletion of Shp-1 resulted in increased PPARγ2 protein amounts (Figure 4A-B), which was not due to higher transcription, since there was no significant difference in the *Pparg* transcript levels between Shp-1 WT and KD cells (Figure 4C). To corroborate these data, we measured PPARγ2 stability in a time-course experiment after treatment of PPARγ2 overexpressing NIH3T3 cells with

cycloheximide to inhibit translation. Whereas PPARγ2 was almost fully degraded after 6 h in Shp-1 WT cells, loss of Shp-1 significantly reduced PPARγ2 degradation (Figure 4D and E). Together, these results show that Shp-1 controls PPARγ2 stability.

SHP-1 regulates PPARγ2-mediated adipogenesis

Finally, we wanted to analyze the molecular details and functional effects of the SHP-1-regulated PPARγ2 stability on PPARγ2 activity. Previously, the tyrosine residue 78 (Y78) has been identified as the major site for tyrosine-phosphorylation in PPARγ2 and Y78 phosphorylation increased the stability of PPARγ2 in HEK293-cells by reducing ubiquitin-dependent degradation (Keshet *et al*, 2014; Choi et al., 2015). To determine whether Y78 residue undergoes phosphorylation in NIH3T3 cells, we treated NIH3T3 cells expressing wild type PPARγ2 or mutant PPARγ2 (Y78F) with the proteasome inhibitor MG132 and bpV(HOpic) and immunoprecipitated phosphorylated PPARγ. We observed that levels of tyrosine phosphorylated PPARγ were significantly lower in the Y78F mutant compared to wild type PPARγ indicating that Y78 is the main residue undergoing tyrosine phosphorylation in NIH3T3 cells (Figure 5A).

Furthermore, we found that the protein amount of a PPARγ2-Y78F mutant, in which the tyrosine 78 is replaced by the non-phosphorylatable phenylalanine, was much lower than PPARγ2-WT in NIH3T3-cells, despite no differences in the transcript levels of these two constructs (Figure S1A and B). However, treatment of these cells with the proteasome inhibitor MG132 restored the stability of the PPARγ2-Y78F mutant to PPARγ2-WT levels (Figure S1C and D) supporting the previously published results that Y78 is the main site regulating PPARγ2 stability.

To understand the role of Y78 in SHP-1-controlled PPARγ2 stability, we compared NIH3T3 cells overexpressing PPARγ2-WT or the PPARγ2-Y78F mutant in the SHP-1-WT and SHP-1-KD background (Figure 5B). As before, we found higher levels of PPARγ2-WT in SHP-1 depleted cells and low amounts of PPARγ2-Y78F in SHP-1-

WT cells. Interestingly, the PPARγ2-Y78F levels were unaffected by the loss of SHP-1 suggesting that the SHP-1 mediated regulation of PPARγ2 stability depends on the presence and probably the phosphorylation of Y78. We ruled out the possibility that the observed effects are due to differences in *Pparg2* transcription, because we did not find a significant difference in the transcript levels of any of the *Pparg2* constructs in SHP-1-WT and SHP-1-KD conditions with or without rosiglitazone treatment (Figure 5C).

To determine the impact of SHP-1 on PPARγ2 activity, we examined the expression of classical PPARγ target genes (*Fabp4* and *Cd36*). Reflecting the PPARγ2 protein levels seen in Figure 5B, *Fabp4* and *Cd36* transcripts significantly increased in cells overexpressing wild-type PPARγ2 in SHP-1-KD cells as compared to SHP-1-WT cells after rosiglitazone treatment (Figure 5D and E). However, there was no significant difference in the low levels of *Fabp4* and *Cd36* transcripts in cells of SHP-1-WT or SHP-1-KD background expressing PPARγ2--Y78F after rosiglitazone treatment.

To analyze whether the impact of SHP-1-mediated regulation of PPARγ2 activity also results in phenotypic changes, we treated PPARγ2-WT and -Y78F overexpressing NIH3T3-cells with rosiglitazone in the SHP-WT or -KD background. Similar to the *Fabp4* and *Cd36* transcript levels and mirroring the PPARγ2 protein levels, loss of SHP-1 caused an increase in lipid content in PPARγ2-WT, but not PPARγ2-Y78F expressing cells, which generally showed reduced lipid content (Figure 5F and G). These findings indicate that SHP-1-mediated regulation of PPARγ2 stability through tyrosine residue Y78 results in altered PPARγ2 activity consequently affecting adipogenesis.

Discussion

In the present study, we show that PPARγ2 is not only a novel interacting partner, but also a substrate of the tyrosine-phosphatase SHP-1. As depicted in the model in

Fig 5H, we found that knockdown of SHP-1 stabilizes PPARγ2-WT protein leading to increased PPARγ2 protein expression as well as enhanced transcription of *Cd36* and *Fabp4* resulting in elevated adipogenesis. Mutation of the tyrosine residue 78 to the non-phosphorylatable phenylalanine, which resulted in a general destabilization of PPARγ2, blunted these SHP-1-dependent effects. Thus, SHP-1-mediated dephosphorylation at the Y78 residue results in the degradation of PPARγ2 and consequently modification of its activity. Since SHP-1 interacted to the same extent with PPARγ2 from untreated or rosiglitazone-treated cells, this SHP-1-mediated regulation seems to be independent of the activation status of PPARγ2. Together, these findings provide the mechanistic insight to explain our previous observations that overexpression of SHP-1 strongly reduced the activity of rosiglitazone-stimulated PPARγ2 (Xu et al., 2014a).

While SHP-1 function has been vastly characterized in the immune system, a much more limited number of SHP-1 substrates is known in metabolic tissues including carcinoembryonic antigen-related cell adhesion molecule 1 (Dubois *et al*, 2006) and phosphatidylinositol 3-kinase regulatory subunit p85 (Lodeiro *et al*, 2011). Our work provides several lines of evidence that establish PPARγ, one of the master regulators of adipogenesis, as a SHP-1 substrate. SHP-1 interacted with PPARγ2 mainly via its N-terminal SH2 domains, which are responsible for the detection of phosphotyrosine residues in SHP-1 target proteins. PPARγ2 bound stronger to a SHP-1 substrate-trapping mutant as compared to wild-type SHP-1. Finally, SHP-1 dephosphorylated PPARγ2 *in vitro*, even better than PTP1B, which has been suggested to be the phosphatase responsible for PPARγ2 dephosphorylation (Choi *et al*, 2015). The identification of PPARγ2 as SHP-1 substrate adds another transcription factor to the short list of transcriptional regulators including β-catenin and TonEBP/OREBP, which have been described as SHP-1 targets (Zhou *et al*, 2010; Simoneau *et al*, 2011). It also underlines that SHP-1 plays an important role in the nucleus of cells, especially epithelial cells, besides its well-known functions as a regulator of several signaling pathways.

The stability of nuclear receptors is influenced by their interaction with coactivators/co-suppressors and phosphorylation-induced ubiquitin-mediated protein degradation (Burns & Vanden Heuvel, 2007; Blanquart *et al*, 2004). We showed that SHP-1 loss increased PPARγ2 stability, an effect that is abrogated by mutation of the tyrosine 78 residue to phenylalanine. Previously, it has been demonstrated that the Y78 residue of PPARγ2 is tyrosine phosphorylated by c-Abl kinase, which leads to PPARγ2 stabilization by inhibiting ubiquitin-dependent degradation (Keshet *et al*, 2014). Therefore, our data imply that by dephosphorylating the Y78 residue SHP-1 negatively regulates the stability of PPARγ2. Previously Xiao et al., 2015 demonstrated that SHP-1 regulates Casitas-B-lineage lymphoma (Cbl)-b protein mediated T-cell response by controlling the tyrosine phosphorylation and ubiquitination of Cbl-b (Xiao *et al*, 2015). It will be interesting in the future to study whether dephosphorylation by SHP-1 controls the stability and activity of other proteins.

PPARγ is mainly expressed in adipose tissue and the immune system, but to a lower extent also in the liver. Knockdown of PPARγ in adipose tissue affects the maturation and integrity of mature adipocytes (He *et al*, 2003; Koutnikova *et al*, 2003). Interestingly, irrespective of the levels of PPARγ in these metabolic tissues, deletion of PPARγ in adipose tissue, liver or muscle has a significant effect on whole-body lipid homeostasis. The adipose tissue-specific deletion of PPARγ results in an increased lipid content and the development of fatty livers (He *et al*, 2003). Under high fat conditions the expression of PPARγ increases in other metabolic tissues such as the liver. Fatty livers exhibit markedly higher levels of PPARγ and high expression of its target genes. It appears that cross-talk between adipose tissue and the liver is important for the maintenance of lipid homeostasis. We have shown that SHP-1 can interact with PPARγ in cell culture models representing liver and adipose tissue. In addition, we discovered that SHP-1 controls adipocyte differentiation *in vitro* by regulating PPARγ stability and activity through dephosphorylation. Future studies will be necessary to determine how this mechanism affects *in vivo* adipogenesis. Another interesting question will be whether our findings can be

extrapolated to other tissues and cells. We previously reported an increase in *Pparg2* mRNA in livers of obese mice with a liver-specific SHP-1 knockout compared to their WT-counterparts (Xu et al., 2014a). During adipogenesis, positive feedback loops for PPARγ activating its own transcription have been proposed (Rosen *et al*, 2002; Wakabayashi *et al*, 2009) and recruitment of PPARγ to the *Pparg2* promoter has been detected (Lee *et al*, 2013). Increased stability of PPARγ2 inducing its own transcription might explain the higher *Pparg2* transcript levels in the livers of mice with deletion of SHP-1, but has to be experimentally verified. Overall, we believe that SHP-1 is an important common switch that fine-tunes the activity of PPARγ not only in adipocytes, but also in other cells including hepatocytes.

Materials availability

Further information and requests for resources and reagents should be directed to and will be fulfilled by the corresponding author, André Marette (Andre.Marette@criucpq.ulaval.ca)

Acknowledgments

This work was supported by a Canadian Institutes of Health Research (CIHR) Foundation grant (FDN-143247) to A.M. A.K. was partially supported by an IUCPQ student grant. A.M. holds a CIHR/Pfizer research Chair in the pathogenesis of insulin resistance and cardiovascular diseases.

Author contributions

M.S., K.B., MLB, A.K., V.H., N.B. and A.M. conceived and designed the project. A.K., M.S., M.L.B, M.F., B.L.L., and K.B. performed experiments. A.K., M.L.B., M.F., V.H., M.S., K.B., M.L.,. and A.M. interpreted the results. A.K., M.S., K.B. and A.M. wrote the manuscript with comments from the other authors.

Declaration of interests

The authors declare no competing interests.

References

1. Bardot O, Aldridge TC, Latruffe N & Green S (1993) PPAR-RXR heterodimer activates a peroxisome proliferator response element upstream of the bifunctional enzyme gene. *Biochem Biophys Res Commun* 192: 37–45

2. Bergeron S, Dubois M-J, Bellmann K, Schwab M, Larochelle N, Nalbantoglu J & Marette A (2011) Inhibition of the protein tyrosine phosphatase SHP-1 increases glucose uptake in skeletal muscle cells by augmenting insulin receptor signaling and GLUT4 expression. *Endocrinology* 152: 4581–4588

3. Blanquart C, Mansouri R, Fruchart J-C, Staels B & Glineur C (2004) Different ways to regulate the PPARalpha stability. *Biochem Biophys Res Commun* 319: 663–670

4. Burns KA & Vanden Heuvel JP (2007) Modulation of PPAR activity via phosphorylation. *Biochim Biophys Acta* 1771: 952–960

5. Choi S, Jung J-E, Yang YR, Kim E-S, Jang H-J, Kim E-K, Kim IS, Lee J-Y, Kim JK, Seo JK, *et al* (2015) Novel phosphorylation of PPARγ ameliorates obesity-induced adipose tissue inflammation and improves insulin sensitivity. *Cell Signal* 27: 2488–2495

6. Cribbs AP, Kennedy A, Gregory B & Brennan FM (2013) Simplified production and concentration of lentiviral vectors to achieve high transduction in primary human T cells. *BMC Biotechnol* 13: 98

7. Dubois M-J, Bergeron S, Kim H-J, Dombrowski L, Perreault M, Fournès B, Faure R, Olivier M, Beauchemin N, Shulman GI, *et al* (2006) The SHP-1 protein tyrosine phosphatase negatively modulates glucose homeostasis. *Nat Med* 12: 549–556

8. Duchesne C, Charland S, Asselin C, Nahmias C & Rivard N (2003) Negative regulation of beta-catenin signaling by tyrosine phosphatase SHP-1 in intestinal epithelial cells. *J Biol Chem* 278: 14274–14283

9. Farmer SR (2006) Transcriptional control of adipocyte formation. *Cell Metabolism* 4: 263–273

10. Floyd ZE & Stephens JM (2002) Interferon-gamma-mediated activation and ubiquitin-proteasome-dependent degradation of PPARgamma in adipocytes. *J Biol Chem* 277: 4062–4068

11. Floyd ZE & Stephens JM (2004) Control of peroxisome proliferator-activated receptor gamma2 stability and activity by SUMOylation. *Obes Res* 12: 921–928

12. Frank C, Burkhardt C, Imhof D, Ringel J, Zschörnig O, Wieligmann K, Zacharias M & Böhmer F-D (2004) Effective dephosphorylation of Src substrates by SHP-1. *J Biol Chem* 279: 11375–11383

13. Garg M, Wahid M & Khan F (2020) Regulation of peripheral and central immunity: Understanding the role of Src homology 2 domain-containing tyrosine phosphatases, SHP-1 & SHP-2. *Immunobiology* 225: 151847

14. Hauser S, Adelmant G, Sarraf P, Wright HM, Mueller E & Spiegelman BM (2000) Degradation of the peroxisome proliferator-activated receptor gamma is linked to ligand-dependent activation. *J Biol Chem* 275: 18527–18533

15. He W, Barak Y, Hevener A, Olson P, Liao D, Le J, Nelson M, Ong E, Olefsky JM & Evans RM (2003) Adipose-specific peroxisome proliferator-activated receptor gamma knockout causes insulin resistance in fat and liver but not in muscle. *Proc Natl Acad Sci U S A* 100: 15712–15717

16. Houseknecht KL, Cole BM & Steele PJ (2002) Peroxisome proliferator-activated receptor gamma (PPARgamma) and its ligands: a review. *Domest Anim Endocrinol* 22: 1–23

17. Keshet R, Bryansker Kraitshtein Z, Shanzer M, Adler J, Reuven N & Shaul Y (2014) c-Abl tyrosine kinase promotes adipocyte differentiation by targeting PPAR-gamma 2. *Proc Natl Acad Sci U S A* 111: 16365–16370

18. Koutnikova H, Cock T-A, Watanabe M, Houten SM, Champy M-F, Dierich A & Auwerx J (2003) Compensation by the muscle limits the metabolic consequences of lipodystrophy in PPAR gamma hypomorphic mice. *Proc Natl Acad Sci U S A* 100: 14457–14462

19. Lee J-E, Wang C, Xu S, Cho Y-W, Wang L, Feng X, Baldridge A, Sartorelli V, Zhuang L, Peng W, *et al* (2013) H3K4 mono- and di-methyltransferase MLL4 is required for enhancer activation during cell differentiation. *Elife* 2: e01503

20. Lefterova MI, Haakonsson AK, Lazar MA & Mandrup S (2014) PPARγ and the global map of adipogenesis and beyond. *Trends Endocrinol Metab* 25: 293–302

21. Lehrke M & Lazar MA (2005) The many faces of PPARgamma. *Cell* 123: 993–999

22. Livak KJ & Schmittgen TD (2001) Analysis of relative gene expression data using real-time quantitative PCR and the 2(-Delta Delta C(T)) Method. *Methods* 25: 402–408

23. Lodeiro M, Alén BO, Mosteiro CS, Beiroa D, Nogueiras R, Theodoropoulou M, Pardo M, Gallego R, Pazos Y, Casanueva FF, *et al* (2011) The SHP-1 protein tyrosine phosphatase negatively modulates Akt signaling in the ghrelin/GHSR1a system. *Mol Biol Cell* 22: 4182–4191

24. Memon RA, Tecott LH, Nonogaki K, Beigneux A, Moser AH, Grunfeld C & Feingold KR (2000) Up-regulation of peroxisome proliferator-activated receptors (PPAR-alpha) and PPAR-gamma messenger ribonucleic acid expression in the liver in murine obesity: troglitazone induces expression of PPAR-gamma-responsive adipose tissue-specific genes in the liver of obese diabetic mice. *Endocrinology* 141: 4021–4031

25. Mizuno K, Katagiri T, Hasegawa K, Ogimoto M & Yakura H (1996) Hematopoietic cell phosphatase, SHP-1, is constitutively associated with the SH2 domain-containing leukocyte protein, SLP-76, in B cells. *J Exp Med* 184: 457–463

26. Nielsen R, Pedersen TÅ, Hagenbeek D, Moulos P, Siersbæk R, Megens E, Denissov S, Børgesen M, Francoijs K-J, Mandrup S, *et al* (2008) Genome-wide profiling of PPARγ:RXR and RNA polymerase II occupancy reveals temporal activation of distinct metabolic pathways and changes in RXR dimer composition during adipogenesis. *Genes Dev* 22: 2953–2967

27. Ohshima T, Koga H & Shimotohno K (2004) Transcriptional activity of peroxisome proliferator-activated receptor gamma is modulated by SUMO-1 modification. *J Biol Chem* 279: 29551–29557

28. Paling NRD & Welham MJ (2005) Tyrosine phosphatase SHP-1 acts at different stages of development to regulate hematopoiesis. *Blood* 105: 4290–4297

29. Pascual G, Fong AL, Ogawa S, Gamliel A, Li AC, Perissi V, Rose DW, Willson TM, Rosenfeld MG & Glass CK (2005) A SUMOylation-dependent pathway mediates transrepression of inflammatory response genes by PPAR-gamma. *Nature* 437: 759–763

30. Plutzky J, Neel BG & Rosenberg RD (1992) Isolation of a src homology 2-containing tyrosine phosphatase. *Proc Natl Acad Sci U S A* 89: 1123–1127

31. Rosen ED, Hsu C-H, Wang X, Sakai S, Freeman MW, Gonzalez FJ & Spiegelman BM (2002) C/EBPalpha induces adipogenesis through PPARgamma: a unified pathway. *Genes Dev* 16: 22–26

32. Schachtrup C, Emmler T, Bleck B, Sandqvist A & Spener F (2004) Functional analysis of peroxisome-proliferator-responsive element motifs in genes of fatty acid-binding proteins. *Biochem J* 382: 239–245

33. Simoneau M, Coulombe G, Vandal G, Vézina A & Rivard N (2011) SHP-1 inhibits β-catenin function by inducing its degradation and interfering with its association with TATA-binding protein. *Cell Signal* 23: 269–279

34. Toobian D, Ghosh P & Katkar GD (2021) Parsing the Role of PPARs in Macrophage Processes. *Front Immunol* 12: 783780

35. Wakabayashi K, Okamura M, Tsutsumi S, Nishikawa NS, Tanaka T, Sakakibara I, Kitakami J, Ihara S, Hashimoto Y, Hamakubo T, *et al* (2009) The peroxisome proliferator-activated receptor gamma/retinoid X receptor alpha heterodimer targets the histone modification enzyme PR-Set7/Setd8 gene and regulates adipogenesis through a positive feedback loop. *Mol Cell Biol* 29: 3544–3555

36. Wang W, Liu L, Song X, Mo Y, Komma C, Bellamy HD, Zhao ZJ & Zhou GW (2011) Crystal structure of human protein tyrosine phosphatase SHP-1 in the open conformation. *J Cell Biochem* 112: 2062–2071

37. Wu D, Eeda V, Undi RB, Mann S, Stout M, Lim H-Y & Wang W (2021) A novel peroxisome proliferator-activated receptor gamma ligand improves insulin sensitivity and promotes browning of white adipose tissue in obese mice. *Mol Metab* 54: 101363

38. Xiao Y, Qiao G, Tang J, Tang R, Guo H, Warwar S, Langdon WY, Tao L & Zhang J (2015) Protein Tyrosine Phosphatase SHP-1 Modulates T Cell Responses by Controlling Cbl-b Degradation. *J Immunol* 195: 4218–4227

39. Xu E, Charbonneau A, Rolland Y, Bellmann K, Pao L, Siminovitch KA, Neel BG, Beauchemin N & Marette A (2012) Hepatocyte-specific Ptpn6 deletion protects from obesity-linked hepatic insulin resistance. *Diabetes* 61: 1949–1958

40. Xu E, Forest M-P, Schwab M, Avramoglu RK, St-Amand E, Caron AZ, Bellmann K, Shum M, Voisin G, Paquet M, *et al* (2014a) Hepatocyte-specific Ptpn6 deletion promotes hepatic lipid accretion, but reduces NAFLD in diet-induced obesity: potential role of PPARγ. *Hepatology* 59: 1803–1815

41. Xu E, Schwab M & Marette A (2014b) Role of protein tyrosine phosphatases in the modulation of insulin signaling and their implication in the pathogenesis of obesity-linked insulin resistance. *Rev Endocr Metab Disord* 15: 79–97

42. Zhang Z, Shen K, Lu W & Cole PA (2003) The role of C-terminal tyrosine phosphorylation in the regulation of SHP-1 explored via expressed protein ligation. *J Biol Chem* 278: 4668–4674

43. Zhou X, Gallazzini M, Burg MB & Ferraris JD (2010) Contribution of SHP-1 protein tyrosine phosphatase to osmotic regulation of the transcription factor TonEBP/OREBP. *PNAS* 107: 7072–7077

Figure legends

Figure 1. SHP-1 interacts with PPARγ mainly through the SH2 domains.
A. Schematic representation of various SHP-1 constructs generated via recombinant DNA technology.
B. HepG2 cells were transfected with the indicated plasmids and cell lysates were immunoprecipitated using anti-FLAG M2 beads. The expression of respective proteins was determined by western blot using the indicated antibodies (representative of three independent experiments).
C. Quantification of immunoprecipitated Myc-PPARγ2 and FLAG-SHP-1 constructs was performed by densitometry using ImageJ (n=3).
D. NIH3T3 cells were transfected with the indicated plasmids and were either treated with DMSO or 100 nM rosiglitazone for 1h. Cell lysates were immunoprecipitated using anti-FLAG M2 beads. The expression of respective proteins was determined by western blot using the indicated antibodies (representative of two independent experiments).
E. Quantification of immunoprecipitated Myc-PPARγ2 and FLAG-SHP-1 was performed by densitometry using ImageJ (n=2).
IP: immunoprecipitation, WCE: whole cell extracts

Figure 2: SHP-1 dephosphorylates PPARγ *in vitro*.
A. HEK293T cells were transfected with an empty *FLAG*-vector or a *FLAG-PPARg2* plasmid. After 24 h cells were treated with bpV(HOpic) (10 µM) for 30 minutes. Lysates were immunoprecipitated with anti-FLAG beads and analyzed by western blot using respective antibodies. IP: immunoprecipitation, WCE: whole cell extracts, 4G10/PY20: mix of phospho-tyrosine-specific antibodies (n=3).
B. HEK293T cells were transfected with *FLAG* empty vector, *FLAG-SHP-1-WT*, *FLAG-SHP-1-DN* or *Myc-PPARg2* plasmids. After 24 h cells were either left untreated or treated with 20 µM bpV(HOpic) for 30 minutes. Myc-precipitated, tyrosine-phosphorylated Myc-PPARγ2 was used as substrate and incubated for 30 min at 37°C with FLAG, FLAG-SHP-1-WT or FLAG-SHP-1-DN eluted from FLAG-beads after FLAG-precipitation or with recombinant λ phosphatase. Tyrosine-phosphorylation of Myc-PPARγ2 was determined by western blot using phospho-tyrosine specific antibodies to measure SHP-1 activity. The expression of respective Myc- and FLAG-constructs was verified by immunoblotting of whole cell extracts with the indicated antibodies (WT: wild type, DN: dominant negative). (Representative of three independent experiments).
C. Quantification of levels of phospho-tyrosine Myc-PPARγ2 and total Myc-PPARγ2 was performed by densitometry using ImageJ (n=3).
D. NIH3T3 cells were either transfected with *V5* empty vector, *PTP1B-V5*, *SHP-1-V5* or *FLAG-PPARg2* constructs. After 24 h cells were either left untreated or treated with 20 µM bpV(HOpic) for 30 minutes. FLAG-PPARγ2 eluted from FLAG-agarose beads was used as substrate and incubated with V5-precipitated V5, PTP1B-V5 or SHP-1-V5 at 37°C for 30 minutes. Tyrosine-phosphorylation of FLAG-PPARγ2 was determined by western blotting using phospho-tyrosine specific antibodies to measure PTP1B and SHP-1 activity. The expression of respective V5- and FLAG-

constructs was verified by immunoblotting of whole cell extracts with the indicated antibodies. (Representative of three independent experiments).
E. Quantification of levels of phospho-tyrosine FLAG-PPARγ2 and total FLAG-PPARγ2 was performed by densitometry using ImageJ (n=3).

F. V5, SHP-1-V5 or PTP1B-V5 immunoprecipitates were incubated with DiFMUP (6,8-Difluoro-4-Methylumbelliferyl Phosphate) substrate. Reaction was performed at 37°C for 30min. Phosphatase activity was assessed by measuring fluorescence at 455 nm (setting: Ex 358/Em 455) (n=2). IP: immunoprecipitation, WCE: whole cell extracts

Figure 3: *CD36* and *FABP4* transcript levels are increased in NIH3T3, but not HepG2 cells in response to rosiglitazone treatment after overexpression of PPARγ2.
A. HepG2 cells and B. NIH3T3 cells were transfected with either *FLAG* empty vector or *FLAG-PPARg2*. After 24 h cells were treated either with DMSO or Rosiglitazone (100nM) for 16h. Expression of indicated proteins was determined by western blot (A and B) using respective antibodies. The amounts of *CD36* and *FABP4* transcripts were evaluated by qPCR (C and D) (n=3).

Figure 4: SHP-1 modulates PPARγ2 stability.
A. NIH3T3 cells were infected with retrovirus encoding empty vector (MSCV) or *PPARg2*. In addition, cells were transduced with lentivirus containing shRNA-control (*Luc*) or shRNA-*Shp-1*. The expression of the indicated proteins was determined by western blotting.
B. Quantification of PPARγ2 amounts was performed by densitometry using ImageJ (n=3).
C. *PPARg2* transcript levels were quantified by qPCR. (n=3).
D. NIH3T3 cells overexpressing *PPARg2* in SHP-1-WT (shRNA *Luc*) and SHP-1-KD (shRNA *Shp-1*) background were treated with cycloheximide (CHX) for the indicated times. The expression of respective proteins was determined by western blotting (n=2).
E. Quantification of PPARγ2 levels was performed by densitometry using ImageJ (n=2).

Figure 5: SHP-1 regulates PPARγ2-mediated adipogenesis through tyrosine residue 78.
A. NIH3T3 cells overexpressing *PPARg2* and *PPARg2 (Y78F*) in SHP-1-WT background were treated with 20 µM MG132 for 1h. In last 30 min of MG132 incubation, cells were treated with 20µM of bpV(HOpic). Protein lysates were prepared and immune-precipitated using a PPARγ-specific antibody. Expression of indicated proteins was determined by western blot using respective antibodies (n=2).

B. Knockdown (KD) of *SHP-1* in NIH3T3 cells stably expressing PPARγ2-WT or PPARγ2-Y78F using lentiviral-mediated shRNA transduction. Expression of indicated proteins was confirmed by western blot (n=2).
C, D and E: mRNA levels of *PPARg2* (C), *Fabp4* (D) and *Cd36* (E) were determined by qPCR in NIH3T3 SHP-1-WT or -KD cells stably transduced with empty vector (Control), PPARγ2-WT or -Y78F. Cells were treated with either DMSO or 100 nM rosiglitazone for 16h (n=3).
F. NIH3T3 cells with or without knockdown of *SHP-1* stably expressing either control retroviral vector, PPARg2-WT or -Y78F were cultured to confluence and then treated with rosiglitazone (100nM). On day 10, cells were fixed and lipid content was determined by oil red O staining.
G. Oil red O-stained NIH3T3 cells were dissolved in isopropanol and intracellular lipid content was quantified by measuring absorbance at 500 nm (n=3).
H: Model depicting the control of PPARγ2 activity by SHP-1.

Figures

Figure 1. SHP-1 interacts with PPARγ mainly through the SH2 domains.

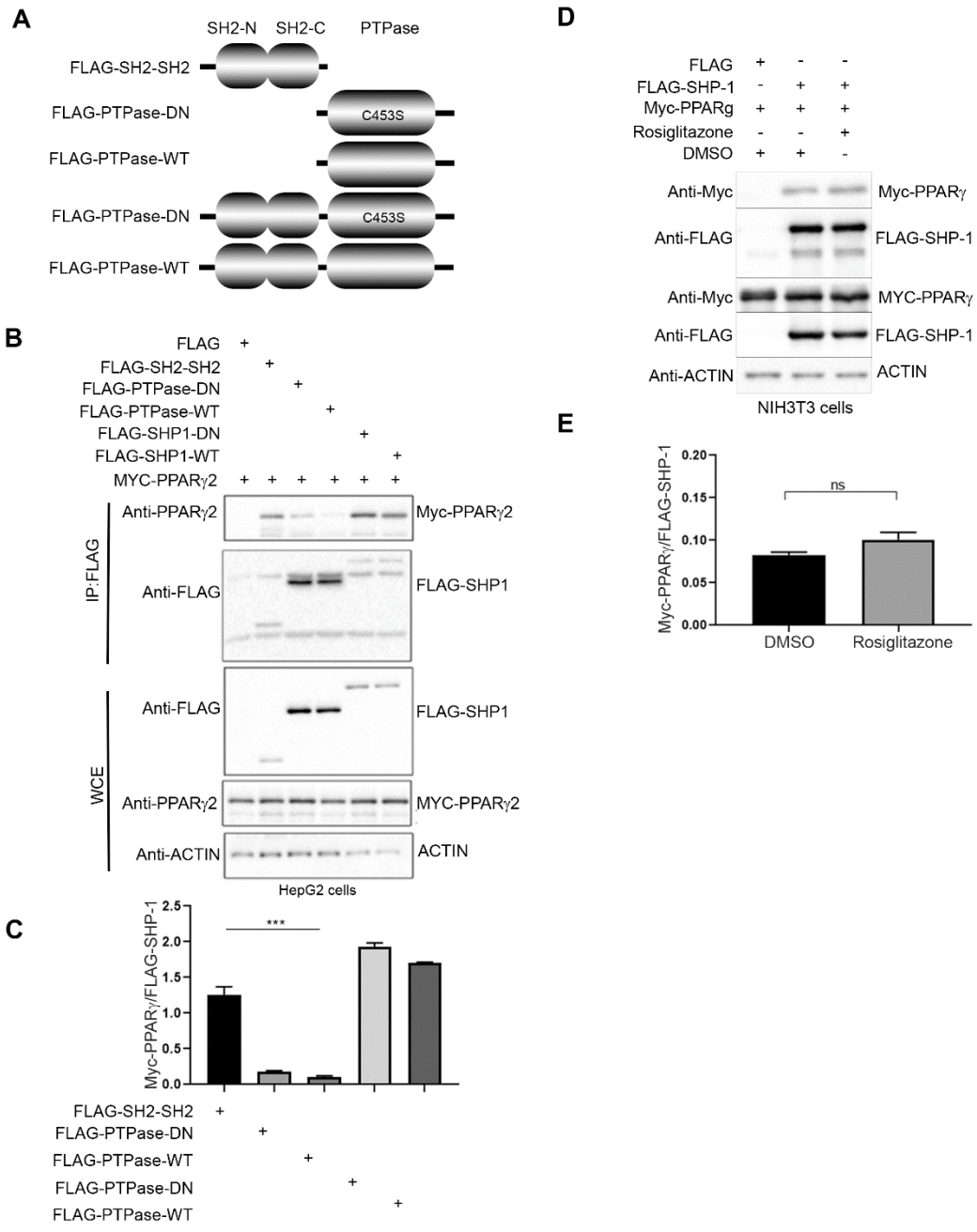

Figure 2. SHP-1 dephosphorylates PPARγ in vitro.

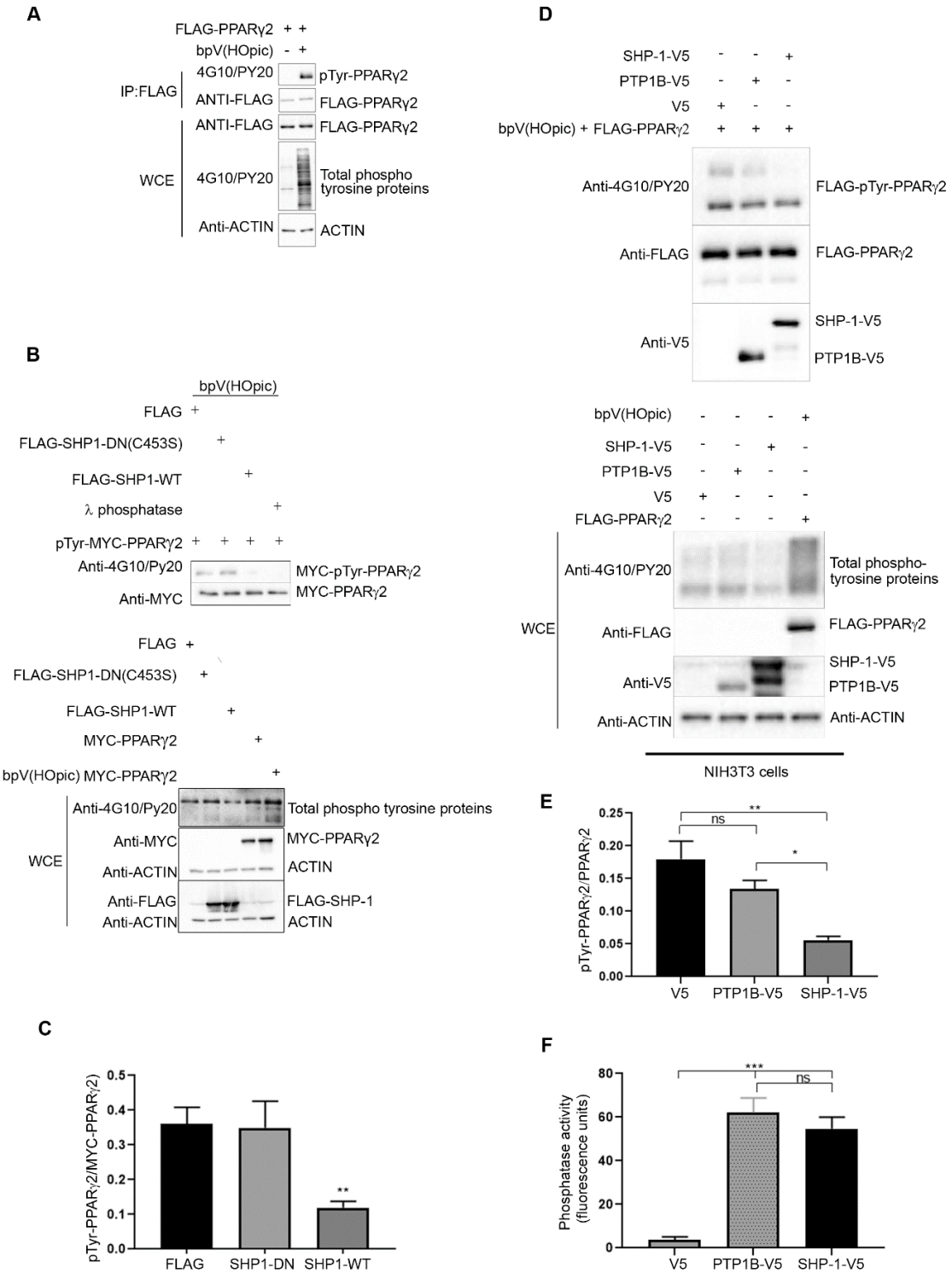

Figure 3. *CD36* and *FABP4* transcript levels are increased in NIH3T3, but not HepG2 cells in response to rosiglitazone treatment after overexpression of PPARγ.

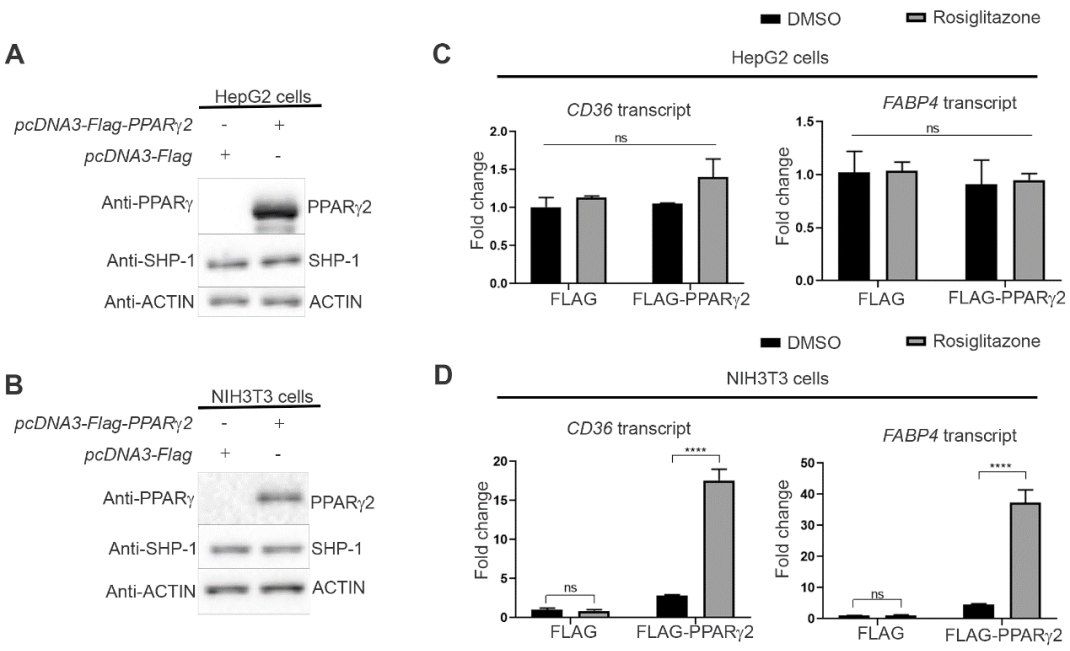

Figure 4. SHP-1 modulates PPARγ2 stability.

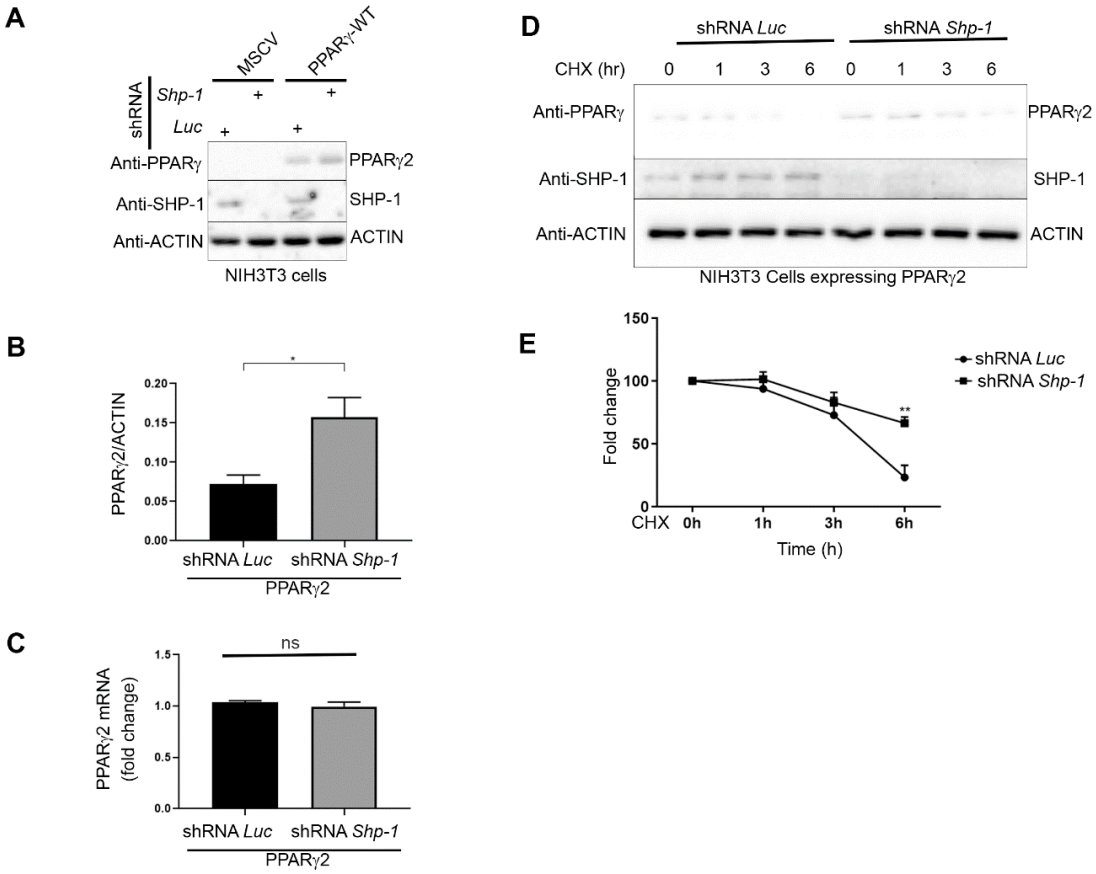

Figure 5. SHP-1 regulates PPARγ2-mediated lipogenesis through tyrosine residue 78.

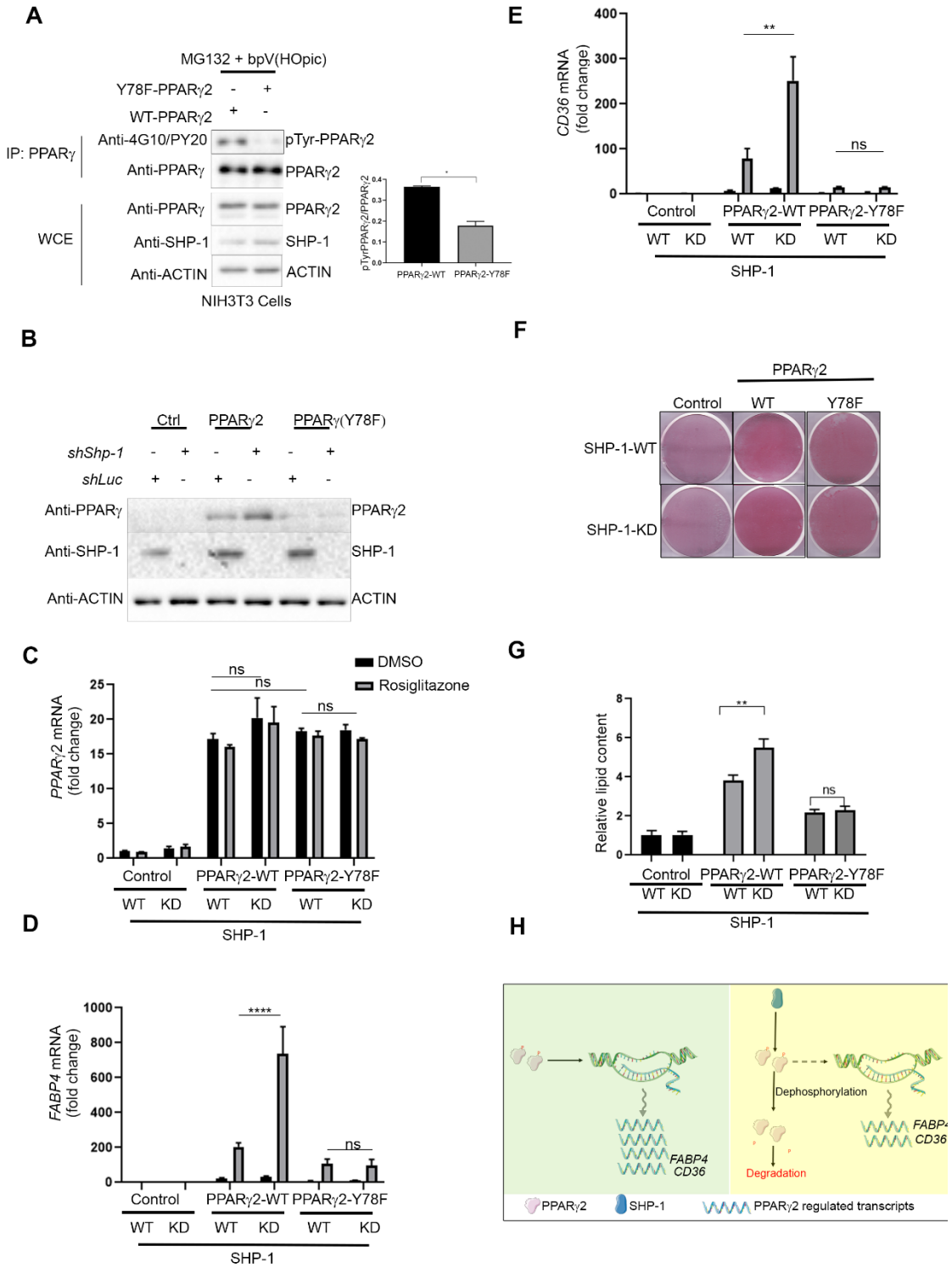

Supplementary Figure

Figure S1. Y78 residue is important for the stability of PPARγ2.

A. Generation of NIH3T3 cells stably expressing wild type PPARγ2 or PPARγ2-Y78F mutant using retroviral infection. Expression of indicated proteins was confirmed by western blotting.

B. *PPARg2* transcript levels in NIH3T3 cells either stably expressing *PPARg2* or *PPARg2-Y78F* was determined by qPCR (n=3).

C. NIH3T3 cells stably expressing *PPARg2* or *PPARg2-Y78F* were treated with proteasomal inhibitor MG132 (20μM) for indicated time points. Protein levels were determined by western blotting using indicated antibodies (n=2).

D. Levels of PPARγ were quantified by densitometry using ImageJ.

Figure S1. Y78 residue is important for the stability of PPARγ2.

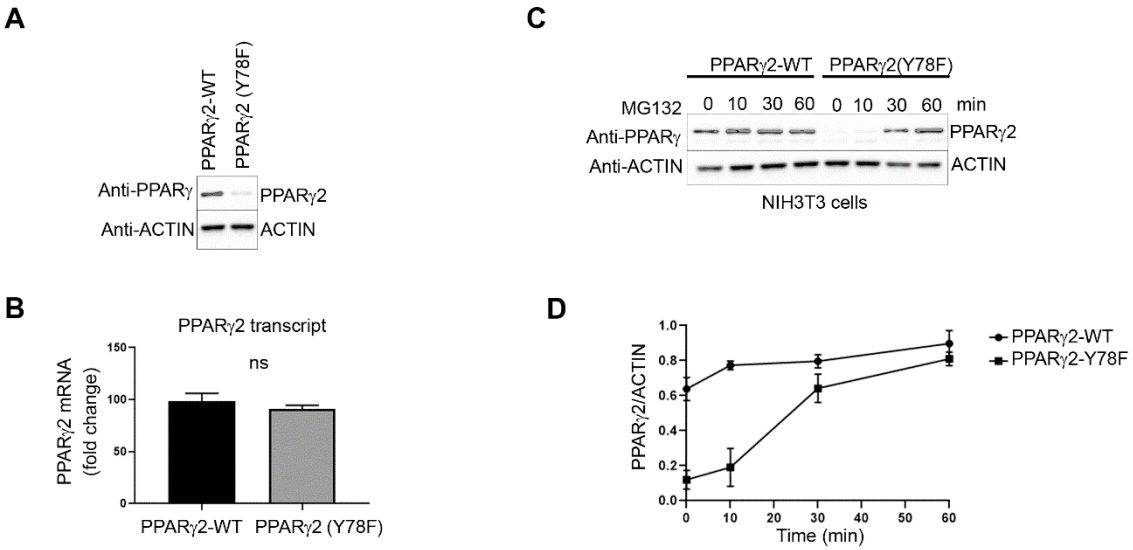

Supplementary information

Table S1. Primer sequences used for RT-qPCR

Gene	Species	Forward Primer	Reverse Primer	Reference
CD36	Human	AGATGCAGCCTCATTTCCAC	GCCTTGGATGGAAGAACAAA	
FABP4	Human	TGGTGGTGGAATGCGTCAT	GGTCAACGTCCCTTGGCTTA	
PPARG2	Human	ATGGGTGAAACTCTGGGAGATTC	TTCTTGTGATATGTTTGCAGACAG	Self designed
HPRT1	Human	AGATGGTCAAGGTCGCAAG	GTATTCATTATAGTCAAGGGCATATCC	(Sulzbach De Oliveira *et al*, 2016)
Cd36	Mouse	GTCCTGGCTGTGTTTGGAGG	GCTGCTACAGCCAGATTCAG	
Fabp4	Mouse	ATCAGCGTAAATGGGGATTTGG	GTCTGCGGTGATTTCATCGAA	(Keshet *et al*, 2014)
Pparg2		TCGCTGATGCACTGCCTATG	GAGAGGTCCACAGAGCTGATT	(Keshet *et al*, 2014)
B2m	Mouse	GGGTGGAACTGTGTTACGTAG	TGGTCTTTCTGGTGCTTGTC	

Table S2. shRNA sequence used in the study

shRNA	Name	Sequence
shShp1.68	TRCN0000028968	CCGGGCTAGACTGTGACATTGATATCTCGAGATATCAATGTCACAGTCTAGCTTTTT

Table S3. List of the antibodies and reagents used in the study.

Antibodies	Source	Identifier
Mouse anti-SHP1	ThermoFischer Scientific	MA5-11669 (1SH01)
Mouse anti-FLAG	Sigma	088K6018
Mouse anti-MYC	Sigma	M4439-100UL
Mouse anti-ACTIN	Millipore	MAB1501
Mouse anti-Phosphotyrosine (4G10)	Millipore	05-321
Mouse anti-Phosphotyrosine (PY20)	Abcam	Ab10321
Rabbit anti-V5	Cell Signaling	13202S
Rabbit anti eEF2	Cell Signaling	2332
Anti-FLAG® M2 Magnetic Beads	Sigma	M8823-5ML
Anti-FLAG® M2 Affinity Gel	Sigma	A2220-5ML
Anti-c-Myc Agarose Conjugate	Sigma	A7470
Mouse IgG2b	Biolegend	MG2b-57
Anti-FLAG® M2 Affinity Gel	Sigma	A2220-5ML
Anti-c-Myc Agarose Conjugate	Sigma	A7470
Mouse IgG2b	Biolegend	MG2b-57
Rabbit-PPARgamma (81B8)	Cell signaling	2443S
Reagents		
Tetracycline	Sigma	T7660-5G
Blasticidin S HCl	Invitrogen	R210-01
Hygromycin B	Invitrogen	10687-010
Zeocin	Invitrogen	R250-01
Puromycin dihydrochloride	Invivogen	ant-pr-1
Insulin (Humulin R)	Eli Lilly	HI0213
Poly-L-lysine hydrobromide	Sigma	P1399-25MG
DMEM low glucose	Wisent Bioproducts	319-010-CL
DMEM high glucose	Wisent Bioproducts	319-005-CL
RPMI	Wisent Bioproducts	350-000-CL
Jet Prime	Polyplus-transfection	114-15

Sodium orthovanadate	Sigma	S6508-50G
Sodium Fluoride	Sigma	S6776-100G
Calcium chloride	Sigma	C3981-500G
Sodium dodecyl sulfate	Sigma	L3771-500G
EDTA	Sigma	60-00-4
EGTA	Sigma	03777
β-glycerophosphate	Sigma	G5422-100G
Triton	Fisher	X-100
SDS	Sigma	L3771-500G
BSA	Sigma	A9647-100G
Glutamax	Gibco	35050-061
FBS	Gibco	16170-078
Advanced qpcr mastermix with supergreen lo-rox	Wisent bioproducts	800-431-UL
QIAquick PCR Purification Kit	Qiagen	28104
Amplex™ Red Glucose/Glucose Oxidase Assay Kit	Invitrogen	A22189
Rosiglitazone	SynFine	010301
bpV(HOpic)	Calbiochem	203701
Cycloheximide	Sigma	01810-1G
MG132	Calbiochem	474787-10mg
3X Flag peptides	Sigma	F4799-4mg
Direct-zol™ RNA MiniPrep	Zymoresearch	R2072
Oil Red O	Sigma	O-0625

Supplementary References

1. Keshet R, Bryansker Kraitshtein Z, Shanzer M, Adler J, Reuven N & Shaul Y (2014) c-Abl tyrosine kinase promotes adipocyte differentiation by targeting PPAR-gamma 2. *Proc Natl Acad Sci U S A* 111: 16365–16370

2. Sulzbach De Oliveira Hs, Biolchi V, Richardt Medeiros Hr, Bizerra Gandor Jantsch Dbg, Knabben De Oliveira Becker Delving Lk, Reckziegel R, Goettert Mi, Brum Is & Pozzobon A (2016) Effect of Helicobacter pylori on NFKB1, p38α and TNF-α mRNA expression levels in human gastric mucosa. *Exp Ther Med* 11: 2365–2372

Chapter III: SHP-1 acts as a co-activator of *PCK1* transcription to control gluconeogenesis

Chapitre III

SHP-1 agit comme un coactivateur de la transcription de PCK1 pour contrôler la gluconéogenèse

Résumé

Nous avons précédemment déterminé que la protéine-tyrosine phosphatase SHP-1 (PTPN6) régule négativement la signalisation de l'insuline, mais son impact sur le métabolisme hépatique du glucose et le contrôle systémique du glucose reste mal compris. Ici, nous montrons un nouveau mécanisme par lequel SHP-1 agit comme un co-activateur pour la transcription du gène de la phosphoénolpyruvate carboxykinase 1 (PCK1) pour augmenter la gluconéogenèse hépatique. SHP-1 est recruté dans les régions régulatrices du gène PCK1 et interagit avec l'ARN polymérase II. Le recrutement de SHP-1 à la chromatine dépend de son association avec le facteur de transcription transducteur de signal et activateur de transcription 5 (STAT5). La perte de SHP-1 ainsi que de STAT5 diminue le recrutement de l'ARN polymérase II vers le promoteur de PCK1 et par conséquent les niveaux d'ARNm de PCK1 conduisant donc à une baisse de la gluconéogenèse. Ce travail met en évidence un nouveau rôle nucléaire de SHP-1 en tant que régulateur transcriptionnel clé de la gluconéogenèse hépatique ajoutant un nouveau mécanisme au répertoire des fonctions de SHP-1 dans le contrôle métabolique.

SHP-1 acts as a co-activator of *PCK1* transcription to control gluconeogenesis

Amit Kumar[1†], Michael Schwab[1†], Maruhen Amir Datsch Silveira[2,3,5], Beisy Laborit Labrada[1], Marilyn Goudreault[6,8], Éric Fournier[2,3,4,5], Kerstin Bellmann[1], Nicole Beauchemin[7], Anne-Claude Gingras[8,9], Steve Bilodeau[2,3,4,5], Mathieu Laplante[1,3], and André Marette[1,10*]

[1]Centre de recherche de l'Institut universitaire de cardiologie et de pneumologie de Québec (CRIUCPQ), Faculté de Médecine, Université Laval, Québec, QC G1V 4G5, Canada.

[2]Centre de Recherche du CHU de Québec - Université Laval, Axe Oncologie, Québec, QC G1V 4G2, Canada.

[3]Centre de Recherche sur le Cancer de l'Université Laval, Québec, QC G1R 3S3, Canada.

[4] Centre de recherche en données massives de l'Université Laval, Québec, QC G1V 0A6, Canada.

[5]Département de biologie moléculaire, biochimie médicale et pathologie, Faculté de Médecine, Université Laval, Québec, QC G1V 0A6, Canada.

[6]Institute for Research in Immunology and Cancer, Université de Montréal, Montréal, QC H3T 1J4, Canada.

[7]Rosalind and Morris Goodman Cancer Research Centre, Depts. of Oncology, Medicine and Biochemistry, McGill University, Montreal, QC H3A 1A3, Canada.

[8]Lunenfeld-Tanenbaum Research Institute, Mount Sinai Hospital, Sinai Health System, Toronto, ON M5G 1X5, Canada.

[9]Department of Molecular Genetics, University of Toronto, Toronto, ON M5S 1A8, Canada.

[10]Institute of Nutrition and Functional Foods, Laval University, Québec, QC G1V 0A6, Canada.

† These authors contributed equally to this work.

* To whom correspondence may be addressed. **Email:** Andre.Marette@criucpq.ulaval.ca

Keywords: SHP-1/PTPN6, PCK1, Gluconeogenesis, Transcription, Liver

Abstract

We previously reported that the protein-tyrosine phosphatase SHP-1 (PTPN6) negatively regulates insulin signaling, but its impact on hepatic glucose metabolism and systemic glucose control remains poorly understood. Here, we show a new mechanism whereby SHP-1 acts as a co-activator for transcription of the phosphoenolpyruvate carboxykinase 1 (*PCK1*) gene to increase liver gluconeogenesis. SHP-1 is recruited to the regulatory regions of the *PCK1* gene and interacts with RNA polymerase II. The recruitment of SHP-1 to chromatin is dependent on its association with the transcription factor signal transducer and activator of transcription 5 (STAT5). Loss of SHP-1 as well as STAT5 decrease RNA polymerase II recruitment to the *PCK1* promoter and consequently *PCK1* mRNA levels leading to blunted gluconeogenesis. This work highlights a novel nuclear role of SHP-1 as a key transcriptional regulator of hepatic gluconeogenesis adding a new mechanism to the repertoire of SHP-1 functions in metabolic control.

Introduction

SHP-1 (encoded by gene *PTPN6*) is a non-membrane protein tyrosine phosphatase that plays important roles in controlling immune signaling pathways and fundamental physiological processes (Abram & Lowell, 2017; Neel *et al*, 2003; Xu *et al*, 2012, 2014a, 2014b). SHP-1 encompasses two SH2 domains at the N-terminus followed by a central phosphatase domain and a C-terminal regulatory tail (Wang *et al*, 2011; Yang *et al*, 2003). SHP-1 mainly exerts its functions by dephosphorylating target proteins in diverse signaling pathways in the cytoplasm, but is also found in the nucleus of epithelial cells (Craggs & Kellie, 2001; Duchesne *et al*, 2003; Rodríguez-Ubreva *et al*, 2010). Although the function of the SHP-1 nuclear pool remains mostly elusive, it has been reported that SHP-1 negatively regulates the activity of some transcription factors by dephosphorylation (Simoneau *et al*, 2011; Zhou *et al*, 2010). While SHP-1 is predominantly expressed in hematopoietic cells of all lineages, we have shown that this phosphatase is also expressed at lower levels in cells of metabolically active tissues such as the liver, skeletal muscle, and adipose tissue, where its expression is increased in obese mice fed a high-fat diet (Xu *et al*, 2012). We first reported that SHP-1 negatively regulates glucose metabolism and insulin action through interfering with the Insulin receptor-Phosphoinositide 3-kinase-AKT (IR-PI3K-AKT) axis, and by inhibiting insulin clearance targeting carcinoembryonic antigen related cell adhesion molecule 1 (CEACAM1) thus ultimately contributing to obesity-linked insulin resistance (Xu *et al*, 2014a; Dubois *et al*, 2006; Xu *et al*, 2009). Pharmacological inhibition and siRNA-mediated SHP-1 down-regulation in diet-induced obese mice improve insulin sensitivity and glucose tolerance (Krüger *et al*, 2016). However, SHP-1 also controls liver metabolism and glucose homeostasis independently from its ability to impede insulin signaling as shown by the lower fasting glucose and markedly decreased hepatic glucose production in mice with hepatocyte-specific conditional deletion of SHP-1 ($Ptpn6^{H\text{-}KO}$) as compared to their wild-type ($Ptpn6^{f/f}$) littermates (Xu *et al*, 2012). The underlying mechanism(s) involved in this liver phenotype remain to be elucidated.

Gluconeogenesis is a process by which the liver can synthesize glucose from non-carbohydrate sources during starvation (Shah & Wondisford, 2020), which can contribute to hyperglycemia in type 2 diabetic patients when not tightly controlled, resulting in increased endogenous glucose production (Boden *et al*, 2001). Phosphoenolpyruvate carboxykinase 1 (PCK1/PEPCK) is the key rate-limiting enzyme controlling gluconeogenesis (Yang *et al*, 2009a, 2009b). PCK1 catalyzes the conversion of oxaloacetate to phosphoenolpyruvate. *Pck1* gene silencing in mouse liver resulted in improved glycemic control and insulin sensitivity (Gómez-Valadés *et al*, 2008) whereas higher levels of *PCK1* transcripts have been reported in diabetic patients (Giralt *et al*, 2018). PCK1 activity is largely correlated with its transcription, which is controlled by several transcription factors and co-regulators, in turn regulated by hormones and diet (Puigserver *et al*, 2003; Koo *et al*, 2005; Yoon *et al*, 2001). Therefore, it is important to fully understand the mechanistic details of *PCK1* regulation at the transcriptional level, since altering hepatic gluconeogenesis by modulating *PCK1* gene expression could be a therapeutic approach to treat diabetes.

Both the nuclear and metabolic function of SHP-1 have been poorly characterized. Here, we describe the RNA polymerase II (RNA pol II) subunit POLR2J as a novel interaction partner of SHP-1. We are demonstrating a novel function of nuclear SHP-1 by acting as a transcriptional coactivator regulating *PCK1* gene expression. We showed that SHP-1 and the transcription factor signal transducer and activator of transcription 5 (STAT5) are interdependently associated with chromatin to control recruitment of RNA pol II to the *PCK1* promoter. Loss of SHP-1 as well as STAT5 inactivation or depletion decreased *PCK1* transcription and consequently gluconeogenesis in hepatocytes. In this study, we have demonstrated a new nuclear mechanism for SHP-1 by which it regulates *PCK1*-transcription and hepatic glucose production.

Materials and Methods

Cell lines and treatment

All cell lines were cultured at 37°C in a humidified atmosphere containing 5% CO2. HepG2 cells were cultured in Dulbecco's modified Eagle's medium (DMEM), low glucose supplemented with 10% fetal bovine serum (FBS). Flp-In™ 293 T-REx cell lines were cultured in DMEM (high glucose) containing 10% FBS. The rat hepatoma FAO cells were cultured in RPMI supplemented with 10% FBS. Primary mouse hepatocytes (PMH) were isolated from wild type mice (*Ptpn6*$^{f/f}$) and mice with liver-specific SHP-1 knock-out (*Ptpn6*$^{H\text{-}KO}$) previously used in our laboratory (Xu *et al*, 2012, 2014a).

Mammalian cell transfection

HepG2 and Flp-In™ 293 T-REx cell lines were transfected using jetPRIME® (Polyplus-transfection) and PureFection™ (System Biosciences) transfection reagents according to the manufacturer's instructions with cell confluence between 60 to 80%.

DNA constructs

To generate inducible *FLAG3-SHP-1* constructs for expression in Flp-In™ 293 T-REx cells, *SHP-1*- and *SHP-1-C453S*-cDNAs were PCR-amplified from existing vectors in our laboratory and cloned using *Hind*III and *Eco*RI restriction sites into pcDNA5/FRT/TO containing a sequence with three consecutive FLAG-epitopes for N-terminal tagging. To create *Myc3-POLR2J*- and *Myc3-POLR2C*-constructs, *POLR2J*- and *POLR2C*-cDNAs (vectors containing Human MGC Verified FL cDNA from OpenBiosystems/ThermoScientific) were PCR-amplified and cloned using *Bam*HI and *Xba*I restriction sites into pcDNA3.1-Myc3 (a kind gift from Dr. Sabine Elowe). The pLX304-STAT5A-V5 plasmid was a kind gift of Dr. Mathieu Laplante. The pAD-CMV-STAT5B-CMV-GFP plasmid was purchased from Addgene (#83257).

Generation of stable Flp-In T-Rex 293 cells inducibly expressing SHP-1 constructs

Flp-In™ 293 T-REx cell lines expressing either *3xFLAG*, *FLAG3-SHP1* (WT), or *FLAG3-SHP1-C453S* (DN) were generated using Flp-In™ T-REx™ 293 cell line system as described by the manufacturer (InVitrogen). Briefly, Flp-In™ T-REx™-293 cell cells were co-transfected with pcDNA5/FRT/TO expression vectors containing either *3xFLAG*, *FLAG3-SHP1* or *FLAG3-SHP1-C453S* together with Flp recombinase vector pOG44. Transfected cells were selected using Hygromycin B (200μg/ml) and expression was confirmed by immunoblotting.

Co-immunoprecipitation, immunoblotting and mass spectrometry

Flp-In T-REx 293 cells stably expressing either 3xFLAG, FLAG3-SHP1, or FLAG3-SHP1-C453S for affinity-purification mass spectrometry (AP-MS) were treated or not with 1 μM insulin for 30 min after serum-deprivation for 39 h. To express inducible constructs, cells were treated with tetracycline (1μg/ml) for 27 h (AP-MS) or 24 h (co-IP) before harvesting. HepG2 cells were co-transfected with either FLAG3-SHP1, FLAG3-SHP1-C453S or empty 3xFLAG vector and 3xMyc-tagged POLR2C, 3xMyc-tagged POLR2J, V5-tagged STAT5A or FLAG-tagged STST5B and harvested after 24h. For co-IP, cells were lysed in lysis buffer containing 20 mM Tris-HCl pH 7.5, 140 mM NaCl, 1 mM of $CaCl_2$ and $MgCl_2$, 10 mM NaF, 1% NP-40, 10% glycerol, 2 mM Na-Vanadate, 1 mM PMSF and protease inhibitors from Roche. Lysates were centrifuged and protein was quantified using the BCA method. 1 mg of total protein was incubated for 2hrs with anti-FLAG M2® affinity gel, anti-FLAG® M2 magnetic beads (Sigma-Aldrich) or Protein G Dynabeads pre-incubated with isotype control mouse IgG2b or anti SHP-1 antibody, followed by 5 washes with buffer containing 1X PBS, 2 mM Na-Vanadate, and protease inhibitor. Proteins were eluted using 1X Laemmli sample buffer. The expression of proteins was determined by immunoblotting, which was done as described before (Xu *et al*, 2014a; Dubois *et al*, 2006), using specific antibodies listed in Sup. table S5.

For AP-MS, samples were prepared as reported before (Chen & Gingras, 2007) and analyzed by liquid chromatography-tandem mass spectrometry on a Thermo LTQ instrument. The *Homo sapiens* RefSeq V29 appended with the reversed decoy

sequences was used for searching with the Mascot search engine allowing for methionine oxidation as a variable parameter. Evaluation of the recovered proteins in the SHP-1 purifications against the 9 selected negative controls was performed using SAINTexpress (Teo *et al*, 2014). Briefly, with each of the two baits (SHP-1 WT and SHP-1 substrate trapping mutant), for each prey (protein detected in a pull-down), the two highest spectral counts across four analyses (from duplicate purifications of samples treated or not with insulin) were selected for SAINTexpress scoring with default options. The SAINTexpress file was downloaded and used as an input for the visualization tool ProHits-viz; high-confidence interactors were those deemed by SAINTexpress to fall within 1% of the Bayesian False Discovery Rate (Knight *et al*, 2017).

Generation of single-cell cultures of SHP-1 KO HepG2 cells

The single guide RNAs (sgRNAs) targeting Shp1 were designed using CRISPR DESIGN (http://crispr.mit.edu) (Ran *et al*, 2013) (Sup. table S6). SgRNA with a high score and low off-target score were selected. Guide RNAs targeting different exons of PTPase domains and non-targeting (NT) guides were synthesized, annealed, and cloned in px459 V2.0 vector as described by Ran et al., 2013 (Ran *et al*, 2013) (Sup. table S2). SgRNA constructs were sequenced using U6 primer. HepG2 cells were seeded in a six-well plate (0.5 million per well) and were either left untransfected or transfected with Sg4, Sg1, and Sg6 (non-targeting guide, NT) constructs. Puromycin was added (2µg/ml) after 24h of transfection for a period of 3 days. After 3 days, cells were counted and 500 cells were seeded in a 150cm dish and incubated for 7-10 days at 37°C with 5%CO_2. Single-cell clones were transferred into 24 well plates using the filter disc method. When single-cell cultures were sufficiently grown, protein lysates were prepared and the expression of SHP-1 was determined by immunoblotting.

Cell fractionation

HepG2-cells expressing WT SHP-1 or CRISPR-KO-SHP-1 cell fractionations were performed using a subcellular protein fractionation kit for cultured cells (ThermoFisher Scientific) as per the manufacturer's instructions. Enrichment of marker proteins and SHP-1 was determined by immunoblotting.

ChIP-seq

HepG2 cells (WT or CRISPR-KO-SHP1) were cultured in 150 mm dishes. Cells were washed 3 times with PBS and $5x10^7$ cells for each ChIP-seq fixed with 1% formaldehyde for 10 min. Cross-linked cells were quenched using glycine for 5 min at room temperature. Cells were washed twice with ice-cold PBS and harvested using a silicon scraper. Cells were transferred to 50 ml falcon and centrifuged at 1350 g for 5 min. Pellets obtained were washed again with ice-cold PBS. Cell pellets were suspended in LB1 buffer (50 mM Hepes-KOH, pH7.5, 140 mM NaCl, 1 mM EDTA, 10 % glycerol, 0.5% IGEPAL, 0.25% Triton X-100, PMSF and protease inhibitor cocktail) and incubated at 4°C for 10 min with rotation. Pellets were obtained using centrifugation. The cell pellet was suspended in LB2 buffer (10 mM Tris-HCl, pH8.0, 200 mM NaCl, 1mM EDTA, and 0.5 mM EGTA supplemented with protease inhibitors) and incubated for 10 min at room temperature with rotation. Lysates were centrifuged at 1350 g for 5 min and pellets were suspended in sonication buffer (20 mM Tris-HCl pH 8.0, 150 mM NaCl, 2 mM EDTA pH 8.0, 0.1 % SDS, and 1% Triton X-100 supplemented with proteinase inhibitors). Lysates were sonicated using Bioruptor instrument (Diagenode) for a total of 6 min (high intensity, 12 cycles of 30 sec ON and 30 sec OFF) at 4°C to obtain a chromatin fragmentation of 200-900 bp. Protein G dynabeads pre-blocked in blocking solution (0.5% BSA in PBS) were incubated with antibodies (RPB1 and pSer2-RPB1) at 4°C for 6 h. Protein G Dynabead-antibody complexes were washed 3 times with 1 ml blocking solution, then added to chromatin preparations and incubated overnight at 4°C. Some portions of the chromatin were left untreated and used as whole-cell extract (WCE) control. Beads were washed once with Wash buffer B (20 mM Tris-HCl pH 8.0, 150 mM NaCl, 2 mM EDTA pH8.0, 0.1% SDS, 1% Triton X-100 and protease inhibitors),

followed by wash buffer C (20 mM Tris-HCl pH 8.0, 500 mM NaCl, 2 mM EDTA pH 8.0, 0.1% SDS, 1% Triton X-100 and protease inhibitors), and Wash Buffer D (10 mM Tris-HCl pH8.0, 250 mM LiCl, 1 mM EDTA pH 8.0, 1% NP40 and protease inhibitor) and TE buffer (10 mM Tris pH 8.0, 1 mM EDTA, 50 mM NaCl and protease inhibitors). Complexes were eluted off the beads using elution buffer containing 50 mM Tris-HCl pH 8.0, 1 mM EDTA pH 8.0, and 50 mM NaCl. Beads were collected and incubated at 65°C overnight to reverse cross-linked. In parallel, WCE were also reverse cross-linked. Samples were subsequently treated with RNase A (Ambion) at 37°C for 2 hours followed by Proteinase K (Invitrogen) treatment at 55°C for 30 min. DNA was purified using the phenol-chloroform method. Libraries were constructed from ChIP- and WCE-samples using NEBNext Ultra II DNA library prep kit (New England Biolabs) according to the manufacturer's instructions and single-end sequenced (50 bp) on an Illumina HiSeq 2500 instrument at the Next-Generation Sequencing Platform of the CHU de Québec-Université Laval Research Center (CRCHUQ).

ChIP-seq data analysis

Analysis of raw sequencing reads was performed using the MUGQIC ChIP-Seq pipeline (Bourgey *et al*, 2019). Briefly, reads were trimmed for adaptor sequences using Trimmomatic (Bolger *et al*, 2014). High-quality reads were aligned to the human reference genome (GRCH38/hg38) with the BWA aligner (Li & Durbin, 2009). Narrow peaks were called using MACS2 (Zhang *et al*, 2008), using the corresponding input DNA as background. For visualization, reads were extended 200 bp using the bamCoverage function from deepTools (Ramírez *et al*, 2016). Gene tracks were created using the University of California, Santa Cruz (USCS) Genome Browser (Kent *et al*, 2002) (Sup. table S6). Differential binding between SHP1-KO and WT was assessed using csaw (Lun & Smyth, 2016).

Micrococcal nuclease ChIP

Frozen cross-linked cell pellets of HepG2 cells (WT or CRISPR-KO-SHP-1) were thawed and suspended in LB1 buffer. Cell pellets were homogenized with 15 strokes of a Dounce glass pestle A and 30 strokes of pestle B on ice. Cell pellets were obtained upon centrifugation, suspended in LB2 buffer, and incubated for 10 min at room temperature with rotation. Lysates were centrifuged and suspended in Mnase digestion buffer (New England Biolabs) containing 500 gel units of Micrococcal nuclease (Fig. S4A). Cell pellets were incubated at 37°C for 20 min with shaking (300rpm). The reaction was stopped by adding EDTA. Cell pellets were centrifuged and suspended in ChIP-SDS lysis buffer (1% SDS, 10mM EDTA, 50mM Tris, pH 8.1). Pellets were homogenized with 100 strokes of Dounce pestle B on ice. Homogenized pellets were observed under the microscope (Fig. S4B). Pellets were subjected to three-freeze thaw cycles using liquid nitrogen. Lysates were diluted in ChIP dilution buffer (0.01% SDS, 1.1% Triton X-100, 1.2mM EDTA, 16.7mM Tris-HCl, pH 8.1, 167mM NaCl) and precleared with pre-blocked Protein G Dynabeads at 4°C for 1 h. At this point, an aliquot of samples was taken for input controls. The precleared lysates were incubated with antibody (SHP-1 or RPB1)-pre-blocked protein G Dynabead complexes overnight at 4°C. Beads were consecutively washed each time for 15 min at 4°C with low salt immune complex wash buffer (0.1% SDS, 1% Triton X-100, 2mM EDTA, 20mM Tris-HCl, pH 8.1, 150mM NaCl), followed by high Salt Immune Complex Wash Buffer (0.1% SDS, 1% Triton X-100, 2mM EDTA, 20mM Tris-HCl, pH 8.1, 500mM NaCl), LiCl Immune Complex Wash Buffer (0.25M LiCl, 1% IGEPAL-CA630, 1% deoxycholic acid (sodium salt), 1mM EDTA, 10mM Tris, pH 8.1.) and finally with TE Buffer (10mM Tris-HCl, 1mM EDTA, pH 8.0.) A small portion of the beads was eluted using Laemmli buffer and the amount of immunoprecipitated SHP-1 was determined by immunoblotting (Fig. S4C). The rest of the complexes were eluted off the beads and reverse cross-linking, RNAse-, and Proteinase K-treatment was done as described earlier. Same treatments were given to the input controls. DNA was purified using Qiagen PCR purification kit as per the manufacturer's instruction. ChIP was analyzed using qPCR. The sequences of the oligonucleotides used in the study are shown in Sup. table S3. The value of enrichment was calculated relative to the input controls.

Lentivirus preparation and generation of knockdown cell lines.

Lentiviruses were prepared by transfecting the lentiviral constructs encoding *shControl* (a kind gift from M. Laplante), *shPtpn6* or *shStat5* (Sup. table S4) along with psPAX2 and pMD2G into 293T cells using JetPRIME transfection reagent as per the manufacturer's instruction. Viruses containing supernatants were collected 48 h after transfection and filtered using a 0.45µm filter (Cribbs *et al*, 2013).
FAO or HepG2 cells were transduced with lentiviral supernatant (*shControl*, *shPtpn6* or *shStat5*) in the presence of polybrene (8 µg/ml). After 24h of infection cells were washed three times with media and maintained in fresh virus-free media for 24h. Then, cells were split and selected using puromycin (2 µg/ml) for 3 days. Knockdown efficiency of shRNAs was assessed by western blotting.

RNA isolation and RT-qPCR

Total RNA was isolated using the Zymo research kit (Irvine, USA) kit) as per the manufacturer's instructions. The purity and quantity of RNA were assessed using Biodrop. Two micrograms of total RNA were reverse transcribed using high capacity cDNA reverse transcription kit (Applied biosystems) supplied with random primers. cDNA was diluted and expression of transcripts was determined using multicell advance qPCR master mix (Wisent). Fold change in transcript levels was determined using 2-delta Ct method (Livak & Schmittgen, 2001) with normalization to the reference genes *HPRT1* or *ACTIN or B2M* (for primary mouse hepatocytes). The sequences of primers used in the study are listed in Sup. table S3.

Hepatocyte isolation and culture

Primary hepatocytes were isolated from 14-17 week old female and male mice with the same genotypes used in our previous study (Xu *et al*, 2012, 2014a). All mice were on a C57BL/6J background. Animals were handled in accordance with the guidelines of the Canadian Council on Animal Care and protocols were approved by the Animal Ethics Committee of Université Laval (CPAUL). The hepatocytes were isolated using the two-step collagenase perfusion method (Seglen, 1976). Briefly,

the liver was infused with 50 ml of perfusion buffer via the vena cava inferior followed by 50 ml of perfusion buffer containing (20 mg collagenase type II, 0.51 mM $CaCl_2$, 137 mM NaCl, 7 mM KCl , 0.7 mM Na_2HPO_4 and 10 mM Hepes). After the perfusion, the liver was excised and disintegrated in cell attachment medium (M199 medium supplemented with 10% fetal bovine serum, 1% penicillin/streptomycin, 500 nM dexamethasone, 10 nM insulin, 200 nM thyroid hormone, 0.1 % BSA and 1X Glutamax). The cellular suspension was centrifuged at 400 rpm for 2 min. The cell viability was measured by trypan blue exclusion assay. The cells were resuspended in cell attachment media and seeded on collagen I pre-coated plates. After the culture medium was changed two hours later for serum-free hepatocyte culture basal medium (M199 supplemented with 50X B27 Supplement, 1X Glutamax, 1 % penicillin/streptomycin, 100 nM dexamethasone and 2 nM nicotinamide) to remove unattached cells, the hepatocytes were used for the experiments.

Hepatic glucose production assay

Hepatic glucose production in FAO cells and PMH was essentially measured as described before (Chevrier *et al*, 2015). FAO cells expressing control shRNA or Ptpn6 shRNA and PMH isolated from *Ptpn6*$^{f/f}$ or *Ptpn6*$^{H\text{-}KO}$ mice were serum-deprived overnight and either left untreated or treated with 50µM Stat5 inhibitor (CAS 285986-31-4). Cells were washed three times with PBS and incubated with hepatic glucose production media (D-MEM without glucose (Sigma #D5030-1L), containing sodium bicarbonate (3.7 g/L), sodium pyruvate (2 mM) and sodium L-lactate (20 mM), pH7.3) (with and without Stat5 inhibitor). After 5 hours, supernatants were collected and glucose levels were determined using Amplex red Glucose/Glucose Oxidase assay kit (Invitrogen). Cells were washed with PBS and lysed in 50 mM NaOH. Protein levels were measured using the BCA method. Levels of glucose produced by the cells were normalized to the protein concentrations. Similarly, glucose production assay was performed in SHP-1 WT and SHP-1-KD FAO cells with or without STAT5-specific shRNA.

Quantification and statistical analysis

All data are reported as means ± SE. Statistical analysis was performed using the GraphPad Prism 8 software. We used an unpaired two-tailed t-test or two-way ANOVA with Tukey's post hoc test. The number of biological repeats included in the experiments is mentioned in the figure legends. Western blots were quantified using ImageJ.

Results

SHP-1 interacts with proteins of the transcriptional machinery.

To characterize new, regulatory metabolic SHP-1-functions, we sought to identify SHP-1-interacting partners using an affinity-purification mass spectrometry approach (Chen & Gingras, 2007). We generated stably transfected Flp-In™ 293 T-REx cells, which inducibly express proteins of interest from a common locus. Total extracts from cells producing FLAG-tagged wild-type (WT) SHP-1 or the SHP-1-C453S substrate-trapping mutant, which was shown to stabilize the association between phosphatase and substrate (Timms *et al*, 1998), were FLAG-immunoprecipitated. The resulting samples were analyzed by liquid chromatography-tandem mass spectrometry. To define specific interactors of SHP-1, cells expressing an empty FLAG-vector and a fusion of FLAG to the green fluorescent protein, described elsewhere (Mellacheruvu *et al*, 2013) were used as controls. SAINTexpress (Teo *et al*, 2014) was used to identify the high-confidence interaction partners for SHP-1 or SHP-1-C453S (Sup. table1). The WT and C453S constructs recovered largely different sets of interaction partners, with the C453S mutant recovering more interaction partners. Interestingly, POLR2J (RPB11), a small subunit of RNA polymerase II, was identified as one of the novel significant SHP-1-C453-associated proteins after FLAG-purification mass spectrometry (Fig. 1A and Sup. table1). Co-immunoprecipitation experiments in the Flp-In™ 293 T-REx cells confirmed the binding of POLR2J to SHP-1 and, consistent with the mass spectrometry analysis, showed that endogenous POLR2J interacted mainly with the

substrate-trapping SHP-1-C453S mutant (Fig. 1B). Although this implies that POLR2J might be a target for SHP-1 phosphatase activity, we were not able to detect tyrosine-phosphorylated POLR2J even after immunoprecipitation from cells treated with the general tyrosine phosphatase inhibitors bpV(pic) and bpV(HOpic) respectively (Fig. S1). This suggests that POLR2J is not a direct substrate of SHP-1, but that its interaction is stabilized by inactivation of the phosphatase by an unknown mechanism.

To validate the association between SHP-1 and POLR2J we performed co-immunoprecipitation experiments in HepG2 hepatic cells. We confirmed that exogenously co-expressed FLAG-tagged SHP-1 interacted with Myc-tagged POLR2J in these cells (Fig. 1C) and that SHP-1 was also bound to POLR2C (RPB3), another subunit of RNA pol II closely associated with POLR2J (Fig. 1D). Together, these data demonstrate a physical interaction between SHP-1 and RNA pol II in hepatic cells suggesting a role for SHP-1 in transcriptional regulation.

SHP-1 localizes to the chromatin-bound nuclear fraction.

SHP-1 exhibits a different intracellular distribution depending on the cell type with a mainly cytoplasmic localization in hematopoietic cells, but predominantly nuclear staining in non-hematopoietic cells (Craggs & Kellie, 2001; Duchesne *et al*, 2003; Rodríguez-Ubreva *et al*, 2010). To study the localization and function of SHP-1 in hepatocytes in more detail, we generated clonal HepG2 cell lines with and without deletion of *PTPN6* by using CRISPR/Cas9 technology. The knockout was confirmed by western blot (Fig. 2A and Fig. S2). Since SHP-1 would require to be localized on the chromatin in order to regulate RNA pol II, we performed subcellular fractionation experiments in HepG2-cells and primary mouse hepatocytes (PMH) isolated from wild type mice (*Ptpn6*$^{f/f}$) and mice with liver-specific SHP-1 knock-out (*Ptpn6*$^{H\text{-}KO}$) previously generated in our laboratory (Xu *et al*, 2012, 2014a). The analyses in both cell types showed that SHP-1 is localized in the cytoplasmic, membrane and nuclear fractions (Fig. 2B and C). Similar to the transcription factor cAMP response element binding protein (CREB), SHP-1 was not only found in the soluble nuclear fraction,

but also in the chromatin-bound nuclear fraction, where RNA pol II represented by its subunit POLR2C was localized (Fig. 2B and C). These experiments demonstrate that SHP-1 is recruited to chromatin, where transcriptional regulation occurs.

SHP-1 regulates *PCK1* transcript levels by controlling recruitment of RNA pol II to the *PCK1* promoter.

The presence of SHP-1 at the chromatin and its physical interaction with a RNA pol II subunit infer its direct role in transcriptional regulation. To investigate the functional relationship between SHP-1 and the transcription machinery, we profiled the genome-wide occupancy of POLR2A/RPB1, the largest subunit of the RNA pol II, in SHP-1 WT and SHP-1 KO HepG2 cells using chromatin immunoprecipitation coupled with massively parallel DNA sequencing (ChIP-seq) (Gade & Kalvakolanu, 2012). As expected, we found a similar number of regions occupied by RPB1 in WT (46,045) and SHP-1 KO (41,605) cells. The distribution of RNA pol II-occupied regions was also similar between the WT and SHP-1 KO cells, with an average of 46% peaks at the promoter (44.6% and 47.4%, respectively), 40% in the gene body (40.4% and 39.4%) and 14.1% at distal regions (15% and 13.2%). To determine the functional consequences on RNA pol II recruitment, differential signal densities between WT and SHP1-KO cells were quantified. A total of 417 genomic regions harbored significant changes in RPB1 signal densities (p<0.001) in SHP-1 KO versus SHP-1 WT cells (Fig. 3A) with a striking bias for RPB1 losses (398 regions) compared to RPB1 gains (19 regions). The majority (60.5%) of RPB1 losses were located at gene promoters, while 25.1% were in the gene body (exon, intron, 5' UTR and 3' UTR) and 14.3% at distal intergenic regions (Fig. 3A). By comparison, the small number of regions gaining RPB1 occupancy were found mostly in the gene body (63.1%). These results suggest that SHP-1 plays a role in the recruitment of RNA pol II at the promoter region at a subset of genes.

Among the genes that were decreased in RNA pol II density at their promoter in SHP-1 KO cells, we found *PCK1*, one of the master regulators of glucose homeostasis, which controls the first step of gluconeogenesis (Yang *et al*, 2009a,

2009b). Since our previous *in vivo* findings showed reduced levels of fasting glucose and a decrease in hepatic gluconeogenesis in mice carrying a liver-specific SHP1-KO as compared to their wild type counterparts (Xu *et al*, 2012, 2014a), we focused our analysis on *PCK1* to expand on the role of SHP-1 in transcription and to further mechanistically understand the impact of SHP-1 on glucose metabolism. RPB1 ChIP-qPCR analysis confirmed the decrease of RNA pol II occupancy at the *PCK1* promoter of SHP-1 KO compared to WT cells observed in the RPB1 ChIP-seq (Fig. 3B and 3C). Observing a decrease in RNA pol II occupancy at the promoter region is not always associated with a loss in transcriptional activity. To ascertain that SHP-1 was modulating the transcriptional activity at the *PCK1* gene, we measured the levels of phosphorylation of RPB1 on serine 2, which is associated with transcriptional elongation (West & Corden, 1995). Density profiles of phospho-Ser2 RPB1 ChIP-seq showed decreased levels at the *PCK1* gene in SHP-1 KO cells (Fig. 3B). Together, these data imply that SHP-1 is involved in the transcriptional regulation of *PCK1*.

To corroborate our ChIP-data and determine whether SHP-1 generally controls the transcription of *PCK1* in hepatic cells, we measured mRNA levels in various liver cell lines and hepatic tissue by qPCR. We found a significant decrease of *PCK1* transcript levels in two independent HepG2 SHP-1 CRISPR KO cell lines (Fig. 3D). To validate the effects of SHP-1 on *PCK1* transcription in another liver cell line, we used *Ptpn6* shRNA to knock down *Ptpn6* by about 50% in FAO rat hepatoma cells as compared to the control shRNA (Fig. S3A). As observed in HepG2 cells, we found a significant decrease in the *Pck1* transcript levels in FAO cells expressing *Ptpn6* shRNA (Fig. 3E). To further establish the *in vivo* relevance of our data, we determined the levels of *PCK1* transcripts in both liver tissues as well as PMH isolated from $Ptpn6^{f/f}$ and $Ptpn6^{H\text{-}KO}$ mice(Xu *et al*, 2014a). We observed a significant decrease in *PCK1* transcript levels in both liver tissue (Fig. 3F) and isolated hepatocytes (Fig. 3G) from mice with a liver-specific ablation of SHP-1. Taken together our data indicate that hepatic SHP-1 positively modulates *PCK1* transcript levels *in vitro* and *in vivo* further substantiating an important role for SHP-1 in transcription in this metabolic organ.

SHP-1 binds STAT5-dependently to the *PCK1* promoter to regulate RNA pol II recruitment and *PCK1* transcription.

Since SHP-1 does not harbor any known DNA- or chromatin-binding domain we postulated that its recruitment to chromatin was transcription factor-dependent. We searched for transcription factor binding motifs in the *PCK1* promoter using the PROMO tool with a dissimilarity rate cutoff set to <15% (Farré *et al*, 2003) and compared the resulting list of transcription factors to the SHP-1-interacting partners listed in BioGRID (Stark *et al*, 2006). As seen in the Venn diagram in Fig. 4A, the only common protein between the two datasets was the transcription factor STAT5, which refers to two nearly identical proteins, STAT5A and STAT5B. Interestingly, STAT5 was already implicated in the control of *PCK1* transcription in mammary gland epithelial cells and adipocytes (Hsieh *et al*, 2011; Kaltenecker *et al*, 2017), but a potential role for SHP-1 in this mechanism has never been reported. Using co-immunoprecipitation experiments, we confirmed the association between STAT5A and STAT5B with SHP-1 (Fig. 4B and 4D). An enzyme-substrate-interaction between SHP-1 and STAT5 was ruled out because STAT5A and STAT5B bound with the same affinity to WT SHP1 and the substrate-trapping SHP-1-C453S mutant (Fig. 4C and E).

We next asked whether STAT5 recruits SHP-1 to the *PCK1* promoter, and how the SHP-1-STAT5 interaction affects the recruitment of RNA Pol II to the *PCK1* promoter. To answer these questions, we knocked down STAT5 in HepG2-WT and HepG2-SHP-1-KO cells using shRNAs and achieved a 50% reduction in STAT5 protein levels (Fig. 5A). Loss of STAT5 in HepG2-WT cells did not affect the total amount of SHP-1 (Fig. 5A and 5B) ruling out that STAT5-mediated effects on SHP-1 are dependent on modulating its expression. We performed SHP-1 and RPB1 ChIP-qPCR analyses targeting the *PCK1* promoter in HepG2-WT and SHP-1-KO cells either expressing control or *STAT5* shRNA. Confirming the previously detected chromatin recruitment (Fig. 2), SHP-1 bound to the *PCK1* promoter in SHP-1-WT cells (Fig. 5C). STAT5 knockdown significantly reduced the recruitment of SHP-1 indicating that STAT5 is required for the binding of SHP-1 to the *PCK1* promoter.

Moreover, we found that the enrichment of RPB1 on the *PCK1* promoter was significantly decreased after knockdown of STAT5 as well as in SHP-1-KO cells, but knockdown of STAT5 in SHP-1 KO cells did not further impact this reduction (Fig. 5D). As analyzed by qPCR, the reduced levels of RNA pol II at the *PCK1* promoter correlated with significantly decreased *PCK1* transcript levels in STAT5 KD, SHP-1 KO and STAT5 KD/SHP-1 KO cells (Fig. 5E). Taken together, these results suggest that STAT5-mediated binding of SHP-1 to the *PCK1* promoter regulates recruitment of RNA pol II to activate transcription.

Gluconeogenesis is controlled by SHP-1 together with STAT5.

PCK1 is a major regulator of gluconeogenesis. To investigate the importance of SHP-1 and STAT5 in a physiological context, we measured *PCK1* transcript levels and glucose production in FAO cells, a well-established model for glucose metabolism studies (Houde *et al*, 2010; Smadja-Lamère *et al*, 2013; Shum *et al*, 2016, 2019). To better understand the relationship between SHP-1 and STAT5 in this process, we used depletion and activation of STAT5 in the SHP-1 WT or SHP-1 knockdown (KD) background and measured *Pck1* transcript levels and glucose production. Knockdown of STAT5 using shRNA in FAO SHP-1-WT and FAO SHP-1-KD cells reduced the levels of STAT5 protein in these cells by 50% (Fig. S3B). We found that depletion of SHP-1 as well as STAT5 significantly decreased *Pck1* transcript levels as well as glucose production (Fig. 6A and B). Importantly, STAT5 knockdown did not further decrease *Pck1* transcript levels and the glucose production capacity in cells depleted of SHP-1, suggesting that SHP-1 and STAT5 act on the same pathway in the regulation of gluconeogenesis mediated by control of *PCK1* transcription. Furthermore, these data confirm the results obtained in HepG2 cells (Fig. 5) and show that the SHP-1-STAT5-mediated modulation of RNA pol II recruitment to the *PCK1* promoter followed by differential *PCK1* transcription is mirrored by metabolic changes as reflected by hepatic glucose production.

To further validate our data obtained in the STAT5 depleted FAO cells, we used a pharmacological approach to inhibit STAT5 in FAO cells but also in freshly isolated

mouse hepatocytes (PMH), the gold standard for *ex vivo* glucose production assays (Nagarajan *et al*, 2019). We treated FAO SHP-1-WT and FAO SHP-1-KD cells, as well as PMH isolated from *Ptpn6*$^{f/f}$ and *Ptpn6*$^{6H\text{-}KO}$ mice with a STAT5 inhibitor (CAS 285986-31-4) (Müller *et al*, 2008) and assessed *PCK1* transcription by qPCR and gluconeogenesis as a functional readout. We found in both hepatic cellular models that STAT5 inhibitor treatment (Stat5i) of SHP-1-WT cells significantly reduced *Pck1* transcript levels, but not to the same extent as observed in SHP-1 knockdown cells exhibiting no further decrease in *Pck1* transcript levels indicating that SHP-1 and STAT5 act on the same pathway (Fig. 6C and D). Matching the *Pck1* transcript level data, we observed a significant decrease of glucose production in FAO-cells and PMH after treatment of SHP-1 WT cells with STAT5 inhibitor. A larger decrease in SHP-1 KD cells, which was not significantly changed after STAT5 inhibitor treatment of these cells, was noticed (Fig. 6E and F).

Discussion

We discovered a new metabolic function for SHP-1 in the liver, whereby the PTPase activates hepatic gluconeogenesis through co-activation of *PCK1*-transcription in liver cells. Moreover, we elucidated the molecular mechanism of this transcriptional regulation by demonstrating that SHP-1 through interaction with the transcription factor STAT5 mediates the recruitment of RNA pol II to the *PCK1* promoter.

SHP-1 is a major regulator of cytokine and immune receptor signaling in hematopoietic cells, and we have shown that it negatively modulates insulin signaling in metabolic tissues (Abram & Lowell, 2017; Xu *et al*, 2014a; Dubois *et al*, 2006). In the present study, we have identified a novel, non-canonical SHP-1 function as a key promoter of hepatic gluconeogenesis. Despite being mainly characterized as a cytoplasmic protein-tyrosine phosphatase, SHP-1 is also found in nuclei of epithelial cells (Craggs & Kellie, 2001; Duchesne *et al*, 2003; Ram & Waxman, 1997). Here, we report for the first time that SHP-1 is associated with the promoter region of the *PCK1* gene. Furthermore, we provide strong evidence that SHP-1 interacts with RNA pol II and the transcription factor STAT5. The recruitment

of SHP-1 to chromatin at the *PCK1* promoter was dependent on STAT5. Depletion of SHP-1 not only reduced recruitment of RNA pol II to the *PCK1* promoter, but also decreased *PCK1* transcript levels and subsequently gluconeogenesis. STAT5 downregulation or inhibition had similar effects on RNA pol II recruitment, *Pck1* transcription and glucose production. Thus, we propose a conceptual model whereby STAT5-bound SHP-1 regulates *Pck1* transcription through RNA polymerase II recruitment to its promoter, thereby modulating glucose production by liver cells (Fig. 6G).

These findings provide a key mechanism to explain our previous observations that mice with hepatocyte-specific deletion of SHP-1 (*Ptpn6*$^{6H\text{-}KO}$) exhibited lower fasting glycemia as compared to their littermate WT controls (Xu *et al*, 2012, 2014a). These mice also exhibited a markedly reduced hepatic glucose production rate (Xu *et al*, 2012). The pathophysiological relevance of these findings is further demonstrated by the observation that SHP-1 expression is increased in the liver of high-fat fed obese mice and that SHP-1 genetic deletion reduced fasting hyperglycemia but also fully blunted the elevated glucose production in these obese mice (Xu *et al*, 2012).

Coactivators are a diverse group of proteins which modulate transcription in a variety of different ways (Näär *et al*, 2001; Spiegelman & Heinrich, 2004). These include modification of chromatin or unraveling DNA through enzymatic action of the coactivators and functioning as an adaptor between the transcription factor and RNA pol II to direct recruitment of the transcriptional apparatus. We found that the tyrosine-phosphatase SHP-1 shows the characteristics of a typical transcriptional coactivator. SHP-1 binds to the transcription factor STAT5, which is required for the association of SHP-1 to chromatin. SHP-1 interacts with RNA pol II and its invalidation reduces recruitment of RNA pol II to the regulatory regions of the *PCK1* gene and *PCK1* transcription. Despite using four different domain prediction tools namely Motif Scan (MyHits, SIB, Switzerland), InterPro 5, MOTIF (GenomeNet, Japan) and CD-Search (Conserved Domain Databases), we were not able to identify a DNA- or chromatin-binding domain in SHP-1 corroborating that the recruitment of SHP-1 to the *PCK1* promoter is mediated by the interaction with promoter-bound STAT5. However, the exact spatial and temporal formation of the SHP-1-STAT5

complex and its association with chromatin has yet to be determined. Since a plethora of transcription factors including cAMP responsive element binding protein (CREB) (Horike *et al*, 2008) and Forkhead box protein O1 (FOXO1) (Puigserver *et al*, 2003) have been described for control of *PCK1* transcription, it will be interesting to elucidate how the SHP-1-STAT5 complex is integrated into this circuitry of transcriptional regulation.

Recently, Phosphatase and tensin homologue deleted on chromosome ten (PTEN), a dual specificity phosphatase (Steinbach *et al*, 2019), as well as the insulin receptor (Hancock *et al*, 2019) were shown to regulate gene transcription in a very similar fashion to SHP-1 by interacting directly with the transcription machinery. These studies did not provide conclusive, mechanistic evidence for the requirement of PTEN phosphatase activity, nor the insulin receptor kinase activity for direct transcriptional regulation. The increased interaction between POLR2J and the substrate-trapping SHP-1-C453S-mutant as compared with the WT form of SHP-1 suggests that POLR2J might be a substrate for SHP-1, but would also be in agreement with a phosphatase activity-independent binding of SHP-1 through its phosphatase-domain to POLR2J. SHP-1 has been implicated in the modulation of transcriptional processes by dephosphorylating different transcription factors (Simoneau *et al*, 2011; Zhou *et al*, 2010), but phosphatase activity-independent functions for SHP-1 have been demonstrated for other cellular processes such as leukocyte-associated immunoglobulin-like receptor 1 and cytokine signaling (Kang *et al*, 2015; Minoo *et al*, 2004).

Phosphorylation of STAT proteins at a C-terminal tyrosine-residue generally leads to transcriptional activation by enhancing dimerization, nuclear localization and binding of STATs to DNA (Levy & Darnell, 2002; Reich & Liu, 2006). While some studies reported that SHP-1 can dephosphorylate STAT5 *in vitro* (Paling & Welham, 2002; Xiao *et al*, 2009), another study suggests that STAT5 is not a substrate of SHP-1, but rather of SHP-2 (Yu *et al*, 2000). In our experiments, tyrosine-phosphorylation does not seem to be required for STAT5-SHP-1 interaction or STAT5-SHP-1-mediated *Pck1* transcriptional regulation. STAT5 bound equally well to WT-SHP-1 and a substrate-trapping SHP-1 mutant inferring, suggesting that their

interaction is tyrosine phosphorylation-independent and STAT5 is not a direct substrate for SHP-1. Our data support tyrosine-phosphorylation-independent mechanisms in this process adding to the growing list of evidence that unphosphorylated STATs (uSTAT) can play important roles in transcriptional regulation (Yang & Stark, 2008). Indeed, uSTAT3 has been reported to form a complex with unphosphorylated NF-κb to translocate into the nucleus and activate a subset of NF-κb dependent genes (Yang *et al*, 2007). Additionally, uSTAT6 cooperates with the transcriptional coactivator p300 to enhance COX-2 expression (Cui *et al*, 2007). Furthermore, uSTAT5 by regulating heterochromatin stability through interaction with HP1α (Hu *et al*, 2013) or in cooperation with the transcription factor CTCF, regulates different transcriptional programs (Park *et al*, 2016).

Our ChIP-analysis revealed that SHP-1 might be involved in the transcriptional modulation of many other genes than *PCK1* that may also carry key functional roles in the modulation of glucose metabolism in liver and other metabolic tissues. Future work beyond the scope of this study will consist of expanding our analysis to determine whether the mechanism by which SHP-1 exerts transcriptional regulation is relevant to other genes. Furthermore, other factors may be involved in the specific interactions between SHP-1, STAT5 and RNA pol II. The interplay of these factors fine-tuning SHP-1 recruitment to chromatin will need to be further investigated.

In summary, we report the novel observation that SHP-1 directly associates with the *PCK1* promoter through STAT5 and RNA pol II and that its presence is required for *PCK1* expression, thereby promoting hepatic gluconeogenesis. Our data suggest that SHP-1 nuclear localization is necessary to control hepatic gluconeogenesis through directly regulating STAT5-mediated *PCK1* transcription, thus adding a novel nuclear mechanism to the repertoire of SHP-1 metabolic functions.

Materials availability

Further information and requests for resources and reagents should be directed to and will be fulfilled by the corresponding author, André Marette (Andre.Marette@criucpq.ulaval.ca)

Data and code availability

The ChIP-seq data discussed in Fig. 3 of this manuscript have been deposited in NCBI's Gene Expression Omnibus (Edgar *et al*, 2002) and are accessible through GEO Series accession number GSE174142 (https://www.ncbi.nlm.nih.gov/geo/query/acc.cgi?acc=GSE174142).

Acknowledgments

This work was supported by a Canadian Institutes of Health Research (CIHR) Foundation grant (FDN-143247) to A.M. A.K. was partially supported by an IUCPQ student grant. A.M. holds a CIHR/Pfizer research Chair in the pathogenesis of insulin resistance and cardiovascular diseases.

Author contributions

M.S., K.B., A.K., N.B. and A.M. conceived and designed the project. A.K., M.S., M.A.D.S., B.L.L., and K.B. performed experiments. A.K., M.S., K.B., M.L., S.B., A.G. and A.M. interpreted the results. A.G. and M.G. performed mass spectrometry and analysed the results. M.A.D.S and S.B. helped with CHIP-seq experiments and analysed the results. E.F. performed computational analysis of ChIP-seq data. A.K., M.S., K.B. and A.M. wrote the manuscript with comments from the other authors.

Declaration of interests

The authors declare no competing interests.

References

1. Abram CL, Lowell CA (2017) Shp1 function in myeloid cells. ***J Leukoc Biol*** **102:** 657–675

2. Boden G, Chen X, Stein TP (2001) Gluconeogenesis in moderately and severely hyperglycemic patients with type 2 diabetes mellitus. ***Am J Physiol Endocrinol Metab*** **280:** E23-30

3. Bolger AM, Lohse M, Usadel B (2014) Trimmomatic: a flexible trimmer for Illumina sequence data. ***Bioinformatics*** **30:** 2114–2120

4. Bourgey M, Dali R, Eveleigh R, Chen KC, Letourneau L, Fillon J, Michaud M, Caron M, Sandoval J, Lefebvre F, *et al* (2019) GenPipes: an open-source framework for distributed and scalable genomic analyses. ***Gigascience*** **8**

5. Chen GI, Gingras A-C (2007) Affinity-purification mass spectrometry (AP-MS) of serine/threonine phosphatases. ***Methods*** **42:** 298–305

6. Chevrier G, Mitchell PL, Rioux L-E, Hasan F, Jin T, Roblet CR, Doyen A, Pilon G, St-Pierre P, Lavigne C, *et al* (2015) Low-Molecular-Weight Peptides from Salmon Protein Prevent Obesity-Linked Glucose Intolerance, Inflammation, and Dyslipidemia in LDLR-/-/ApoB100/100 Mice. ***J Nutr*** **145:** 1415–1422

7. Craggs G, Kellie S (2001) A functional nuclear localization sequence in the C-terminal domain of SHP-1. ***J Biol Chem*** **276:** 23719–23725

8. Cribbs AP, Kennedy A, Gregory B, Brennan FM (2013) Simplified production and concentration of lentiviral vectors to achieve high transduction in primary human T cells. ***BMC Biotechnol*** **13:** 98

9. Cui X, Zhang L, Luo J, Rajasekaran A, Hazra S, Cacalano N, Dubinett SM (2007) Unphosphorylated STAT6 contributes to constitutive cyclooxygenase-2 expression in human non-small cell lung cancer. ***Oncogene*** **26:** 4253–4260

10. Dubois M-J, Bergeron S, Kim H-J, Dombrowski L, Perreault M, Fournès B, Faure R, Olivier M, Beauchemin N, Shulman GI, *et al* (2006) The SHP-1 protein tyrosine phosphatase negatively modulates glucose homeostasis. ***Nat Med*** **12:** 549–556

11. Duchesne C, Charland S, Asselin C, Nahmias C, Rivard N (2003) Negative regulation of beta-catenin signaling by tyrosine phosphatase SHP-1 in intestinal epithelial cells. ***J Biol Chem*** **278:** 14274–14283

12. Edgar R, Domrachev M, Lash AE (2002) Gene Expression Omnibus: NCBI gene expression and hybridization array data repository. ***Nucleic Acids Res*** **30:** 207–210

13. Farré D, Roset R, Huerta M, Adsuara JE, Roselló L, Albà MM, Messeguer X (2003) Identification of patterns in biological sequences at the ALGGEN server: PROMO and MALGEN. ***Nucleic Acids Res* 31:** 3651–3653

14. Gade P, Kalvakolanu DV (2012) Chromatin Immunoprecipitation Assay as a Tool for Analyzing Transcription Factor Activity. ***Methods Mol Biol* 809:** 85–104

15. Giralt A, Denechaud P-D, Lopez-Mejia IC, Delacuisine B, Blanchet E, Bonner C, Pattou F, Annicotte J-S, Fajas L (2018) E2F1 promotes hepatic gluconeogenesis and contributes to hyperglycemia during diabetes. ***Mol Metab* 11:** 104–112

16. Gómez-Valadés AG, Méndez-Lucas A, Vidal-Alabró A, Blasco FX, Chillon M, Bartrons R, Bermúdez J, Perales JC (2008) Pck1 Gene Silencing in the Liver Improves Glycemia Control, Insulin Sensitivity, and Dyslipidemia in db/db Mice. ***Diabetes* 57:** 2199–2210

17. Hancock ML, Meyer RC, Mistry M, Khetani RS, Wagschal A, Shin T, Ho Sui SJ, Näär AM, Flanagan JG (2019) Insulin Receptor Associates with Promoters Genome-wide and Regulates Gene Expression. ***Cell* 177:** 722-736.e22

18. Horike N, Sakoda H, Kushiyama A, Ono H, Fujishiro M, Kamata H, Nishiyama K, Uchijima Y, Kurihara Y, Kurihara H, *et al* (2008) AMP-activated protein kinase activation increases phosphorylation of glycogen synthase kinase 3beta and thereby reduces cAMP-responsive element transcriptional activity and phosphoenolpyruvate carboxykinase C gene expression in the liver. ***J Biol Chem* 283:** 33902–33910

19. Houde VP, Brûlé S, Festuccia WT, Blanchard P-G, Bellmann K, Deshaies Y, Marette A (2010) Chronic Rapamycin Treatment Causes Glucose Intolerance and Hyperlipidemia by Upregulating Hepatic Gluconeogenesis and Impairing Lipid Deposition in Adipose Tissue. ***Diabetes* 59:** 1338–1348

20. Hsieh C-W, Huang C, Bederman I, Yang J, Beidelschies M, Hatzoglou M, Puchowicz M, Croniger CM (2011) Function of phosphoenolpyruvate carboxykinase in mammary gland epithelial cells. ***J Lipid Res* 52:** 1352–1362

21. Hu X, Dutta P, Tsurumi A, Li J, Wang J, Land H, Li WX (2013) Unphosphorylated STAT5A stabilizes heterochromatin and suppresses tumor growth. ***Proc Natl Acad Sci U S A* 110:** 10213–10218

22. Kaltenecker D, Mueller KM, Benedikt P, Feiler U, Themanns M, Schlederer M, Kenner L, Schweiger M, Haemmerle G, Moriggl R (2017) Adipocyte STAT5 deficiency promotes adiposity and impairs lipid mobilisation in mice. ***Diabetologia* 60:** 296–305

23. Kang X, Lu Z, Cui C, Deng M, Fan Y, Dong B, Han X, Xie F, Tyner JW, Coligan JE, *et al* (2015) The ITIM-containing receptor LAIR1 is essential for acute myeloid leukaemia development. ***Nat Cell Biol* 17:** 665–677

24. Kent WJ, Sugnet CW, Furey TS, Roskin KM, Pringle TH, Zahler AM, Haussler and D (2002) The Human Genome Browser at UCSC. ***Genome Res* 12:** 996–1006

25. Knight JDR, Choi H, Gupta GD, Pelletier L, Raught B, Nesvizhskii AI, Gingras A-C (2017) ProHits-viz: a suite of web tools for visualizing interaction proteomics data. ***Nat Methods* 14:** 645–646

26. Koo S-H, Flechner L, Qi L, Zhang X, Screaton RA, Jeffries S, Hedrick S, Xu W, Boussouar F, Brindle P, *et al* (2005) The CREB coactivator TORC2 is a key regulator of fasting glucose metabolism. ***Nature* 437:** 1109–1111

27. Krüger J, Wellnhofer E, Meyborg H, Stawowy P, Östman A, Kintscher U, Kappert K (2016) Inhibition of Src homology 2 domain-containing phosphatase 1 increases insulin sensitivity in high-fat diet-induced insulin-resistant mice. ***FEBS Open Bio* 6:** 179–189

28. Levy DE, Darnell JE (2002) Stats: transcriptional control and biological impact. ***Nat Rev Mol Cell Biol* 3:** 651–662

29. Li H, Durbin R (2009) Fast and accurate short read alignment with Burrows-Wheeler transform. ***Bioinformatics* 25:** 1754–1760

30. Livak KJ, Schmittgen TD (2001) Analysis of relative gene expression data using real-time quantitative PCR and the 2(-Delta Delta C(T)) Method. ***Methods* 25:** 402–408

31. Lun ATL, Smyth GK (2016) csaw: a Bioconductor package for differential binding analysis of ChIP-seq data using sliding windows. ***Nucleic Acids Res* 44:** e45

32. Mellacheruvu D, Wright Z, Couzens AL, Lambert J-P, St-Denis NA, Li T, Miteva YV, Hauri S, Sardiu ME, Low TY, *et al* (2013) The CRAPome: a contaminant repository for affinity purification-mass spectrometry data. ***Nat Methods* 10:** 730–736

33. Minoo P, Zadeh MM, Rottapel R, Lebrun J-J, Ali S (2004) A novel SHP-1/Grb2–dependent mechanism of negative regulation of cytokine-receptor signaling: contribution of SHP-1 C-terminal tyrosines in cytokine signaling. ***Blood* 103:** 1398–1407

34. Müller J, Sperl B, Reindl W, Kiessling A, Berg T (2008) Discovery of chromone-based inhibitors of the transcription factor STAT5. ***Chembiochem*** **9:** 723–727

35. Näär AM, Lemon BD, Tjian R (2001) Transcriptional coactivator complexes. ***Annu Rev Biochem*** **70:** 475–501

36. Nagarajan SR, Paul-Heng M, Krycer JR, Fazakerley DJ, Sharland AF, Hoy AJ (2019) Lipid and glucose metabolism in hepatocyte cell lines and primary mouse hepatocytes: a comprehensive resource for in vitro studies of hepatic metabolism. ***Am J Physiol Endocrinol Metab*** **316:** E578–E589

37. Neel BG, Gu H, Pao L (2003) The 'Shp'ing news: SH2 domain-containing tyrosine phosphatases in cell signaling. ***Trends Biochem Sci*** **28:** 284–293

38. Paling NRD, Welham MJ (2002) Role of the protein tyrosine phosphatase SHP-1 (Src homology phosphatase-1) in the regulation of interleukin-3-induced survival, proliferation and signalling. ***Biochem J*** **368:** 885–894

39. Park HJ, Li J, Hannah R, Biddie S, Leal-Cervantes AI, Kirschner K, Flores Santa Cruz D, Sexl V, Göttgens B, Green AR (2016) Cytokine-induced megakaryocytic differentiation is regulated by genome-wide loss of a uSTAT transcriptional program. ***EMBO J*** **35:** 580–594

40. Puigserver P, Rhee J, Donovan J, Walkey CJ, Yoon JC, Oriente F, Kitamura Y, Altomonte J, Dong H, Accili D, *et al* (2003) Insulin-regulated hepatic gluconeogenesis through FOXO1–PGC-1α interaction. ***Nature*** **423:** 550–555

41. Ram PA, Waxman DJ (1997) Interaction of growth hormone-activated STATs with SH2-containing phosphotyrosine phosphatase SHP-1 and nuclear JAK2 tyrosine kinase. ***J Biol Chem*** **272:** 17694–17702

42. Ramírez F, Ryan DP, Grüning B, Bhardwaj V, Kilpert F, Richter AS, Heyne S, Dündar F, Manke T (2016) deepTools2: a next generation web server for deep-sequencing data analysis. ***Nucleic Acids Res*** **44:** W160-165

43. Ran FA, Hsu PD, Wright J, Agarwala V, Scott DA, Zhang F (2013) Genome engineering using the CRISPR-Cas9 system. ***Nature Protocols*** **8:** 2281–2308

44. Reich NC, Liu L (2006) Tracking STAT nuclear traffic. ***Nat Rev Immunol*** **6:** 602–612

45. Rodríguez-Ubreva FJ, Cariaga-Martinez AE, Cortés MA, Romero-De Pablos M, Ropero S, López-Ruiz P, Colás B (2010) Knockdown of protein tyrosine phosphatase SHP-1 inhibits G1/S progression in prostate cancer cells

through the regulation of components of the cell-cycle machinery. ***Oncogene* 29:** 345–355

46. Seglen PO (1976) Preparation of isolated rat liver cells. ***Methods Cell Biol* 13:** 29–83

47. Shah AM, Wondisford FE (2020) Tracking the carbons supplying gluconeogenesis. ***J Biol Chem* 295:** 14419–14429

48. Shum M, Bellmann K, St-Pierre P, Marette A (2016) Pharmacological inhibition of S6K1 increases glucose metabolism and Akt signalling in vitro and in diet-induced obese mice. ***Diabetologia* 59:** 592–603

49. Shum M, Houde VP, Bellemare V, Junges Moreira R, Bellmann K, St-Pierre P, Viollet B, Foretz M, Marette A (2019) Inhibition of mitochondrial complex 1 by the S6K1 inhibitor PF-4708671 partly contributes to its glucose metabolic effects in muscle and liver cells. ***J Biol Chem* 294:** 12250–12260

50. Simoneau M, Coulombe G, Vandal G, Vézina A, Rivard N (2011) SHP-1 inhibits β-catenin function by inducing its degradation and interfering with its association with TATA-binding protein. ***Cell Signal* 23:** 269–279

51. Smadja-Lamère N, Shum M, Déléris P, Roux PP, Abe J-I, Marette A (2013) Insulin activates RSK (p90 ribosomal S6 kinase) to trigger a new negative feedback loop that regulates insulin signaling for glucose metabolism. ***J Biol Chem* 288:** 31165–31176

52. Spiegelman BM, Heinrich R (2004) Biological control through regulated transcriptional coactivators. ***Cell* 119:** 157–167

53. Stark C, Breitkreutz B-J, Reguly T, Boucher L, Breitkreutz A, Tyers M (2006) BioGRID: a general repository for interaction datasets. ***Nucleic Acids Res* 34:** D535–D539

54. Steinbach N, Hasson D, Mathur D, Stratikopoulos EE, Sachidanandam R, Bernstein E, Parsons RE (2019) PTEN interacts with the transcription machinery on chromatin and regulates RNA polymerase II-mediated transcription. ***Nucleic Acids Res* 47:** 5573–5586

55. Teo G, Liu G, Zhang J, Nesvizhskii AI, Gingras A-C, Choi H (2014) SAINTexpress: improvements and additional features in Significance Analysis of INTeractome software. ***J Proteomics* 100:** 37–43

56. Timms JF, Carlberg K, Gu H, Chen H, Kamatkar S, Nadler MJ, Rohrschneider LR, Neel BG (1998) Identification of major binding proteins and substrates for the SH2-containing protein tyrosine phosphatase SHP-1 in macrophages. ***Mol Cell Biol* 18:** 3838–3850

57. Wang W, Liu L, Song X, Mo Y, Komma C, Bellamy HD, Zhao ZJ, Zhou GW (2011) Crystal structure of human protein tyrosine phosphatase SHP-1 in the open conformation. ***J Cell Biochem*** **112:** 2062–2071

58. West ML, Corden JL (1995) Construction and analysis of yeast RNA polymerase II CTD deletion and substitution mutations. ***Genetics*** **140:** 1223–1233

59. Xiao W, Hong H, Kawakami Y, Kato Y, Wu D, Yasudo H, Kimura A, Kubagawa H, Bertoli LF, Davis RS, *et al* (2009) Tumor suppression by phospholipase C-beta3 via SHP-1-mediated dephosphorylation of Stat5. ***Cancer Cell*** **16:** 161–171

60. Xu E, Charbonneau A, Rolland Y, Bellmann K, Pao L, Siminovitch KA, Neel BG, Beauchemin N, Marette A (2012) Hepatocyte-specific Ptpn6 deletion protects from obesity-linked hepatic insulin resistance. ***Diabetes*** **61:** 1949–1958

61. Xu E, Dubois M-J, Leung N, Charbonneau A, Turbide C, Avramoglu RK, DeMarte L, Elchebly M, Streichert T, Lévy E, *et al* (2009) Targeted disruption of carcinoembryonic antigen-related cell adhesion molecule 1 promotes diet-induced hepatic steatosis and insulin resistance. ***Endocrinology*** **150:** 3503–3512

62. Xu E, Forest M-P, Schwab M, Avramoglu RK, St-Amand E, Caron AZ, Bellmann K, Shum M, Voisin G, Paquet M, *et al* (2014a) Hepatocyte-specific Ptpn6 deletion promotes hepatic lipid accretion, but reduces NAFLD in diet-induced obesity: potential role of PPARγ. ***Hepatology*** **59:** 1803–1815

63. Xu E, Schwab M, Marette A (2014b) Role of protein tyrosine phosphatases in the modulation of insulin signaling and their implication in the pathogenesis of obesity-linked insulin resistance. ***Rev Endocr Metab Disord*** **15:** 79–97

64. Yang J, Kalhan SC, Hanson RW (2009a) What Is the Metabolic Role of Phosphoenolpyruvate Carboxykinase? ***J Biol Chem*** **284:** 27025–27029

65. Yang J, Liao X, Agarwal MK, Barnes L, Auron PE, Stark GR (2007) Unphosphorylated STAT3 accumulates in response to IL-6 and activates transcription by binding to NFkappaB. ***Genes Dev*** **21:** 1396–1408

66. Yang J, Liu L, He D, Song X, Liang X, Zhao ZJ, Zhou GW (2003) Crystal structure of human protein-tyrosine phosphatase SHP-1. ***J Biol Chem*** **278:** 6516–6520

67. Yang J, Reshef L, Cassuto H, Aleman G, Hanson RW (2009b) Aspects of the control of phosphoenolpyruvate carboxykinase gene transcription. ***J Biol Chem*** **284:** 27031–27035

68. Yang J, Stark GR (2008) Roles of unphosphorylated STATs in signaling. ***Cell Res* 18:** 443–451

69. Yoon JC, Puigserver P, Chen G, Donovan J, Wu Z, Rhee J, Adelmant G, Stafford J, Kahn CR, Granner DK, *et al* (2001) Control of hepatic gluconeogenesis through the transcriptional coactivator PGC-1. ***Nature* 413:** 131–138

70. Yu CL, Jin YJ, Burakoff SJ (2000) Cytosolic tyrosine dephosphorylation of STAT5. Potential role of SHP-2 in STAT5 regulation. ***J Biol Chem* 275:** 599–604

71. Zhang Y, Liu T, Meyer CA, Eeckhoute J, Johnson DS, Bernstein BE, Nusbaum C, Myers RM, Brown M, Li W, *et al* (2008) Model-based analysis of ChIP-Seq (MACS). ***Genome Biol* 9:** R137

72. Zhou X, Gallazzini M, Burg MB, Ferraris JD (2010) Contribution of SHP-1 protein tyrosine phosphatase to osmotic regulation of the transcription factor TonEBP/OREBP. ***PNAS* 107:** 7072–7077

Figure Legends

Figure 1. **SHP-1 interacts with proteins of the transcriptional machinery.**
A. Dot plot of the confident interactions identified by mass spectrometry after co-immunoprecipitation with SHP-1 in Flp-In T-REx 293 cells. The color-coding maps to average spectral counts (capped at 25), and the size of the circle to the relative spectral abundance across the baits. The edge color represents the Bayesian False Discovery Rate (BFDR); see legend inset for details.
B. Western blot analysis of co-immunoprecipitation showing binding of inducibly expressed FLAG3-SHP-1 constructs to endogenous POLR2J in Flp-In T-REx 293 cells (representative of three experiments).
C and D. Co-immunoprecipitation experiments showing the association of transiently expressed FLAG3-SHP-1 with Myc3-POLR2J and Myc3-POLR2C in HepG2 cells (representative of three experiments), WCE: whole cell lysate.

Figure 2. SHP-1 localizes to the chromatin bound nuclear fraction.
A. Representative western blot confirming CRISPR-mediated *SHP-1 KO* in HepG2 cells (WT(UT): untransfected, WT(NT): non-targeting construct, KO: SHP-1 targeting constructs), ns: non-specific band.
B. Western blot of HepG2 cell-fractionation assay showing the presence of SHP-1 in cytosolic, membrane, soluble nuclear and chromatin bound nuclear fraction. Marker proteins confirming enrichment of different fractions (representative three experiments).
C. Western blot of PMH isolated from *Ptpn6*$^{f/f}$ and *Ptpn6*$^{H\text{-}KO}$ mice cell-fractionation assay showing the presence of SHP-1 in cytosolic, membrane, soluble nuclear and chromatin bound nuclear fraction. Marker proteins confirming enrichment of different fractions (representative figure of three mice in each group).

Figure 3. Genome wide mapping of RPB1 binding regions in liver cells reveals the master regulator of gluconeogenesis *PCK1* as a target for SHP-1-mediated transcription regulation.
A. Distribution of significantly different RPB1 signal densities classified by human genomic annotations (hg38) in SHP-1 KO compared to SHP-1 WT cells.
B. Visualization of ChIP-seq data in the UCSC genome browser. Chip-seq distribution for RPB1 and phospho-RPB1-Ser2 at *PCK1* gene.
C. ChIP-qPCR validation of RPB1 binding on *PCK1* promoter. (n=3) (*p<0.05).
D. Expression levels of *PCK1* transcripts in SHP1 WT and KO HepG2 cells analyzed by qPCR. ****p < 0.0001 (n=3).
E. *PCK1*-mRNA levels in FAO cells with (*Ptpn6* shRNA) or without (control shRNA) knockdown of *SHP-1* determined by qPCR (n=3). **p<0.01 (n=3).
F. Levels of *PCK1* transcripts in liver lysates of *Ptpn6*$^{f/f}$ and *Ptpn6*$^{H\text{-}KO}$ mice analyzed by qPCR. ***p<0.001 (n=4).
G. Levels of *PCK1* transcripts in primary hepatocytes isolated from *Ptpn6*$^{f/f}$ and *Ptpn6*$^{H\text{-}KO}$ mice analyzed by qPCR. **p<0.05 (n=4).

Figure 4. SHP-1 interacts with STAT5 *in vitro* and shares a common binding region at the *PCK1*-promoter.

A. Venn diagram predicting common factors by comparing transcription factors that bind to *PCK1*-promoter (PROMO) and proteins that interact with SHP-1 (BioGRID).

B. Western blot analysis of co-immunoprecipitation showing interaction of SHP-1 and STAT5A in HepG2 cells using co-expression of V5-tagged *STAT5A* and FLAG-tagged *SHP-1*.

C. Quantification of SHP-1/STAT5A binding determined by densitometry using Image J (n=2).

D. Western blot analysis of co-immunoprecipitation showing interaction of SHP-1 and STAT5B in HepG2 cells using co-expression of FLAG-tagged *STAT5B* and FLAG-tagged *SHP-1*. Immunoprecipitation was performed using a SHP-1-specific antibody.

E. Quantification of SHP-1/STAT5B binding determined by densitometry using Image J (n=2).

Figure 5. STAT5-dependent recruitment of SHP-1 is required for the enrichment of RPB1 to the *PCK1* promoter thereby regulating *PCK1* transcription.

A. Confirmation by western blot of STAT5 knockdown in HepG2 cells (SHP-1-WT or SHP-1-KO) using lentiviral infection with constructs carrying luciferase-specific (control) or *STAT5*-specific shRNA. Quantification of STAT5 knockdown levels determined by densitometry using Image J (n=2).

B. Quantification of SHP-1 levels in HepG2 WT-cells with (*shSTAT5*) or without (shControl) knock down of STAT5 carrying either control shRNA or STAT5-specific shRNA determined by densitometry using Image J (n=2).

C-D: SHP-1 (C) and RPB1 (D) ChIP-qPCR at the *PCK1* promoter (n=3). *p<0.05, **p<0.01.

E. *PCK1*-mRNA levels in HepG2 cells with (*STAT5* shRNA) or without (Luc shRNA) knockdown of *STAT5* determined by qPCR (n=3). ***p<0.001, **p<0.01, ns: non-significant.

Figure 6. Gluconeogenesis is controlled by SHP-1 via STAT5.

A. *Pck1*-mRNA levels in in SHP-1 WT and SHP-1-KD FAO cells with or without STAT5-specific shRNA determined by qPCR (n=3). **** p<0.0001, **p<0.01.

B. Determination of hepatic glucose production in SHP-1 WT and SHP-1-KD FAO cells with or without STAT5-specific shRNA (n=3). *** p<0.001, *p<0.05.

C *Pck1*-mRNA levels in FAO cells with (*Ptpn6* shRNA) or without (control shRNA) knockdown of *SHP-1* in response to DMSO or STAT5 inhibitor determined by qPCR (n=4). ***p<0.001, *p<0.05.

D. *Pck1*-mRNA levels in PMH isolated from *Ptpn6*$^{f/f}$ and *Ptpn6*$^{H\text{-}KO}$ mice in response to DMSO or STAT5 inhibitor determined by qPCR (n=4). **** p<0.0001, ***p<0.001, *p<0.05.

E. Determination of hepatic glucose production in FAO cells with (*Ptpn6* shRNA) or without (control shRNA) *SHP-1* knockdown in response to DMSO or STAT5 inhibitor. (n=4) **** p<0.0001, **p<0.01, *p<0.05.

F. Determination of hepatic glucose production in PMH isolated from $Ptpn6^{f/f}$ and $Ptpn6^{H\text{-}KO}$ in response to DMSO or STAT5 inhibitor (n=4). *** $p<0.001$, *$p<0.05$.
G. Model depicting transcriptional regulation of *PCK1* transcription mediated by SHP-1, STAT5 and RNA pol II resulting in control of gluconeogenesis.

Figures

Figure 1. SHP-1 interacts with proteins of the transcriptional machinery.

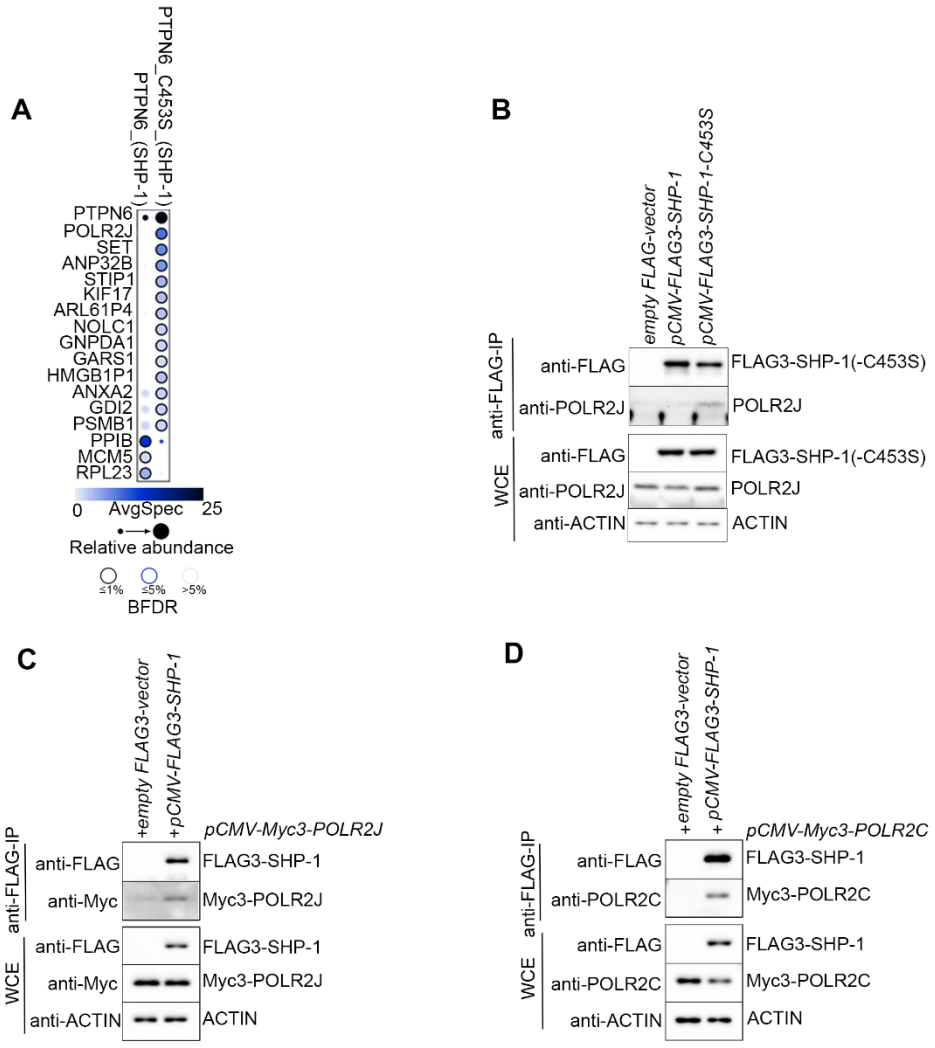

Figure 2. SHP-1 localizes to the chromatin bound nuclear fraction.

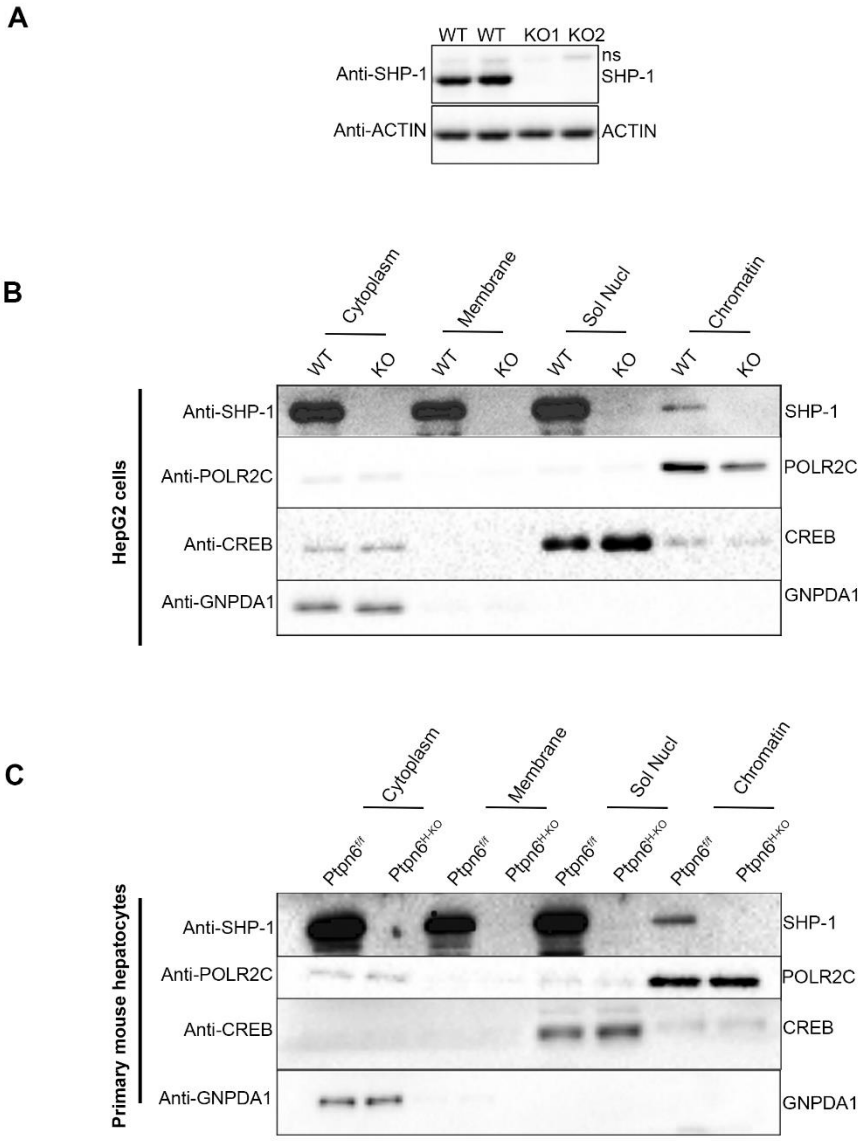

Figure 3. Genome wide mapping of RPB1 binding regions in liver cells reveals the master regulator of gluconeogenesis *PCK1* as a target for SHP-1-mediated transcription regulation.

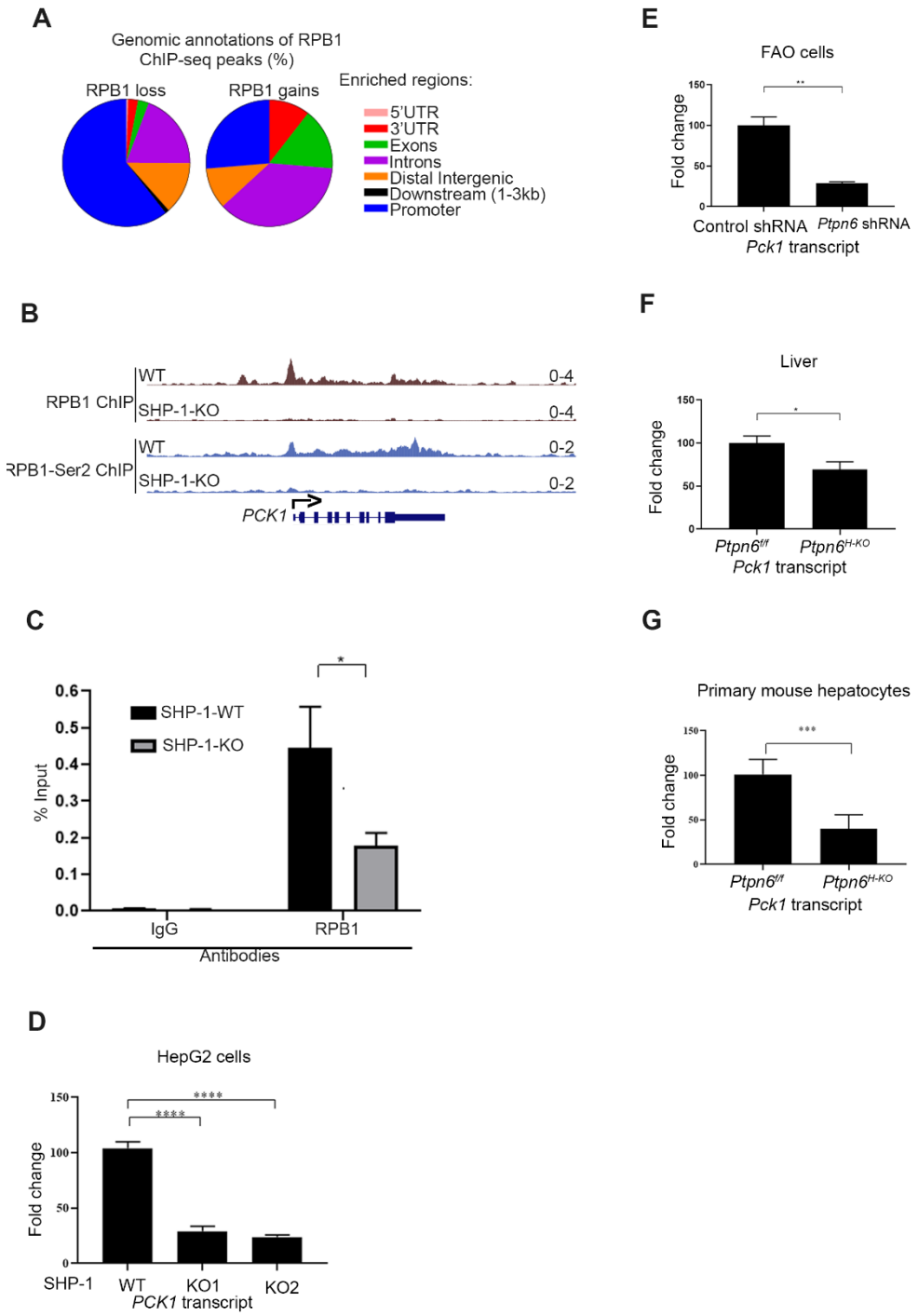

Figure 4. SHP-1 interacts with STAT5 in vitro and shares a common binding region at the *PCK1*-promoter.

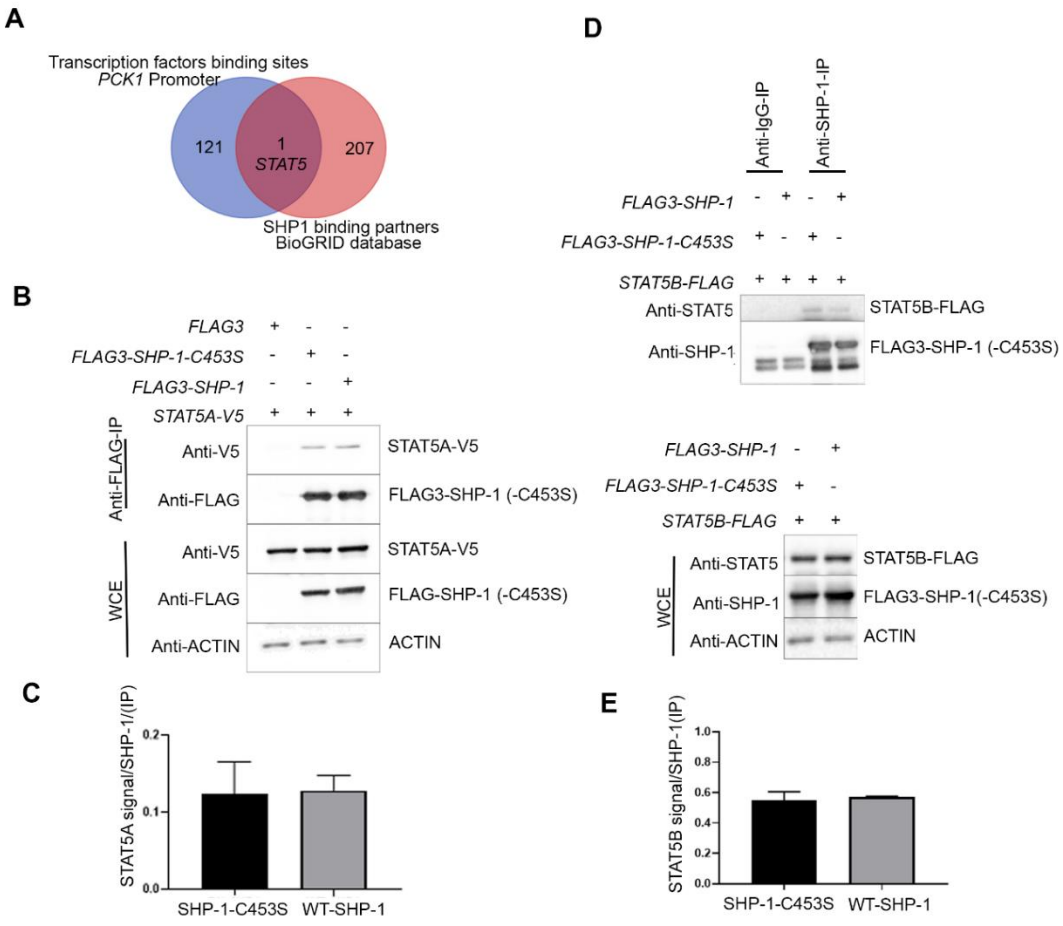

Figure 5. STAT5-dependent recruitment of SHP-1 is required for the enrichment of RPB1 to the PCK1 promoter thereby regulating PCK1 transcription.

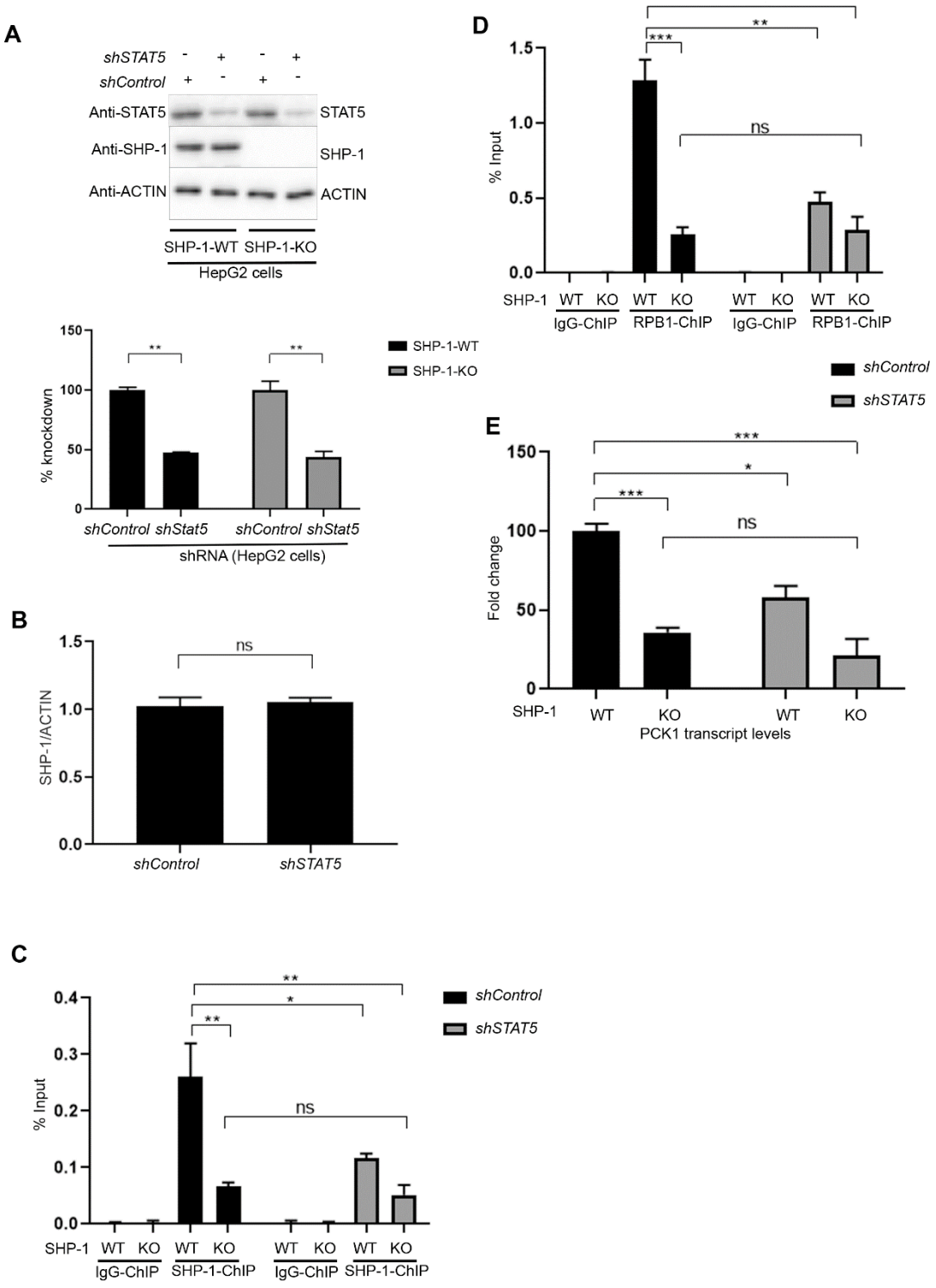

Figure 6. Gluconeogenesis is controlled by SHP-1 via STAT5.

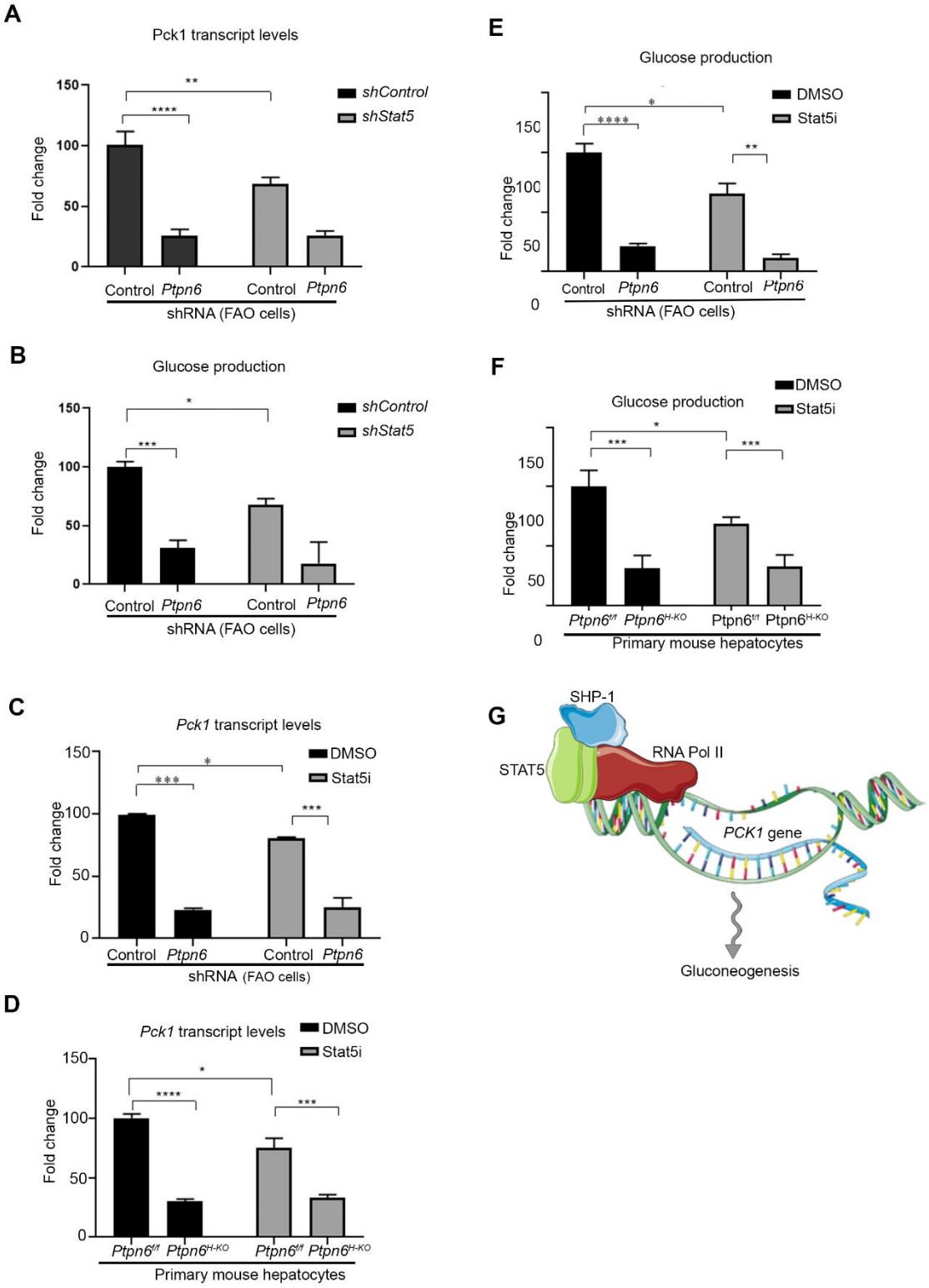

Supplementary Figure Legends

Figure S1. POLR2J is not tyrosine-phosphorylated.
Western blot analysis of immunoprecipitations of Myc-tagged POLR2J showing no tyrosine-phosphorylation of POLR2J in Flp-In T-Rex 293- (A) or HepG2-cells (B). Flp-In T-Rex- or HepG2-cells were transfected with an empty Myc3-vector or Myc3-POLR2J-expressing plasmid and treated with 20 μM bpV(pic)/bpV(HOpic) for 30 min or left untreated. Tyrosine-phosphorylation of Myc3-POLR2J precipitated with anti-Myc agarose beads was analyzed in immunoblots with phospho-tyrosine-specific antibodies.

Figure S2. Generation and validation of CRISPR mediated SHP-1 knockout HepG2 cells.
HepG2 cells were transfected with pX459/SHP1 sgRNA #1 (A) or pX459/SHP sgRNA#4 (A) or pX459/non targeting sgRNA. Single cell clones were selected with puromycin. Expression of SHP-1 was determined by western blot using anti-Shp1 antibody (B & C). Sequencing chromatograms of genomic PCR products spanning single guide sites amplified from SHP-1 KO cells. Sequencing results of clones derived from sgRNA1 (D) and sgRNA4 (E) is shown.

Figure S3. Knock down efficiency of shRNA in FAO cells.
A. Confirmation by western blot of SHP1 knockdown in FAO cells using lentiviral infection with constructs carrying luciferase-specific (control) or *SHP-1* (*Ptpn6*)-specific shRNA. Quantification of SHP1 knockdown levels determined by densitometry using Image J (n=3).
B. Confirmation by western blot of STAT5 knockdown in FAO cells (SHP-1-WT or SHP-1-KD) using lentiviral infection with constructs carrying either scramble control or *STAT5*-specific shRNA. Quantification of STAT5 knockdown levels determined by densitometry using Image J (n=2).

Figure S4. Optimization of Chromatin immunoprecipitation PCR using Micrococcal Nucleases.
A. Representative agarose gel analysis of Mnase digested chromatin.
B. Representative photographs of cross-linked cell pellets before and after Mnase digestion.
C. Efficiency of SHP-1 antibody in immunoprecipitation of chromatin fixed HepG2 cells analysed by western blotting.

Supplementary Figures

Figure S1. POLR2J is not tyrosine-phosphorylated.

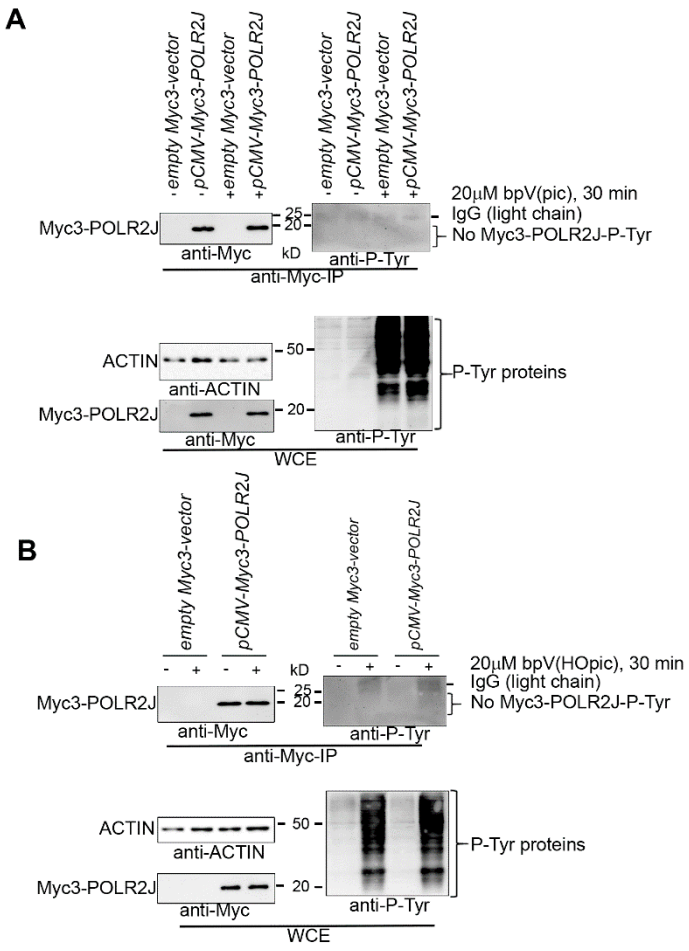

Figure S2. Generation and validation of CRISPR mediated SHP-1 knockout HepG2 cells.

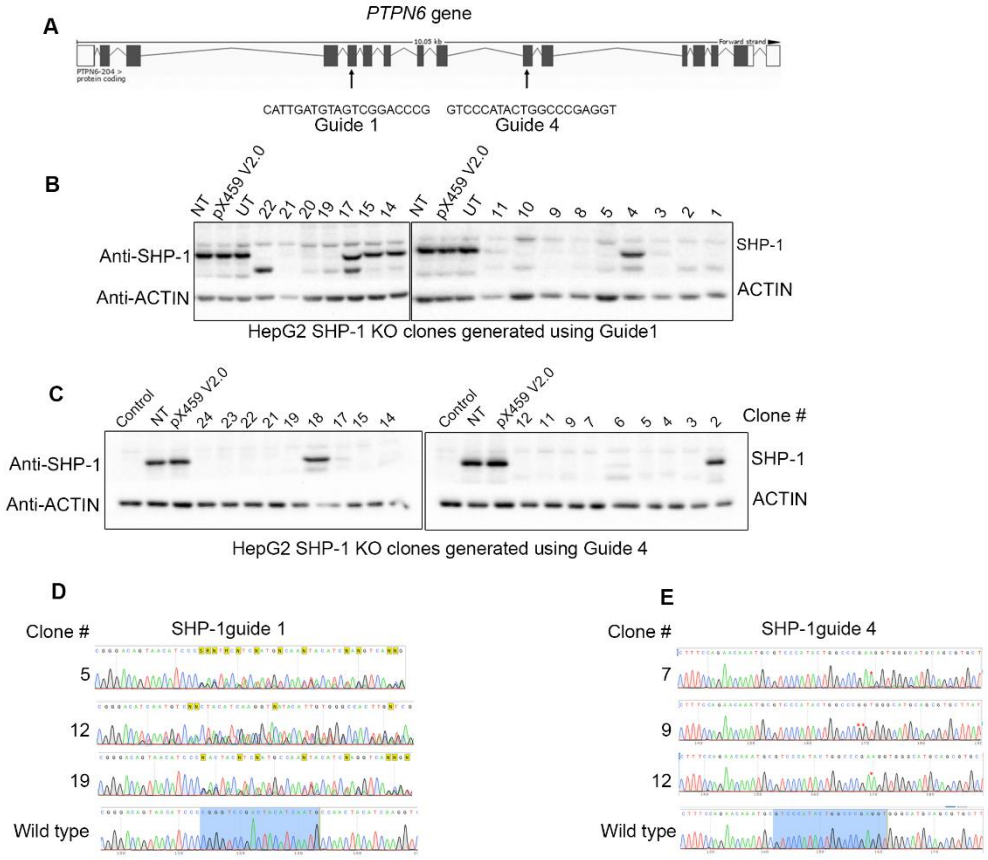

Figure S3. Knock down efficiency of shRNA in FAO cells.

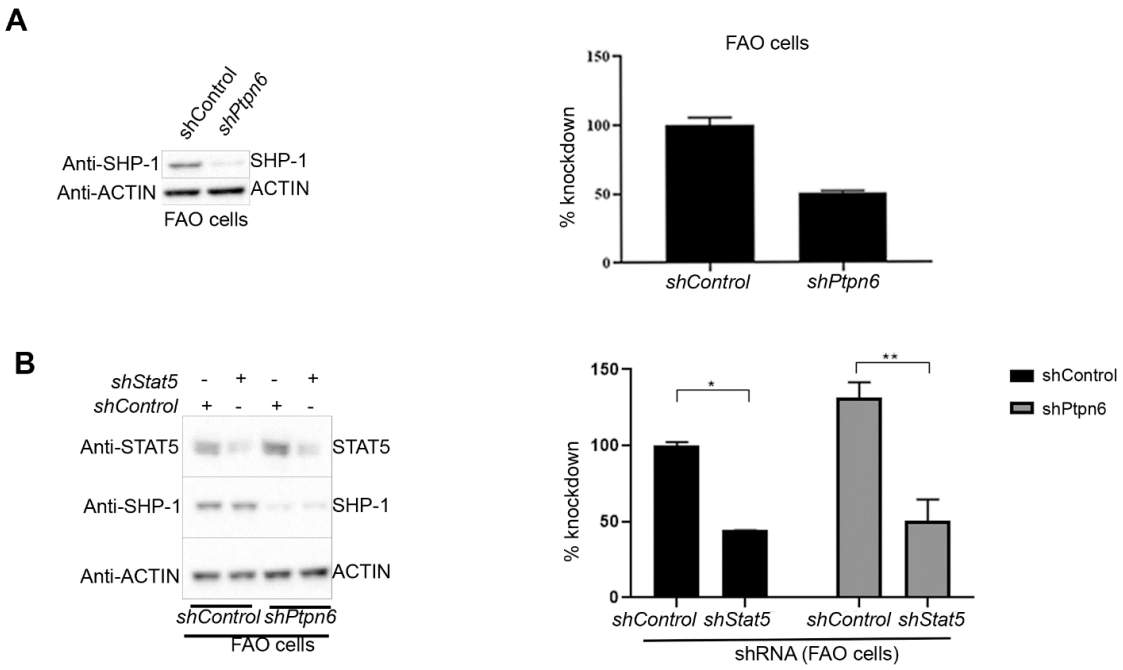

Figure S4. Optimization of Chromatin immunoprecipitation PCR using Micrococcal Nucleases.

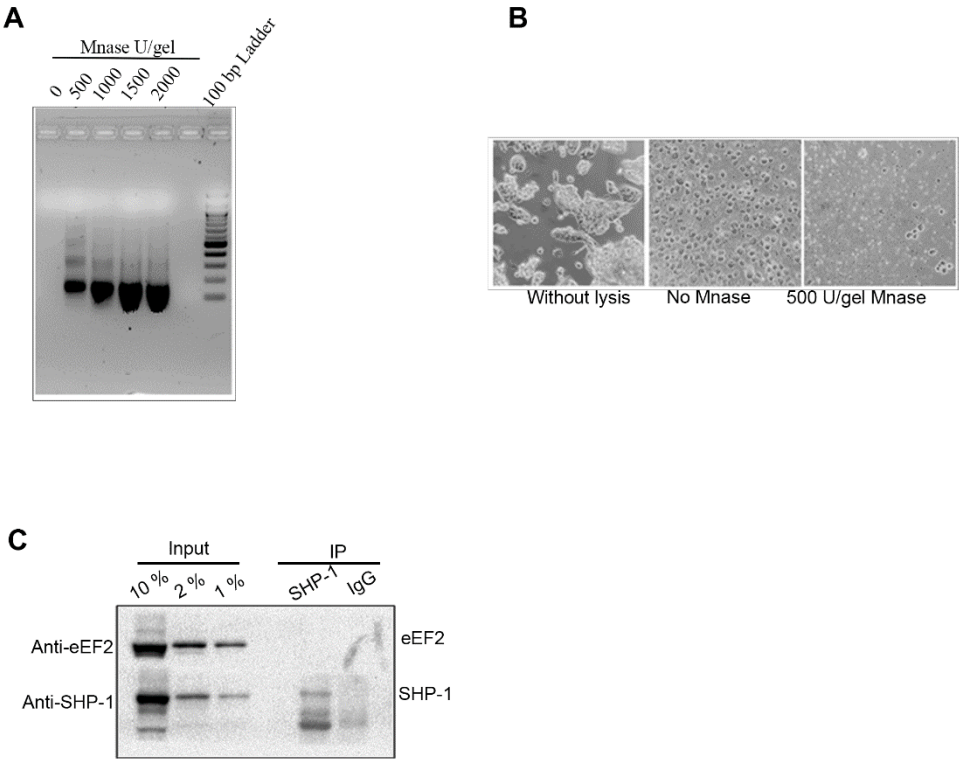

Supplementary information

Table S1. SAINTexpress analysis related to Fig. 1A.

Bait	Prey Gene	AvgSpec	FoldChange	BFDR	PreySequence Length
Ptpn6_C453S_(Shp1)	ANP32B	5.75	57.5	0	251
Ptpn6_C453S_(Shp1)	ANXA2	1.75	17.5	0.01	339
Ptpn6_C453S_(Shp1)	ARL6IP4	3	13.5	0.01	338
Ptpn6_C453S_(Shp1)	GARS1	1.25	12.5	0.01	739
Ptpn6_C453S_(Shp1)	GDI2	1.75	17.5	0	445
Ptpn6_C453S_(Shp1)	GNPDA1	1.5	15	0	289
Ptpn6_C453S_(Shp1)	HMGB1P1	2.75	27.5	0	211
Ptpn6_C453S_(Shp1)	KIF17	3	30	0	1029
Ptpn6_(Shp1)	MCM5	1.25	12.5	0.01	734
Ptpn6_C453S_(Shp1)	NOLC1	1.75	17.5	0.01	699
Ptpn6_C453S_(Shp1)	POLR2J	8.5	76.5	0	117
Ptpn6_(Shp1)	PPIB	13.25	17.04	0	216
Ptpn6_C453S_(Shp1)	PSMB1	1.5	15	0	241
Ptpn6_C453S_(Shp1)	PTPN6	392.5	3925	0	624
Ptpn6_(Shp1)	PTPN6	155.25	1552.5	0	624
Ptpn6_(Shp1)	RPL23	4.5	10.12	0	140
Ptpn6_C453S_(Shp1)	SET	6.75	67.5	0	277
Ptpn6_C453S_(Shp1)	STIP1	4	12	0.01	543

Table S2. Oligos used in the cloning of guide RNAs in pX459.

SgRNA	Species	Forward Primer	Reverse Primer
Sg1	Human	CACC G CATTGATGTAGTCGG ACCCG	AAAC CGGGTCCGACTACATCAATGC
Sg4	Human	CACC GTCCCATACTGGCCC GAGGT	AAAC ACCTCGGGCCAGTATGGGAC
Sg6	Human	CACC GGGCCCGCATAGGAT ATCGC	AAAC GCGATATCCTATGCGGGCCC

Table S3. Primer sequences used for RT-qPCR and ChIP-qPCR.

Gene	Species	Forward Primer	Reverse Primer	Reference
Pck1	Rat	TGCCCAAGATCTTC CACGTC	TCAAGTTCAGGGCGTCTT CC	(Li *et al*, 2015)
Actin	Rat	CGTCTTCCCCTCCA TCGT	GGAGTCCTTCTGACCCAT ACC	(Li *et al*, 2015)
PCK1	Human	ATCTTTGGTGGCC GTAGACCT	CCGAAGTTGTAGCCGAAG AA	(Wang *et al*, 2014)
HPRT 1	Human	AGATGGTCAAGGT CGCAAG	GTATTCATTATAGTCAAG GGCATATCC	(Sulzbach De Oliveira *et al*, 2016)
PCK1	Mouse	GGCGATGACATTG CCTGGATGA	TGTCTTCACTGAGGTGCC AGGA	(Stanford *et al*, 2017)
B2M	Mouse	GGGTGGAACTGTG TTACGTAG	TGGTCTTTCTGGTGCTTG TC	
Chip-*PCK1*	Human	TGACCCACCTGCC TGTTAAG	ACTTCGAGCCCTCAACCA AC	Self designed

Table S4. shRNA sequence used in the study

shRNA	Name	Sequence
shShp1.68	TRCN0000028968	CCGGGCTAGACTGTGACATTGATAT CTCGAGATATCAATGTCACAGTCTAGCTTTTT
shSTAT5A	TRCN0000232134	GGACCTTCTTGTTGCGCTTTA
shSTAT5B	TRCN0000232140	TATGTCCCTGAAACGAATTAA
shSTAT5B	TRCN0000012557	GACTCTCAGGAGAGAATGTTT
STAT5B	TRCN0000421057	GAATTTGCCAGGACGGAATTA
STAT5A	TRCN0000231567	CGAGGTCTTTGCCAAGTATTA
STAT5A	TRCN0000231566	GCCATTCACGACGCGAGATTT

Table S5. List of the antibodies and reagents used in the study.

Antibodies	Source	Identifier
Mouse anti-SHP1	ThermoFischer Scientific	MA5-11669 (1SH01)
Rabbit anti-POLR2J	Proteintech	16403-1-AP
Rabbit anti-POLR2C	Proteintech	13428-1-AP
Mouse anti-FLAG	Sigma	088K6018
Mouse anti-MYC	Sigma	M4439-100UL
Mouse anti-ACTIN	Millipore	MAB1501
Mouse anti-Phosphotyrosine (4G10)	Millipore	05-321
Mouse anti-Phosphotyrosine (PY20)	Abcam	Ab10321
Rabbit anti-CREB	Cell Signaling	9197S
Rabbit anti-GNPDA1	Abcam	ab106563
Rabbit anti-pSer2-RPB1 (anti-RNAPII-CTD-pSer2)	Abcam	ab5095
Mouse anti-RPB1 (anti-RNAPII-CTD)	Abcam	ab817
Rabbit anti-V5	Cell Signaling	13202S
Rabbit anti-STAT5	New England Biolabs	94205S
Rabbit anti eEF2	Cell Signaling	2332
Anti-FLAG® M2 Magnetic Beads	Sigma	M8823-5ML
Anti-FLAG® M2 Affinity Gel	Sigma	A2220-5ML
Anti-c-Myc Agarose Conjugate	Sigma	A7470
Mouse IgG2b	Biolegend	MG2b-57
Tetracycline	Sigma	T7660-5G
Blasticidin S HCl	Invitrogen	R210-01
Hygromycin B	Invitrogen	10687-010
Zeocin	Invitrogen	R250-01
Puromycin dihydrochloride	Invivogen	ant-pr-1
Insulin (Humulin R)	Eli Lilly	HI0213

Poly-L-lysine hydrobromide	Sigma	P1399-25MG
STAT5 inhibitor	Sigma	573108-10MG-M
DMEM low glucose	Wisent Bioproducts	319-010-CL
DMEM high glucose	Wisent Bioproducts	319-005-CL
RPMI	Wisent Bioproducts	350-000-CL
Jet Prime	Polyplus-transfection	114-15
PureFection	System Biosciences	LV750A-1
Dynabeads protein G	Thermo Fisher Scientific	10003D
Sodium orthovanadate	Sigma	S6508-50G
Sodium Fluoride	Sigma	S6776-100G
Calcium chloride	Sigma	C3981-500G
Sodium dodecyl sulfate	Sigma	L3771-500G
EDTA	Sigma	60-00-4
EGTA	Sigma	03777
β-glycerophosphate	Sigma	G5422-100G
Triton	Fisher	X-100
SDS	Sigma	L3771-500G
dexamethasone	Sigma	D-1756
BSA	Sigma	A9647-100G
Glutamax	Gibco	35050-061
FBS	Gibco	16170-078
RNase A	Invitrogen	12091021
Proteinase K	Invitrogen	25530049
Micrococcal Nuclease	New England Biolabs	M0247S
Advanced qpcr mastermix with supergreen lo-rox	Wisent bioproducts	800-431-UL
Subcellular Protein Fractionation Kit for Cultured Cells	Thermo Fischer Scientific	78840
QIAquick PCR Purification Kit	Qiagen	28104
Amplex™ Red Glucose/Glucose Oxidase Assay Kit	Invitrogen	A22189

Table S6. Softwares and alogarithms used in the study.

Software	Source	Identifier
Generunner	Hastings Software. Inc. Hastings, NY, USA	www.generunner.net
BioGRID	(Stark *et al*, 2006)	thebiogrid.org
PROMO 3.02	(Farré *et al*, 2003)	http://alggen.lsi.upc.es/cgi-bin/promo_v3/promo/promoinit.cgi?dirDB=TF_8.3
Venn Diagram	Bioinformatics & Evolutionary Genomics, BELGIUM	http://bioinformatics.psb.ugent.be/webtools/Venn/
UCSC browser	(Kent *et al*, 2002)	https://genome.ucsc.edu/
CRISPR design tool	(Ran *et al*, 2013)	http://crispr.mit.edu/

Supplementary References

1. Farré D, Roset R, Huerta M, Adsuara JE, Roselló L, Albà MM, Messeguer X (2003) Identification of patterns in biological sequences at the ALGGEN server: PROMO and MALGEN. ***Nucleic Acids Res*** **31:** 3651–3653

2. Kent WJ, Sugnet CW, Furey TS, Roskin KM, Pringle TH, Zahler AM, Haussler and D (2002) The Human Genome Browser at UCSC. ***Genome Res*** **12:** 996–1006

3. Li L, Yoshitomi H, Wei Y, Qin L, Zhou J, Xu T, Wu X, Zhou T, Sun W, Guo X, *et al* (2015) Tang-Nai-Kang Alleviates Pre-diabetes and Metabolic Disorders and Induces a Gene Expression Switch toward Fatty Acid Oxidation in SHR.Cg-Leprcp/NDmcr Rats. ***PLOS ONE*** **10:** e0122024

4. Ran FA, Hsu PD, Wright J, Agarwala V, Scott DA, Zhang F (2013) Genome engineering using the CRISPR-Cas9 system. ***Nature Protocols*** **8:** 2281–2308

5. Stanford KI, Takahashi H, So K, Alves-Wagner AB, Prince NB, Lehnig AC, Getchell KM, Lee M-Y, Hirshman MF, Goodyear LJ (2017) Maternal Exercise Improves Glucose Tolerance in Female Offspring. ***Diabetes*** **66:** 2124–2136

6. Stark C, Breitkreutz B-J, Reguly T, Boucher L, Breitkreutz A, Tyers M (2006) BioGRID: a general repository for interaction datasets. ***Nucleic Acids Res*** **34:** D535–D539

7. Sulzbach De Oliveira HS, Biolchi V, Richardt Medeiros HR, Bizerra Gandor Jantsch DBG, Knabben De Oliveira Becker Delving LK, Reckziegel R, Goettert MI, Brum IS, Pozzobon A (2016) Effect of Helicobacter pylori on NFKB1, p38α and TNF-α mRNA expression levels in human gastric mucosa. ***Exp Ther Med*** **11:** 2365–2372

8. Wang C, Chen Z, Li S, Zhang Y, Jia S, Li J, Chi Y, Miao Y, Guan Y, Yang J (2014) Hepatic Overexpression of ATP Synthase β Subunit Activates PI3K/Akt Pathway to Ameliorate Hyperglycemia of Diabetic Mice. ***Diabetes*** **63:** 947–959

CONCLUSION

The role of SHP-1 in regulating glucose and lipid metabolism is well known (Xu *et al*, 2012, 2014a, 2014b, 2014c). However, there is a scarcity of data describing mechanistic details showing the impact of SHP-1 on these processes. Previous findings from our laboratory showed the negative regulation of PPARγ activity by SHP-1. In chapter II of this thesis, we have studied in depth the relationship between SHP-1 and PPARγ. Our studies showed that SHP-1 directly interacts with PPARγ mainly via its N-terminus followed by its phosphatase domain. The dual affinity of SHP-1 domains towards PPARγ suggests that PPARγ could be a substrate of SHP-1, which we further demonstrated by phosphatase assay. A previous report showed that depletion of PTP1B resulted in increased phosphorylation of PPARγ (Choi *et al*, 2015). We have also included PTP1B in our dephosphorylation assay and our data showed that SHP-1 efficiently dephosphorylates PPARγ but not PTP1B. Previously tyrosine residue 78 (Y78) has been shown to be phosphorylated in PPARγ. We did not find Y78 residue in our mass spectrometry analysis, suggesting the limitation of this technique (Dephoure *et al*, 2013). We also attempted to discover novel tyrosine residues that could be phosphorylated using mass spectrometry. We indeed found a few novel sites that have not been reported elsewhere. However, using co-immunoprecipitation studies we were not able to validate those sites (Figure 1). Therefore, we focused on the Y78 residue of PPARγ.

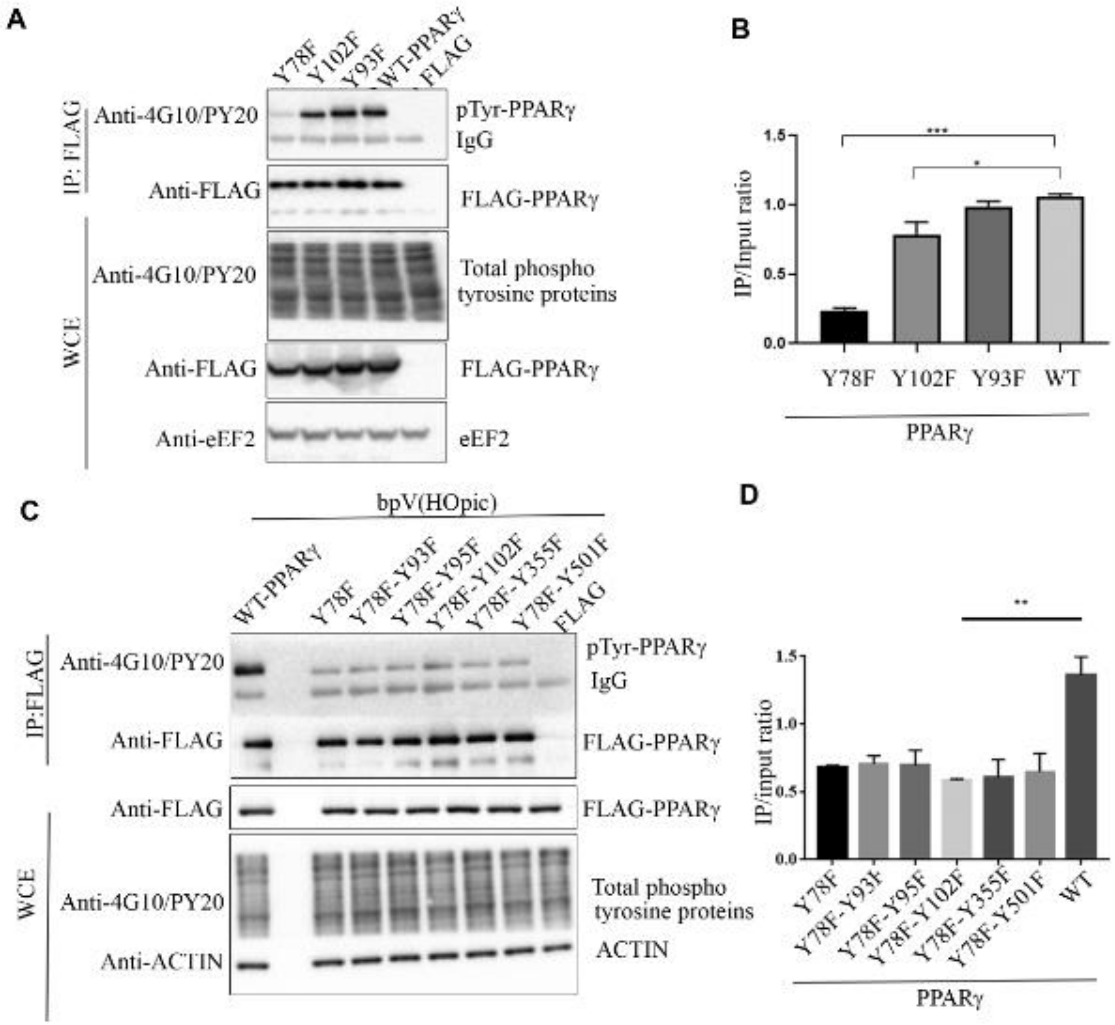

Figure 1. Profiling of tyrosine phosphorylation sites in PPARγ. A. 293T cells were transfected with either empty FLAG vector or FLAG- PPARγ WT or Flag-PPARγ mutants (as shown in the figure). Cells were treated with 10µm bpV(HOpic) for 30 minutes. Lysates were immunoprecipitated using anti-FLAG-M2 beads and the expression of proteins was determined using western blotting using indicated antibodies.

B. Quantification of levels of phospho-Tyr- PPARγ was performed by densitometry using ImageJ (n=3).

C. Determination of levels of PPARγ tyrosine phosphorylation in double PPARγ mutants using immuno-precipitation study.

D. Quantification of levels of phospho-Tyr- PPARγ was performed by densitometry using ImageJ (n=3).

SHP-1 depletion resulted in increased tyrosine phosphorylation of wild-type PPARγ protein but not of PPARγ (Y78F) mutant protein suggesting that Y78 could be the main tyrosine residue that could be targeted by SHP-1. Furthermore, SHP-1 depletion resulted in higher levels of PPAR gamma protein levels without affecting its transcript levels indicating SHP-1 mediated PPARγ regulation may be at post-translational level. Our results provide evidence that in the presence of SHP-1, PPARγ is dephosphorylated resulting in its degradation and hence lower levels of PPARγ transactivation were observed. SHP-1 depletion was concomitant with reduced expression of classical PPARγ transcripts (*FABP4* and *CD36*) and a low level of relative lipid contents. These findings are in agreement with *in vivo* phenotypes observed in a previous study published from our laboratory (Xu *et al*, 2014a). Interestingly, Choi et al., 2015 demonstrated that PPARγ-Y78F mutant was associated with enhanced expression of a set of genes involved in inflammation (Choi et al., 2015). This report is in contrast to our findings where we found that expression of classical PPARγ gene was decreased when Y78 residue was mutated to F.

We have deciphered the relationship between SHP-1 and PPARγ using different cellular models (293T cells, human hepatoma cells, HepG2, and mouse fibroblast NIH3T3 cells). Our data add PPARγ to the short list of SHP-1 substrate that are transcription regulators including b-catenin and TonEBP/OREBP (Zhou *et al*, 2010; Simoneau *et al*, 2011). Previously, Xiao et al.,2015 demonstrated that SHP-1 control the tyrosine phosphorylation and ubiquitination of Casitas-B-lineage lymphoma (Cbl)-b protein that ultimately affects T cell response (Xiao *et al*, 2009). Therefore, it would be interesting to discover other metabolically important proteins that stability is affected by SHP-1. Furthermore, several studies demonstrated that PPARγ can itself activates its own transcription by positive feedback loop mechanisms (Rosen *et al*, 2002; Wakabayashi *et al*, 2009; Dephoure *et al*, 2013). Therefore, it can be speculated that in the absence of SHP-1, PPARγ is more stable in the mice liver, which may drive its own transcription (Xu *et al*, 2014a) . However, these observations need experimental validation.

In chapter II, the data derived from *in vitro* studies and therefore have its limitations. These *in vitro* models suggest that SHP-1 mediated dephosphorylation might trigger the degradation of PPARγ, however, these findings need to be validated by *in vivo* studies.

In chapter III of the thesis, we took a challenge to discover novel interacting partners of SHP-1. The immunoprecipitation of SHP-1 from SHP-1 overexpressing cell lines followed by mass spectrometry revealed several novel interacting partners of SHP-1. Unfortunately, we did not find PPARγ in our mass spectrometry analysis the reason being we have used 293T cells that do not express PPARγ protein. Unexpectedly, we found POLR2J, a subunit of RNA polymerase II as a novel interacting partner of SHP-1. Although we confirmed the direct interaction between SHP-1 and POLR2J, we were not able to prove a substrate (POLR2J) - enzyme (SHP-1) relationship between these two proteins. Despite of being mainly characterized as cytoplasmic protein tyrosphosphatase, SHP-1 is also found in the nucleus of epithelial cells (Ram & Waxman, 1997; Craggs & Kellie, 2001; Duchesne *et al*, 2003). Our subcellular fractionation of liver cells (primary mouse hepatocytes and HepG2 cells) revealed that the large fraction of SHP-1 localized in the nuclear fraction and some amount was in the chromatin fraction where actual transcription takes place. This is the fraction where RNA polymerase II resides and carries out its biological function. We speculate SHP-1 may be a “binding partner” of PolR2J that may regulate the transcription of a class of genes. CHIP-seq analysis of SHP-1 expressing and SHP-1 KO cells revealed modulation of several classes of genes including genes involved in lipid and glucose metabolism. The top five enrichment category in a KEGG pathway analysis were insulin resistance, JAK-STAT signaling pathway, tight junction, PPAR signaling pathway and insulin signaling pathway (Table 1).

Table 1. The top five enrichment pathways obtained by comparing HepG2-WT vs HepG2-SHP-1 KO cells revealed by Kyoto encyclopedia of Genes and Genomes (KEGG) analysis.

Term	p value	-log10(p)	Fold enrichment	Gene list
Insulin resistance	0.004	2.3	5.5	*PPARA, PCK1, PRKCZ, PPP1R3C, RPS6KA1, SLC27A3*
JAK-STAT signaling pathway	0.02	1.6	3.7	*JAK1, JAK3, AOX1, IFNLR1, IL22RA1, PDGFP*
Tight junction	0.02	1.5	3.5	*ARHGEF18, CLDN19, CLDN4, PRKCZ, TJAP1, TUBA4A*
PPAR signaling pathway	0.03	1.4	5.3	*APOA5, FABP3, PPARA, PCK1*
Insulin signaling pathway	0.04	1.3	3.6	*MKNK1, INPPL1, PCK1, PRKCZ, PPP1R3C*

We chose *PCK1* gene since it regulates the key step in gluconeogenesis as a prototype gene to test the non-conventional role of SHP-1 protein. SHP-1 absence reduced the transcript levels of *PCK1 in vitro* (liver cell lines), *ex vivo* (primary mouse hepatocytes), and *in vivo* (mouse liver). We found a decrease of RNA pol II occupancy at the *PCK1* promoter of cells lacking SHP-1 as compared to SHP-1 expressing cells. Our *in silico* analysis suggested that STAT5 could be the transcription factor that could assist in the binding of SHP-1 protein to the chromatin where it might interact with RNA polymerase II. STAT5 knockdown significantly decreased the recruitment of SHP-1 to the *PCK1* promoter. This was corroborated by reduced recruitment of RPB1 (RNA polymerase II largest subunit) to the *PCK1* promoter upon depletion of STAT5 or SHP-1, but knockdown of STAT5 in SHP-1 KO cells did not further impact this reduction. These findings suggest that STAT5 governs the binding of SHP-1 to the *PCK1* promoter as STAT5 knockdown had no further impact on *PCK1* transcript levels and the glucose output in cells depleted of SHP-1. From these findings, we conclude that SHP-1 and STAT5 might act on the same pathway in the regulation of gluconeogenesis mediated by control of *PCK1* transcription. These findings were further validated using a pharmacological approach to inhibit STAT5 in FAO cells and primary mouse hepatocytes. Our data indicate that treatment of SHP-1 expressing cells with a STAT5 inhibitor (Stat5i) reduced *PCK1* transcript levels, but not to the same extent as observed in SHP-1 knockdown cells exhibiting no further decrease in *PCK1* transcript levels. Similarly, we found a significant decrease in glucose production in FAO-cells and PMH after treatment of SHP-1 WT cells with STAT5i. A significant drop in glucose production capacity in SHP-1 KD cells, which was not significantly altered after STAT5i treatment was observed. Taken together these data provide a key mechanism to explain in vivo phenotypes observed in mice with hepatocyte specific deletion of SHP-1 that exhibits lower glycemia compared to control littermates (Xu *et al*, 2012, 2014a). Furthermore, these mice also display reduced hepatic glucose production capacity (Xu *et al*, 2012) that maybe partly due to regulation of PCK1 expression by SHP-1-STAT5-RNAPII pathway. Furthermore, our data suggest that SHP-1 displays the characteristics of a typical transcriptional activator (Näär *et al*, 2001; Spiegelman

& Heinrich, 2004). There are several transcription factors including CREB (Horike *et al*, 2008) and FOXO1 (Puigserver *et al*, 2003; O-Sullivan *et al*, 2015) that controls the transcription of PCK1. Therefore, it will be interesting to discover novel collaborations of SHP-1 with other transcription factor on PCK1 promoter.

Phosphorylation of STAT5 at a C terminal tyrosine residue 694 leads to transcriptional activation by promoting STAT5-STAT5 dimer formation, nuclear localization and binding of STAT5 to the target DNA (Levy & Darnell, 2002). To investigate whether tyrosine phosphorylation of STAT5 plays a role in SHP-1 mediated gluconeogenesis we used growth hormone in our experiments. Growth hormone (GH)-mediated activation of STAT5 has been implicated in the control of glucose production (Kim *et al*, 2012). To examine whether growth hormone can influence SHP-1-STAT5-mediated gluconeogenesis in FAO cells, we performed time course experiments with FAO-SHP-1-WT or FAO SHP1-KD cells treated with rat growth hormone (rGH). We observed a similar increase in pSTAT5(Tyr694) levels in FAO-SHP-1-WT and FAO-SHP1-KD cells in a time-dependent manner (Figure 2A). STAT5 can be dephosphorylated in vitro by both SHP-1 (Paling & Welham, 2002; Xiao *et al*, 2009) as well as by SHP-2 (Yu *et al*, 2000). In our hand, we did not find an increase in the levels of pSTAT5(Tyr694) levels in SHP-1-KD condition. Furthermore, we did not find a significant difference in the binding of STAT5 to SHP-1-WT or a substrate trapping mutant of SHP-1 suggesting STAT5 is not a direct substrate of SHP-1.

Furthermore, rGH did not lead to any significant changes in *PCK1* transcript levels both in SHP-1 WT and KD cells across the time points, but overall *PCK1* mRNA was significantly reduced in SHP-1 depleted cells as observed earlier (Figure 2B). In contrast, transcript levels of *Socs3*, a GH-induced STAT5 target (Adams *et al*, 1998; Cui *et al*, 2007; Davey *et al*, 1999), transiently increased under the same conditions in both SHP-1 WT and KD cells with no significant difference confirming that FAO cells are responsive to GH treatment (Figure 2C). Altogether with the *PCK1* transcript levels, we observed a significant reduction in gluconeogenesis in SHP-1 KD cells, but we did not find a significant increase in glucose production capacity in FAO-SHP-1-WT or FAO-SHP-1-KD cells in response to GH treatment (Figure 2D).

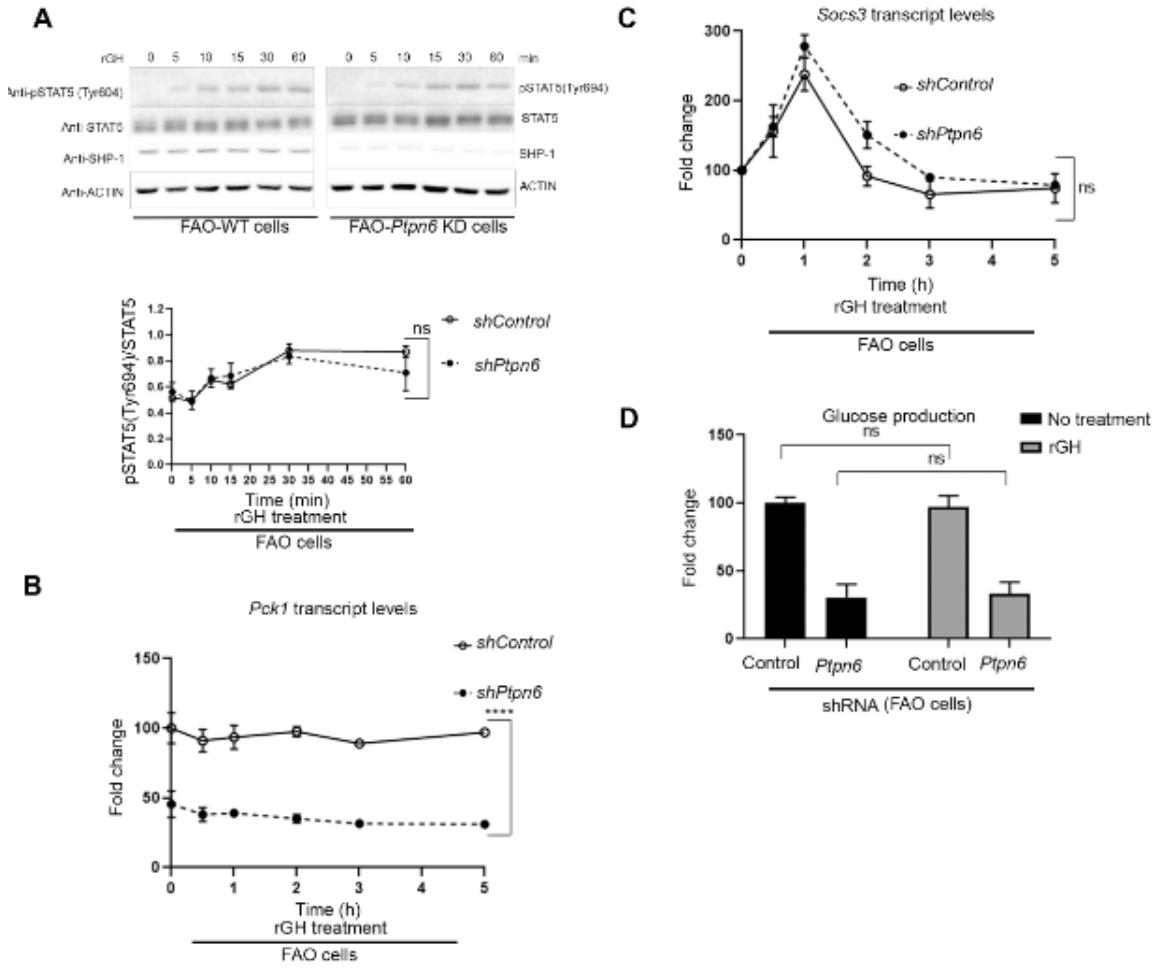

Figure 2. Growth hormone does not influence *PCK1* expression and gluconeogenesis. A. Upper panel, Western blot showing phosphorylation and total amounts of various proteins in FAO cells with or without *SHP-1* knockdown in response to recombinant rat growth hormone treatment at various time points (n=2). Lower panel: Quantification of pSTAT5/total STAT5 determined by densitometry using Image J (n=2).
B-D*. PCK1*- (B) and *Socs3*- (C) transcript levels in FAO cells with or without *SHP-1* knockdown in response to recombinant rat growth hormone treatment at different time points determined by qPCR (n=2).
D. Determination of hepatic glucose production in FAO cells with (*Ptpn6* shRNA) or without (control shRNA) *SHP-1* knockdown in response to recombinant rat growth hormone treatment (n=3), ns: non-significant.

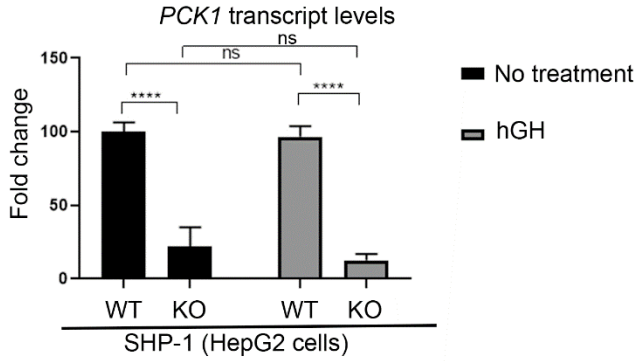

Figure 3. Growth hormone does not influence PCK1 expression in HepG2 cells. *PCK1*-transcript levels in HepG2 cells with or without SHP-1 knockout in response to recombinant human growth hormone treatment at different time points determined by qPCR (n=3) ns: non-significant **** p<0.0001.

As in FAO cells, we did not find any induction of *PCK1* transcription in HepG2 cells in response to human GH treatment (Figure 3). From these results, we conclude that SHP-1-STAT5-mediated regulation of *PCK1* transcription is independent of the activation state of STAT5 and therefore is a novel mechanism regulating hepatic gluconeogenesis. Our data is in agreement to a growing list of studies where tyrosine phosphorylation-independent STATs activities have been demonstrated (Yang *et al*, 2007; Cui *et al*, 2007; Yang & Stark, 2008; Hu *et al*, 2013; Park *et al*, 2016). In addition to this, recently PTEN a phosphatase (Steinbach *et al*, 2019) and insulin receptor (Hancock *et al*, 2019) were shown to regulate the transcription of a set of genes in a very similar manner to SHP-1 by directly interacting with the chromatin. However, our *in vitro* and *ex vivo* findings need *in vivo* validation. Liver-specific STAT5 KO and SHP-1/STAT5 double KO mice could be useful in this regard. The glucose production data from liver-specific SHP-1 KO mice could be compared with liver-specific double knockout (SHP-1 and STAT5) and wild type mice using conventional oGTT or pyruvate tolerance tests. Since the generation of double KO mice (SHP-1/STAT5) can be a time-consuming process, alternatively the expression of STAT5 can be knocked down in mouse liver using shRNA expression via adenoviruses and using liver-specific promoters. Glucose levels could be compared

with appropriate littermates. In addition, CHIP analysis could be performed in liver lysates of these mice, which could further confirm the “the binding partner” role of SHP-1 in regulating gluconeogenesis.

Taken together, in this thesis we have discovered two novel mechanisms by which SHP-1 participates in lipid and glucose metabolism. The first is a phosphatase dependent role of SHP-1: we have shown how SHP-1-mediated dephosphorylation of PPARγ makes it susceptible to degradation and finally affects adipogenesis. PPARγ has been shown to enhance high fat diet induced hypertrophy, therefore a drug that promotes the activity of SHP-1 could be potentially helpful in treating obesity. Secondly, we have shown a phosphatase-independent control of glucose metabolism by SHP-1. In future, discovery of more non-canonical targets of SHP-1 could further give insight into the novel biological functions of SHP-1.

References

1. Abd El-Kader SM & El-Den Ashmawy EMS (2015) Non-alcoholic fatty liver disease: The diagnosis and management. *World J Hepatol* 7: 846–858

2. Abel ED, Peroni O, Kim JK, Kim YB, Boss O, Hadro E, Minnemann T, Shulman GI & Kahn BB (2001) Adipose-selective targeting of the GLUT4 gene impairs insulin action in muscle and liver. *Nature* 409: 729–733

3. Abram CL & Lowell CA (2017) Shp1 function in myeloid cells. *J Leukoc Biol* 102: 657–675

4. Adámková L, Soucková K & Kovarík J (2007) Transcription protein STAT1: biology and relation to cancer. *Folia Biol (Praha)* 53: 1–6

5. Adams TE, Hansen JA, Starr R, Nicola NA, Hilton DJ & Billestrup N (1998) Growth hormone preferentially induces the rapid, transient expression of SOCS-3, a novel inhibitor of cytokine receptor signaling. *J Biol Chem* 273: 1285–1287

6. Adeva-Andany MM, Pérez-Felpete N, Fernández-Fernández C, Donapetry-García C & Pazos-García C (2016) Liver glucose metabolism in humans. *Biosci Rep* 36: e00416

7. Aguirre V, Uchida T, Yenush L, Davis R & White MF (2000) The c-Jun NH(2)-terminal kinase promotes insulin resistance during association with insulin receptor substrate-1 and phosphorylation of Ser(307). *J Biol Chem* 275: 9047–9054

8. Ahmadian M, Suh JM, Hah N, Liddle C, Atkins AR, Downes M & Evans RM (2013) PPARγ signaling and metabolism: the good, the bad and the future. *Nat Med* 19: 10.1038/nm.3159

9. Ahmed SA & Shalayel MH (1999) Role of cortisol in the deterioration of glucose tolerance in Sudanese pregnant women. *East Afr Med J* 76: 465–467

10. Akira S (1999) Functional roles of STAT family proteins: lessons from knockout mice. *Stem Cells* 17: 138–146

11. Akt phosphorylates insulin receptor substrate to limit PI3K-mediated PIP3 synthesis | eLife

12. Al Rifai M, Silverman MG, Nasir K, Budoff MJ, Blankstein R, Szklo M, Katz R, Blumenthal RS & Blaha MJ (2015) The association of nonalcoholic fatty liver disease, obesity, and metabolic syndrome, with systemic inflammation and subclinical atherosclerosis: the Multi-Ethnic Study of Atherosclerosis (MESA). *Atherosclerosis* 239: 629–633

13. Allen BL & Taatjes DJ (2015) The Mediator complex: a central integrator of transcription. *Nat Rev Mol Cell Biol* 16: 155–166

14. Alonso A, Sasin J, Bottini N, Friedberg I, Friedberg I, Osterman A, Godzik A, Hunter T, Dixon J & Mustelin T (2004) Protein tyrosine phosphatases in the human genome. *Cell* 117: 699–711

15. Amador M, Meza CA, McAinch AJ, King GA, Covington JD & Bajpeyi S (2020) Exercise-Induced Improvements in Insulin Sensitivity Are Not Attenuated by a Family History of Type 2 Diabetes. *Front Endocrinol (Lausanne)* 11: 120

16. Amemiya-Kudo M, Shimano H, Hasty AH, Yahagi N, Yoshikawa T, Matsuzaka T, Okazaki H, Tamura Y, Iizuka Y, Ohashi K, *et al* (2002) Transcriptional activities of nuclear SREBP-1a, -1c, and -2 to different target promoters of lipogenic and cholesterogenic genes. *J Lipid Res* 43: 1220–1235

17. Andersen CJ, Murphy KE & Fernandez ML (2016) Impact of Obesity and Metabolic Syndrome on Immunity12. *Adv Nutr* 7: 66–75

18. Andersen JN, Mortensen OH, Peters GH, Drake PG, Iversen LF, Olsen OH, Jansen PG, Andersen HS, Tonks NK & Møller NPH (2001) Structural and Evolutionary Relationships among Protein Tyrosine Phosphatase Domains. *Mol Cell Biol* 21: 7117–7136

19. Anja B & Laura R (2017) The cost of diabetes in Canada over 10 years: applying attributable health care costs to a diabetes incidence prediction model. *Health Promot Chronic Dis Prev Can* 37: 49–53

20. Aprile M, Cataldi S, Ambrosio MR, D'Esposito V, Lim K, Dietrich A, Blüher M, Savage DB, Formisano P, Ciccodicola A, *et al* (2018) PPARγΔ5, a Naturally Occurring Dominant-Negative Splice Isoform, Impairs PPARγ Function and Adipocyte Differentiation. *Cell Rep* 25: 1577-1592.e6

21. Araki E, Lipes MA, Patti ME, Brüning JC, Haag B, Johnson RS & Kahn CR (1994) Alternative pathway of insulin signalling in mice with targeted disruption of the IRS-1 gene. *Nature* 372: 186–190

22. Arck P, Toth B, Pestka A & Jeschke U (2010) Nuclear Receptors of the Peroxisome Proliferator-Activated Receptor (PPAR) Family in Gestational Diabetes: From Animal Models to Clinical Trials1. *Biology of Reproduction* 83: 168–176

23. Atkinson MA, Eisenbarth GS & Michels AW (2014) Type 1 diabetes. *Lancet* 383: 69–82

24. Au-Yeung N, Mandhana R & Horvath CM (2013) Transcriptional regulation by STAT1 and STAT2 in the interferon JAK-STAT pathway. *JAKSTAT* 2: e23931

25. Baeuerle PA & Baltimore D (1988) I kappa B: a specific inhibitor of the NF-kappa B transcription factor. *Science* 242: 540–546

26. Bakan I & Laplante M (2012) Connecting mTORC1 signaling to SREBP-1 activation. *Curr Opin Lipidol* 23: 226–234

27. Banerji J, Rusconi S & Schaffner W (1981) Expression of a beta-globin gene is enhanced by remote SV40 DNA sequences. *Cell* 27: 299–308

28. Banting FG, Best CH, Collip JB, Campbell WR & Fletcher AA (1922a) Pancreatic Extracts in the Treatment of Diabetes Mellitus. *Can Med Assoc J* 12: 141–146

29. Banting FG, Best CH, Collip JB, Macleod JJR & Noble EC (1922b) The effect of pancreatic extract (insulin) on normal rabbits. *American Journal of Physiology-Legacy Content* 62: 162–176

30. Banville D, Stocco R & Shen SH (1995) Human protein tyrosine phosphatase 1C (PTPN6) gene structure: alternate promoter usage and exon skipping generate multiple transcripts. *Genomics* 27: 165–173

31. Barash I (2006) Stat5 in the mammary gland: controlling normal development and cancer. *J Cell Physiol* 209: 305–313

32. Bataller R & Brenner DA (2005) Liver fibrosis. *J Clin Invest* 115: 209–218

33. van Beekum O, Fleskens V & Kalkhoven E (2009) Posttranslational modifications of PPAR-gamma: fine-tuning the metabolic master regulator. *Obesity (Silver Spring)* 17: 213–219

34. Bergeron S, Dubois M-J, Bellmann K, Schwab M, Larochelle N, Nalbantoglu J & Marette A (2011) Inhibition of the protein tyrosine phosphatase SHP-1 increases glucose uptake in skeletal muscle cells by augmenting insulin receptor signaling and GLUT4 expression. *Endocrinology* 152: 4581–4588

35. van den Berghe G (1991) The role of the liver in metabolic homeostasis: Implications for inborn errors of metabolism. *J Inherit Metab Dis* 14: 407–420

36. Beurel E, Grieco SF & Jope RS (2015) Glycogen synthase kinase-3 (GSK3): regulation, actions, and diseases. *Pharmacol Ther* 0: 114–131

37. Bian X, Gao P, Xiong X, Xu H, Qian M & Liu S (2000) Risk factors for development of diabetes mellitus in women with a history of gestational diabetes mellitus. *Chin Med J (Engl)* 113: 759–762

38. Bianco ME & Josefson JL (2019) Hyperglycemia During Pregnancy and Long-Term Offspring Outcomes. *Curr Diab Rep* 19: 143

39. Bogan JS & Kandror KV (2010) Biogenesis and regulation of insulin-responsive vesicles containing GLUT4. *Curr Opin Cell Biol* 22: 506–512

40. Böhmer F, Szedlacsek S, Tabernero L, Ostman A & den Hertog J (2013) Protein tyrosine phosphatase structure-function relationships in regulation and pathogenesis. *FEBS J* 280: 413–431

41. Bolino A, Muglia M, Conforti FL, LeGuern E, Salih MA, Georgiou DM, Christodoulou K, Hausmanowa-Petrusewicz I, Mandich P, Schenone A, *et al* (2000) Charcot-Marie-Tooth type 4B is caused by mutations in the gene encoding myotubularin-related protein-2. *Nat Genet* 25: 17–19

42. Bonofiglio D, Cione E, Qi H, Pingitore A, Perri M, Catalano S, Vizza D, Panno ML, Genchi G, Fuqua SAW, *et al* (2009) Combined low doses of PPARgamma and RXR ligands trigger an intrinsic apoptotic pathway in human breast cancer cells. *Am J Pathol* 175: 1270–1280

43. Boos LA, Dettmer M, Schmitt A, Rudolph T, Steinert H, Moch H, Sobrinho-Simões M, Komminoth P & Perren A (2013) Diagnostic and prognostic implications of the PAX8-PPARγ translocation in thyroid carcinomas-a TMA-based study of 226 cases. *Histopathology* 63: 234–241

44. Bossé Y, Lamontagne M, Gaudreault N, Racine C, Levesque M-H, Smith BM, Auger D, Clemenceau A, Paré M-È, Laviolette L, *et al* (2019) Early-onset emphysema in a large French-Canadian family: a genetic investigation. *Lancet Respir Med* 7: 427–436

45. Boucher J, Kleinridders A & Kahn CR (2014) Insulin Receptor Signaling in Normal and Insulin-Resistant States. *Cold Spring Harb Perspect Biol* 6

46. Bouzid D, Fourati H, Amouri A, Marques I, Abida O, Haddouk S, Ben Ayed M, Tahri N, Penha-Gonçalves C & Masmoudi H (2013) Association of ZAP70 and PTPN6, but Not BANK1 or CLEC2D, with inflammatory bowel disease in the Tunisian population. *Genet Test Mol Biomarkers* 17: 321–326

47. Braissant O, Foufelle F, Scotto C, Dauça M & Wahli W (1996) Differential expression of peroxisome proliferator-activated receptors (PPARs): tissue distribution of PPAR-alpha, -beta, and -gamma in the adult rat. *Endocrinology* 137: 354–366

48. Bren-Mattison Y, Van Putten V, Chan D, Winn R, Geraci MW & Nemenoff RA (2005) Peroxisome proliferator-activated receptor-gamma (PPAR(gamma)) inhibits tumorigenesis by reversing the undifferentiated phenotype of metastatic non-small-cell lung cancer cells (NSCLC). *Oncogene* 24: 1412–1422

49. Bruecher-Encke B, Griffin JD, Neel BG & Lorenz U (2001) Role of the tyrosine phosphatase SHP-1 in K562 cell differentiation. *Leukemia* 15: 1424–1432

50. Brunmeir R & Xu F (2018) Functional Regulation of PPARs through Post-Translational Modifications. *Int J Mol Sci* 19: E1738

51. Buitenhuis M, Baltus B, Lammers J-WJ, Coffer PJ & Koenderman L (2003) Signal transducer and activator of transcription 5a (STAT5a) is required for eosinophil differentiation of human cord blood-derived CD34+ cells. *Blood* 101: 134–142

52. Bulger M & Groudine M (2011) Functional and mechanistic diversity of distal transcription enhancers. *Cell* 144: 327–339

53. Bult CJ, Eppig JT, Blake JA, Kadin JA, Richardson JE, & the Mouse Genome Database Group (2016) Mouse genome database 2016. *Nucleic Acids Research* 44: D840–D847

54. Burchell A & Hume R (1995) The glucose-6-phosphatase system in human development. *Histol Histopathol* 10: 979–993

55. Burns KA & Vanden Heuvel JP (2007) Modulation of PPAR activity via phosphorylation. *Biochim Biophys Acta* 1771: 952–960

56. Buscà R, Pouysségur J & Lenormand P (2016) ERK1 and ERK2 Map Kinases: Specific Roles or Functional Redundancy? *Front Cell Dev Biol* 0

57. Butler AE, Janson J, Bonner-Weir S, Ritzel R, Rizza RA & Butler PC (2003) Beta-cell deficit and increased beta-cell apoptosis in humans with type 2 diabetes. *Diabetes* 52: 102–110

58. Caër C, Rouault C, Le Roy T, Poitou C, Aron-Wisnewsky J, Torcivia A, Bichet J-C, Clément K, Guerre-Millo M & André S (2017) Immune cell-derived cytokines contribute to obesity-related inflammation, fibrogenesis and metabolic deregulation in human adipose tissue. *Sci Rep* 7: 3000

59. Camp HS, Tafuri SR & Leff T (1999) c-Jun N-Terminal Kinase Phosphorylates Peroxisome Proliferator-Activated Receptor-γ1 and Negatively Regulates Its Transcriptional Activity. *Endocrinology* 140: 392–397

60. Cantley J & Ashcroft FM (2015) Q&A: insulin secretion and type 2 diabetes: why do β-cells fail? *BMC Biol* 13: 33

61. Cargnello M & Roux PP (2011) Activation and Function of the MAPKs and Their Substrates, the MAPK-Activated Protein Kinases. *Microbiol Mol Biol Rev* 75: 50–83

62. Carpenter G, King L & Cohen S (1978) Epidermal growth factor stimulates phosphorylation in membrane preparations in vitro. *Nature* 276: 409–410

63. Cartee GD (2015) Roles of TBC1D1 and TBC1D4 in insulin- and exercise-stimulated glucose transport of skeletal muscle. *Diabetologia* 58: 19–30

64. Casqueiro J, Casqueiro J & Alves C (2012) Infections in patients with diabetes mellitus: A review of pathogenesis. *Indian J Endocrinol Metab* 16 Suppl 1: S27-36

65. Cassuto H, Kochan K, Chakravarty K, Cohen H, Blum B, Olswang Y, Hakimi P, Xu C, Massillon D, Hanson RW, *et al* (2005) Glucocorticoids regulate transcription of the gene for phosphoenolpyruvate carboxykinase in the liver via an extended glucocorticoid regulatory unit. *J Biol Chem* 280: 33873–33884

66. Cataldi S, Costa V, Ciccodicola A & Aprile M (2021) PPARγ and Diabetes: Beyond the Genome and Towards Personalized Medicine. *Curr Diab Rep* 21: 18

67. Cerf ME (2013) Beta Cell Dysfunction and Insulin Resistance. *Front Endocrinol (Lausanne)* 4: 37

68. Chadt A & Al-Hasani H (2020) Glucose transporters in adipose tissue, liver, and skeletal muscle in metabolic health and disease. *Pflugers Arch - Eur J Physiol* 472: 1273–1298

69. Chakravarty K, Cassuto H, Reshef L & Hanson RW (2005) Factors that control the tissue-specific transcription of the gene for phosphoenolpyruvate carboxykinase-C. *Crit Rev Biochem Mol Biol* 40: 129–154

70. Chan LSA & Wells RA (2009) Cross-Talk between PPARs and the Partners of RXR: A Molecular Perspective. *PPAR Res* 2009: 925309

71. Chandra V, Huang P, Hamuro Y, Raghuram S, Wang Y, Burris TP & Rastinejad F (2008) Structure of the intact PPAR-gamma-RXR- nuclear receptor complex on DNA. *Nature* 456: 350–356

72. Chen C, Cohrs CM, Stertmann J, Bozsak R & Speier S (2017a) Human beta cell mass and function in diabetes: Recent advances in knowledge and

technologies to understand disease pathogenesis. *Molecular Metabolism* 6: 943–957

73. Chen EI, Hewel J, Krueger JS, Tiraby C, Weber MR, Kralli A, Becker K, Yates JR & Felding-Habermann B (2007) Adaptation of energy metabolism in breast cancer brain metastases. *Cancer Res* 67: 1472–1486

74. Chen L, Deng H, Cui H, Fang J, Zuo Z, Deng J, Li Y, Wang X & Zhao L (2017b) Inflammatory responses and inflammation-associated diseases in organs. *Oncotarget* 9: 7204–7218

75. Chiba Y, Nakazawa S, Todoroki M, Shinozaki K, Sakai H & Misawa M (2009) Interleukin-13 augments bronchial smooth muscle contractility with an up-regulation of RhoA protein. *Am J Respir Cell Mol Biol* 40: 159–167

76. Choi S, Jung J-E, Yang YR, Kim E-S, Jang H-J, Kim E-K, Kim IS, Lee J-Y, Kim JK, Seo JK, *et al* (2015) Novel phosphorylation of PPARγ ameliorates obesity-induced adipose tissue inflammation and improves insulin sensitivity. *Cell Signal* 27: 2488–2495

77. Choubey A, Girdhar K, Kar AK, Kushwaha S, Yadav MK, Ghosh D & Mondal P (2020) Low-dose naltrexone rescues inflammation and insulin resistance associated with hyperinsulinemia. *J Biol Chem* 295: 16359–16369

78. Christensen MD & Geisler C (2000) Recruitment of SHP-1 protein tyrosine phosphatase and signalling by a chimeric T-cell receptor-killer inhibitory receptor. *Scand J Immunol* 51: 557–564

79. Christofides A, Konstantinidou E, Jani C & Boussiotis VA (2021) The role of peroxisome proliferator-activated receptors (PPAR) in immune responses. *Metabolism* 114: 154338

80. Christophi GP, Hudson CA, Gruber R, Chrisophi CP & Massa PT (2008) Promoter-specific induction of the phosphatase SHP-1 by viral infection and cytokines in CNS glia. *J Neurochem* 105: 2511–2523

81. Chung ST, Chacko SK, Sunehag AL & Haymond MW (2015) Measurements of Gluconeogenesis and Glycogenolysis: A Methodological Review. *Diabetes* 64: 3996–4010

82. Coelho M, Oliveira T & Fernandes R (2013) Biochemistry of adipose tissue: an endocrine organ. *Arch Med Sci* 9: 191–200

83. Conaway JW, Bond MW & Conaway RC (1987) An RNA polymerase II transcription system from rat liver. Purification of an essential component. *J Biol Chem* 262: 8293–8297

84. Cooke M, Orlando U, Maloberti P, Podestá EJ & Cornejo Maciel F (2011) Tyrosine phosphatase SHP2 regulates the expression of acyl-CoA synthetase ACSL4. *J Lipid Res* 52: 1936–1948

85. Corden JL (1990) Tails of RNA polymerase II. *Trends Biochem Sci* 15: 383–387

86. Craggs G & Kellie S (2001) A functional nuclear localization sequence in the C-terminal domain of SHP-1. *J Biol Chem* 276: 23719–23725

87. Cramer P (2001) Structural Basis of Transcription: RNA Polymerase II at 2.8 Angstrom Resolution. *Science* 292: 1863–1876

88. Croker BA, Lawson BR, Berger M, Eidenschenk C, Blasius AL, Moresco EMY, Sovath S, Cengia L, Shultz LD, Theofilopoulos AN, *et al* (2008) Inflammation and autoimmunity caused by a SHP1 mutation depend on IL-1, MyD88, and a microbial trigger. *Proc Natl Acad Sci U S A* 105: 15028–15033

89. Cui Y, Hosui A, Sun R, Shen K, Gavrilova O, Chen W, Cam MC, Gao B, Robinson GW & Hennighausen L (2007) Loss of signal transducer and activator of transcription 5 leads to hepatosteatosis and impaired liver regeneration. *Hepatology* 46: 504–513

90. Da Silva Xavier G (2018) The Cells of the Islets of Langerhans. *J Clin Med* 7: 54

91. Daniel PV, Dogra S, Rawat P, Choubey A, Khan AS, Rajak S, Kamthan M & Mondal P (2021) NF-κB p65 regulates hepatic lipogenesis by promoting nuclear entry of ChREBP in response to a high carbohydrate diet. *Journal of Biological Chemistry* 296

92. Davey HW, McLachlan MJ, Wilkins RJ, Hilton DJ & Adams TE (1999) STAT5b mediates the GH-induced expression of SOCS-2 and SOCS-3 mRNA in the liver. *Mol Cell Endocrinol* 158: 111–116

93. Decker T & Kovarik P (2000) Serine phosphorylation of STATs. *Oncogene* 19: 2628–2637

94. Dephoure N, Gould KL, Gygi SP & Kellogg DR (2013) Mapping and analysis of phosphorylation sites: a quick guide for cell biologists. *Mol Biol Cell* 24: 535–542

95. Diagnosis and Classification of Diabetes Mellitus (2009) *Diabetes Care* 32: S62–S67

96. Dias MMG, Batista FAH, Tittanegro TH, de Oliveira AG, Le Maire A, Torres FR, Filho HVR, Silveira LR & Figueira ACM (2020) PPARγ S273

Phosphorylation Modifies the Dynamics of Coregulator Proteins Recruitment. *Front Endocrinol (Lausanne)* 11: 561256

97. Dickie MM, Southard JL & Farnsworth RT (1969) Two unusual dominant mutations in the mouse. *J Hered* 60: 84–86

98. Diezko R & Suske G (2013) Ligand binding reduces SUMOylation of the peroxisome proliferator-activated receptor γ (PPARγ) activation function 1 (AF1) domain. *PLoS One* 8: e66947

99. Drapeau N, Lizotte F, Denhez B, Guay A, Kennedy CR & Geraldes P (2013) Expression of SHP-1 induced by hyperglycemia prevents insulin actions in podocytes. *Am J Physiol Endocrinol Metab* 304: E1188-1198

100. Dubois M-J, Bergeron S, Kim H-J, Dombrowski L, Perreault M, Fournès B, Faure R, Olivier M, Beauchemin N, Shulman GI, *et al* (2006) The SHP-1 protein tyrosine phosphatase negatively modulates glucose homeostasis. *Nat Med* 12: 549–556

101. Duchesne C, Charland S, Asselin C, Nahmias C & Rivard N (2003) Negative regulation of beta-catenin signaling by tyrosine phosphatase SHP-1 in intestinal epithelial cells. *J Biol Chem* 278: 14274–14283

102. Eckhart W, Hutchinson MA & Hunter T (1979) An activity phosphorylating tyrosine in polyoma T antigen immunoprecipitates. *Cell* 18: 925–933

103. Edgerton DS, Ramnanan CJ, Grueter CA, Johnson KMS, Lautz M, Neal DW, Williams PE & Cherrington AD (2009) Effects of insulin on the metabolic control of hepatic gluconeogenesis in vivo. *Diabetes* 58: 2766–2775

104. Eick D & Geyer M (2013) The RNA Polymerase II Carboxy-Terminal Domain (CTD) Code. *Chem Rev* 113: 8456–8490

105. Ellard S, Bellanné-Chantelot C, Hattersley AT, & European Molecular Genetics Quality Network (EMQN) MODY group (2008) Best practice guidelines for the molecular genetic diagnosis of maturity-onset diabetes of the young. *Diabetologia* 51: 546–553

106. Ellulu MS, Patimah I, Khaza'ai H, Rahmat A & Abed Y (2017) Obesity and inflammation: the linking mechanism and the complications. *Arch Med Sci* 13: 851–863

107. Emhoff C-AW, Messonnier LA, Horning MA, Fattor JA, Carlson TJ & Brooks GA (2013) Gluconeogenesis and hepatic glycogenolysis during

exercise at the lactate threshold. *Journal of Applied Physiology* 114: 297–306

108. Engin A (2017) The Definition and Prevalence of Obesity and Metabolic Syndrome. *Adv Exp Med Biol* 960: 1–17

109. Eriksen KW, Woetmann A, Skov L, Krejsgaard T, Bovin LF, Hansen ML, Grønbaek K, Billestrup N, Nissen MH, Geisler C, *et al* (2010) Deficient SOCS3 and SHP-1 expression in psoriatic T cells. *J Invest Dermatol* 130: 1590–1597

110. Esmaeili MA, Yadav S, Gupta RK, Waggoner GR, Deloach A, Calingasan NY, Beal MF & Kiaei M (2016) Preferential PPAR-α activation reduces neuroinflammation, and blocks neurodegeneration in vivo. *Hum Mol Genet* 25: 317–327

111. Evren S, Wan S, Ma X-Z, Fahim S, Mody N, Sakac D, Jin T & Branch DR (2013) Characterization of SHP-1 protein tyrosine phosphatase transcripts, protein isoforms and phosphatase activity in epithelial cancer cells. *Genomics* 102: 491–499

112. Feng G-S (2006) Shp2 as a therapeutic target for leptin resistance and obesity. *Expert Opin Ther Targets* 10: 135–142

113. Feng GS, Hui CC & Pawson T (1993) SH2-containing phosphotyrosine phosphatase as a target of protein-tyrosine kinases. *Science* 259: 1607–1611

114. Feng Y, Feng Q, Qu H, Song X, Hu J, Xu X, Zhang L & Yin S (2020) Stress adaptation is associated with insulin resistance in women with gestational diabetes mellitus. *Nutr Diabetes* 10: 1–4

115. Firdous P, Nissar K, Ali S, Ganai BA, Shabir U, Hassan T & Masoodi SR (2018) Genetic Testing of Maturity-Onset Diabetes of the Young Current Status and Future Perspectives. *Front Endocrinol (Lausanne)* 9: 253

116. Frackelton AR, Ross AH & Eisen HN (1983) Characterization and use of monoclonal antibodies for isolation of phosphotyrosyl proteins from retrovirus-transformed cells and growth factor-stimulated cells. *Mol Cell Biol* 3: 1343–1352

117. Freund P, Kerenyi MA, Hager M, Wagner T, Wingelhofer B, Pham HTT, Elabd M, Han X, Valent P, Gouilleux F, *et al* (2017) O-GlcNAcylation of STAT5 controls tyrosine phosphorylation and oncogenic transcription in STAT5-dependent malignancies. *Leukemia* 31: 2132–2142

118. Fulton DL, Sundararajan S, Badis G, Hughes TR, Wasserman WW, Roach JC & Sladek R (2009) TFCat: the curated catalog of mouse and human transcription factors. *Genome Biology* 10: R29

119. Gaál Z & Balogh I (2019) Monogenic Forms of Diabetes Mellitus. *Exp Suppl* 111: 385–416

120. Gamdzyk M, Doycheva DM, Malaguit J, Enkhjargal B, Tang J & Zhang JH (2018) Role of PPAR-β/δ/miR-17/TXNIP pathway in neuronal apoptosis after neonatal hypoxic-ischemic injury in rats. *Neuropharmacology* 140: 150–161

121. Gamero AM, Young MR, Mentor-Marcel R, Bobe G, Scarzello AJ, Wise J & Colburn NH (2010) STAT2 contributes to promotion of colorectal and skin carcinogenesis. *Cancer Prev Res (Phila)* 3: 495–504

122. Gao M, Piernas C, Astbury NM, Hippisley-Cox J, O'Rahilly S, Aveyard P & Jebb SA (2021) Associations between body-mass index and COVID-19 severity in 6·9 million people in England: a prospective, community-based, cohort study. *Lancet Diabetes Endocrinol* 9: 350–359

123. Gao Z, Hwang D, Bataille F, Lefevre M, York D, Quon MJ & Ye J (2002) Serine phosphorylation of insulin receptor substrate 1 by inhibitor kappa B kinase complex. *J Biol Chem* 277: 48115–48121

124. Garrington TP & Johnson GL (1999) Organization and regulation of mitogen-activated protein kinase signaling pathways. *Current Opinion in Cell Biology* 11: 211–218

125. Gavrilova O, Haluzik M, Matsusue K, Cutson JJ, Johnson L, Dietz KR, Nicol CJ, Vinson C, Gonzalez FJ & Reitman ML (2003) Liver peroxisome proliferator-activated receptor gamma contributes to hepatic steatosis, triglyceride clearance, and regulation of body fat mass. *J Biol Chem* 278: 34268–34276

126. GBD 2015 Obesity Collaborators, Afshin A, Forouzanfar MH, Reitsma MB, Sur P, Estep K, Lee A, Marczak L, Mokdad AH, Moradi-Lakeh M, *et al* (2017) Health Effects of Overweight and Obesity in 195 Countries over 25 Years. *N Engl J Med* 377: 13–27

127. Geiss-Friedlander R & Melchior F (2007) Concepts in sumoylation: a decade on. *Nat Rev Mol Cell Biol* 8: 947–956

128. Germolec DR, Shipkowski KA, Frawley RP & Evans E (2018) Markers of Inflammation. *Methods Mol Biol* 1803: 57–79

129. Gibcus JH & Dekker J (2012) The context of gene expression regulation. *F1000 Biol Rep* 4: 8

130. Giguère V (1999) Orphan Nuclear Receptors: From Gene to Function*. *Endocrine Reviews* 20: 689–725

131. Giralt A, Denechaud P-D, Lopez-Mejia IC, Delacuisine B, Blanchet E, Bonner C, Pattou F, Annicotte J-S & Fajas L (2018) E2F1 promotes hepatic gluconeogenesis and contributes to hyperglycemia during diabetes. *Mol Metab* 11: 104–112

132. Godoy-Matos AF, Silva Júnior WS & Valerio CM (2020) NAFLD as a continuum: from obesity to metabolic syndrome and diabetes. *Diabetology & Metabolic Syndrome* 12: 60

133. Gómez-Valadés AG, Méndez-Lucas A, Vidal-Alabró A, Blasco FX, Chillon M, Bartrons R, Bermúdez J & Perales JC (2008) Pck1 Gene Silencing in the Liver Improves Glycemia Control, Insulin Sensitivity, and Dyslipidemia in db/db Mice. *Diabetes* 57: 2199–2210

134. Gotthardt D, Putz EM, Grundschober E, Prchal-Murphy M, Straka E, Kudweis P, Heller G, Bago-Horvath Z, Witalisz-Siepracka A, Cumaraswamy AA, *et al* (2016) STAT5 Is a Key Regulator in NK Cells and Acts as a Molecular Switch from Tumor Surveillance to Tumor Promotion. *Cancer Discov* 6: 414–429

135. Gouilleux F, Wakao H, Mundt M & Groner B (1994) Prolactin induces phosphorylation of Tyr694 of Stat5 (MGF), a prerequisite for DNA binding and induction of transcription. *EMBO J* 13: 4361–4369

136. Grasmann G, Smolle E, Olschewski H & Leithner K (2019) Gluconeogenesis in cancer cells - Repurposing of a starvation-induced metabolic pathway? *Biochim Biophys Acta Rev Cancer* 1872: 24–36

137. Greeley SAW, Naylor RN, Philipson LH & Bell GI (2011) Neonatal diabetes: an expanding list of genes allows for improved diagnosis and treatment. *Curr Diab Rep* 11: 519–532

138. Green MC & Shultz LD (1975) Motheaten, an immunodeficient mutant of the mouse. I. Genetics and pathology. *J Hered* 66: 250–258

139. Guo S, Rena G, Cichy S, He X, Cohen P & Unterman T (1999) Phosphorylation of serine 256 by protein kinase B disrupts transactivation by FKHR and mediates effects of insulin on insulin-like growth factor-binding protein-1 promoter activity through a conserved insulin response sequence. *J Biol Chem* 274: 17184–17192

140. Haberle V & Stark A (2018) Eukaryotic core promoters and the functional basis of transcription initiation. *Nat Rev Mol Cell Biol* 19: 621–637

141. Haeusler RA, Hartil K, Vaitheesvaran B, Arrieta-Cruz I, Knight CM, Cook JR, Kammoun HL, Febbraio MA, Gutierrez-Juarez R, Kurland IJ, *et al* (2014) Integrated control of hepatic lipogenesis versus glucose production requires FoxO transcription factors. *Nat Commun* 5: 5190

142. Hajri T, Zaiou M, Fungwe TV, Ouguerram K & Besong S (2021) Epigenetic Regulation of Peroxisome Proliferator-Activated Receptor Gamma Mediates High-Fat Diet-Induced Non-Alcoholic Fatty Liver Disease. *Cells* 10: 1355

143. Hakimi P, Johnson MT, Yang J, Lepage DF, Conlon RA, Kalhan SC, Reshef L, Tilghman SM & Hanson RW (2005) Phosphoenolpyruvate carboxykinase and the critical role of cataplerosis in the control of hepatic metabolism. *Nutr Metab (Lond)* 2: 33

144. Hall JA, Ramachandran D, Roh HC, DiSpirito JR, Belchior T, Zushin P-JH, Palmer C, Hong S, Mina AI, Liu B, *et al* (2020) Obesity-Linked PPARγ S273 Phosphorylation Promotes Insulin Resistance through Growth Differentiation Factor 3. *Cell Metab* 32: 665-675.e6

145. Hall RK, Sladek FM & Granner DK (1995) The orphan receptors COUP-TF and HNF-4 serve as accessory factors required for induction of phosphoenolpyruvate carboxykinase gene transcription by glucocorticoids. *Proc Natl Acad Sci U S A* 92: 412–416

146. Hamer M, Gale CR, Kivimäki M & Batty GD (2020) Overweight, obesity, and risk of hospitalization for COVID-19: A community-based cohort study of adults in the United Kingdom. *PNAS* 117: 21011–21013

147. Hamman RF, Wing RR, Edelstein SL, Lachin JM, Bray GA, Delahanty L, Hoskin M, Kriska AM, Mayer-Davis EJ, Pi-Sunyer X, *et al* (2006) Effect of weight loss with lifestyle intervention on risk of diabetes. *Diabetes Care* 29: 2102–2107

148. Han TS & Lean ME (2016) A clinical perspective of obesity, metabolic syndrome and cardiovascular disease. *JRSM Cardiovasc Dis* 5: 2048004016633371

149. Hancock ML, Meyer RC, Mistry M, Khetani RS, Wagschal A, Shin T, Ho Sui SJ, Näär AM & Flanagan JG (2019) Insulin Receptor Associates with Promoters Genome-wide and Regulates Gene Expression. *Cell* 177: 722-736.e22

150. Hansen LH, Abrahamsen N & Nishimura E (1995) Glucagon receptor mRNA distribution in rat tissues. *Peptides* 16: 1163–1166

151. Hanson RW & Reshef L (1997) Regulation of phosphoenolpyruvate carboxykinase (GTP) gene expression. *Annu Rev Biochem* 66: 581–611

152. Hattersley AT, Greeley SAW, Polak M, Rubio-Cabezas O, Njølstad PR, Mlynarski W, Castano L, Carlsson A, Raile K, Chi DV, *et al* (2018) ISPAD Clinical Practice Consensus Guidelines 2018: The diagnosis and management of monogenic diabetes in children and adolescents. *Pediatr Diabetes* 19 Suppl 27: 47–63

153. Heinäniemi M, Uski JO, Degenhardt T & Carlberg C (2007) Meta-analysis of primary target genes of peroxisome proliferator-activated receptors. *Genome Biology* 8: R147

154. Hendriks WJAJ & Pulido R (2013) Protein tyrosine phosphatase variants in human hereditary disorders and disease susceptibilities. *Biochim Biophys Acta* 1832: 1673–1696

155. Hernandez-Quiles M, Broekema MF & Kalkhoven E (2021) PPARgamma in Metabolism, Immunity, and Cancer: Unified and Diverse Mechanisms of Action. *Front Endocrinol* 0

156. Herzig S, Long F, Jhala US, Hedrick S, Quinn R, Bauer A, Rudolph D, Schutz G, Yoon C, Puigserver P, *et al* (2001) CREB regulates hepatic gluconeogenesis through the coactivator PGC-1. *Nature* 413: 179–183

157. Hinton SD (2019) The role of pseudophosphatases as signaling regulators. *Biochimica et Biophysica Acta (BBA) - Molecular Cell Research* 1866: 167–174

158. Hoelbl A, Schuster C, Kovacic B, Zhu B, Wickre M, Hoelzl MA, Fajmann S, Grebien F, Warsch W, Stengl G, *et al* (2010) Stat5 is indispensable for the maintenance of bcr/abl-positive leukaemia. *EMBO Mol Med* 2: 98–110

159. Hof P, Pluskey S, Dhe-Paganon S, Eck MJ & Shoelson SE (1998) Crystal structure of the tyrosine phosphatase SHP-2. *Cell* 92: 441–450

160. Hollenberg SM, Weinberger C, Ong ES, Cerelli G, Oro A, Lebo R, Thompson EB, Rosenfeld MG & Evans RM (1985) Primary structure and expression of a functional human glucocorticoid receptor cDNA. *Nature* 318: 635–641

161. Honzawa N & Fujimoto K (2021) The Plasticity of Pancreatic β-Cells. *Metabolites* 11: 218

162. Horike N, Sakoda H, Kushiyama A, Ono H, Fujishiro M, Kamata H, Nishiyama K, Uchijima Y, Kurihara Y, Kurihara H, *et al* (2008) AMP-activated protein kinase activation increases phosphorylation of glycogen synthase kinase 3beta and thereby reduces cAMP-responsive element transcriptional activity and phosphoenolpyruvate carboxykinase C gene expression in the liver. *J Biol Chem* 283: 33902–33910

163. Horton JD, Goldstein JL & Brown MS (2002) SREBPs: activators of the complete program of cholesterol and fatty acid synthesis in the liver. *J Clin Invest* 109: 1125–1131

164. Hou J, Schindler U, Henzel WJ, Ho TC, Brasseur M & McKnight SL (1994) An interleukin-4-induced transcription factor: IL-4 Stat. *Science* 265: 1701–1706

165. Hruby A & Hu FB (2015) The Epidemiology of Obesity: A Big Picture. *Pharmacoeconomics* 33: 673–689

166. Hsin J-P & Manley JL (2012) The RNA polymerase II CTD coordinates transcription and RNA processing. *Genes Dev* 26: 2119–2137

167. Hu E, Kim JB, Sarraf P & Spiegelman BM (1996) Inhibition of adipogenesis through MAP kinase-mediated phosphorylation of PPARgamma. *Science* 274: 2100–2103

168. Hu E, Tontonoz P & Spiegelman BM (1995) Transdifferentiation of myoblasts by the adipogenic transcription factors PPAR gamma and C/EBP alpha. *Proc Natl Acad Sci U S A* 92: 9856–9860

169. Hu X, Dutta P, Tsurumi A, Li J, Wang J, Land H & Li WX (2013) Unphosphorylated STAT5A stabilizes heterochromatin and suppresses tumor growth. *Proc Natl Acad Sci U S A* 110: 10213–10218

170. Hunter T (2014) The genesis of tyrosine phosphorylation. *Cold Spring Harb Perspect Biol* 6: a020644

171. Hunter T & Sefton BM (1980) Transforming gene product of Rous sarcoma virus phosphorylates tyrosine. *Proc Natl Acad Sci U S A* 77: 1311–1315

172. Ihle JN (1996) STATs: Signal Transducers and Activators of Transcription. *Cell* 84: 331–334

173. Imai E, Miner JN, Mitchell JA, Yamamoto KR & Granner DK (1993) Glucocorticoid receptor-cAMP response element-binding protein interaction and the response of the phosphoenolpyruvate carboxykinase gene to glucocorticoids. *J Biol Chem* 268: 5353–5356

174. Ipsen DH, Lykkesfeldt J & Tveden-Nyborg P (2018) Molecular mechanisms of hepatic lipid accumulation in non-alcoholic fatty liver disease. *Cell Mol Life Sci* 75: 3313–3327

175. Iwashita A, Muramatsu Y, Yamazaki T, Muramoto M, Kita Y, Yamazaki S, Mihara K, Moriguchi A & Matsuoka N (2007) Neuroprotective efficacy of the peroxisome proliferator-activated receptor delta-selective agonists in vitro and in vivo. *J Pharmacol Exp Ther* 320: 1087–1096

176. Jarvie JL, Pandey A, Ayers CR, McGavock JM, Sénéchal M, Berry JD, Patel KV & McGuire DK (2019) Aerobic Fitness and Adherence to Guideline-Recommended Minimum Physical Activity Among Ambulatory Patients With Type 2 Diabetes Mellitus. *Diabetes Care* 42: 1333–1339

177. Ji S, Park SY, Roth J, Kim HS & Cho JW (2012) O-GlcNAc modification of PPARγ reduces its transcriptional activity. *Biochem Biophys Res Commun* 417: 1158–1163

178. Jiang G & Zhang BB (2003) Glucagon and regulation of glucose metabolism. *American Journal of Physiology-Endocrinology and Metabolism* 284: E671–E678

179. Jiang X, Ye X, Guo W, Lu H & Gao Z (2014) Inhibition of HDAC3 promotes ligand-independent PPARγ activation by protein acetylation. *J Mol Endocrinol* 53: 191–200

180. Jin YJ, Yu CL & Burakoff SJ (1999) Human 70-kDa SHP-1L differs from 68-kDa SHP-1 in its C-terminal structure and catalytic activity. *J Biol Chem* 274: 28301–28307

181. Jones JR, Barrick C, Kim K-A, Lindner J, Blondeau B, Fujimoto Y, Shiota M, Kesterson RA, Kahn BB & Magnuson MA (2005) Deletion of PPARgamma in adipose tissues of mice protects against high fat diet-induced obesity and insulin resistance. *Proc Natl Acad Sci U S A* 102: 6207–6212

182. Katafuchi T, Holland WL, Kollipara RK, Kittler R, Mangelsdorf DJ & Kliewer SA (2018) PPARγ-K107 SUMOylation regulates insulin sensitivity but not adiposity in mice. *PNAS* 115: 12102–12111

183. Katome T, Obata T, Matsushima R, Masuyama N, Cantley LC, Gotoh Y, Kishi K, Shiota H & Ebina Y (2003) Use of RNA interference-mediated gene silencing and adenoviral overexpression to elucidate the roles of AKT/protein kinase B isoforms in insulin actions. *J Biol Chem* 278: 28312–28323

184. Kearney AL, Norris DM, Ghomlaghi M, Kin Lok Wong M, Humphrey SJ, Carroll L, Yang G, Cooke KC, Yang P, Geddes TA, *et al* (2021) Akt phosphorylates insulin receptor substrate to limit PI3K-mediated PIP3 synthesis. *Elife* 10: e66942

185. Kerenyi MA, Grebien F, Gehart H, Schifrer M, Artaker M, Kovacic B, Beug H, Moriggl R & Müllner EW (2008) Stat5 regulates cellular iron uptake of erythroid cells via IRP-2 and TfR-1. *Blood* 112: 3878–3888

186. Kersten S (2001) Mechanisms of nutritional and hormonal regulation of lipogenesis. *EMBO Rep* 2: 282–286

187. Keshet R, Bryansker Kraitshtein Z, Shanzer M, Adler J, Reuven N & Shaul Y (2014) c-Abl tyrosine kinase promotes adipocyte differentiation by targeting PPAR-gamma 2. *Proc Natl Acad Sci U S A* 111: 16365–16370

188. Kido Y, Nakae J & Accili D (2001) The Insulin Receptor and Its Cellular Targets1. *The Journal of Clinical Endocrinology & Metabolism* 86: 972–979

189. Kim T-K & Shiekhattar R (2015) Architectural and functional commonalities between enhancers and promoters. *Cell* 162: 948–959

190. Kim YD, Li T, Ahn S-W, Kim D-K, Lee J-M, Hwang S-L, Kim Y-H, Lee C-H, Lee I-K, Chiang JYL, *et al* (2012) Orphan nuclear receptor small heterodimer partner negatively regulates growth hormone-mediated induction of hepatic gluconeogenesis through inhibition of signal transducer and activator of transcription 5 (STAT5) transactivation. *J Biol Chem* 287: 37098–37108

191. Kim YJ, Björklund S, Li Y, Sayre MH & Kornberg RD (1994) A multiprotein mediator of transcriptional activation and its interaction with the C-terminal repeat domain of RNA polymerase II. *Cell* 77: 599–608

192. Kirken RA, Malabarba MG, Xu J, DaSilva L, Erwin RA, Liu X, Hennighausen L, Rui H & Farrar WL (1997a) Two discrete regions of interleukin-2 (IL2) receptor beta independently mediate IL2 activation of a PD98059/rapamycin/wortmannin-insensitive Stat5a/b serine kinase. *J Biol Chem* 272: 15459–15465

193. Kirken RA, Malabarba MG, Xu J, Liu X, Farrar WL, Hennighausen L, Larner AC, Grimley PM & Rui H (1997b) Prolactin stimulates serine/tyrosine phosphorylation and formation of heterocomplexes of multiple Stat5 isoforms in Nb2 lymphocytes. *J Biol Chem* 272: 14098–14103

194. Kirkman MS, Briscoe VJ, Clark N, Florez H, Haas LB, Halter JB, Huang ES, Korytkowski MT, Munshi MN, Odegard PS, *et al* (2012) Diabetes in Older Adults. *Diabetes Care* 35: 2650–2664

195. Kleiman LB, Maiwald T, Conzelmann H, Lauffenburger DA & Sorger PK (2011) Rapid phospho-turnover by receptor tyrosine kinases impacts downstream signaling and drug binding. *Mol Cell* 43: 723–737

196. Klip A, McGraw TE & James DE (2019) Thirty sweet years of GLUT4. *J Biol Chem* 294: 11369–11381

197. Klover PJ, Zimmers TA, Koniaris LG & Mooney RA (2003) Chronic Exposure to Interleukin-6 Causes Hepatic Insulin Resistance in Mice. *Diabetes* 52: 2784–2789

198. Kolodziej P & Young RA (1989) RNA polymerase II subunit RPB3 is an essential component of the mRNA transcription apparatus. *Mol Cell Biol* 9: 5387–5394

199. Koo S-H, Flechner L, Qi L, Zhang X, Screaton RA, Jeffries S, Hedrick S, Xu W, Boussouar F, Brindle P, *et al* (2005) The CREB coactivator TORC2 is a key regulator of fasting glucose metabolism. *Nature* 437: 1109–1111

200. Kosan C, Ginter T, Heinzel T & Krämer OH (2013) STAT5 acetylation. *JAKSTAT* 2: e26102

201. Kroll TG, Sarraf P, Pecciarini L, Chen CJ, Mueller E, Spiegelman BM & Fletcher JA (2000) PAX8-PPARgamma1 fusion oncogene in human thyroid carcinoma [corrected]. *Science* 289: 1357–1360

202. Krüger J, Wellnhofer E, Meyborg H, Stawowy P, Östman A, Kintscher U & Kappert K (2016) Inhibition of Src homology 2 domain-containing phosphatase 1 increases insulin sensitivity in high-fat diet-induced insulin-resistant mice. *FEBS Open Bio* 6: 179–189

203. Kubota T, Koshizuka K, Williamson EA, Asou H, Said JW, Holden S, Miyoshi I & Koeffler HP (1998) Ligand for peroxisome proliferator-activated receptor gamma (troglitazone) has potent antitumor effect against human prostate cancer both in vitro and in vivo. *Cancer Res* 58: 3344–3352

204. Lambert SA, Jolma A, Campitelli LF, Das PK, Yin Y, Albu M, Chen X, Taipale J, Hughes TR & Weirauch MT (2018) The Human Transcription Factors. *Cell* 172: 650–665

205. Laplante M & Sabatini DM (2009) An emerging role of mTOR in lipid biosynthesis. *Curr Biol* 19: R1046–R1052

206. Lazarow PB & De Duve C (1976) A fatty acyl-CoA oxidizing system in rat liver peroxisomes; enhancement by clofibrate, a hypolipidemic drug. *Proc Natl Acad Sci U S A* 73: 2043–2046

207. Lee TI & Young RA (2013) Transcriptional regulation and its misregulation in disease. *Cell* 152: 1237–1251

208. Leithner K, Hrzenjak A, Trötzmüller M, Moustafa T, Köfeler HC, Wohlkoenig C, Stacher E, Lindenmann J, Harris AL, Olschewski A, *et al* (2015) PCK2 activation mediates an adaptive response to glucose depletion in lung cancer. *Oncogene* 34: 1044–1050

209. Leitner DR, Frühbeck G, Yumuk V, Schindler K, Micic D, Woodward E & Toplak H (2017) Obesity and Type 2 Diabetes: Two Diseases with a Need for Combined Treatment Strategies - EASO Can Lead the Way. *Obes Facts* 10: 483–492

210. Lenormand P, Sardet C, Pagès G, L'Allemain G, Brunet A & Pouysségur J (1993) Growth factors induce nuclear translocation of MAP kinases (p42mapk and p44mapk) but not of their activator MAP kinase kinase (p45mapkk) in fibroblasts. *J Cell Biol* 122: 1079–1088

211. Leon BM & Maddox TM (2015) Diabetes and cardiovascular disease: Epidemiology, biological mechanisms, treatment recommendations and future research. *World J Diabetes* 6: 1246–1258

212. Levy DE & Darnell JE (2002) Stats: transcriptional control and biological impact. *Nat Rev Mol Cell Biol* 3: 651–662

213. Li H, Zhang Z, Wang B, Zhang J, Zhao Y & Jin Y (2007) Wwp2-mediated ubiquitination of the RNA polymerase II large subunit in mouse embryonic pluripotent stem cells. *Mol Cell Biol* 27: 5296–5305

214. Li S, Brown MS & Goldstein JL (2010) Bifurcation of insulin signaling pathway in rat liver: mTORC1 required for stimulation of lipogenesis, but not inhibition of gluconeogenesis. *Proc Natl Acad Sci U S A* 107: 3441–3446

215. Li WX (2008) Canonical and non-canonical JAK–STAT signaling. *Trends in Cell Biology* 18: 545–551

216. Li Y, Luo S, Ma R, Liu J, Xu P, Zhang H, Tang K, Ma J, Zhang Y, Liang X, *et al* (2015) Upregulation of cytosolic phosphoenolpyruvate carboxykinase is a critical metabolic event in melanoma cells that repopulate tumors. *Cancer Res* 75: 1191–1196

217. Lim H-J, Lee S, Park J-H, Lee K-S, Choi H-E, Chung K-S, Lee H-H & Park H-Y (2009) PPAR delta agonist L-165041 inhibits rat vascular smooth

muscle cell proliferation and migration via inhibition of cell cycle. *Atherosclerosis* 202: 446–454

218. Lin L, Jian J, Song C-Y, Chen F, Ding K, Xie W-F & Hu P-F (2020) SHP-1 ameliorates nonalcoholic steatohepatitis by inhibiting proinflammatory cytokine production. *FEBS Lett* 594: 2965–2974

219. Liss KHH & Finck BN (2017) PPARs and Nonalcoholic Fatty Liver Disease. *Biochimie* 136: 65–74

220. Liu W, Yin Y, Wang M, Fan T, Zhu Y, Shen L, Peng S, Gao J, Deng G, Meng X, *et al* (2020) Disrupting phosphatase SHP2 in macrophages protects mice from high-fat diet-induced hepatic steatosis and insulin resistance by elevating IL-18 levels. *J Biol Chem* 295: 10842–10856

221. Liu X, Robinson GW, Gouilleux F, Groner B & Hennighausen L (1995) Cloning and expression of Stat5 and an additional homologue (Stat5b) involved in prolactin signal transduction in mouse mammary tissue. *Proc Natl Acad Sci U S A* 92: 8831–8835

222. Liu X, Robinson GW, Wagner KU, Garrett L, Wynshaw-Boris A & Hennighausen L (1997) Stat5a is mandatory for adult mammary gland development and lactogenesis. *Genes Dev* 11: 179–186

223. Liu Y, Colby JK, Zuo X, Jaoude J, Wei D & Shureiqi I (2018) The Role of PPAR-δ in Metabolism, Inflammation, and Cancer: Many Characters of a Critical Transcription Factor. *Int J Mol Sci* 19: 3339

224. Lizotte F, Denhez B, Guay A, Gévry N, Côté AM & Geraldes P (2016) Persistent Insulin Resistance in Podocytes Caused by Epigenetic Changes of SHP-1 in Diabetes. *Diabetes* 65: 3705–3717

225. López-Ruiz P, Rodriguez-Ubreva J, Cariaga AE, Cortes MA & Colás B (2011) SHP-1 in cell-cycle regulation. *Anticancer Agents Med Chem* 11: 89–98

226. Lorenz U (2009) SHP-1 and SHP-2 in T cells: two phosphatases functioning at many levels. *Immunol Rev* 228: 342–359

227. Lorenz U, Ravichandran KS, Pei D, Walsh CT, Burakoff SJ & Neel BG (1994) Lck-dependent tyrosyl phosphorylation of the phosphotyrosine phosphatase SH-PTP1 in murine T cells. *Mol Cell Biol* 14: 1824–1834

228. Lu J, Zhao J, Meng H & Zhang X (2019) Adipose Tissue-Resident Immune Cells in Obesity and Type 2 Diabetes. *Front Immunol* 0

229. Lu M, Wan M, Leavens KF, Chu Q, Monks BR, Fernandez S, Ahima RS, Ueki K, Kahn CR & Birnbaum MJ (2012) Insulin regulates liver

metabolism in vivo in the absence of hepatic Akt and Foxo1. *Nat Med* 18: 388–395

230. Luo J, Field SJ, Lee JY, Engelman JA & Cantley LC (2005) The p85 regulatory subunit of phosphoinositide 3-kinase down-regulates IRS-1 signaling via the formation of a sequestration complex. *J Cell Biol* 170: 455–464

231. Luo W, Xu Q, Wang Q, Wu H & Hua J (2017) Effect of modulation of PPAR-γ activity on Kupffer cells M1/M2 polarization in the development of non-alcoholic fatty liver disease. *Sci Rep* 7: 44612

232. Ma L, Gao J, Guan Y, Shi X, Zhang H, Ayrapetov MK, Zhang Z, Xu L, Hyun Y-M, Kim M, *et al* (2010) Acetylation modulates prolactin receptor dimerization. *Proc Natl Acad Sci U S A* 107: 19314–19319

233. Marette A (2021) The fascinating physiology of insulin: celebrating a centennial hormone. *Am J Physiol Endocrinol Metab* 320: E1

234. Marín-Juez R, Jong-Raadsen S, Yang S & Spaink HP (2014) Hyperinsulinemia induces insulin resistance and immune suppression via Ptpn6/Shp1 in zebrafish. *J Endocrinol* 222: 229–241

235. Martin S, Millar CA, Lyttle CT, Meerloo T, Marsh BJ, Gould GW & James DE (2000) Effects of insulin on intracellular GLUT4 vesicles in adipocytes: evidence for a secretory mode of regulation. *J Cell Sci* 113 Pt 19: 3427–3438

236. Matsui T, Segall J, Weil PA & Roeder RG (1980) Multiple factors required for accurate initiation of transcription by purified RNA polymerase II. *J Biol Chem* 255: 11992–11996

237. Matsumoto M, Pocai A, Rossetti L, DePinho RA & Accili D (2007) Impaired Regulation of Hepatic Glucose Production in Mice Lacking the Forkhead Transcription Factor Foxo1 in Liver. *Cell Metabolism* 6: 208–216

238. Matsusue K, Haluzik M, Lambert G, Yim S-H, Gavrilova O, Ward JM, Brewer B, Reitman ML & Gonzalez FJ (2003) Liver-specific disruption of PPARgamma in leptin-deficient mice improves fatty liver but aggravates diabetic phenotypes. *J Clin Invest* 111: 737–747

239. Mattei AM, Smailys JD, Hepworth EMW & Hinton SD (2021) The Roles of Pseudophosphatases in Disease. *Int J Mol Sci* 22: 6924

240. Matthews RJ, Bowne DB, Flores E & Thomas ML (1992) Characterization of hematopoietic intracellular protein tyrosine phosphatases: description of a phosphatase containing an SH2 domain and

another enriched in proline-, glutamic acid-, serine-, and threonine-rich sequences. *Mol Cell Biol* 12: 2396–2405

241. Mazaira GI, Zgajnar NR, Lotufo CM, Daneri-Becerra C, Sivils JC, Soto OB, Cox MB & Galigniana MD (2018) The Nuclear Receptor Field: A Historical Overview and Future Challenges. *Nucl Receptor Res* 5: 101320

242. McCullough AJ (2006) Pathophysiology of nonalcoholic steatohepatitis. *J Clin Gastroenterol* 40 Suppl 1: S17-29

243. McIntyre HD, Catalano P, Zhang C, Desoye G, Mathiesen ER & Damm P (2019) Gestational diabetes mellitus. *Nat Rev Dis Primers* 5: 47

244. Meirhaeghe A & Amouyel P (2004) Impact of genetic variation of PPARgamma in humans. *Mol Genet Metab* 83: 93–102

245. Melkonian EA, Asuka E & Schury MP (2021) Physiology, Gluconeogenesis. In *StatPearls* Treasure Island (FL): StatPearls Publishing

246. Meraz MA, White JM, Sheehan KC, Bach EA, Rodig SJ, Dighe AS, Kaplan DH, Riley JK, Greenlund AC, Campbell D, *et al* (1996) Targeted disruption of the Stat1 gene in mice reveals unexpected physiologic specificity in the JAK-STAT signaling pathway. *Cell* 84: 431–442

247. Mezza T, Cinti F, Cefalo CMA, Pontecorvi A, Kulkarni RN & Giaccari A (2019) β-Cell Fate in Human Insulin Resistance and Type 2 Diabetes: A Perspective on Islet Plasticity. *Diabetes* 68: 1121–1129

248. Miele C, Caruso M, Calleja V, Auricchio R, Oriente F, Formisano P, Condorelli G, Cafieri A, Sawka-Verhelle D, Van Obberghen E, *et al* (1999) Differential role of insulin receptor substrate (IRS)-1 and IRS-2 in L6 skeletal muscle cells expressing the Arg1152 --> Gln insulin receptor. *J Biol Chem* 274: 3094–3102

249. Mirza S, Hossain M, Mathews C, Martinez P, Pino P, Gay JL, Rentfro A, McCormick JB & Fisher-Hoch SP (2012) Type 2-Diabetes is Associated With Elevated Levels of TNF-alpha, IL-6 and Adiponectin and Low Levels of Leptin in a Population of Mexican American: A Cross-Sectional Study. *Cytokine* 57: 136–142

250. Mitra S, De A & Chowdhury A (2020) Epidemiology of non-alcoholic and alcoholic fatty liver diseases. *Transl Gastroenterol Hepatol* 5: 16

251. Moosazadeh M, Asemi Z, Lankarani KB, Tabrizi R, Maharlouei N, Naghibzadeh-Tahami A, Yousefzadeh G, Sadeghi R, Khatibi SR, Afshari M, *et al* (2017) Family history of diabetes and the risk of gestational diabetes

mellitus in Iran: A systematic review and meta-analysis. *Diabetes Metab Syndr* 11 Suppl 1: S99–S104

252. Mothe I & Van Obberghen E (1996) Phosphorylation of insulin receptor substrate-1 on multiple serine residues, 612, 632, 662, and 731, modulates insulin action. *J Biol Chem* 271: 11222–11227

253. Mueller E, Sarraf P, Tontonoz P, Evans RM, Martin KJ, Zhang M, Fletcher C, Singer S & Spiegelman BM (1998) Terminal differentiation of human breast cancer through PPAR gamma. *Mol Cell* 1: 465–470

254. Muller WA, Faloona GR & Unger RH (1971) The influence of the antecedent diet upon glucagon and insulin secretion. *N Engl J Med* 285: 1450–1454

255. Näär AM, Lemon BD & Tjian R (2001) Transcriptional coactivator complexes. *Annu Rev Biochem* 70: 475–501

256. Nagy L & Schwabe JWR (2004) Mechanism of the nuclear receptor molecular switch. *Trends Biochem Sci* 29: 317–324

257. Nakae J, Park B-C & Accili D (1999) Insulin Stimulates Phosphorylation of the Forkhead Transcription Factor FKHR on Serine 253 through a Wortmannin-sensitive Pathway*. *Journal of Biological Chemistry* 274: 15982–15985

258. Nakase K, Cheng J, Zhu Q & Marasco WA (2009) Mechanisms of SHP-1 P2 promoter regulation in hematopoietic cells and its silencing in HTLV-1-transformed T cells. *J Leukoc Biol* 85: 165–174

259. Nakata K, Suzuki Y, Inoue T, Ra C, Yakura H & Mizuno K (2011) Deficiency of SHP1 leads to sustained and increased ERK activation in mast cells, thereby inhibiting IL-3-dependent proliferation and cell death. *Mol Immunol* 48: 472–480

260. Nassir F, Rector RS, Hammoud GM & Ibdah JA (2015) Pathogenesis and Prevention of Hepatic Steatosis. *Gastroenterol Hepatol (N Y)* 11: 167–175

261. Neculai D, Neculai AM, Verrier S, Straub K, Klumpp K, Pfitzner E & Becker S (2005) Structure of the unphosphorylated STAT5a dimer. *J Biol Chem* 280: 40782–40787

262. Nesterovitch AB, Gyorfy Z, Hoffman MD, Moore EC, Elbuluk N, Tryniszewska B, Rauch TA, Simon M, Kang S, Fisher GJ, *et al* (2011) Alteration in the gene encoding protein tyrosine phosphatase nonreceptor

type 6 (PTPN6/SHP1) may contribute to neutrophilic dermatoses. *Am J Pathol* 178: 1434–1441

263. Nikolov DB & Burley SK (1997) RNA polymerase II transcription initiation: A structural view. *PNAS* 94: 15–22

264. Nirupama R, Devaki M & Yajurvedi HN (2012) Chronic stress and carbohydrate metabolism: persistent changes and slow return to normalcy in male albino rats. *Stress* 15: 262–271

265. Novac N & Heinzel T (2004) Nuclear receptors: overview and classification. *Curr Drug Targets Inflamm Allergy* 3: 335–346

266. Nteeba J, Ortinau LC, Perfield JW & Keating AF (2013) Diet-induced obesity alters immune cell infiltration and expression of inflammatory cytokine genes in mouse ovarian and peri-ovarian adipose depot tissues. *Mol Reprod Dev* 80: 948–958

267. O'Brien RM, Lucas PC, Forest CD, Magnuson MA & Granner DK (1990) Identification of a sequence in the PEPCK gene that mediates a negative effect of insulin on transcription. *Science* 249: 533–537

268. Oh S, Shao J, Mitra J, Xiong F, D'Antonio M, Wang R, Garcia-Bassets I, Ma Q, Zhu X, Lee J-H, *et al* (2021) Enhancer release and retargeting activates disease-susceptibility genes. *Nature* 595: 735–740

269. Oka T, Yoshino T, Hayashi K, Ohara N, Nakanishi T, Yamaai Y, Hiraki A, Sogawa CA, Kondo E, Teramoto N, *et al* (2001) Reduction of Hematopoietic Cell-Specific Tyrosine Phosphatase SHP-1 Gene Expression in Natural Killer Cell Lymphoma and Various Types of Lymphomas/Leukemias. *Am J Pathol* 159: 1495–1505

270. Osman S & Cramer P (2020) Structural Biology of RNA Polymerase II Transcription: 20 Years On. *Annu Rev Cell Dev Biol* 36: 1–34

271. O-Sullivan I, Zhang W, Wasserman DH, Liew CW, Liu J, Paik J, DePinho RA, Stolz DB, Kahn CR, Schwartz MW, *et al* (2015) FoxO1 integrates direct and indirect effects of insulin on hepatic glucose production and glucose utilization. *Nat Commun* 6: 7079

272. Owen OE, Felig P, Morgan AP, Wahren J & Cahill GF (1969) Liver and kidney metabolism during prolonged starvation. *J Clin Invest* 48: 574–583

273. Paling NRD & Welham MJ (2002) Role of the protein tyrosine phosphatase SHP-1 (Src homology phosphatase-1) in the regulation of

interleukin-3-induced survival, proliferation and signalling. *Biochem J* 368: 885–894

274. Panigrahi A & O'Malley BW (2021) Mechanisms of enhancer action: the known and the unknown. *Genome Biol* 22: 108

275. Panuganti KK, Nguyen M & Kshirsagar RK (2021) Obesity. In *StatPearls* Treasure Island (FL): StatPearls Publishing

276. Pao LI, Lam K-P, Henderson JM, Kutok JL, Alimzhanov M, Nitschke L, Thomas ML, Neel BG & Rajewsky K (2007) B Cell-Specific Deletion of Protein-Tyrosine Phosphatase Shp1 Promotes B-1a Cell Development and Causes Systemic Autoimmunity. *Immunity* 27: 35–48

277. Paredes-Flores MA & Mohiuddin SS (2021) Biochemistry, Glycogenolysis. In *StatPearls* Treasure Island (FL): StatPearls Publishing

278. Park HJ, Li J, Hannah R, Biddie S, Leal-Cervantes AI, Kirschner K, Flores Santa Cruz D, Sexl V, Göttgens B & Green AR (2016) Cytokine-induced megakaryocytic differentiation is regulated by genome-wide loss of a uSTAT transcriptional program. *EMBO J* 35: 580–594

279. Paul RG, Hennebry AS, Elston MS, Conaglen JV & McMahon CD (2019) Regulation of murine skeletal muscle growth by STAT5B is age- and sex-specific. *Skeletal Muscle* 9: 19

280. Pedchenko TV, Gonzalez AL, Wang D, DuBois RN & Massion PP (2008) Peroxisome proliferator-activated receptor beta/delta expression and activation in lung cancer. *Am J Respir Cell Mol Biol* 39: 689–696

281. Pei D, Lorenz U, Klingmüller U, Neel BG & Walsh CT (1994) Intramolecular regulation of protein tyrosine phosphatase SH-PTP1: a new function for Src homology 2 domains. *Biochemistry* 33: 15483–15493

282. Perry RJ, Zhang D, Guerra MT, Brill AL, Goedeke L, Nasiri AR, Rabin-Court A, Wang Y, Peng L, Dufour S, *et al* (2020) Glucagon stimulates gluconeogenesis by INSP3R1-mediated hepatic lipolysis. *Nature* 579: 279–283

283. Plaschka C, Larivière L, Wenzeck L, Seizl M, Hemann M, Tegunov D, Petrotchenko EV, Borchers CH, Baumeister W, Herzog F, *et al* (2015) Architecture of the RNA polymerase II-Mediator core initiation complex. *Nature* 518: 376–380

284. Plutzky J, Neel BG & Rosenberg RD (1992) Isolation of a src homology 2-containing tyrosine phosphatase. *Proc Natl Acad Sci U S A* 89: 1123–1127

285. Poole AW & Jones ML (2005) A SHPing tale: perspectives on the regulation of SHP-1 and SHP-2 tyrosine phosphatases by the C-terminal tail. *Cell Signal* 17: 1323–1332

286. Porstmann T, Santos CR, Griffiths B, Cully M, Wu M, Leevers S, Griffiths JR, Chung Y-L & Schulze A (2008) SREBP activity is regulated by mTORC1 and contributes to Akt-dependent cell growth. *Cell Metab* 8: 224–236

287. Pouwels S, Sakran N, Graham Y, Leal A, Pintar T, Yang W, Kassir R, Singhal R, Mahawar K & Ramnarain D (2022) Non-alcoholic fatty liver disease (NAFLD): a review of pathophysiology, clinical management and effects of weight loss. *BMC Endocr Disord* 22: 63

288. Powell E, Kuhn P & Xu W (2007) Nuclear Receptor Cofactors in PPARγ-Mediated Adipogenesis and Adipocyte Energy Metabolism. *PPAR Res* 2007: 53843

289. Princen F, Bard E, Sheikh F, Zhang SS, Wang J, Zago WM, Wu D, Trelles RD, Bailly-Maitre B, Kahn CR, *et al* (2009) Deletion of Shp2 tyrosine phosphatase in muscle leads to dilated cardiomyopathy, insulin resistance, and premature death. *Mol Cell Biol* 29: 378–388

290. Puigserver P, Rhee J, Donovan J, Walkey CJ, Yoon JC, Oriente F, Kitamura Y, Altomonte J, Dong H, Accili D, *et al* (2003) Insulin-regulated hepatic gluconeogenesis through FOXO1–PGC-1α interaction. *Nature* 423: 550–555

291. Pulido R & Lang R (2019) Dual Specificity Phosphatases: From Molecular Mechanisms to Biological Function. *International Journal of Molecular Sciences* 20: 4372

292. Qayyum A, Nystrom M, Noworolski SM, Chu P, Mohanty A & Merriman R (2012) MRI steatosis grading: development and initial validation of a color mapping system. *AJR Am J Roentgenol* 198: 582–588

293. Ram PA & Waxman DJ (1997) Interaction of growth hormone-activated STATs with SH2-containing phosphotyrosine phosphatase SHP-1 and nuclear JAK2 tyrosine kinase. *J Biol Chem* 272: 17694–17702

294. Rasmussen EB & Lis JT (1993) In vivo transcriptional pausing and cap formation on three Drosophila heat shock genes. *Proc Natl Acad Sci U S A* 90: 7923–7927

295. Reginato MJ, Krakow SL, Bailey ST & Lazar MA (1998) Prostaglandins promote and block adipogenesis through opposing effects

on peroxisome proliferator-activated receptor gamma. *J Biol Chem* 273: 1855–1858

296. Rengachari S, Schilbach S, Aibara S, Dienemann C & Cramer P (2021) Structure of the human Mediator-RNA polymerase II pre-initiation complex. *Nature* 594: 129–133

297. Riazi K, Azhari H, Charette JH, Underwood FE, King JA, Afshar EE, Swain MG, Congly SE, Kaplan GG & Shaheen A-A (2022) The prevalence and incidence of NAFLD worldwide: a systematic review and meta-analysis. *Lancet Gastroenterol Hepatol* 7: 851–861

298. Ristow M, Müller-Wieland D, Pfeiffer A, Krone W & Kahn CR (1998) Obesity associated with a mutation in a genetic regulator of adipocyte differentiation. *N Engl J Med* 339: 953–959

299. Robinson PJ, Trnka MJ, Bushnell DA, Davis RE, Mattei P-J, Burlingame AL & Kornberg RD (2016) Structure of a Complete Mediator-RNA Polymerase II Pre-Initiation Complex. *Cell* 166: 1411-1422.e16

300. Rochel N, Krucker C, Coutos-Thévenot L, Osz J, Zhang R, Guyon E, Zita W, Vanthong S, Hernandez OA, Bourguet M, *et al* (2019) Recurrent activating mutations of PPARγ associated with luminal bladder tumors. *Nat Commun* 10: 253

301. Rodríguez-Ubreva FJ, Cariaga-Martinez AE, Cortés MA, Romero-De Pablos M, Ropero S, López-Ruiz P & Colás B (2010) Knockdown of protein tyrosine phosphatase SHP-1 inhibits G1/S progression in prostate cancer cells through the regulation of components of the cell-cycle machinery. *Oncogene* 29: 345–355

302. Roeder RG & Rutter WJ (1969) Multiple Forms of DNA-dependent RNA Polymerase in Eukaryotic Organisms. *Nature* 224: 234–237

303. Root-Bernstein R, Podufaly A & Dillon PF (2014) Estradiol Binds to Insulin and Insulin Receptor Decreasing Insulin Binding in vitro. *Front Endocrinol* 0

304. Rosen ED, Hsu C-H, Wang X, Sakai S, Freeman MW, Gonzalez FJ & Spiegelman BM (2002) C/EBPalpha induces adipogenesis through PPARgamma: a unified pathway. *Genes Dev* 16: 22–26

305. Rosen ED, Sarraf P, Troy AE, Bradwin G, Moore K, Milstone DS, Spiegelman BM & Mortensen RM (1999) PPAR gamma is required for the differentiation of adipose tissue in vivo and in vitro. *Mol Cell* 4: 611–617

306. Rougvie AE & Lis JT (1988) The RNA polymerase II molecule at the 5' end of the uninduced hsp70 gene of D. melanogaster is transcriptionally engaged. *Cell* 54: 795–804

307. Rui L (2014) Energy Metabolism in the Liver. *Compr Physiol* 4: 177–197

308. Sacks DA, Hadden DR, Maresh M, Deerochanawong C, Dyer AR, Metzger BE, Lowe LP, Coustan DR, Hod M, Oats JJN, *et al* (2012) Frequency of gestational diabetes mellitus at collaborating centers based on IADPSG consensus panel-recommended criteria: the Hyperglycemia and Adverse Pregnancy Outcome (HAPO) Study. *Diabetes Care* 35: 526–528

309. Salehi-sahlabadi A, Sadat S, Beigrezaei S, Pourmasomi M, Feizi A, Ghiasvand R, Hadi A, Clark CCT & Miraghajani M (2021) Dietary patterns and risk of non-alcoholic fatty liver disease. *BMC Gastroenterology* 21: 41

310. Saltiel AR & Kahn CR (2001) Insulin signalling and the regulation of glucose and lipid metabolism. *Nature* 414: 799–806

311. Salzberg SL (2018) Open questions: How many genes do we have? *BMC Biology* 16: 94

312. Samuel VT & Shulman GI (2012) Mechanisms for insulin resistance: common threads and missing links. *Cell* 148: 852–871

313. Samuels M & Sharp PA (1986) Purification and characterization of a specific RNA polymerase II transcription factor. *J Biol Chem* 261: 2003–2013

314. Sanders FWB & Griffin JL (2016) De novo lipogenesis in the liver in health and disease: more than just a shunting yard for glucose. *Biol Rev Camb Philos Soc* 91: 452–468

315. Sarraf P, Mueller E, Jones D, King FJ, DeAngelo DJ, Partridge JB, Holden SA, Chen LB, Singer S, Fletcher C, *et al* (1998) Differentiation and reversal of malignant changes in colon cancer through PPARgamma. *Nat Med* 4: 1046–1052

316. Sarraf P, Mueller E, Smith WM, Wright HM, Kum JB, Aaltonen LA, de la Chapelle A, Spiegelman BM & Eng C (1999) Loss-of-function mutations in PPAR gamma associated with human colon cancer. *Mol Cell* 3: 799–804

317. Sato R, Okamoto A, Inoue J, Miyamoto W, Sakai Y, Emoto N, Shimano H & Maeda M (2000) Transcriptional regulation of the ATP citrate-lyase gene by sterol regulatory element-binding proteins. *J Biol Chem* 275: 12497–12502

318. Sayre MH, Tschochner H & Kornberg RD (1992) Reconstitution of transcription with five purified initiation factors and RNA polymerase II from Saccharomyces cerevisiae. *J Biol Chem* 267: 23376–23382

319. Schindler C, Shuai K, Prezioso VR & Darnell JE (1992) Interferon-dependent tyrosine phosphorylation of a latent cytoplasmic transcription factor. *Science* 257: 809–813

320. Serfaty L & Lemoine M (2008) Definition and natural history of metabolic steatosis: clinical aspects of NAFLD, NASH and cirrhosis. *Diabetes Metab* 34: 634–637

321. Shen S-H, Bastien L, Posner BI & Chrétien P (1991) A protein-tyrosine phosphatase with sequence similarity to the SH2 domain of the protein-tyrosine kinases. *Nature* 352: 736–739

322. Sherwani SI, Khan HA, Ekhzaimy A, Masood A & Sakharkar MK (2016) Significance of HbA1c Test in Diagnosis and Prognosis of Diabetic Patients. *Biomark Insights* 11: 95–104

323. Shin HY & Reich NC (2013) Dynamic trafficking of STAT5 depends on an unconventional nuclear localization signal. *J Cell Sci* 126: 3333–3343

324. Simoneau M, Coulombe G, Vandal G, Vézina A & Rivard N (2011) SHP-1 inhibits β-catenin function by inducing its degradation and interfering with its association with TATA-binding protein. *Cell Signal* 23: 269–279

325. Sims RJ, Rojas LA, Beck DB, Bonasio R, Schüller R, Drury WJ, Eick D & Reinberg D (2011) The C-terminal domain of RNA polymerase II is modified by site-specific methylation. *Science* 332: 99–103

326. Sindhu S, Thomas R, Shihab P, Sriraman D, Behbehani K & Ahmad R (2015) Obesity Is a Positive Modulator of IL-6R and IL-6 Expression in the Subcutaneous Adipose Tissue: Significance for Metabolic Inflammation. *PLOS ONE* 10: e0133494

327. Skolnik EY, Batzer A, Li N, Lee CH, Lowenstein E, Mohammadi M, Margolis B & Schlessinger J (1993a) The function of GRB2 in linking the insulin receptor to Ras signaling pathways. *Science* 260: 1953–1955

328. Skolnik EY, Lee CH, Batzer A, Vicentini LM, Zhou M, Daly R, Myers MJ, Backer JM, Ullrich A & White MF (1993b) The SH2/SH3 domain-containing protein GRB2 interacts with tyrosine-phosphorylated IRS1 and Shc: implications for insulin control of ras signalling. *EMBO J* 12: 1929–1936

329. Slot JW, Geuze HJ, Gigengack S, Lienhard GE & James DE (1991) Immuno-localization of the insulin regulatable glucose transporter in brown adipose tissue of the rat. *J Cell Biol* 113: 123–135

330. Smale ST & Kadonaga JT (2003) The RNA polymerase II core promoter. *Annu Rev Biochem* 72: 449–479

331. Smith A, Baumgartner K & Bositis C (2019) Cirrhosis: Diagnosis and Management. *Am Fam Physician* 100: 759–770

332. Socolovsky M, Fallon AE, Wang S, Brugnara C & Lodish HF (1999) Fetal anemia and apoptosis of red cell progenitors in Stat5a-/-5b-/- mice: a direct role for Stat5 in Bcl-X(L) induction. *Cell* 98: 181–191

333. Song Z, Xiaoli AM & Yang F (2018) Regulation and Metabolic Significance of De Novo Lipogenesis in Adipose Tissues. *Nutrients* 10: 1383

334. de Souza MM, Zerlotini A, Geistlinger L, Tizioto PC, Taylor JF, Rocha MIP, Diniz WJS, Coutinho LL & Regitano LCA (2018) A comprehensive manually-curated compendium of bovine transcription factors. *Sci Rep* 8: 13747

335. Spanakis EK & Golden SH (2013) Race/Ethnic Difference in Diabetes and Diabetic Complications. *Curr Diab Rep* 13: 10.1007/s11892-013-0421–9

336. Spiegelman BM & Heinrich R (2004) Biological control through regulated transcriptional coactivators. *Cell* 119: 157–167

337. Steinbach N, Hasson D, Mathur D, Stratikopoulos EE, Sachidanandam R, Bernstein E & Parsons RE (2019) PTEN interacts with the transcription machinery on chromatin and regulates RNA polymerase II-mediated transcription. *Nucleic Acids Res* 47: 5573–5586

338. Stenlöf K, Wernstedt I, Fjällman T, Wallenius V, Wallenius K & Jansson J-O (2003) Interleukin-6 levels in the central nervous system are negatively correlated with fat mass in overweight/obese subjects. *J Clin Endocrinol Metab* 88: 4379–4383

339. Stępień M, Stępień A, Wlazeł RN, Paradowski M, Banach M & Rysz J (2014) Obesity indices and inflammatory markers in obese non-diabetic normo- and hypertensive patients: a comparative pilot study. *Lipids Health Dis* 13: 29

340. Stöckli J, Davey JR, Hohnen-Behrens C, Xu A, James DE & Ramm G (2008) Regulation of Glucose Transporter 4 Translocation by the Rab

Guanosine Triphosphatase-Activating Protein AS160/TBC1D4: Role of Phosphorylation and Membrane Association. *Mol Endocrinol* 22: 2703–2715

341. Streuli M, Krueger NX, Thai T, Tang M & Saito H (1990) Distinct functional roles of the two intracellular phosphatase like domains of the receptor-linked protein tyrosine phosphatases LCA and LAR. *EMBO J* 9: 2399–2407

342. Struhl K (1989) Helix-turn-helix, zinc-finger, and leucine-zipper motifs for eukaryotic transcriptional regulatory proteins. *Trends Biochem Sci* 14: 137–140

343. Su L, Zhao Z, Bouchard P, Banville D, Fischer EH, Krebs EG & Shen SH (1996) Positive effect of overexpressed protein-tyrosine phosphatase PTP1C on mitogen-activated signaling in 293 cells. *J Biol Chem* 271: 10385–10390

344. Swain MG, Ramji A, Patel K, Sebastiani G, Shaheen AA, Tam E, Marotta P, Elkhashab M, Bajaj HS, Estes C, *et al* (2020) Burden of nonalcoholic fatty liver disease in Canada, 2019-2030: a modelling study. *CMAJ Open* 8: E429–E436

345. Szabo SJ, Sullivan BM, Peng SL & Glimcher LH (2003) Molecular mechanisms regulating Th1 immune responses. *Annu Rev Immunol* 21: 713–758

346. Takahashi Y & Fukusato T (2014) Histopathology of nonalcoholic fatty liver disease/nonalcoholic steatohepatitis. *World J Gastroenterol* 20: 15539–15548

347. Tamemoto H, Kadowaki T, Tobe K, Yagi T, Sakura H, Hayakawa T, Terauchi Y, Ueki K, Kaburagi Y & Satoh S (1994) Insulin resistance and growth retardation in mice lacking insulin receptor substrate-1. *Nature* 372: 182–186

348. Tan S-X, Ng Y, Burchfield JG, Ramm G, Lambright DG, Stöckli J & James DE (2012) The Rab GTPase-Activating Protein TBC1D4/AS160 Contains an Atypical Phosphotyrosine-Binding Domain That Interacts with Plasma Membrane Phospholipids To Facilitate GLUT4 Trafficking in Adipocytes. *Mol Cell Biol* 32: 4946–4959

349. Tautz L, Pellecchia M & Mustelin T (2006) Targeting the PTPome in human disease. *Expert Opin Ther Targets* 10: 157–177

350. Timson DJ (2019) Fructose 1,6-bisphosphatase: getting the message across. *Biosci Rep* 39: BSR20190124

351. Titchenell PM, Chu Q, Monks BR & Birnbaum MJ (2015) Hepatic Insulin Signaling is Dispensable for Suppression of Glucose Output by Insulin in Vivo. *Nat Commun* 6: 7078

352. Titchenell PM, Quinn WJ, Lu M, Chu Q, Lu W, Li C, Chen H, Monks BR, Chen J, Rabinowitz JD, *et al* (2016) Direct Hepatocyte Insulin Signaling Is Required for Lipogenesis but Is Dispensable for the Suppression of Glucose Production. *Cell Metab* 23: 1154–1166

353. Toker A & Cantley LC (1997) Signalling through the lipid products of phosphoinositide-3-OH kinase. *Nature* 387: 673–676

354. Tome JM, Tippens ND & Lis JT (2018) Single-molecule nascent RNA sequencing identifies regulatory domain architecture at promoters and enhancers. *Nat Genet* 50: 1533–1541

355. Tonks NK (2006) Protein tyrosine phosphatases: from genes, to function, to disease. *Nat Rev Mol Cell Biol* 7: 833–846

356. Tonks NK, Diltz CD & Fischer EH (1988) Purification of the major protein-tyrosine-phosphatases of human placenta. *J Biol Chem* 263: 6722–6730

357. Tontonoz P, Hu E, Graves RA, Budavari AI & Spiegelman BM (1994a) mPPAR gamma 2: tissue-specific regulator of an adipocyte enhancer. *Genes Dev* 8: 1224–1234

358. Tontonoz P, Hu E & Spiegelman BM (1994b) Stimulation of adipogenesis in fibroblasts by PPAR gamma 2, a lipid-activated transcription factor. *Cell* 79: 1147–1156

359. Trefts E, Gannon M & Wasserman DH (2017) The liver. *Curr Biol* 27: R1147–R1151

360. Tsui HW, Hasselblatt K, Martin A, Mok SC & Tsui FWL (2002) Molecular mechanisms underlying SHP-1 gene expression. *Eur J Biochem* 269: 3057–3064

361. Tuo L, Xiang J, Pan X, Hu J, Tang H, Liang L, Xia J, Hu Y, Zhang W, Huang A, *et al* (2019) PCK1 negatively regulates cell cycle progression and hepatoma cell proliferation via the AMPK/p27Kip1 axis. *J Exp Clin Cancer Res* 38: 50

362. Tyagi S, Gupta P, Saini AS, Kaushal C & Sharma S (2011) The peroxisome proliferator-activated receptor: A family of nuclear receptors role in various diseases. *J Adv Pharm Technol Res* 2: 236–240

363. Udy GB, Towers RP, Snell RG, Wilkins RJ, Park SH, Ram PA, Waxman DJ & Davey HW (1997) Requirement of STAT5b for sexual dimorphism of body growth rates and liver gene expression. *Proc Natl Acad Sci U S A* 94: 7239–7244

364. Ueki K, Kondo T & Kahn CR (2004) Suppressor of Cytokine Signaling 1 (SOCS-1) and SOCS-3 Cause Insulin Resistance through Inhibition of Tyrosine Phosphorylation of Insulin Receptor Substrate Proteins by Discrete Mechanisms. *Mol Cell Biol* 24: 5434–5446

365. Unkeless JC & Jin J (1997) Inhibitory receptors, ITIM sequences and phosphatases. *Curr Opin Immunol* 9: 338–343

366. Urakami T (2019) Maturity-onset diabetes of the young (MODY): current perspectives on diagnosis and treatment. *Diabetes Metab Syndr Obes* 12: 1047–1056

367. Ushiro H & Cohen S (1980) Identification of phosphotyrosine as a product of epidermal growth factor-activated protein kinase in A-431 cell membranes. *J Biol Chem* 255: 8363–8365

368. Van Nguyen T, Angkasekwinai P, Dou H, Lin F-M, Lu L-S, Cheng J, Chin YE, Dong C & Yeh ETH (2012) SUMO-Specific Protease 1 Is Critical for Early Lymphoid Development through Regulation of STAT5 Activation. *Mol Cell* 45: 210–221

369. Vaquerizas JM, Kummerfeld SK, Teichmann SA & Luscombe NM (2009) A census of human transcription factors: function, expression and evolution. *Nat Rev Genet* 10: 252–263

370. Varga T, Czimmerer Z & Nagy L (2011) PPARs are a unique set of fatty acid regulated transcription factors controlling both lipid metabolism and inflammation. *Biochim Biophys Acta* 1812: 1007–1022

371. Varone A, Spano D & Corda D (2020) Shp1 in Solid Cancers and Their Therapy. *Frontiers in Oncology* 10: 935

372. Ventre J, Doebber T, Wu M, MacNaul K, Stevens K, Pasparakis M, Kollias G & Moller DE (1997) Targeted disruption of the tumor necrosis factor-alpha gene: metabolic consequences in obese and nonobese mice. *Diabetes* 46: 1526–1531

373. Verhoeven Y, Tilborghs S, Jacobs J, De Waele J, Quatannens D, Deben C, Prenen H, Pauwels P, Trinh XB, Wouters A, *et al* (2020) The potential and controversy of targeting STAT family members in cancer. *Seminars in Cancer Biology* 60: 41–56

374. Vuppalanchi R & Chalasani N (2009) Non-alcoholic fatty liver disease and non-alcoholic steatohepatitis. *Hepatology* 49: 306–317

375. Wadosky KM & Willis MS (2012) The story so far: post-translational regulation of peroxisome proliferator-activated receptors by ubiquitination and SUMOylation. *Am J Physiol Heart Circ Physiol* 302: H515-526

376. Wakabayashi K, Okamura M, Tsutsumi S, Nishikawa NS, Tanaka T, Sakakibara I, Kitakami J, Ihara S, Hashimoto Y, Hamakubo T, *et al* (2009) The peroxisome proliferator-activated receptor gamma/retinoid X receptor alpha heterodimer targets the histone modification enzyme PR-Set7/Setd8 gene and regulates adipogenesis through a positive feedback loop. *Mol Cell Biol* 29: 3544–3555

377. Wakao H, Gouilleux F & Groner B (1994) Mammary gland factor (MGF) is a novel member of the cytokine regulated transcription factor gene family and confers the prolactin response. *EMBO J* 13: 2182–2191

378. Wan M, Leavens KF, Saleh D, Easton RM, Guertin DA, Peterson TR, Kaestner KH, Sabatini DM & Birnbaum MJ (2011) Postprandial hepatic lipid metabolism requires signaling through Akt2 independent of the transcription factors FoxA2, FoxO1, and SREBP1c. *Cell Metab* 14: 516–527

379. Wang W, Liu L, Song X, Mo Y, Komma C, Bellamy HD, Zhao ZJ & Zhou GW (2011) Crystal structure of human protein tyrosine phosphatase SHP-1 in the open conformation. *J Cell Biochem* 112: 2062–2071

380. Wang Y, Vera L, Fischer WH & Montminy M (2009) The CREB coactivator CRTC2 links hepatic ER stress and fasting gluconeogenesis. *Nature* 460: 534–537

381. Warden A, Truitt J, Merriman M, Ponomareva O, Jameson K, Ferguson LB, Mayfield RD & Harris RA (2016) Localization of PPAR isotypes in the adult mouse and human brain. *Sci Rep* 6: 27618

382. Werner ED, Lee J, Hansen L, Yuan M & Shoelson SE (2004) Insulin Resistance Due to Phosphorylation of Insulin Receptor Substrate-1 at Serine 302 *. *Journal of Biological Chemistry* 279: 35298–35305

383. Weykamp C (2013) HbA1c: A Review of Analytical and Clinical Aspects. *Ann Lab Med* 33: 393–400

384. Wilcox G (2005) Insulin and Insulin Resistance. *Clin Biochem Rev* 26: 19–39

385. Wild T & Cramer P (2012) Biogenesis of multisubunit RNA polymerases. *Trends in Biochemical Sciences* 37: 99–105

386. Wlodarski P, Zhang Q, Liu X, Kasprzycka M, Marzec M & Wasik MA (2007) PU.1 activates transcription of SHP-1 gene in hematopoietic cells. *J Biol Chem* 282: 6316–6323

387. Wo Tsui H, Siminovitch KA, de Souza L & Tsui FWL (1993) Motheaten and viable motheaten mice have mutations in the haematopoietic cell phosphatase gene. *Nat Genet* 4: 124–129

388. Woerle HJ, Pimenta WP, Meyer C, Gosmanov NR, Szoke E, Szombathy T, Mitrakou A & Gerich JE (2004) Diagnostic and Therapeutic Implications of Relationships Between Fasting, 2-Hour Postchallenge Plasma Glucose and Hemoglobin A1c Values. *Archives of Internal Medicine* 164: 1627–1632

389. Wu C, Sun M, Liu L & Zhou GW (2003) The function of the protein tyrosine phosphatase SHP-1 in cancer. *Gene* 306: 1–12

390. Wu Y, Ding Y, Tanaka Y & Zhang W (2014) Risk Factors Contributing to Type 2 Diabetes and Recent Advances in the Treatment and Prevention. *Int J Med Sci* 11: 1185–1200

391. Xiao W, Hong H, Kawakami Y, Kato Y, Wu D, Yasudo H, Kimura A, Kubagawa H, Bertoli LF, Davis RS, *et al* (2009) Tumor suppression by phospholipase C-beta3 via SHP-1-mediated dephosphorylation of Stat5. *Cancer Cell* 16: 161–171

392. Xu D, Wang Z, Xia Y, Shao F, Xia W, Wei Y, Li X, Qian X, Lee J-H, Du L, *et al* (2020) The gluconeogenic enzyme PCK1 phosphorylates INSIG1/2 for lipogenesis. *Nature* 580: 530–535

393. Xu E, Charbonneau A, Rolland Y, Bellmann K, Pao L, Siminovitch KA, Neel BG, Beauchemin N & Marette A (2012) Hepatocyte-specific Ptpn6 deletion protects from obesity-linked hepatic insulin resistance. *Diabetes* 61: 1949–1958

394. Xu E, Forest M-P, Schwab M, Avramoglu RK, St-Amand E, Caron AZ, Bellmann K, Shum M, Voisin G, Paquet M, *et al* (2014a) Hepatocyte-specific Ptpn6 deletion promotes hepatic lipid accretion, but reduces NAFLD in diet-induced obesity: potential role of PPARγ. *Hepatology* 59: 1803–1815

395. Xu E, Schwab M & Marette A (2014b) Role of protein tyrosine phosphatases in the modulation of insulin signaling and their implication in the pathogenesis of obesity-linked insulin resistance. *Rev Endocr Metab Disord* 15: 79–97

396. Xu E, Schwab M & Marette A (2014c) Role of protein tyrosine phosphatases in the modulation of insulin signaling and their implication in

the pathogenesis of obesity-linked insulin resistance. *Rev Endocr Metab Disord* 15: 79–97

397. Yamashita H, Nevalainen MT, Xu J, LeBaron MJ, Wagner KU, Erwin RA, Harmon JM, Hennighausen L, Kirken RA & Rui H (2001) Role of serine phosphorylation of Stat5a in prolactin-stimulated beta-casein gene expression. *Mol Cell Endocrinol* 183: 151–163

398. Yang J, Liao X, Agarwal MK, Barnes L, Auron PE & Stark GR (2007) Unphosphorylated STAT3 accumulates in response to IL-6 and activates transcription by binding to NFkappaB. *Genes Dev* 21: 1396–1408

399. Yang J, Liu L, He D, Song X, Liang X, Zhao ZJ & Zhou GW (2003) Crystal structure of human protein-tyrosine phosphatase SHP-1. *J Biol Chem* 278: 6516–6520

400. Yang J & Stark GR (2008) Roles of unphosphorylated STATs in signaling. *Cell Res* 18: 443–451

401. Yao Z, Cui Y, Watford WT, Bream JH, Yamaoka K, Hissong BD, Li D, Durum SK, Jiang Q, Bhandoola A, *et al* (2006) Stat5a/b are essential for normal lymphoid development and differentiation. *PNAS* 103: 1000–1005

402. Yecies JL, Zhang HH, Menon S, Liu S, Yecies D, Lipovsky AI, Gorgun C, Kwiatkowski DJ, Hotamisligil GS, Lee C-H, *et al* (2011) Akt stimulates hepatic SREBP1c and lipogenesis through parallel mTORC1-dependent and independent pathways. *Cell Metab* 14: 21–32

403. Yoon JC, Puigserver P, Chen G, Donovan J, Wu Z, Rhee J, Adelmant G, Stafford J, Kahn CR, Granner DK, *et al* (2001) Control of hepatic gluconeogenesis through the transcriptional coactivator PGC-1. *Nature* 413: 131–138

404. You M & Zhao Z (1997) Positive effects of SH2 domain-containing tyrosine phosphatase SHP-1 on epidermal growth factor- and interferon-gamma-stimulated activation of STAT transcription factors in HeLa cells. *J Biol Chem* 272: 23376–23381

405. Yu CC, Tsui HW, Ngan BY, Shulman MJ, Wu GE & Tsui FW (1996) B and T cells are not required for the viable motheaten phenotype. *J Exp Med* 183: 371–380

406. Yu CL, Jin YJ & Burakoff SJ (2000) Cytosolic tyrosine dephosphorylation of STAT5. Potential role of SHP-2 in STAT5 regulation. *J Biol Chem* 275: 599–604

407. Yu J, Deng R, Zhu HH, Zhang SS, Zhu C, Montminy M, Davis R & Feng G-S (2013) Modulation of fatty acid synthase degradation by concerted action of p38 MAP kinase, E3 ligase COP1, and SH2-tyrosine phosphatase Shp2. *J Biol Chem* 288: 3823–3830

408. Yu JH, Zhu B-M, Riedlinger G, Kang K & Hennighausen L (2012) The liver-specific tumor suppressor STAT5 controls expression of the reactive oxygen species-generating enzyme NOX4 and the proapoptotic proteins PUMA and BIM in mice. *Hepatology* 56: 2375–2386

409. Yu S, Meng S, Xiang M & Ma H (2021) Phosphoenolpyruvate carboxykinase in cell metabolism: Roles and mechanisms beyond gluconeogenesis. *Mol Metab* 53: 101257

410. Yue X, Han T, Hao W, Wang M & Fu Y (2020) SHP2 knockdown ameliorates liver insulin resistance by activating IRS-2 phosphorylation through the AKT and ERK1/2 signaling pathways. *FEBS Open Bio* 10: 2578–2587

411. Yung JHM & Giacca A (2020) Role of c-Jun N-terminal Kinase (JNK) in Obesity and Type 2 Diabetes. *Cells* 9: 706

412. Zapata PD, Ropero RM, Valencia AM, Buscail L, López JI, Martín-Orozco RM, Prieto JC, Angulo J, Susini C, López-Ruiz P, *et al* (2002) Autocrine regulation of human prostate carcinoma cell proliferation by somatostatin through the modulation of the SH2 domain containing protein tyrosine phosphatase (SHP)-1. *J Clin Endocrinol Metab* 87: 915–926

413. Zaret KS & Carroll JS (2011) Pioneer transcription factors: establishing competence for gene expression. *Genes Dev* 25: 2227–2241

414. Zhang EE, Chapeau E, Hagihara K & Feng G-S (2004) Neuronal Shp2 tyrosine phosphatase controls energy balance and metabolism. *Proc Natl Acad Sci U S A* 101: 16064–16069

415. Zhang H & Zhang C (2010) Adipose “Talks” to Distant Organs to Regulate Insulin Sensitivity and Vascular Function. *Obesity (Silver Spring)* 18: 2071–2076

416. Zhang W, Patil S, Chauhan B, Guo S, Powell DR, Le J, Klotsas A, Matika R, Xiao X, Franks R, *et al* (2006) FoxO1 Regulates Multiple Metabolic Pathways in the Liver: EFFECTS ON GLUCONEOGENIC, GLYCOLYTIC, AND LIPOGENIC GENE EXPRESSION*. *Journal of Biological Chemistry* 281: 10105–10117

417. Zhang X, Yang S, Chen J & Su Z (2018) Unraveling the Regulation of Hepatic Gluconeogenesis. *Front Endocrinol (Lausanne)* 9: 802

418. Zhang Z, Shen K, Lu W & Cole PA (2003) The role of C-terminal tyrosine phosphorylation in the regulation of SHP-1 explored via expressed protein ligation. *J Biol Chem* 278: 4668–4674

419. Zhou X, Gallazzini M, Burg MB & Ferraris JD (2010) Contribution of SHP-1 protein tyrosine phosphatase to osmotic regulation of the transcription factor TonEBP/OREBP. *PNAS* 107: 7072–7077

420. Zhu Y, Qi C, Korenberg JR, Chen XN, Noya D, Rao MS & Reddy JK (1995) Structural organization of mouse peroxisome proliferator-activated receptor gamma (mPPAR gamma) gene: alternative promoter use and different splicing yield two mPPAR gamma isoforms. *Proc Natl Acad Sci U S A* 92: 7921–7925

421. Zhuang X, Ma J, Xu S, Sun Z, Zhang R, Zhang M & Xu G (2021) SHP-1 suppresses endotoxin-induced uveitis by inhibiting the TAK1/JNK pathway. *J Cell Mol Med* 25: 147–160

422. Zisman A, Peroni OD, Abel ED, Michael MD, Mauvais-Jarvis F, Lowell BB, Wojtaszewski JF, Hirshman MF, Virkamaki A, Goodyear LJ, *et al* (2000) Targeted disruption of the glucose transporter 4 selectively in muscle causes insulin resistance and glucose intolerance. *Nat Med* 6: 924–928

423. Zoete V, Grosdidier A & Michielin O (2007) Peroxisome proliferator-activated receptor structures: ligand specificity, molecular switch and interactions with regulators. *Biochim Biophys Acta* 1771: 915–925